Synthesis of ferrocenyl derivatives as novel nucleic analogue monomers

by

Antoine Sallustrau

UNIVERSITY OF
BIRMINGHAM

A thesis submitted to
The University of Birmingham
For the degree of
DOCTOR OF PHILOSOPHY

School of Chemistry
College of Engineering and Physical Sciences
University of Birmingham
June 2013

Abstract

Bioorganometallic chemistry is a growing field of research in which organometallic chemistry is combined with biology to achieve novel molecules with novel properties at the biological level. In this area, the tagging of DNA with bioorganometallic molecules such as ferrocene has been the object of much attention over the past few decades. In recent years, a novel approach has been developed consisting of replacing parts of nucleic acids with organic groups including metal-binding ligands. Considering this approach, it was decided to investigate the replacement of DNA dinucleotides with a tetra-substituted ferrocenyl monomer containing nucleobases, leading to the formation of a novel nucleic acid analogue called *ferrocene nucleic acid* (FcNA). The synthesis of several monomers containing adenine and uracil has been the subject of this thesis. Coupling nucleobases to form bis-substituted ferrocenes was first investigated as a model for the subsequent synthesis of tetra-substituted ferrocenyl monomers with high chiral purity. The compounds were characterised using a range of spectroscopic and analytical techniques, including X-ray crystallography. The influence of the nucleobases and the nature of the linker to the ferrocenyl group have also been investigated using electrochemistry. The work has also led to investigations to develop ferrocene compounds as potential organometallic drugs.

Table of contents

A special thanks to my friends in Paris: Oliv, Elo, Tib, PEM, Yann and the others but especially to Raph, my best friend, for her support and all the good moments we spent during the writing-up. I also would like to thank my parents and my brother and sisters, Xavier, Claire and Helene! I love you guys!

Finally, I would like to make a very special thank and dedicate this thesis to my beautiful love, Franciane, without whom I would not have made it! I know it has not been easy everyday, but thanks for your strength, your support, your patience, your understanding and your love!

List of abbreviations

$[\alpha]_D$	Specific optical rotation
2-AP	2-Amino purine
Ar	Aromatic
Bn	Benzyl group
Bz	Benzoyl group
c	Concentration
$CDCl_3$	Deuterated chloroform
COSY	Correlation spectroscopy
Cp	Cyclopentadienyl
CV	Cyclic voltammetry
δ	Chemical shift
d	Doublet (NMR)
DCA	Dichloroacetic acid
DCM	Dichloromethane
dd	Doublet of doublet (NMR)
DEAD	Diethyl azodicarboxylate
DIAD	Diisopropyl azodicarboxylate
DMAP	4-Dimethylaminopyridine
DMF	Dimethylformamide
dmfc	Decamethylferrocene
DMSO	Dimethylsulfoxide
DMSO-d_6	Deuterated dimethylsulfoxide

dt	Doublet of triplet
D_2O	Deuterated water
ΔE_p	Peak separation
E	Potential (V)
E°'	Formal potential (V)
ee	Enantiomeric excess
eq	Equivalent
ES	Electrospray ionisation
EtOAc	Ethyl acetate
EtOH	Ethanol
Et_2O	Diethylether
Fc	Ferrocene
FcNA	Ferrocenyl nucleic acid
FEN	Ferronucleobase
FRET	Fluorescence resonance energy transfer
GNA	Glycol nucleic acid
HMBC	Heteronuclear multiple bond correlation
HPLC	High performance liquid chromatography
HSQC	Heteronuclear single quantum coherence
IPA	Isopropylamine
I	current (A)
ipso	Ipso carbon
^{i}Pr	Isopropyl group
IR	Infrared spectroscopy

J	Coupling constant (Hz)
LNA	Locked nucleic acid
NMR	Nuclear magnetic resonance spectroscopy
NBS	*N*-Bromosuccinimide
m	NMR multiplet
Me	Methyl
MeOD-d$_4$	Deuterated methanol
MeOH	Methanol
Mp	Melting point
v	Scan rate (mV.s^{-1})
Ph	Phenyl group
PNA	Peptide nucleic acid
RNA	Ribonucleic acid
R.T.	Room temperature
s	Singlet (NMR)
SNA	Serinol nucleic acid
T	Absolute temperature (K)
t	Triplet (NMR)
TBA·PF$_6$	Tetrabutylammonium hexafluorophosphate
TBDPS	*tert*-Butyldiphenylsilyl group
TCA	Trichloroacetic acid
TEA	Triethylamine
TFA	Tetrafluoroacetic Acid
THF	Tetrahydrofuran

T$_m$	Melting temperature
TMEDA	Tetramethylethylenediamine
α-TNA	α-Threoninol nucleic acid
TNA	Threose nucleic acid
vs.	Versus
w/w	Mass percent

CHAPTER 1: INTRODUCTION

Sixty years ago in 1953, Edmund Hillary & Tensing Norkay reached summit of Everest for the first time, the Pulitzer prize was awarded to Ernest Hemingway for his book *The Old Man and The Sea* and in the same year, a famous paper in the scientific journal *Nature* written by Watson and Crick,[1] elucidated for the first time the structure of DNA. In this paper, they wrote: "We wish to suggest a structure for the salt of deoxyribonucleic acid. This structure has novel features which are of considerable biological interest". This discovery started a revolution in molecular biology that reached its culmination point with the sequencing of the entire human genome and just recently, the synthesis of a genome by artificial means and its incorporation in a cell.[2] These breakthroughs have enhanced genomics, chemical biology, and have even inspired recent development in the field of artificial nucleic acid.

1.1 DNA

DNA is a macromolecule that is essential for all forms of life. Using the four canonical nucleobases: adenine (A), thymine (T), cytosine (C) and guanine (G), the nucleic acid assembly encodes the genetic information and blueprint of living organisms. Nucleobases, the central building blocks of this giant molecule, are connected to a deoxyribose sugar via the *N*-1 atom for pyrimidines (T and C) and the *N*-9 atom for purines (A and G) to form nucleosides. Nucleosides are linked together via phosphodiester bridges to form nucleotides. Most DNAs are double stranded duplexes in nature, where two complementary single strands pair together in an anti-parallel orientation. Each single strand of DNA is

defined by a specific sequence of these nucleotides. The double stranded helical shape of DNA comes from the ability of nucleotides to selectively form hydrogen bonds between their respective nucleobases, which play a determinant role in the stability and the specificity of duplex formation. Adenine creates two hydrogen bonds with thymine and guanine three with cytosine (Figure 1-1). The duplex is also stabilised by base stacking interactions. Those two types of interaction are the building blocks of the secondary structure of DNA.
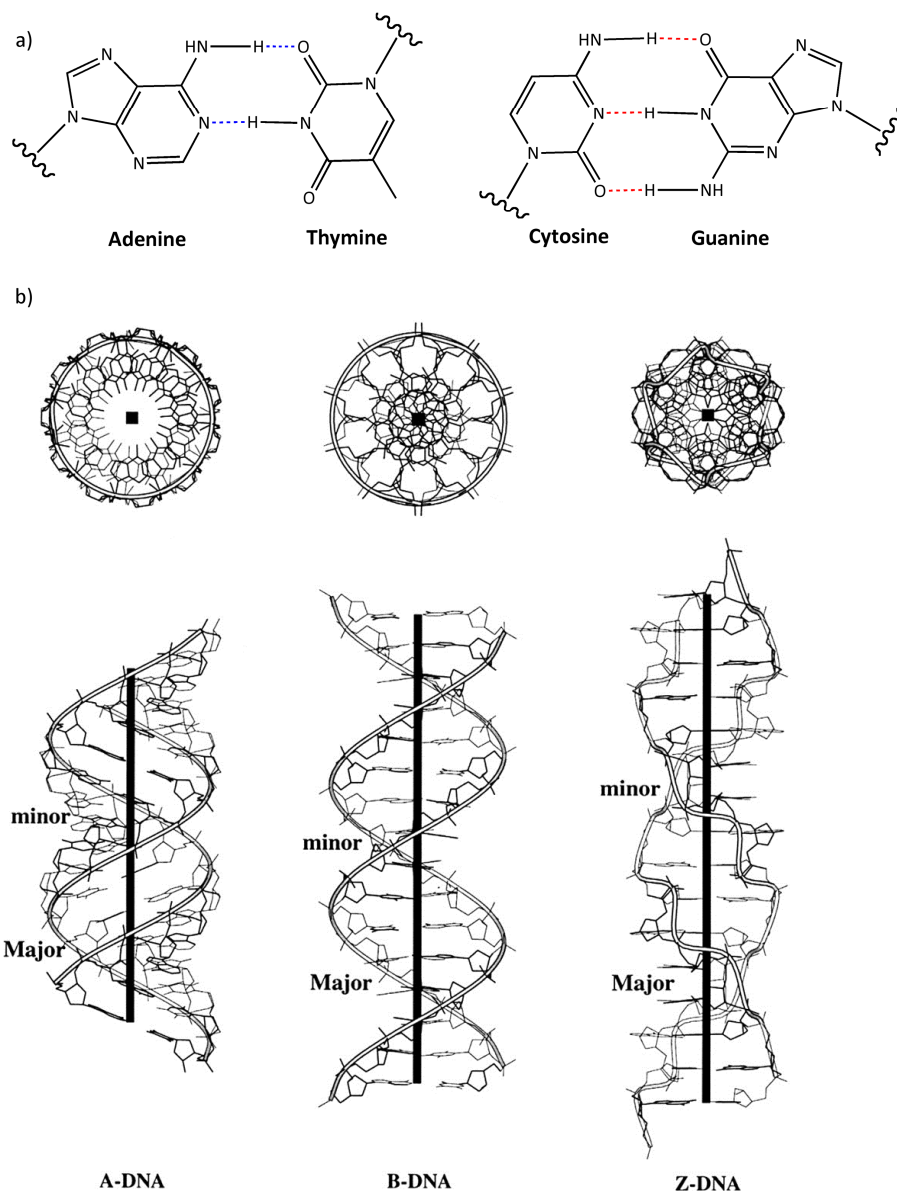
Figure 1-1: a) The four canonical bases forming A-T and C-G H-bonding base pairs, b) Three conformational shapes of DNA duplex (http://x3dna.org/articles/seeing-is-understanding-as-well-as-believing)

The tertiary structure of DNA corresponds to the 3 dimensional shape of the double stranded helix. Three different structural conformations of DNA have been reported: A, B and Z (Figure 1-1).[3] A-DNA structure is a short and thick helix that contains a deep and narrow major groove and a superficial minor groove. This conformation is usually favoured at low water concentration. B-DNA conformation is thinner and longer than A-DNA. It presents a wide major groove that facilitates protein anchorage and a narrow minor groove. This is the most common structure of DNA found *in vivo* and is favoured at high water concentrations. Z-DNA is thinner and more elongated than B-DNA with a deeper minor groove and a shallower major groove. This conformation can be formed in high salt concentration conditions but it is not encountered *in vivo*.

The base pairing and base stacking are disrupted during DNA replication and its transcription into ribonucleic acids (RNA). RNA also consists of a chain of nucleotides but is usually much shorter than DNA and often found as a single strand *in vivo*. RNA contains ribose sugars and uracil replaces thymine as the complementary base to adenine.

1.2   Oligomer synthesis

Directly after the structural elucidation of DNA in the early 1950's and the publication of amino acid sequence of insulin by Sanger in 1955, studying genes and their influence on cell behaviour became a major goal for molecular biologists. DNA has quickly become a significant tool and target in many domains such as nanotechnology[4], disease diagnostics[5] and gene therapy.[6] From here, chemists have started to develop ways to mimic and modify its supramolecular structure. However before gene sequences could be studied and

eventually manipulated, it was important to develop a convenient way of synthesising DNA through chemical means. The development of automated DNA synthesis using phosphoramidite chemistry played a significant role in addressing this challenge.

Automated oligonucleotide synthesis[7] is based on a succession of cycles involving four major steps. The synthesis starts from the solid support where the first protected nucleoside (n) is attached; it then continues over each cycle with the incorporation of each new nucleoside as a phosphoramadite ($n+1$) and finally ends up with the release of the desired oligonucleotide. (Figure 1-2)
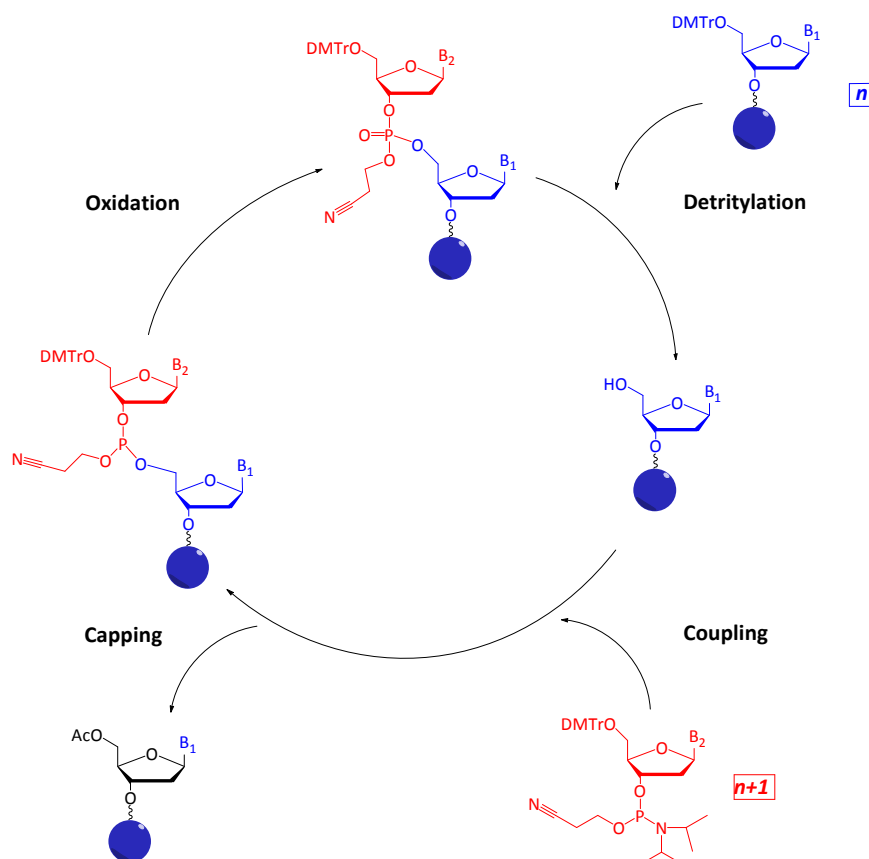
Figure 1-2: *Oligonucleotide synthesis cycle*

The first step of the cycle is a detritylation of the first nucleoside *(n)*. Cleavage of dimethoxytrityl (DMT) group is usually obtained by acid treatment with trichloroacetic acid

(TCA) or dichloroacetic acid (DCA) in order to obtain the free 5'-OH. The second step consists of coupling the activated nucleoside (*n*) and the new phosphoramidite (*n+1*). This reacts with the 5'-OH of *n* in the presence of tetrazole. In practice, the reaction is never completely quantitative; consequently the third step called capping is important since it allows unreacted deprotected nucleosides *n* to be removed before the next cycle. Acetic acid is used to acetylate the free hydroxyl, avoiding side reactions and truncated sequences. The phosphite triester synthesized in the coupling step is relatively unstable. Oxidation of the phosphite to the corresponding phosphate diester stabilizes the oligonucleotide before coupling with the next nucleoside.

The development of efficient chemical synthesis of DNA has enabled the widescale availability of primers, linkers and probes, for example for sensing applications. In the context of nucleic acid modifications for biological purposes, novel strategies have emerged. One of them consists of replacing parts of a nucleic acid with other organic groups that has led to the development of various DNA mimics and analogues. The first test of a DNA analogue is its ability to form complexes with DNA/RNA or with itself in the same way that natural duplexes are formed. Moreover these analogues should ideally enhance pre-existent natural DNA/RNA properties or confer new properties, leading to a new range of applications. Consequently, many different types of DNA modification have been investigated over the past decades varying from simple tagging to more drastic changes such as nucleobase and backbone replacement. Some examples are presented in the following section.

1.3 DNA functionalisation and DNA analogues

1.3.1 Fluorophore functionalization

One popular way to functionalise a nucleic acid is to attach a fluorophore as a label for sensing applications. Fluorophores are fluorescent species that can re-emit light after light excitation, which may be detected at very low concentrations. They can be used as dyes for staining certain structures or tissues and as markers when attached to macromolecules. Different types of fluorophores have been incorporated into nucleic acids. Fluorescein and rhodamine, which are two of the most commonly used fluorophores, have been incorporated into oligonucleotides as phosphoramidites via automated synthesis[8]. (Figure 1-3)

Rhodamine   **Fluorescein**
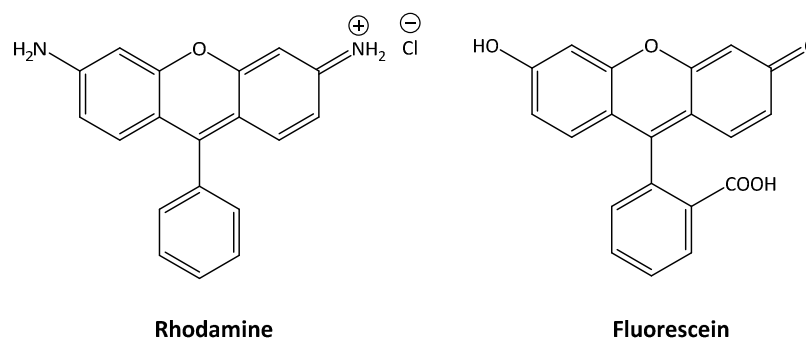
Figure 1-3: Rhodamine and Fluorescein structures

Fluorescein and rhodamine have been used in the widely utilised Taqman® assay.[9] This assay detects polymerase chain reaction (PCR) products by hybridisation and cleavage of a double-labelled probe called a Taqman probe. The latter contains fluorescein as fluorescent dye and rhodamine as quencher dye respectively attached to the 5' and 3'-end of the oligonucleotide sequence.[10] If both dyes are close enough to each other, rhodamine quenches fluorescence emission of fluorescein by fluorescence resonance energy transfer (FRET). During the PCR, the Taq polymerase replicates the targeted sequence by recognition of unmodified primers

until it reaches the hybridised Taqman probe. The nuclease activity of the polymerase degrades the Taqman probe releasing the fluorescein, which is no longer quenched. The increase of fluorescence intensity reveals formation of the PCR product (Figure 1-4).[11] This technique has been used in numerous applications, for example in the diagnostic of base variation in DNA.
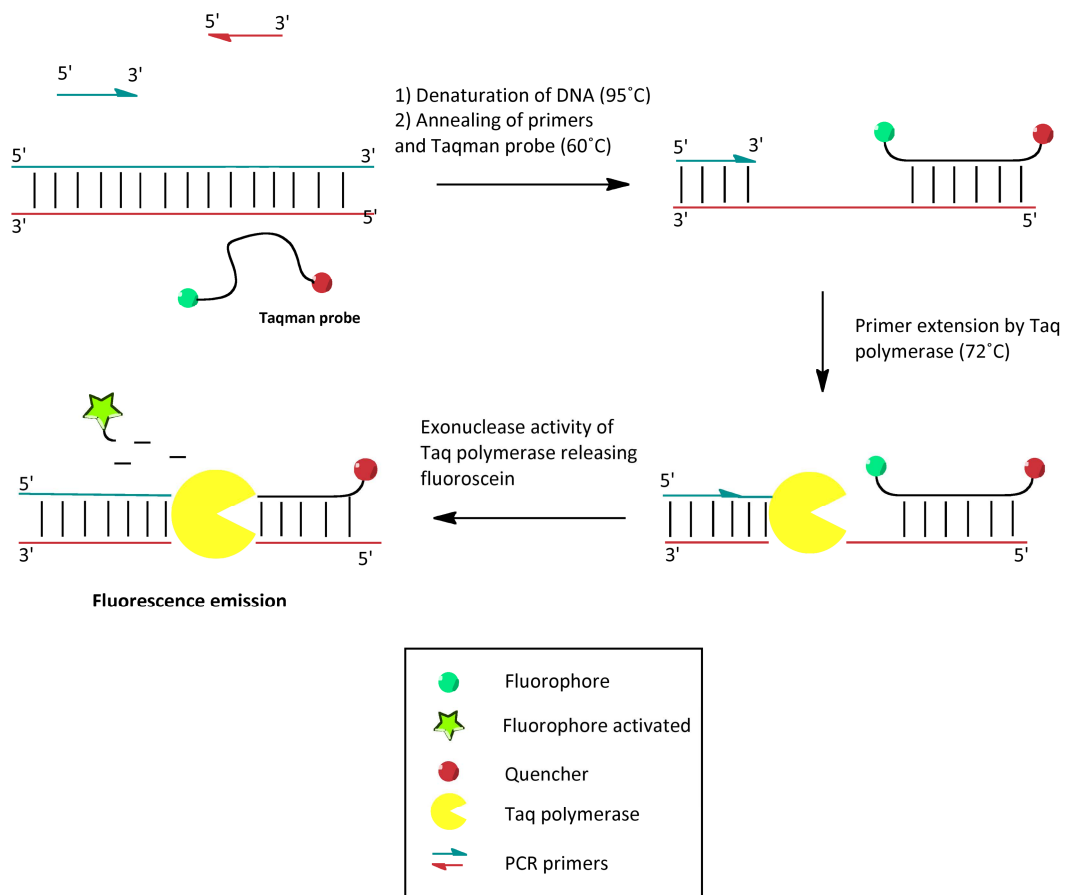
Figure 1-4: *Taqman® assay principle*

In another example of luminescent dyes inserted into DNA sequence, Mesmaeker *et al.*[12] described how they incorporated a ruthenium complex into the middle of a strand sequence. As soon as the probe hybridised with the target sequence, the luminescent signal produced by the complex was quenched through photo-induced electron transfer (PET) from the guanine nucleobases of the target strand. In the same way, pyrene is known for its

sensitivity towards quenchers[13, 14] and has also been used as a DNA tag.[15,16] For example, in 2001, Yamana *et al.* attached a pyrene to the 2' position of the sugar of a nucleotide that showed an enhancement of fluorescence when pairing with the complementary RNA target.[17]
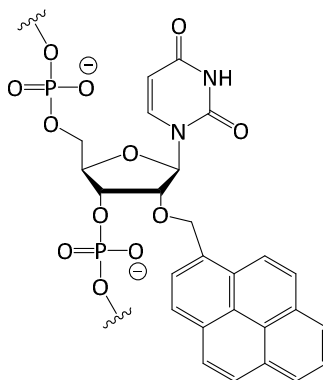
Figure 1-5: *Pyrene attached to nucleotide sugar by Yamana[15]*

1.3.2   Fluorescent base analogues

As described above, fluorescent tags can be connected to DNA via a linker, but this approach often places the fluorophore relatively far away from the duplex. Furthermore, the freedom given by the flexibility of the linker enables the dye to move around, which affects the ability to accurately predict the orientation of the fluorophore. However the use of a fluorescent base analogue avoids this problem since the analogue is tightly located inside the duplex. Fluorescent base analogues have the ability to be fluorescent and to form hydrogen bonds with complementary bases. As an example, 2-aminopurine (2-AP), which is one of the most frequently used fluorescent base analogues, is highly fluorescent and its UV band is at a longer wavelength than normal bases. This means it is possible to selectively excite it even in presence of a large excess of natural bases. As an adenine analogue 2-AP can pair with thymine and uracil but also with cytosine[18], as shown in Figure 1-6.
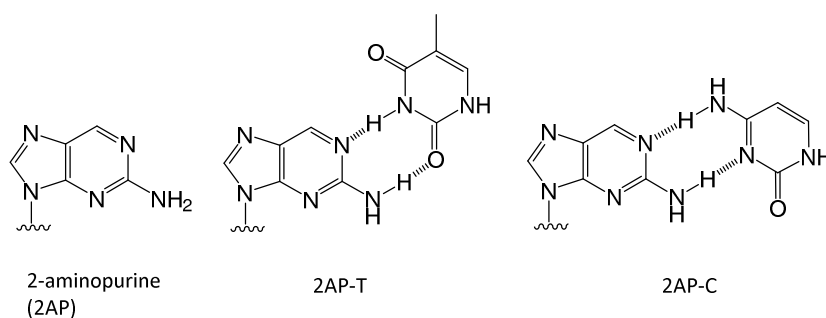
Figure 1-6: *2-Aminopurine pairing with thymine and cytosine via hydrogen bonding*

However, the utilisation of 2-AP has its limitations such as having less specific and less efficient base pairing than natural adenine, which perturbs the native structure of DNA. Its fluorescence depends on its proximate environment and it is considerably quenched when incorporated into a duplex[19] but this sensitivity to its microenvironment has been used in many investigations including nucleic acid structure analysis and DNA-protein interactions.[20, 21, 22]

1.3.3   Metal-mediated base pairing and base pair analogue

A couple of decades ago, interest in the substitution of natural DNA base-pairs with metal complexes started to develop. In this context, the development of ligand-like nucleobases containing metals led to the creation of "metal base-pair" systems. In these systems, Watson and Crick hydrogen bonds are replaced by interactions between a metal acting as a guest species and nucleobases, or their derivatives or mimics, acting as ligands. As described later, metal introduction can result in increased stability of the duplex and in certain cases, magnetic or conducting properties.

In 1963, Katz described insertion of one atom of Hg^{2+} between two natural thymines of a DNA duplex.[23] He hypothesised a slippage process as shown on Figure 1-7, that would bring the thymines together to form a Hg^{2+} base pair.
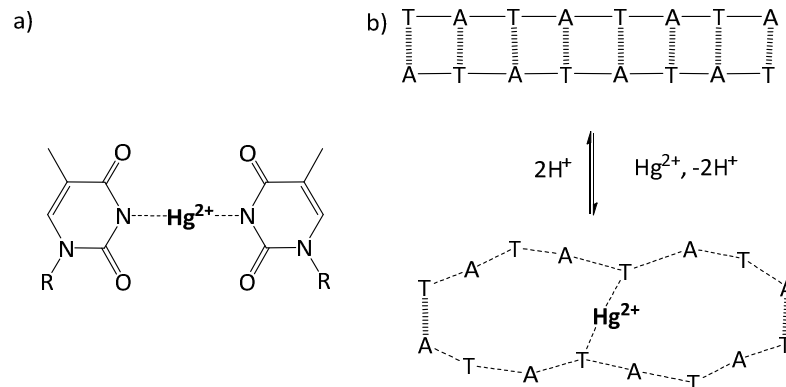
Figure 1-7: *a) The base pair structure proposed by Katz[23]. b) Formation of the base pair by a slippage process*

This concept was verified and supported by many subsequent studies, and most recently, by Ono *et al.*,[24] who through melting-curve studies and ESI mass spectrometry data, demonstrated the formation of stacking interactions between three consecutive T-Hg-T base-pairs, as shown in Figure 1-8.
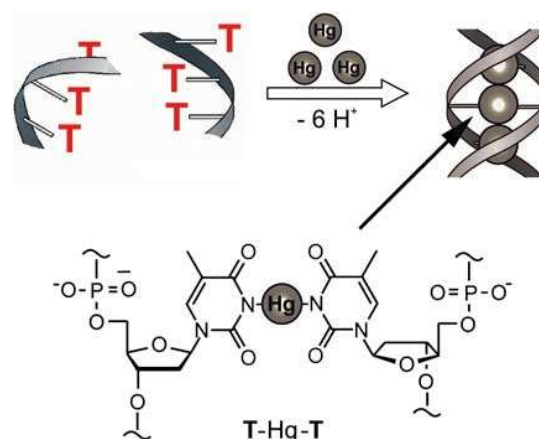
Figure 1-8: *Incorporation of three consecutive T-Hg-T base pairs in a DNA duplex.[24]*

Numerous examples demonstrated that modified nucleobases could also take part in metal base pairing. Meggers, Romesberg and Schultz described the first example of metal-base pairing with synthetic ligands in 2000.[25] They synthesised a planar pyridine dicarboxylate (Dipic) as a tridentate ligand and a pyridine nucleobase as the complementary donor ligand. The Dipic:Py pair was incorporated into the middle of a 15-oligonucleotide and Cu^{2+} was added. Formation of a copper bridge between the couple tridentate ligand-pyridine ("copper base-pair" formation) stabilized the modified DNA duplex almost as well as a dA:dT natural base pair at the same site. The tight binding to copper comes from the tridentate character of the Dipic ligand. Several other types of metals such as Ni^{2+}, Pd^{2+} or Pt^{2+} were studied but none of them stabilized the duplex formation as well as copper. Compared to Ni^{2+} or Zn^{2+}, Cu^{2+} has the highest complex formation constant. On the other hand, Pd^{2+} and Pt^{2+} are bigger and do not fit into the binding site of the tridentate ligand, which explains why copper has a higher affinity than these softer transition metals.[26]
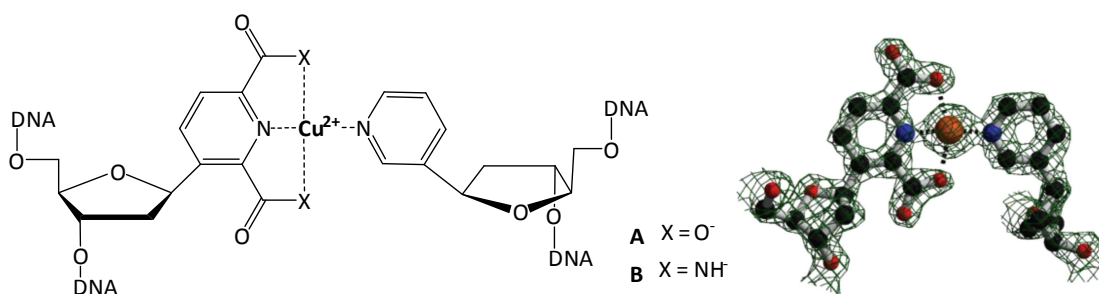
Figure 1-9: Schultz's "Dipic:Py pair"and its crystalline structure[25]

Schultz's group also inserted two Dipic-Py metal base pairs into a dodecamer and successfully obtained the first crystal structure of a metal-base pair in a DNA duplex.[27] Another copper base pair derivative (**B** in Figure 1-9) containing a pyridine 2,6 dicarboxamide ligand (Dipam) was also incorporated into an oligonucleotide and revealed an

improvement in duplex stabilisation of 3˚C and 4˚C compared to normal base pairs dG:dC and dA:dT respectively.

In 2002, Shionoya and Tanaka[28] prepared a "silver base-pair" complex with a pyridine mono-ligand that allowed formation of duplexes and triplexes. They also designed a dihydroxypyridone complex binding Cu^{2+} inside a DNA duplex (Figure 1-10).
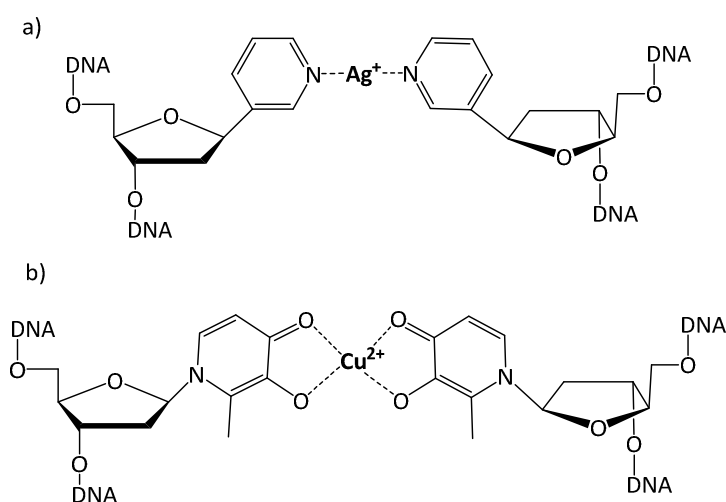
Figure 1-10: *Shionoya's metal base-pair complexes. a) Silver base pair. b) dihydroxypyridone base pair.[28]*

In 2003, they synthesised a short oligonucleotide made of five consecutive hydroxypyridone ligand complexes pairing with five Cu^{2+} ions and flanked with one natural base-pair on both 5' and 3' sides, called d(5'-GH$_5$C-3').[29]
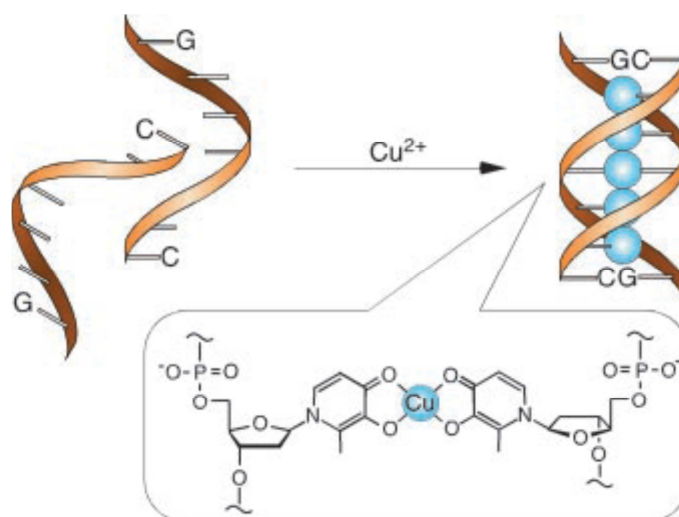
Figure 1-11: Complexation scheme of d(5'-GH$_5$C-3') and 5 eq of Cu^{2+} [29]

The chosen hydroxypyridone nucleobase was a bidentate ligand that formed a neutral complex in presence of the copper. The lack of charge decreased electrostatic repulsion between adjacent Cu^{2+} ions and consequently increased the thermal stability of the duplex. UV studies clearly showed that no duplexes were formed without presence of copper but the absorption at 280 nm and 307 nm changed significantly and simultaneously with addition of Cu^{2+} to the modified oligonucleotide. (Figure 1-12A)
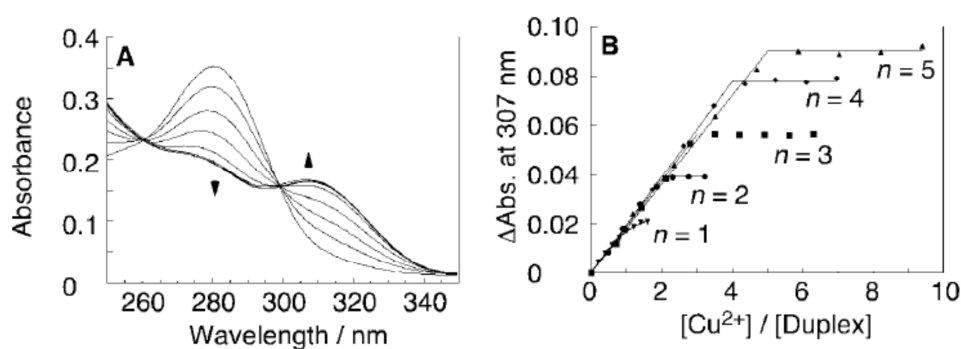
Figure 1-12: UV spectrum of d(5'-GH$_5$C-3') in presence of an increasing amount of Cu^{2+}

The possibility of secondary structures like hairpin or loop was excluded by electrospray ionisation mass spectrometry. Further results showed that Cu^{2+} ions were coupled

ferromagnetically with one another through unpaired d electrons to form magnetic chains. The authors hypothesised that these results could lead to the development of metal-base molecular devices like molecular wires. Meggers *et al.*[30] described in 2005 the synthesis of a copper base pair using hydroxyquinolines (HQ) as ligands and a deoxyribose phosphate or a propylene glycol as backbone. (Figure 1-13)
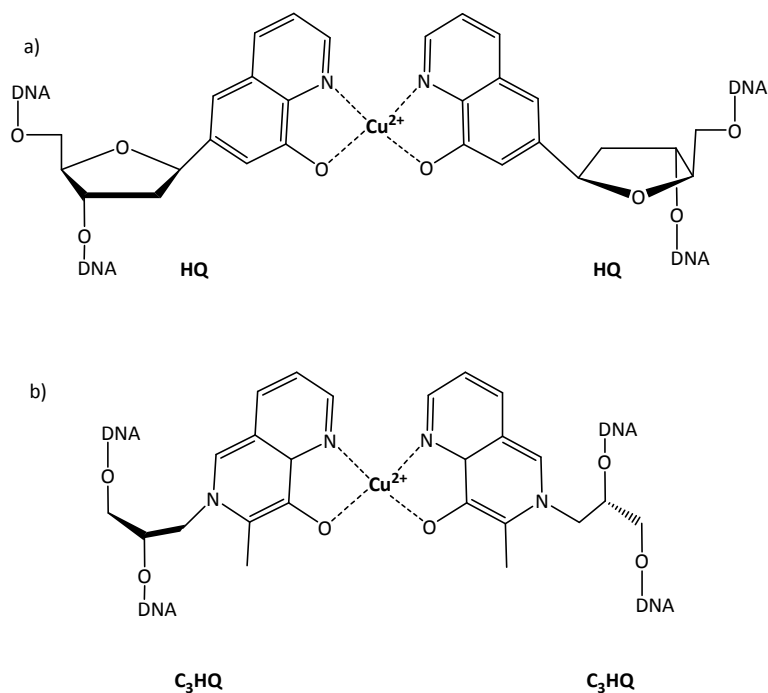
Figure 1-13: *Meggers's hydroxyquinoline base pair with a deoxyribose phosphate or a propanediol phosphate backbone.[30]*

Melting temperature (T_m) measurements on a HQ:HQ duplex pairs showed that even without metals, the complex could form stable base pairs due to the high hydrophobicity of HQ. However, from a value of 36°C without copper, the T_m could reach a temperature of 65°C in presence of one equivalent of Cu^{2+}, that is 20°C more than natural dA-dT or dG-dC base pairing.
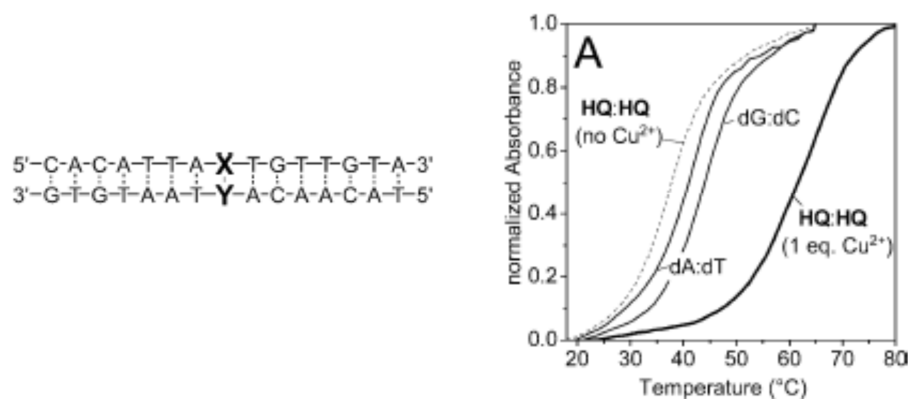
Figure 1-14: *Thermal studies of HQ:HQ duplex stability with or without Cu^{2+} ions*[30]

As a result of the exceptional high stabilization of the duplex, HQ:HQ base pairing was selected to be a starting point for the investigation of a complete backbone modification. As a way of reducing the complexity of the backbone, the natural deoxyribose sugar was exchanged with an artificial derivative of glycidol and led to the synthesis of a new monomer: C$_3$HQ. To synthesise a C$_3$HQ unit, a tritylated epoxide *S*-(-)-glycidol **A** was first selectively opened via a magnesium derivative of **B**. The TBS protecting group was then exchanged for a pivaloyl group followed by phosphitylation to afford **D**.
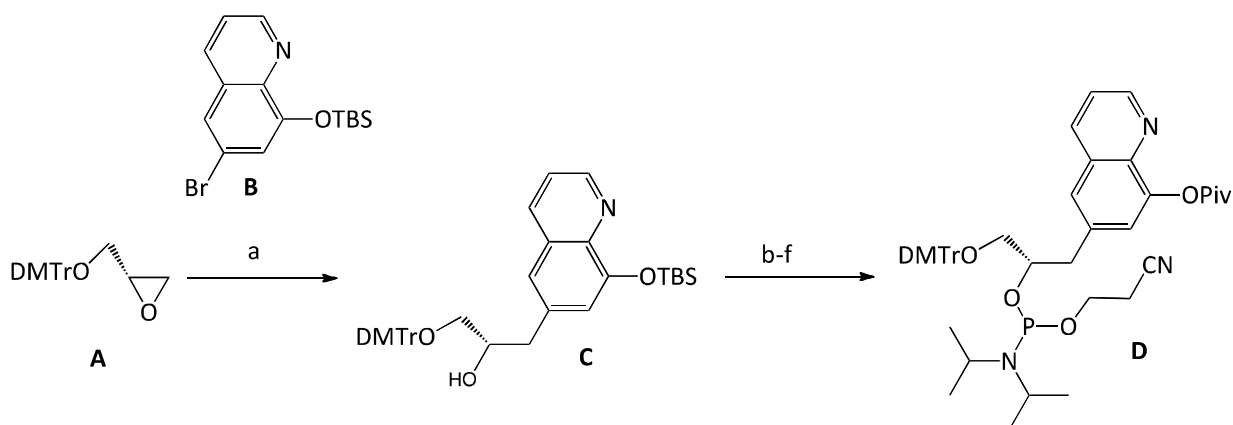
a) Addition of *sec*-BuLi (THF,-78˚C) to **B**, MgBr$_2$ and cat. CuI, epoxide **A** (69%).
b) TBSCl, DMAP, imidazole.
c) Cs$_2$CO$_3$.
d) *t*BuCOCl, DMAP.
e) TBAF
f) (*i*Pr$_2$N)(OCH$_2$CH$_2$CN)PCl, (*i*Pr)EtN (49% overall yield for step b-f).

Scheme 1-1: *Synthesis of the propylene glycol unit developed by Meggers et al.*[30]

An investigation of the stability of the homopair $C_3HQ:C_3HQ$ incorporated into a DNA duplex revealed that without Cu^{2+} no duplex was formed. However with one equivalent of Cu^{2+}, UV melting studies indicated a T_m of 70.5 ˚C. The increased stability of $C_3HQ:C_3HQ$ compared to HQ:HQ (ΔT_m + 5.5 °C) was explained by a less hindered acyclic backbone that would give more conformational flexibility and help duplex formation (Scheme 1-1). The structural backbone change leading to the design of C_3HQ was inspired by Eschenmoser's l-α-threofuranosyl oligonucleosides studies.[31] His studies were done in the context of defining a "chemical etiology of nucleic acid structure" where Eschenmoser tried to find the answer to the question "Was RNA the first genetic material or was it preceded by a simpler genetic material?".[32] The results of his investigations led to the development of new carbohydrate phosphodiester-based DNA analogues such as GNAs or TNAs as described below.

1.3.4 Backbone analogues

1.3.4.1 TNA

In his quest to understand the different criteria selected by Nature to choose ribo- and deoxyribonucleic acids as genetic supports, Eschenmoser emphasised that fully hydroxylated hexopyranosyl oligonucleotides gave weaker base pairing than RNA for steric reasons.[33] These findings orientated his research towards less bulkier pentopyranosyl oligonucleotides, which gave much stronger Watson and Crick base pairing than RNA.[34] He therefore emphasised the possibility of using other types of sugar than those in DNA/RNA to support Watson-Crick base pairing. In 2000, the synthesis of the first Threose Nucleic Acid (TNA) was described.[35] TNAs are composed of repeated units of threoses linked together by phosphodiester bonds and have proven to be able to pair with DNA, RNA and with

themselves (Figure 1-15). Ichida *et al.* polymerized more than 50 nucleotides of TNA from a

DNA template via a mutant polymerase called therminator DNA polymerase.[36]
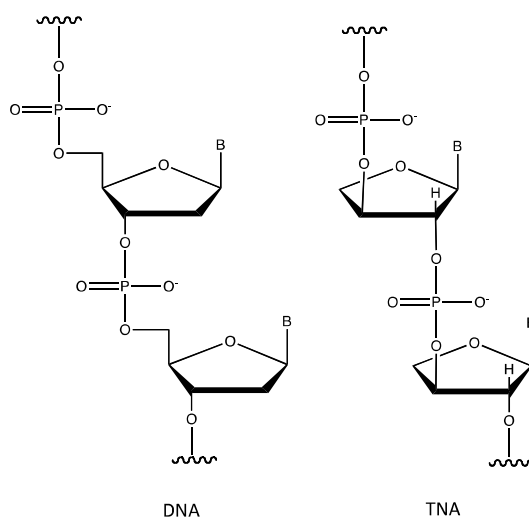
Figure 1-15: *DNA and its analogue TNA*

1.3.4.2   GNA

Another nucleic acid analogue emerged in 2005 when Meggers *et al*. described the synthesis

of a glycol nucleic acid (GNA), where the sugar of natural DNA/RNA nucleotides was replaced

by an acyclic three-carbon propylene glycol.[37]
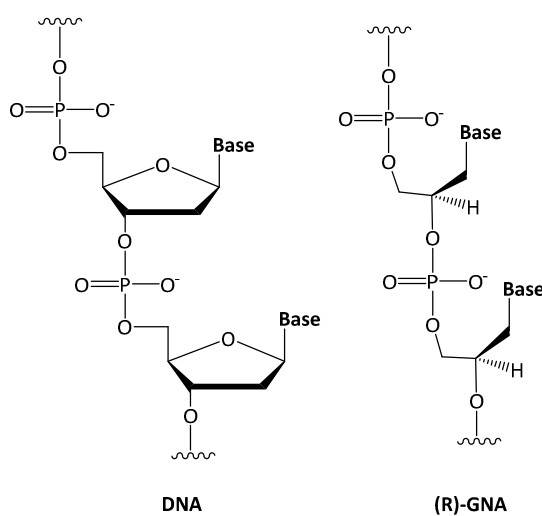
Figure 1-16: *The phosphodiester DNA analogues, GNA*

Thermal stability studies of GNA duplex formation gave T_m values that were 20.5 ˚C and 22.5 ˚C greater than the corresponding DNA (T_m = 40.5 ˚C) and RNA (T_m = 42.5 ˚C) duplexes respectively. To prove that the duplex consisted of a proper Watson and Crick base pairing, they studied the stability of a duplex where one strand included a T:T mismatch. They noticed an important decrease in stability with a T_m = 55 ˚C, showing that hybridisation mainly depends on nucleobase pairing interactions.

1.3.4.3 α-TNA and SNA

In a direct continuation of Meggers's work, Asanuma *et al.* published in 2010 a novel acyclic nucleic acid from D-threoninol.[38] Their α-Threoninol Nucleic Acid (α-TNA) presented interesting features compared to DNA and GNA: duplex formation via complementary base pairing occurred in an antiparallel manner and α-TNA duplex stability was higher than DNA and GNA duplexes. Furthermore, due to the flexibility of the acyclic backbone, the single-strand of α-TNA did not need to adopt the characteristic pre-organised conformation to form the duplex. It had previously been demonstrated that oligomers had to present a conformational "pre-organisation" to allow duplex formation.[39, 40, 41] However, the nucleic acid backbone was not flexible enough to allow cross-pairing with DNA or RNA. Consequently, one year later they published a new example of a nucleic acid analogue that overcame this problem.
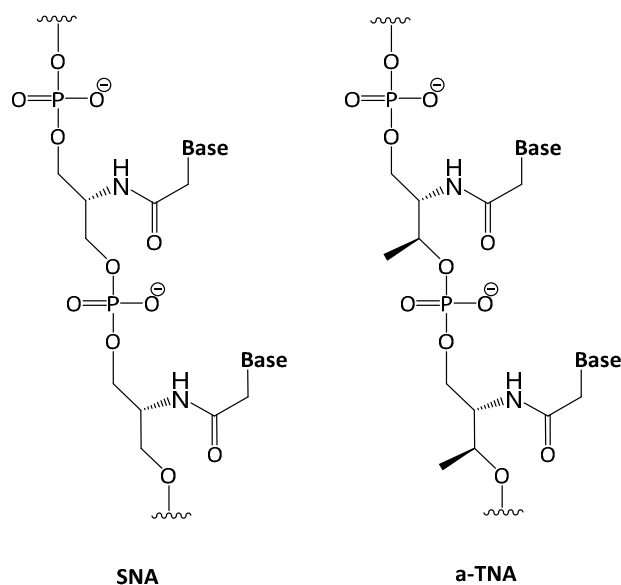
Figure 1-17: *SNA and α-TNA*

They synthesised a Serinol Nucleic Acid (SNA)[42], based on an achiral amino-propanediol (serinol) scaffold, which is more flexible than threoninol. Duplex formation occurred in an antiparallel fashion and presented significantly higher stability compared to DNA and RNA. SNA was able to cross-hybridise with DNA and RNA in contrary to GNA and α-TNA and can therefore be used as antigene/antisense agents.

1.3.4.4   LNA

The sugar moiety in DNA and RNA can adopt two representative favoured conformations: C_2-*endo* and C_3-*endo*, also called the B-form and A-form respectively. Nucleosides exist as an equilibrium mixture of these two conformations but the B-form conformation is dominant in DNA and the A-form is dominant in RNA (Figure 1-18). The reduction of flexibility through synthetic modifications of the sugar could help to improve binding affinities between a new type of nucleic acid and DNA/RNA.
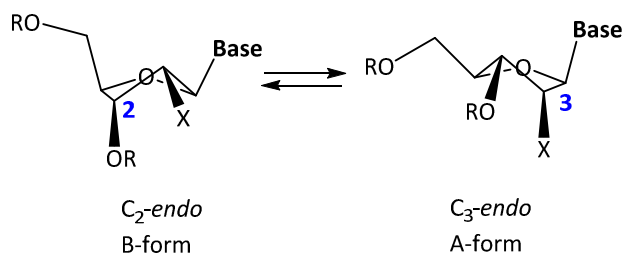
Figure 1-18: Two favoured representative conformations of a nucleoside.

In 1997, Imanishi *et al.*[43], described the synthesis of two "locked" nucleosides **A** and **B**, which they called Locked Nucleic Acid (LNA) in reference to the conformational restriction brought by the introduction of an ether group between the 2'-O and the 4'-C to the sugar moiety (Figure 1-19). The bridge "locks" the ribose in a specific conformation (A-form in this case) that enhances base stacking and backbone pre-organisation.

A: Base = uracil
B: Base = cytosine
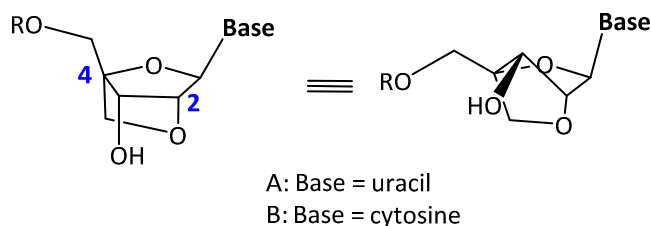
Figure 1-19: Locked Nucleic Acid

A couple of months later, Wengel *et al.*[44], described the synthesis of the same monomer that they incorporated into a 9-mer, giving a stabilizing effect on duplex formation compared to DNA and RNA.

1.3.4.5   PNA

A more radical approach to DNA analogues would be to introduce a completely new backbone linking nucleobases via amide bonds rather than via phosphodiester bonds. In 1991, Nielsen and co-workers described a design of a new type of oligomer called Peptide

Nucleic Acid (PNA) that could form duplexes/triplexes with natural DNA/RNA or with itself. [45] (Figure 1-20) The first homo-thymine PNA they synthesised could mimic an oligonucleotide and selectively form a triplex with a double-stranded DNA, via Hoogsteen base pairing. The nucleic acid analogue consisted of repeating aminoethylglycine units linked by amide bonds and attached to nucleobases through methylene carbonyl linkages. (Figure 1-20)
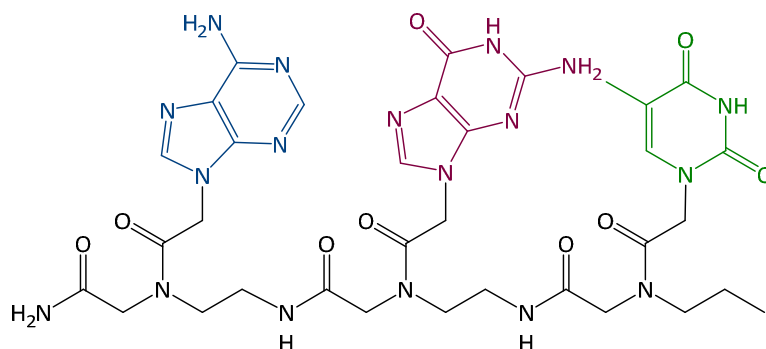
Figure 1-20: *PNA linked to Adenine (A), Guanine (G) and Thymine (T)*

PNAs are acyclic, achiral and neutral and consequently, they can bind complementary nucleic acids in both antiparallel and parallel orientations. PNA can form PNA/DNA and PNA/RNA duplexes that are more stable than DNA/DNA and DNA/RNA but still not as stable as 2PNA/DNA triplexes.

They are now many types of nucleic acid analogues known as XNAs, they are currently being investigated for their ability to mimic DNA function for example by acting as templates for enzymatic nucleic acid synthesis. [46]

1.4   Bioorganometallic chemistry and Ferrocene

The field of bioorganometallic chemistry concerns the synthesis and the study of organometallic species in biological structures and biological systems. Following the discovery of ferrocene and its "sandwich structure", active research grew around the

understanding of metal-carbon bonds (σ, π and δ) such as metallocene, carbonyls and carbenes. Ferrocene was first reported by Pauson in 1951[47,48] as a compound containing one atom of iron linked to each cyclopentadienyl rings by a single atom of carbon as presented in Scheme 1-2. Ferrocene was synthesised via reaction of the Grignard reagent cyclopentadienyl magnesium bromide with iron chloride in diethyl ether.

$$2\ C_5H_5MgBr + FeCl_2 \longrightarrow Fe(C_5H_5)_2 + MgCl_2 + MgBr_2$$

$$Fe(C_5H_5)_2$$
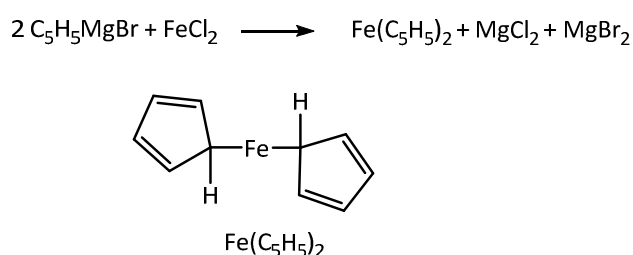
Scheme 1-2: First reported synthesis of ferrocene

The right structure of the metallocene was determined by Wilkinson and Woodward a year later.[49] They demonstrated via early proton NMR characterisation that the five protons of each Cp rings were equivalent, leading to the correct structural representation of ferrocene. (Figure 1-21)

Fe
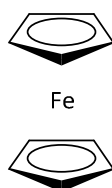
Figure 1-21: Wilkinson representation of Ferrocene

Ferrocene has proven to possess high chemical stability and electrochemical properties that made it a very popular molecule for biological applications, asymmetric catalysis[50], biomaterials,[51] DNA analysis[52] and DNA sensing. The stability of ferrocene enables

functionalization of one or both rings leading to the synthesis of large range of derivatives and their conjugation with biomolecules such as proteins or nucleic acids.

The first work on ferrocene linked to nucleosides was published by Gautheron *et al.*[53] twenty years ago. They reported the synthesis of several "metallocenonucleosides" in which ferrocene was attached to adenosine, deoxyuridine or uridine via a two carbon linker. This was made possible by the condensation of a 5-halogeno nucleosides with zirconylated derivatives of ferrocene using $(C_6H_5CN)_2$-$PdCl_2$ as a catalyst.
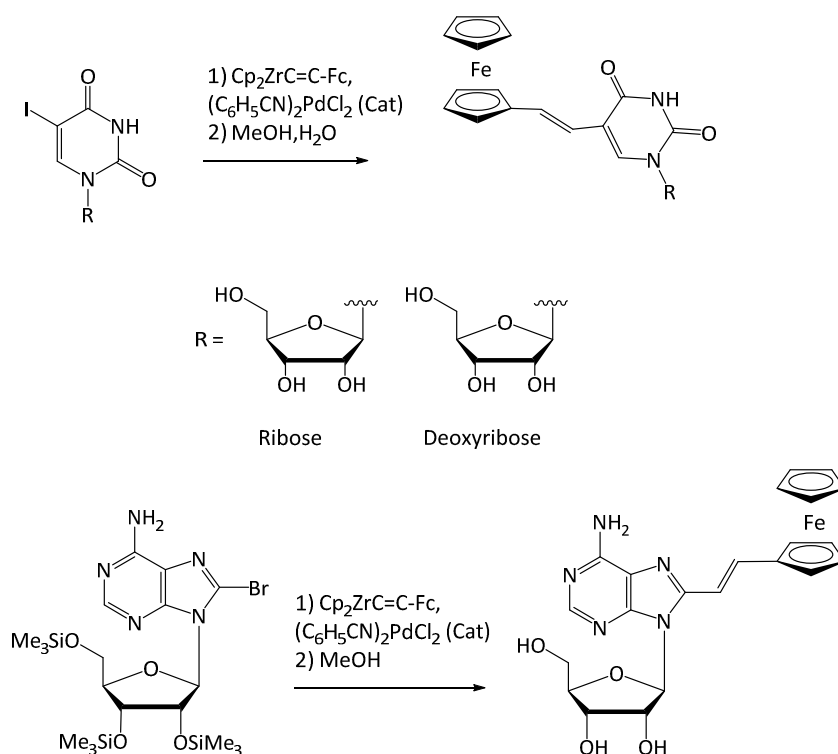
Scheme 1-3: *Ferrocenonucleosides developed by Gautheron*

It was also possible to couple ethynylferrocene to 5-iodouracil, iodouridine, 2-desoxyiodouridine and bromoadenosine via a Sonogashira coupling in presence of $(Ph_3P)PdCl_2$ to give the corresponding 5-ethynylferrocenyl nucleobases. Interestingly, It was

described that 5-ethynylferrocenyluracil derivatives could be cyclised in presence of triethylamine with heat. (Scheme 1-4)
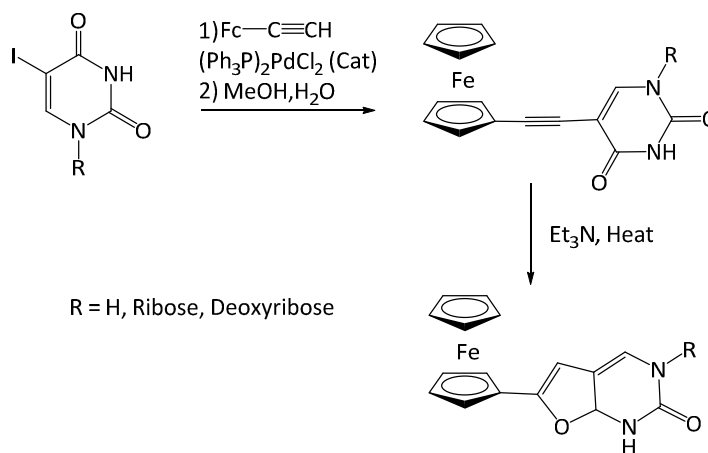
Scheme 1-4: *Ferrocenonucleosides via Sonogashira coupling*

This side reaction is due to a stabilisation of a positive charge on the first carbon of the ethynyl linker by the ferrocenyl group,[54] inducing an oxygen-attack of the uracil on the stabilised carbon. Houlton *et al.*[55] reported that cyclisation could be avoided by running the Sonogashira coupling at room temperature.

Another approach developed by Houlton *et al.*[56] consisted of coupling different nucleobase derivatives with the trimethyl(ferrocenylmethyl)ammonium iodide salt. An example is presented in Scheme 1-5.
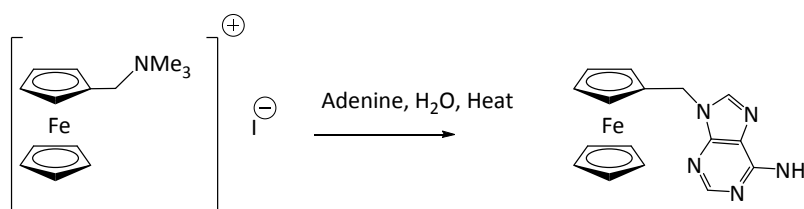
Scheme 1-5: *Ferrocenonucleobase by Houlton*

Ganesh *et al.*[57] used a completely different way to couple ferrocene to nucleobases. Thymine and uracil were attached to mono and bis-ferrocene via 1 and 4 carbon linkers using the Mitsunobu reaction. The one-carbon systems were synthesised from the bis-carboxaldehyde ferrocene, which was reduced to the corresponding bis-hydroxylmethyl ferrocene. The two nucleobases were attached to the bis-hydroxymethyl ferrocene via a Mitsunobu reaction in presence of DIAD, triphenylphosphine in THF, followed by a deprotection of the nucleobases using potassium carbonate. (Scheme 1-6)
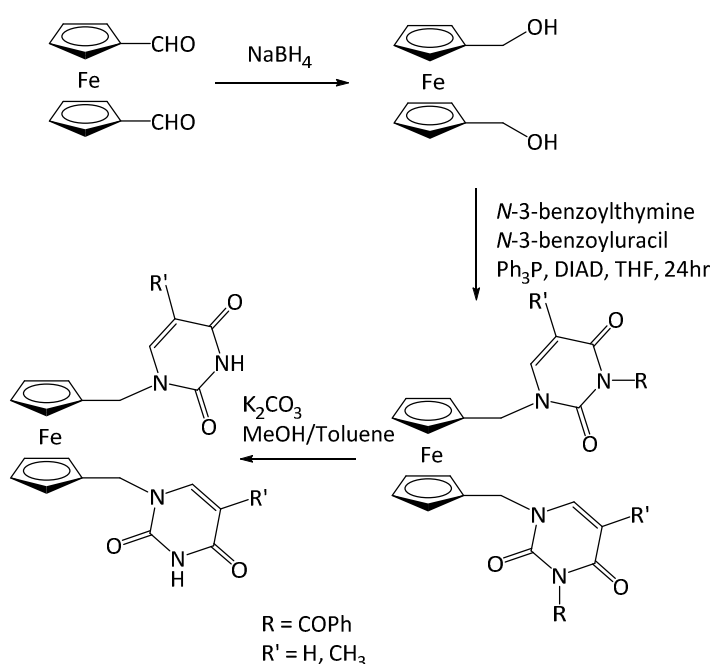
Scheme 1-6: *Synthesis scheme of bis-methyl ferrocenyl thymine and uracil by Ganesh*

The synthesis of the ferrocenyl derivatives containing a butyl spacer was achieved by first reacting ferrocene was first reacted with succinic anhydride using Friedel-Crafts acylation. The carbonyl group and the ester moiety were then reduced to give the corresponding alcohol, which was then reacted with uracil or thymine under Mitsunobu conditions. The bases were then debenzoylated in presence of potassium carbonate to afford the target compounds. (Scheme 1-7)
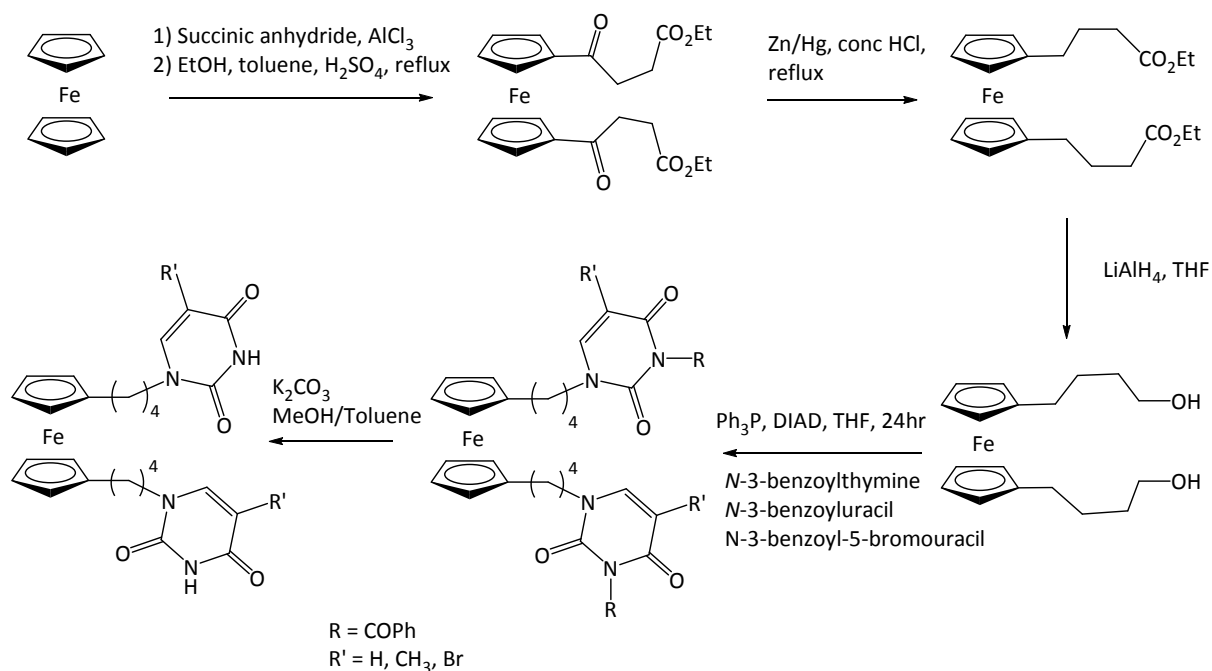
Scheme 1-7: *Ferrocenonucleoside with a butyl linker chain by Ganesh*

The tagging of ferrocene to nucleic acids has become a topical theme, mainly due to continued interest in the electrochemical sensing of various biomolecules and biological units.[58] In 2001, Yu and coworkers[59] described an early example where they synthesized two electrochemically different ferrocenyl monomers by introducing ferrocene derivatives on to the sugar of a nucleoside (Figure 1-22). The monomers were then incorporated into oligonucleotide probes using automated DNA synthesis.
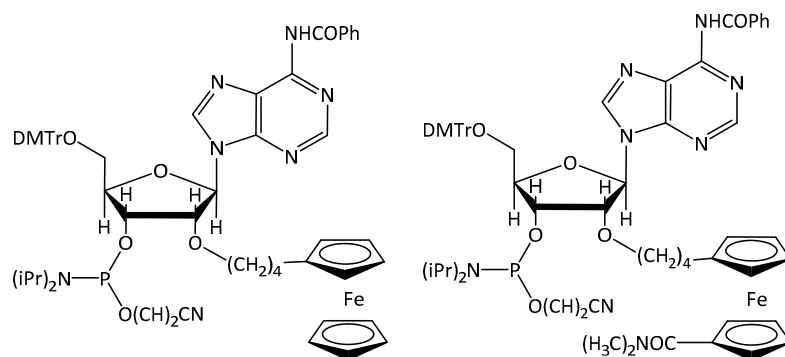
Figure 1-22: *Two electrochemically different ferrocenyl complexes developed by Yu and coworkers[59]*

The two investigated targets differed by a single-base mismatch at the same position. Each probe synthesized was sequence-specific for only one of these targets. Because the two ferrocenyl-complexes appeared as two different electrochemical peaks in alternative current voltammetry, it was possible to discriminate the two different targets and consequently the two different mismatches. The detection of these mismatches was performed on a chip-array coupled to an electrochemical detector. As a result, a direct application of this study is the detection of SNPs.

Another interesting example of a ferrocene tag was described by Ricci and coworkers[60] in 2007. Ferrocene was coupled to the end of an oligonucleotide to sense nucleotide hybridization. The technique was based on the disappearance of the electrochemical signal upon hybridization. (Figure 1-23)
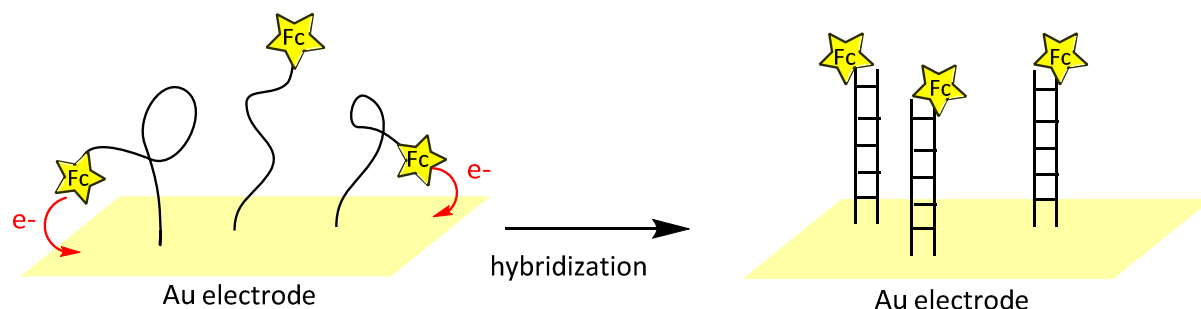
Figure 1-23: *Detection of targeted oligonucleotides hybridisation by Ricci and al.[60]*

The probe was bound to a gold electrode as shown in Figure 1-23. When the sequence is target-free, the sensor gives a well-defined voltammetry peak. When the target complexes the probe, the current is largely reduced. This can be explained by a gain in rigidity of the double strands compared to the single strand, which leads to an increase in the distance between ferrocene and the electrode.

Another example of tagging is the gene sensing method for diagnosis developed in 2002 by Nakayama and Ihara[61]. This method is based on the formation of a ternary complex that gives an electrochemical response when the targeted sequence is present. The ternary complex is formed when the target hybridises to the single strand oligonucleotide, which is attached on the surface of a gold electrode, and to the sensing probe containing a ferrocene moiety. (Figure 1-24)
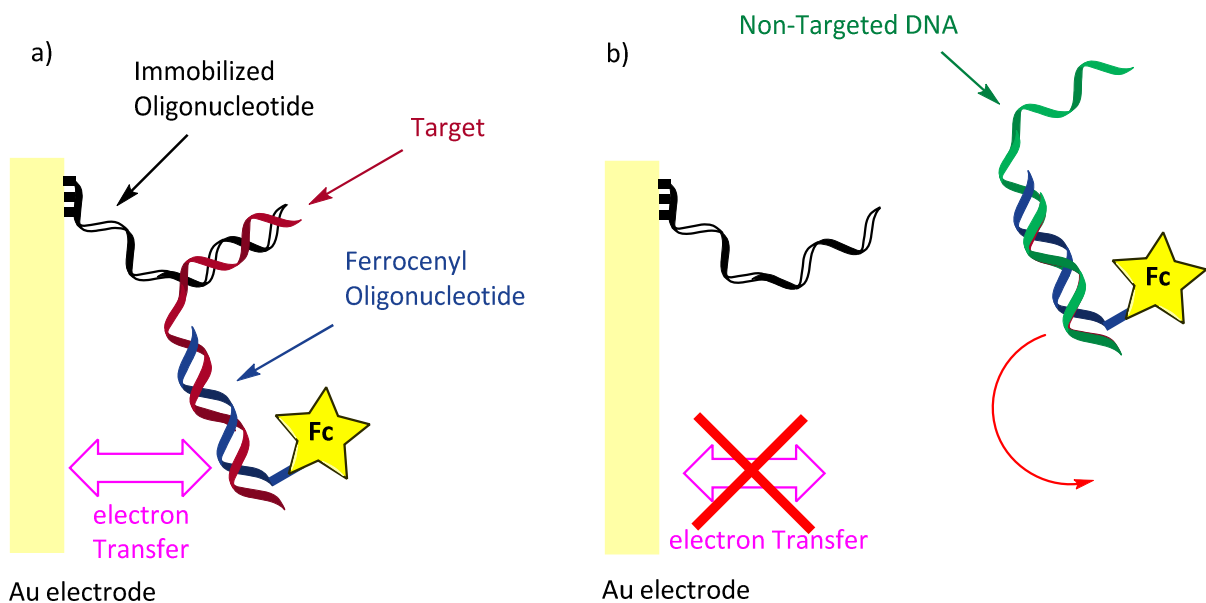
Figure 1-24: *Electrochemical gene sensing method by Ihara[61]*

If the target fully matches with the probe and the oligonucleotide attached to the electrode, the ternary complex is formed and the ferrocene stays close to the electrode. This creates a electrochemical signal and a high peak appears on a differential pulse voltammogram due to the oxidation of the metallocene (plain line in Figure 1-25). However if the target is a mutant (single-base mismatch), the ternary complex cannot efficiently be formed any more resulting in a drop of the electrochemical signal (dashed line), as shown in Figure 1-25.
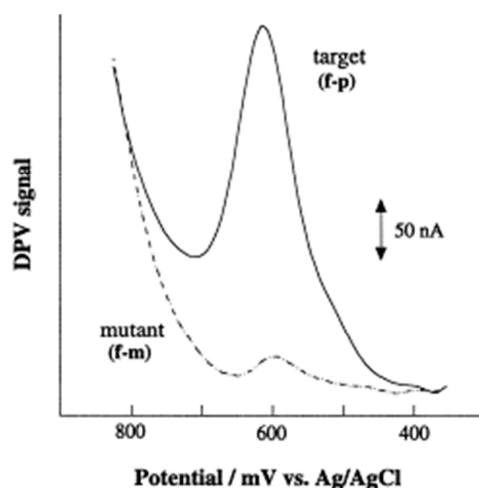
Figure 1-25: DVP of the electrode by two different treatments[61]

However this method has its limitations. Although longer sequences would result in a stronger signal, they would be less specific and would be more tolerant to mismatches. The distance between the ferrocene and the electrode could also affect the detection.

Ferrocenyl monomers have also been attached to PNA by Metzler-Nolte and coworkers,[62, 63] who described in 1999 the first organometallic PNA monomer system, with ferrocene incorporated at the end of an oligomer.

1.5   Incorporation of ferrocene into the backbone of DNA

Another interesting way to use ferrocene in a nucleic acid is to incorporate it directly into an oligonucleotide backbone. Brisset and his team[64] described such an example in 2004 by inserting a ferrocenyl-phosphoramidite into a DNA chain (Figure 1-26).
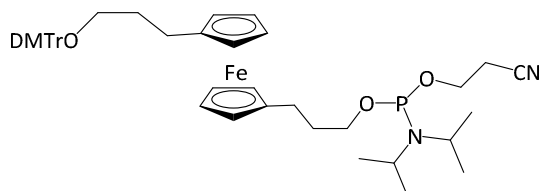
Figure 1-26: *Ferrocenyl phosphoramidite developed by Brisset*

The monomer was synthesised via a Wittig-Horner reaction involving 1-1'-bis-formylferrocene and a triethyl phosphonoacetate followed by hydrogenation of the corresponding double bonds and a reduction of the ester functions using LiAlH$_4$. The 1-1'-bis-propanolferrocene was tritylated and the final phosphoramidite was then obtained via phosphitylation. (Scheme 1-8)
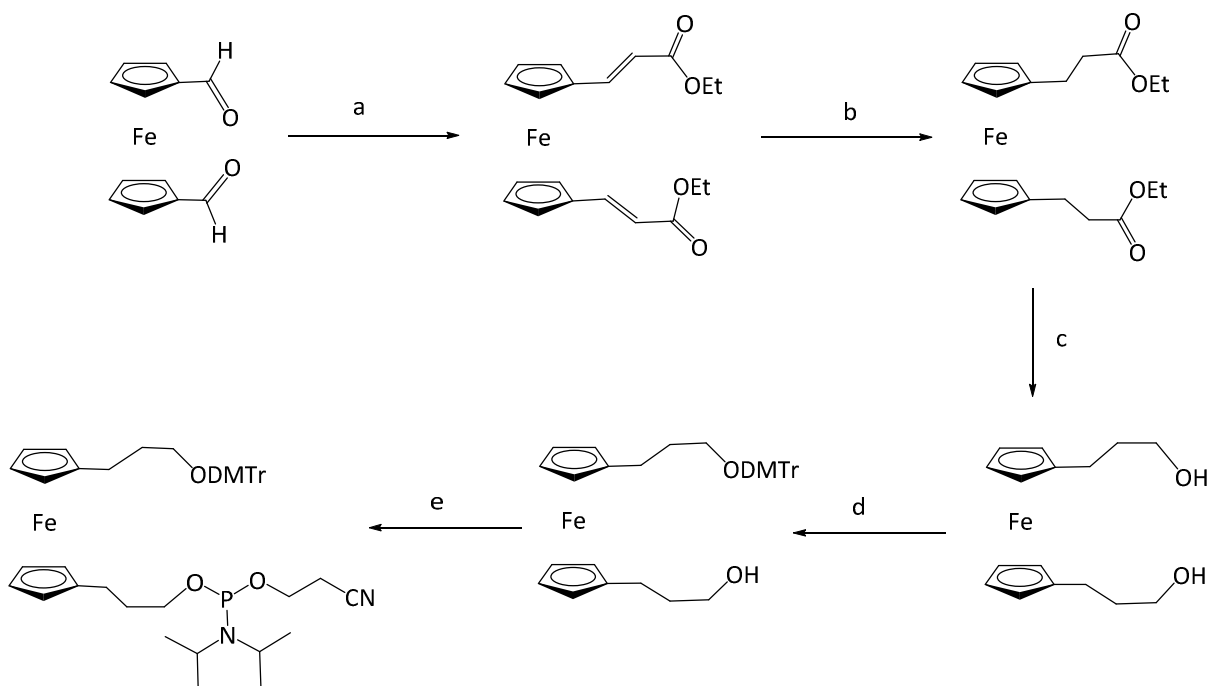
(a) Triethyl phosphonoacetate, Na, EtOH, 1hr
(b) Pd/C, ethylacetate, H$_2$, 24 h.
(c) AlLiH$_4$, diethyl ether, 1h.
(d) Dimethoxytritylchloride, THF, 4hr.
(e) 2-cyanoethyldiisopropylchlorophosphoramidite, THF, 4.5hr.

Scheme 1-8: *Ferrocenyl derivative synthesis by Brisset*

 The ferrocenyl monomer was then incorporated into specific oligonucleotides sequences using an automated synthesizer at various positions along the sequence. The study revealed that all the oligonucleotides were detectable by electrochemistry and the detection could be optimized by the introduction of several ferrocenyl derivatives into the sequence.

Other related work was reported by Ihara and co-workers[65] in 2009, who also described the direct incorporation of ferrocenyl monomers into the DNA-backbone. The influence of the DNA-structure on the redox potential of different ferrocene conjugates was investigated. Inspired by Brisset's work, they synthesised similar bis-substituted ferrocenyl derivatives **A**, **C**, and **D** as shown in Scheme 1-9. The synthesis of monomer **A** was done following Brisset's procedure, although they used $NaBH_4$ in presence of CuCl instead Pd/C catalysis in presence of H_2 for the hydrogenation step. Extension of hydroxyl linker chain of **C** and **E** was performed via Williamson ether synthesis involving the protected bromide **B** and the 15-crown-5-ether. DMTr protection and phosphitylation were achieved as previously described in Brisset's work.
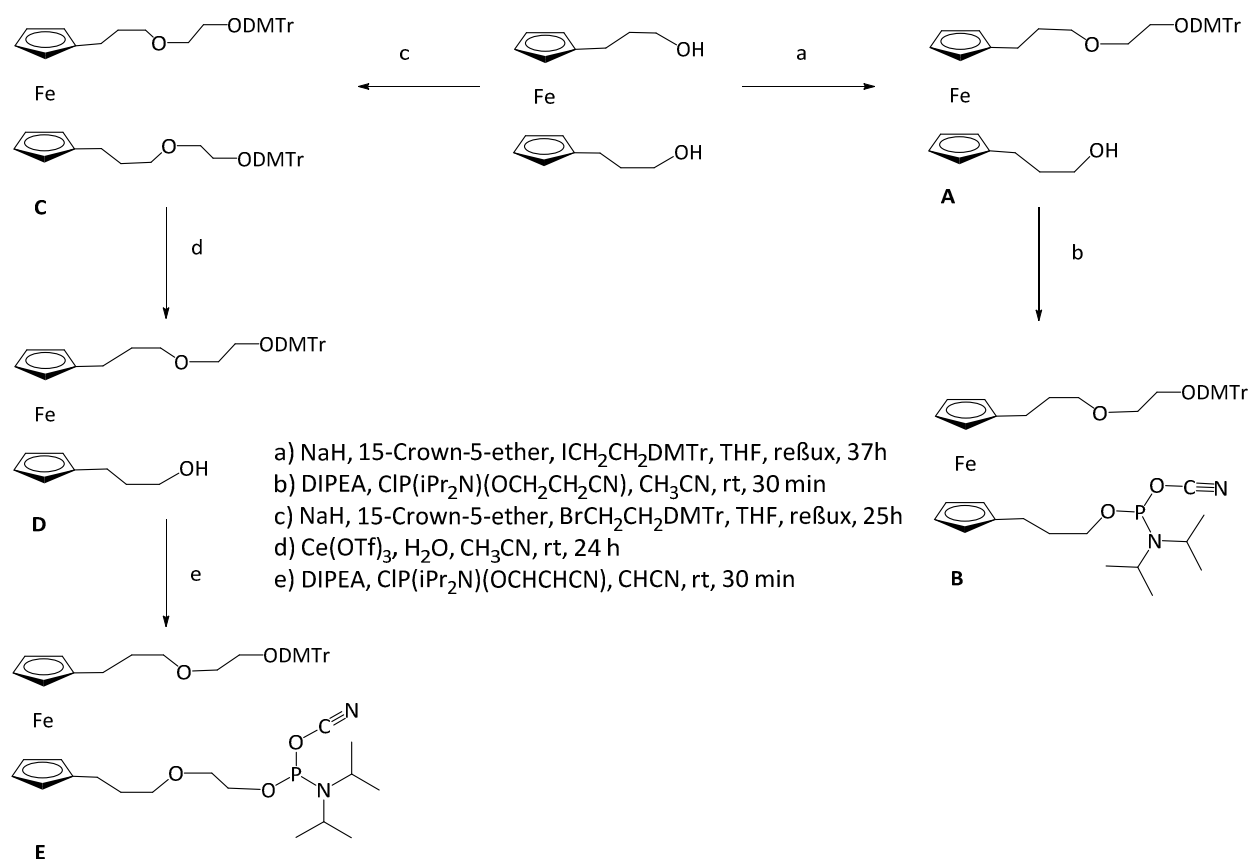
Scheme 1-9: *Fc-based Amidites with different linker chains*

Thermal analysis of duplex and hairpin DNA structures via UV melting experiments revealed a destabilisation of the duplex structure, which was probably due to the flexibility of the Fc unit inserted, since the continuity of the sequence was broken. This tendency increased with the length of the linker chain. Contrary to the duplex, insertion of ferrocene into the loop of the hairpins seemed to have a stabilization effect on the structure. Electrochemical studies revealed that the potential of ferrocene in the two different structures shifted in opposite directions: to negative potentials for the duplex and to positive potentials for the hairpin structure. This could be due to the differences in hydrophilicity between the two structures.

In the light of these inspiring works on nucleic acid analogues and ferrocenyl conjugates, our group decided to investigate a way to develop a novel type of nucleic acid combining Brisset's and Ganesh's independent works. It consisted of linking ferrocene with nucleobases to obtain a ferrocenyl monomer, which could be incorporated into an oligonucleotide sequence or oligomerised. The rationale for this novel *Ferrocene Nucleic Acid* is detailed in the following section.

1.6 Aims

Inspired by the previously described work on metal-containing nucleic acids, the thesis describes the design and synthesis of novel ferrocenyl monomers that make up the component of a bioorganometallic nucleic acid analogue, called *Ferrocene Nucleic Acid* (FcNA). The idea is based on the incorporation of a ferrocenyl monomer into the backbone of a nucleic acid, replacing an entire dinucleotide sugar-phosphate-sugar (SPS) unit by the Cp-M-Cp motif of the monomer (Figure 1-27). One justification for this approach comes from the similar distance between the two cyclopentadienyl rings (3.3 Å)[66] of the ferrocene and the distance between two stacked nucleobases in natural B-DNA (3.4 Å).[67] In this context, the two rings would replace two sugars and the iron atom would replace one linking phosphodiester unit. Another interesting property of ferrocene is that the Cp rings have the ability to rotate independently around the iron axis, giving to the monomer more conformational freedom. It is assumed that this would limit the disruption to the hydrogen bonding and stacking interactions during duplex formation. Additional preliminary computational studies processed by Tiffany Walsh in Warwick and Mark Rodger in

Birmingham, indicated that one ferrocenyl monomer would fit if designed with a two carbons linker between each nucleobase and the ferrocene unit.
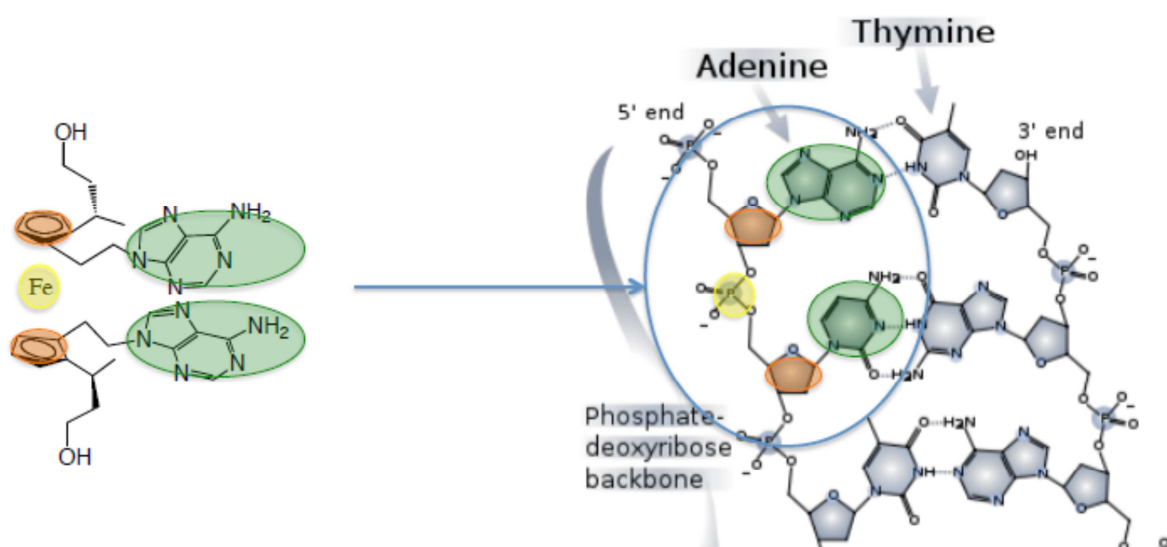
Figure 1-27: *Scheme of incorporation of tetra-substituted ferrocene into DNA*

In order to obtain the target oligomer, tetra-substituted ferrocene monomers would first have to be made. The synthetic design was framed by the fact that both Cp rings would form a part of the backbone. As shown in Figure 1-27, each ring would then be di-substituted, with one linker to the phosphodiester part of DNA and one linker to the nucleobase. The "DNA-linker" was designed to contain three carbons following previous literature results.[68] Acting as a cornerstone of the monomer synthesis, chirality also would have to be carefully controlled.

The thesis is organised in the following way: In Chapter 2, an investigation into the coupling of one or two adenine, uracil and cytosine units to ferrocene is described. The electrochemical properties of these derivatives have also been studied via cyclic voltammetry. In Chapter 3, the synthesis of a tetra-substituted ferrocenes coupled to

adenine, uracil and cytosine will be described, that are monomeric precursors to FcNA oligomers. The final results chapter, Chapter 4, describes the development of bioorganometallic nucleoside drug mimetics via the synthesis of various ferrocene monomers.

1.7 References

1.   Watson and Crick, *Nature*, **1953**, *171*, 737-738.
2.   D. G. Gibson, J. I. Glass, C. Lartigue, V. N. Noskov, R.-Y. Chuang, M. A. Algire, G. A. Benders, M. G. Montague, L. Ma, M. M. Moodie, C. Merryman, S. Vashee, R. Krishnakumar, N. A. Garcia, C. Andrews-Pfannkoch, E. A. Denisova, L. Young, Z.-Q. Qi, T. H. Segall-Shapiro, C. H. Calvey, P. P. Parmar, C. A. Hutchison III, H. O. Smith, J. C. Venter, *Science*, **2010**, *329*, 52-56.
3.   R. E. Dickerson, H. R. Drew, B. N. Conner, R. M. Wing, A. V. Fratini, M. L. Kopka, *Science*, **1982**, *216*, 475-485.
4.   R. P. Goodman, I. A. T. Schaap, C. F. Tardin, C. M. Erben, R. M. Berry, C. F. Schmidt, A. J. Turberfield, *Science,* **2005***, 310*, 1661-1665; B. Yurke, A. J. Turberfield, A. P. Mills Jr, F. C. Simmel, and J. L. Neumann, *Nature*, **2000**, *406*, 605-608.
5.   J. Murrel, M. Farlow, B. Ghetti, M. D. Benson, *Science,* **1991**, *254*, 97-99.
6.   B. J. Culliton, *Science*, **1990**, *249*, 1372.
7.   M. D. Matteucci and M. H. Caruthers, *J. Am. Chem. Soc.*, **1981**, *103*, 3185-3191.
8.   S. L. Beaucage and R. P. Iyer, *Tetrahedron*, **1993**, *49*, 1925-1963.
9.   P. M. Holland, R. D. Abramson, R. Watson, D. H. Gelfand, *Proc. Natl. Acad. Sci. U. S. A.*, **1991**, *88*, 7276-7280.
10.   K. J. Livak, S. A. J. Flood, J. Marmaro, W. Giusti, K. Deetz, *PCR Methods Appl.*, **1995**, 357.
11.   L. G. Lee, C. R. Connell, W. Bloch, *Nucleic Acids Res.*, **1993**, *21*, 3761-3766.
12.   I. Ortmans, S. Content, N. Boutonnet, A. K.-D. Mesmaeker, W. Bannwarth, J.-F. Constant, *Chem. Eur. J.,* **1999**, *5*, 2712-2721.
13.   Y. Shafirovich, S. H. Courtney, N. Ya, and N. E. Geacintov, *J. Am. Chem. Soc.,* **1995**, *117*, 4920-4929.
14.   G. T. Hwang, Y. J. Seo, S. J. Kim, B. H. Kim, *Tetrahedron Letters,* **2004**, *45*, 3543-3546.
15.   R. X.-F. Ren, N. C. Chaudhuri, P. L. Paris, S. Rumney, E. T. Kool, *J. Am. Chem. Soc.,* **1996**, *118*, 7671-7678.
16.   J. D. Frazer, S. M. Horner, and S. A. Woski, *Tetrahedron Letters,* **1998**, *39*, 1279-1282.
17.   K. Yamana, H. Zako, K. Asazuma, R. Iwase, H. Nakano, and A. Murakami, *Angew. Chem. Int. Ed.,* **2001**, *40*, 1104-1106.
18.   L. C. Sowers, G. V. Fazakerley, R. Eritja, B. E. Kaplan, and M. F. Goodman*, Proc. Natl.*

Acad. Sci., **1986,** *83*, 5434-5438.

19.   D. C. Ward, E. Reich, L. Stryer, *J. Biol. Chem.*, **1969**, *244*, 1228-1237.

20.   B. W. Allan and N. O. Reich, *Biochemistry*, **1996**, *35*, 14757-14762. Interaction with the EcoRI DNA methyltransferase.

21.   J. T. Stivers, K. W. Pankiewicz, K. A. Watanabe, *Biochemistry*, **1999**, *38*, 952-963. Interaction with uracil DNA glycosylate.

22.   R. K. Neely, D. Daujotyte, S. Grazulis, S. W. Magennis, D. T. F. Dryden, S. Klimasauskas, A.C. Jones, *Nucleic Acids Research*, **2005**, *33*, 6953-6960.

23.   S. Katz, *Biochim. Biophys. Acta*, **1963**, *68*, 240-253.

24.   Y. Miyake, H. Togashi, M. Tashiro, H. Yamaguchi, S. Oda, M. Kudo, Y. Tanaka, Y. Kondo, R. Sawa, T. Fujimoto, T. Machinami, A. Ono, *J. Am. Chem. Soc.*, **2006**, *128*, 2172-2173.

25.   E. Meggers, P. L. Holland, W. B. Tolman, F. E. Romesberg, P. G. Schultz, *J. Am. Chem. Soc.*, **2000**, *122*, 10714-10715.

26.   P. Espinet, J. A. Miguel, S. Garcia-Granda, D. Miguel, *Inorg. Chem.,* **1996**, *35*, 2287-2291.

27.   S. Atwell, E. Meggers, G. Spraggon, P. G. Schultz, *J. Am. Chem Soc.*, **2001**, *123*, 12364-12367.

28.   K. Tanaka, Y. Yamada, M. Shionoya, *J. Am. Chem. Soc.*, **2002**, *124*, 8802-8803; K. Tanaka, A. Tengeiji, T. Kato, N. Toyama, M. Shiro, M. Shionoya, *J. Am. Chem. Soc.*, **2002**, *124*, 12494-12498.

29.   K. Tanaka, A. Tengeiji, T. Kato, N. Toyama, M. Shionoya, *Science*, **2003**, *299*, 1212-1213.

30.   L. Zhang and E. Meggers, *J. Am. Chem. Soc.*, **2005**, *127*, 74-75.

31.   K.-U. Schoning, P. Scholz, S. Guntha, X. Wu, R. Krishnamurthy, A. Eschenmoser, *Science,* **1999**, *284*, 2118-2124.

32.   L. E. Orgel, *Trends. Biochem. Sci.*, **1998**, *23*, 491-495.

33.   J. Hunziker, H.-J. Roth, M. Bohringer, A. Giger, U. Diederichsen, M. Gobel, R. Krishnan, B. Jaun, C. Leumann, A. Eschenmoser, *Helv. Chim. Acta*, **1993**, *76*, 259-352 (abstract).

34.   M. Beier, F. Reck, T. Wagner, R. Krishnamurthy, A. Eschenmoser, *Science*, **1999**, *283*, 699-703.

35.   K.-U. Schoning, P. Scholz, S. Guntha, X. Wu, R. Krishnamurthy, A. Eschenmoser, *Science*, **2000**, *290*, 1347-1351.

36.   J. K. Ichida, K. Zou, A. Horhota, B. Yu, L. W. McLaughlin, J. W. Szostak, *J. Am. Chem. Soc.*, **2005**, *127*, 2802-2803.

37.   L. Zhang, A. Peritz, E. Meggers, *J. Am. Chem. Soc.*, **2005**, *127*, 4174-4175.

38.   H. Asanuma, T. Toda, K. Murayama, X. Liang, H. Kashida, *J. Am. Chem. Soc.*, **2010**, *132*, 14702-14703.

39.   K. C. Schneider and S. A. Benner, *J. Am. Chem. Soc.*, **1990**, *112,* 453-455.

40.   M. Tarkoy and C. Leumann, *Angew. Chem. Int. Ed. Engl.*, **1993**, *32*, 1432-1434.

41.   E. T. Kool, *Chem. Rev.*, **1997**, *97*, 1473-1488.

42.   H. Kashida, K. Murayama, T. Toda, H. Asanuma, *Angew. Chem. Int. Ed.*, **2011**, *50*, 1285-1288.

43.   S. Obika, D. Nanbu, A. Hari, K.-I. Morio, Y. In, T. Ishida, T. Imanishi, *Tetrahedron Letters*,

1997, *38*, 8735-8738.

44.   A. A. Koshkin, S. K. Singh, P. Nielsen, V. K. Rajwanshi, R. Kumar, M. Meldgaard, C. E. Olsen, J. Wengel, *Tetrahedron,* **1998***, 54,* 3607-3630.

45.   P. E. Nielsen, M. Egholm, R. H. Berg, and O. Buchardt, *Science*, **1991**, *254*, 1497-1500; K. L. Dueholm, M. Egholm, C. Behrens, L. Christensen, H. F. Hansen, T. Vulpius, K. H. Petersen, R. H. Berg, P. E. Nielsen, O. Buchardt, *J. Org. Chem.*, **1994**, *59*, 5767-5773.

46.   V. B. Pinheiro and P. Holliger, *Current Opinion in Chemical Biology,* **2012**, *16*, 245–252.

47.   T. J. Kealy and P. L. Pauson, *Nature*, **1951**, *168*, 1039-1040.

48.   S. A. Miller, J. A. Tebboth, J. F. Tremaine, *J. Chem. Soc.*, **1952**, 632-635.

49.   G. Wilkinson, M. Rosenblum, M. C. Whiting, R. B. Woodward, *J. Am. Chem. Soc.*, **1952**, *74*, 2125-2126.

50.   K. M. Joly, C. Wilson, A. J. Blake, J. H. R. Tucker, C. J. Moody, *Chem. Commun*., **2008**, *41*, 5191-5193.

51.   J.-D. Qiu, R. Wang, R.-P. Liang, X-H. Xia, *Biosensors and Bioelectronics,* **2009**, *24*, 2920-2925.

52.   X. Luo, T. M. -H. Lee, I.-M. Hsing, *Anal. Chem.,* **2008**, *80,* 7341-7346.

53.   P. Meunier, I. Ouattara, B. Gautheron, J. Tirouflet, D. Camboli, J. Besancon, F. Boulay, *Eur. J. Med. Chem.*, **1991**, *26*, 351-362.

54.   A. Appel, F. Jakle, T. Priermeier, R. Schmid, M. Wagner*, Organometallics*, **1996**, *15*, 1188-1194.

55.   A. R. Pike, L. C. Ryder, B. R. Horrocks, W. Clegg, M. R. J. Elsegood, B. A. Connolly, A. Houlton, *Chem. Eur. J.*, **2002**, *8*, 2891-2899.

56.   C. Price, M. Aslanoglu, C. J. Isaac, M. R. J. Elsegood, W. Clegg, B. R. Horrocks, A. Houlton, *J. Chem. Soc. Dalton Trans.*, **1996**, 4115; A. Houlton, C. J. Isaac, A. E. Gibson, B. R. Horrocks, W. Clegg, M. R. J. Elsegood, *J. Chem. Soc. Dalton Trans.,* **1999**, 3229-3234.

57.   A. N. Patwa, S. Gupta, R. G. Gonnade, V. A. Kumar, M. M. Bhadbhade, and K. N. Ganesh, *J. Org. Chem.*, **2008**, *73*, 1508-1515.

58.   H.-B. Kraatz, *Journal of Inorganic and Organometallic Polymers and Materials*, **2005**, *15*, 83-106.

59.   C. J. Yu, Y. Wan, H. Yowanto, J. Li, C. Tao, M. D. James, C. L. Tan, G. F. Blackburn, T. J. Meade*, J. Am. Chem. Soc.*, **2001,** *123,* 11155-11161.

60.   F. Ricci, R. Y. Laiab, K. W. Plaxco, *Chem. Commun.,* **2007**, 3768-3770.

61.   M. Nakayama, T. Ihara, K. Nakano, M. Maeda, *Talanta*, **2002**, *56*, 857-866.

62.   A. Hess and N. Metzler-Nolte, *Chem. Commun*., **1999**, 885-886.

63.   J. C. Verheijen, G. A. van der Marel, J. H. van Boom, N. Metzler-Nolte, *Bioconjugate Chem.*, **2000**, *11*, 741-743.

64.   A.-E. Navarro, N. Spinelli, C. Moustrou, C. Chaix, B. Mandrand, H. Brisset, *Nucleic Acids research*, **2004**, *32*, 5310-5319.

65.   T. Ihara, D. Sasahara, M. Shimizu, A. Jyo, *Supramolecular Chemistry*, **2009**, *21*, 207-217.

66.   A. J. Deeming in *Comprehensive Organometallic Chemistry*, Vol. 4 (Eds. : G. Wilkinson, F. G. A. Stone), Pergamon, Oxford, **1982**, 475-512.

67. W. Saenger, *Principles of Nucleic Acid Structure*, Springer, New York, **1984**.

68. G. Chatelain, H. Brisset, C. Chaix, *New J. Chem.*, **2009**, *33*, 1139-1147.

CHAPTER 2: MONO AND BIS-SUBSTITUTED FERROCENES

2.1 Introduction

To investigate the best way to attach nucleobases to ferrocene, it was decided to investigate various model compounds consisting of mono and bis-substituted ferrocenes obtained through various coupling routes. According to the literature, there are a number of examples of ferrocene being linked to nucleobases. As briefly described in the previous chapter, Ganesh and coworkers[1] synthesised ferrocene-linked nucleobases conjugates from mono and bis-(hydroxybutyl)-ferrocene via a Mitsunobu reaction. (Figure 2-1)
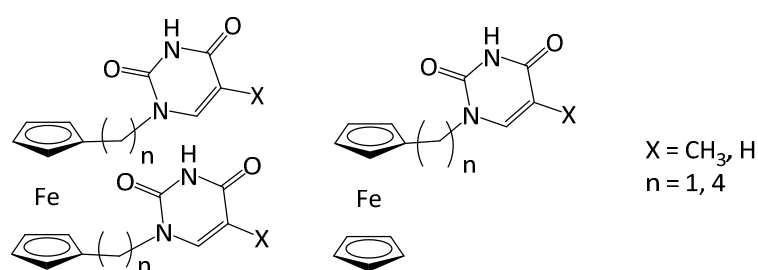
Figure 2-1: *Bis-uracil and bis-thymine ferrocene with 1 and 4 carbons space linkers by Ganesh[1,2]*

Crystallographic structure analysis of bis-thymine and bis-uracil ferrocene conjugates revealed self-assembled motifs consisting of Watson-Crick base pairing. In 2010,[2] Ganesh and coworkers compared these results with new supramolecular assemblies they obtained using a methylene linker instead of a butylene. They concluded that nature of the spacer induced a specific orientation of Cp rings with both contributing to the formation of these specific assemblies. (Figure 2-2)
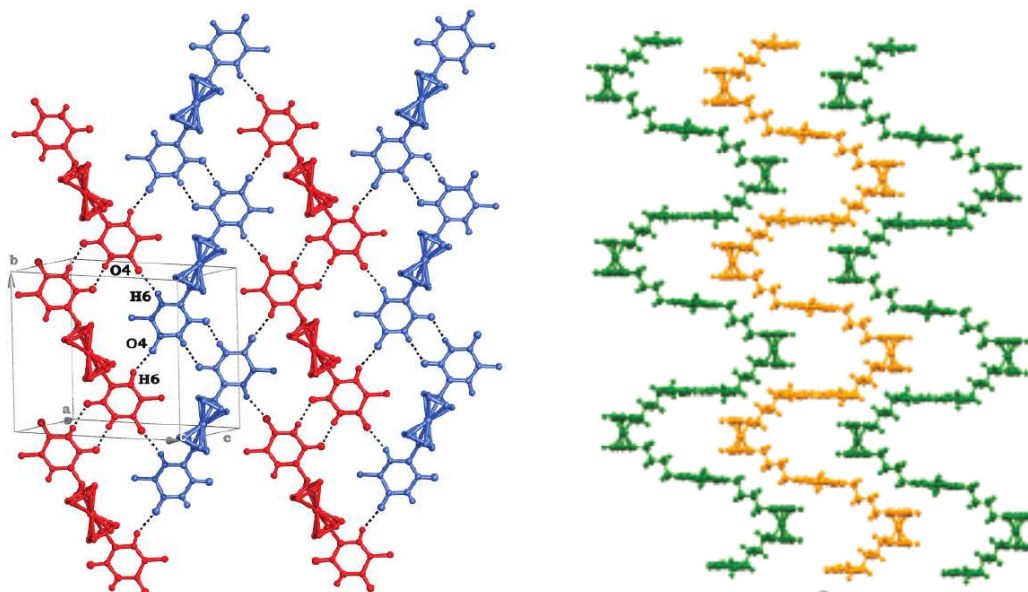
Figure 2-2: *Different crystalline structures of bis thymine ferrocenyl compounds depending on the nature of the spacer (Methyl spacer in red and blue and Butyl space linker in green and yellow)[2]*

In earlier work, Houlton[3] developed another method to couple ferrocene to nucleobases. Mono-substituted ferrocenes linked to thymine, uracil, cytosine and purine derivatives were synthesised by refluxing an aqueous solution of trimethylammonio-methylferrocene iodide with a nucleobase. Adenine-containing ferrocene derivatives are less common than their thymine and uracil analogues. However, Houlton coupled a mono functionalised ferrocene to adenine through a methylene linker using the same method.[4] In addition, Kumar reported that an assembly of four adenine ferrocenylpropanones formed an elegant quartet structure (Figure 2-3). [5, 6]
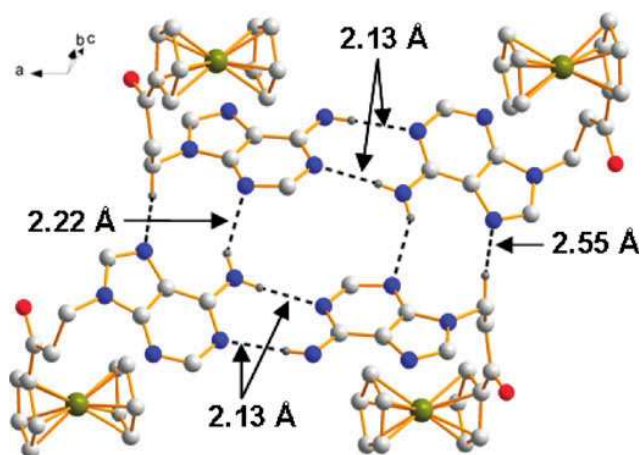
Figure 2-3: *Adenine-ferrocene derivatives forming a quartet via hydrogen bonding[5,6]*

Enlightened by these studies, different coupling methods were investigated to generate the targets in Figure 2-4 including the Horner-Wittig reaction, the Mitsunobu reaction and a bromide substitution. Adenine, uracil and cytosine also had to be suitably protected to enable their use as appropriate reagents in these coupling.
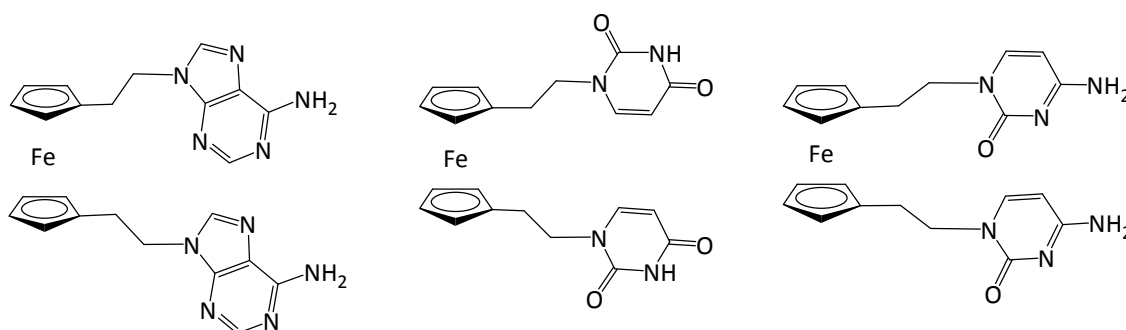
Figure 2-4: *Targets: ferrocene-containing adenine, uracil and cytosine*

2.2   Coupling: Horner-Wittig approach

2.2.1   Literature background

Amongst others, the Horner-Wittig reaction, which is a variant of the Wittig reaction, has been used to couple nucleobases to different types of compounds. For example, Dahl and

coworkers[7] prepared a series of alkenyl adenine and thymine derivatives via this reaction. To begin with, they synthesised phosphonates and phosphine oxide derivatives of the nucleobases. Alkylated bases were then protected with a benzoyl group or a dibutylformamidine group to avoid side reactions during the following step. The bases were then coupled with various carbonyls such as benzaldehyde, leading to the desired alkenes. Replacing benzaldehyde with ferrocene was a new approach that the Tucker group decided to investigate in order to synthesise the target compounds.

First reported in 1953 by Wittig and Geissler,[8] the Wittig reaction and its derivatives are characterised by treatment of a ketone with a phosphonium ylid to give an alkene. Ylids are neutral compounds containing opposite charges on two adjacent atoms. The positive charge is located on the phosphorus and the negative on the carbon (Scheme 2-1). Ylids are usually produced via deprotonation of phosphonium salts with a strong base such as butyllithium, *tert*-butoxide or sodium hydride.
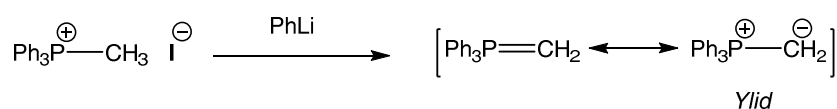
Scheme 2-1: Formation of an ylid by deprotonation of a phosphonium salt

The mechanism of the Wittig reaction is based on the intramolecular formation of an intermediate called oxaphosphetane (Scheme 2-2). First, the nucleophilic carbanion of the ylid attacks the carbonyl. The lone pair on the oxygen attacks the phosphonium forming a four-membered ring. The unstable oxaphosphetane undergoes elimination to give an alkene

and a phosphine oxide as a side-product. The phosphorus-oxygen double bond is very strong and drives the reaction forward.
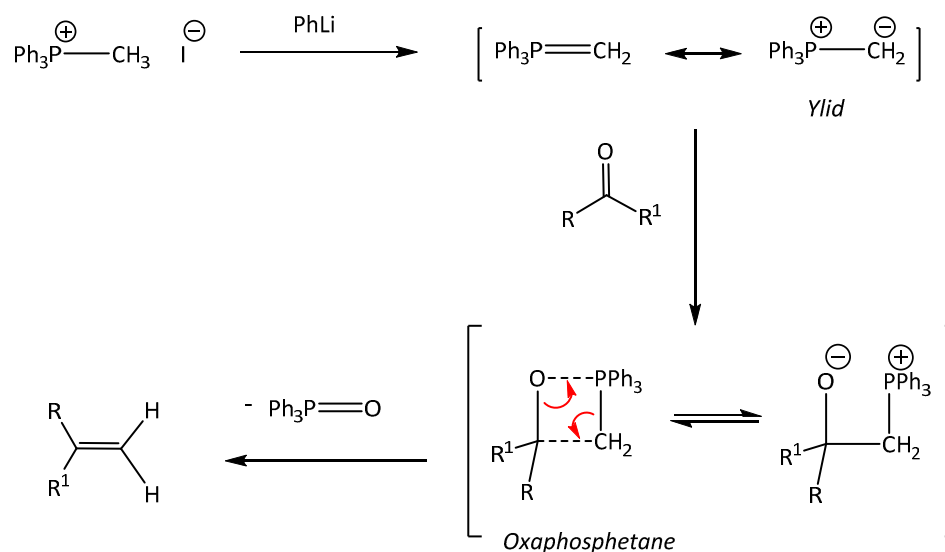
Scheme 2-2: *Wittig reaction mechanism*

The Wittig reaction is regioselective and stereoselective. Indeed, when a substituted ylid reacts with an aldehyde, both *Z* and *E* alkene isomers are formed. The stereoselectivity essentially depends on the type of the ylid involved in the reaction and consequently on the nature of its substituents. Ylids can be divided into two categories: ylids with anion-stabilizing substituents and ylids without. In the first category, the negative charge on the carbon is stabilized not only by the phosphorus but also by adjacent conjugating substituents. They are called stabilized ylids and give mainly *E*-isomers. The others are called unstabilized ylids and give mainly *Z*-isomers.

It is important to consider the relationship between the nature of the ylid and the stereoselectivity of Wittig reaction. Addition of the ylid to the carbonyl produces two diastereoisomers of the oxaphosphetane: **A** and **B** (Scheme 2-3). In the case of stabilised

ylids, the stereoselectivity of the reaction is thermodynamically controlled. The formation of

A and **B** is reversible because of the high stability of the ylid. Consequently, the

oxaphosphetane diastereoisomers can interconvert and the equilibrium of the reaction

turns towards formation of the more stable intermediate **A**. It is reasonable to assume that

the *trans* is the more stable isomer for steric reasons. The two largest groups are on

opposite sides of the ring, reducing steric hindrance. Stereospecific elimination of the

intermediate gives mainly the *E*-alkene isomer.
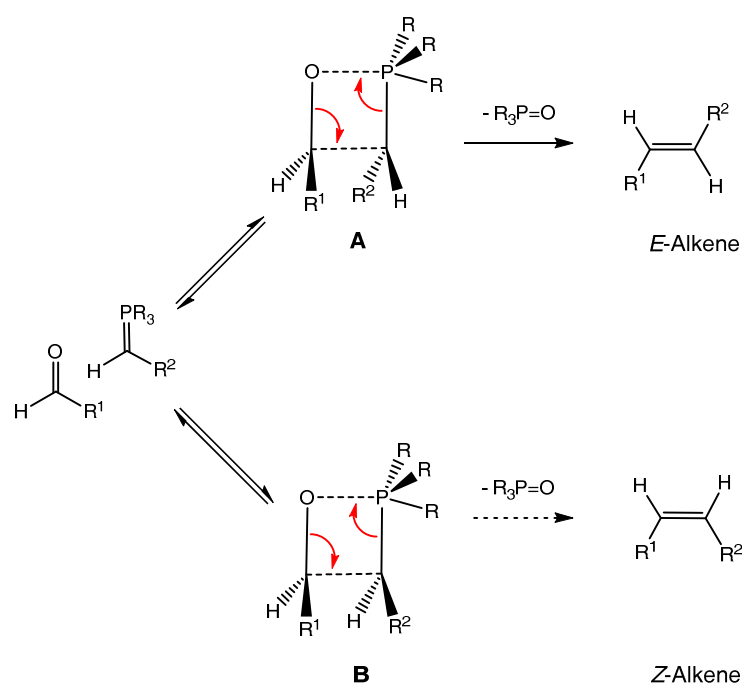
Scheme 2-3: *Wittig mechanism with stabilised ylid*

In the case of unstabilized ylids, the formation of the oxaphosphetane intermediate is

irreversible because of the unstable nature of the ylid. The stereoselectivity of this step is

kinetically controlled and the *cis*-diastereoisomer is formed preferentially. As shown in

scheme 2-4, the ylid and the aldehyde approach each other perpendicularly and form a

"puckered" oxaphosphetane ring. The transition state is formed in a way that steric

hindrance is reduced, leading to the *cis*-oxaphosphetane **A**. This isomer is probably less

stable, but is formed quicker than the *trans*. Stereospecific elimination of the intermediary leads to the formation of *Z*-alkene.
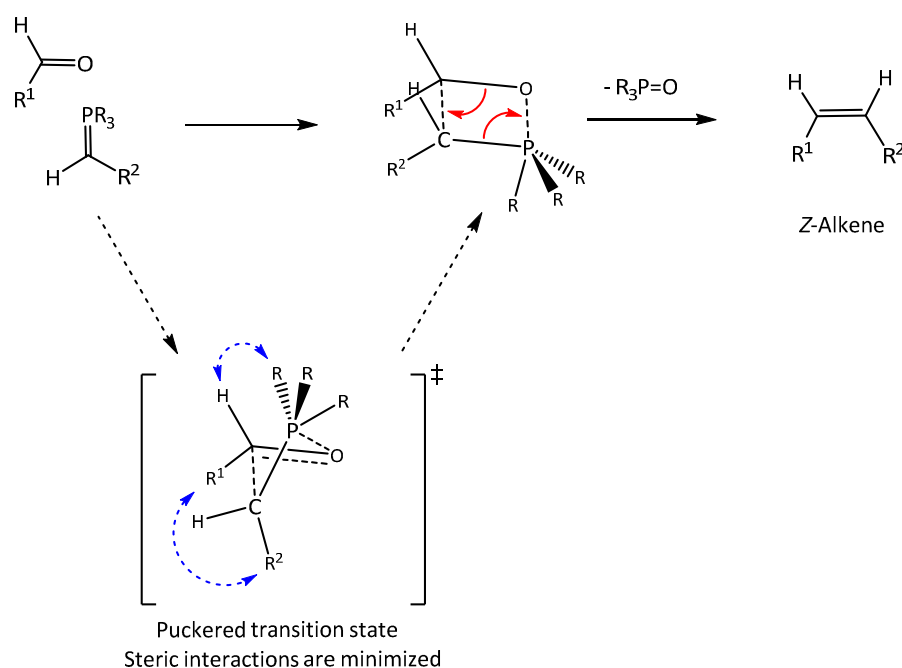
Scheme 2-4: *Wittig mechanism with unstabilized ylid via a puckered transition state*

Variants of the Wittig reaction have been developed to optimise stereoselectivity. Amongst others, the Horner-Wittig reaction is one that is characterised by the use of diphenylphosphine oxide ylids. Horner was the first to use those ylids in order to produce an alkene. Isomeric *Z* and *E*-alkenes were formed directly, but using lithium bases enabled isolation of intermediates **C** and **D** (Figure 2-5). The separated intermediaries could then be treated separately with a base to obtain the corresponding pure isomer of the alkene. The Horner-Wittig reaction can also be carried out without isolation of the intermediates. In this case, the nature of the ylid plays again a significant role in the *Z:E* ratio. When the ylid is unstabilized, the stereoselectivity of the reaction is not really well controlled but tends to go towards the *Z*-alkene if R_1 and R_2 are bulky.
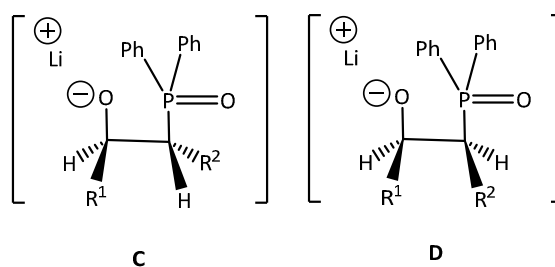
Figure 2-5: stabilised intermediates via lithium salt formation

The following section will discuss the utilisation of the Horner-Wittig reaction as a way to couple ferrocene with adenine and cytosine. The *N*-9 position of adenine was alkylated following the usual procedure but with the *N*-6 position first protected to avoid side-reactions. In the same way, cytosine was alkylated at the *N*-1 position and protected at the *N*-4 position.

2.2.2   Synthesis results

2.2.2.1   Adenine/cytosine alkylation

In the procedure reported by Dahl and coworkers,[7] adenine is alkylated and coupled with benzaldehyde via the Horner-Wittig reaction. To begin with, the alkylated adenine is synthesised. The deprotonation at the *N*-9 position with NaH in DMF is followed by addition of the (4-nitrophenylsulfonyloxymethyl) diphenyl phosphine oxide. After stirring for four days, *N,N*-dibutylformamide dimethyl acetal is added and reacted for three more days to protect the alkylated base. (Scheme 2-5)
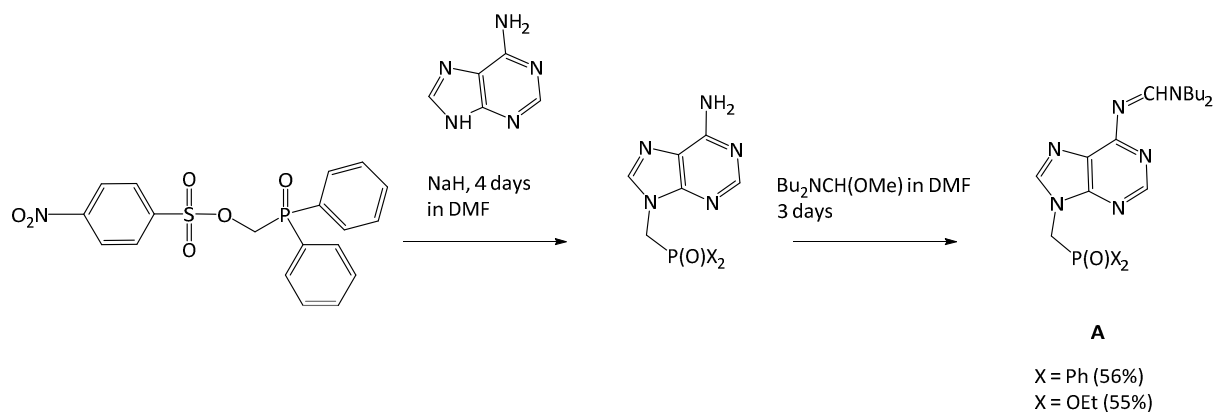
Scheme 2-5: *Alkylation and protection of adenine by Dahl[7]*

Following this method, alkylation and protection of adenine was investigated. Diphenylphosphine chloride **1** was treated with hydrochloric acid and formaldehyde at 50˚C overnight to give the (hydroxymethyl)diphenyl phosphine oxide **2** in 84% yield as reported by Marmor and Seyferth.[9] Adenine is a poor nucleophile and nucleophilic substitution on the α carbon of a phosphine oxide is difficult. To overcome this problem, 4-nitrophenylsulfonyl was used as a good leaving group and linked to the (hydroxymethyl)diphenyl phosphine oxide to aid the alkylation of adenine. Substitution of **2** with the 4-nitrophenylsulfonyl chloride **3** was catalysed by DMAP acting as an activator of **3** with triethylamine deprotonating the alcohol. The alcohol attacked the sulfonyl to form the desired (4-nitrophenylsulfonyloxymethyl) diphenyl phosphine oxide **4** in 55% yield. (Scheme 2-6)
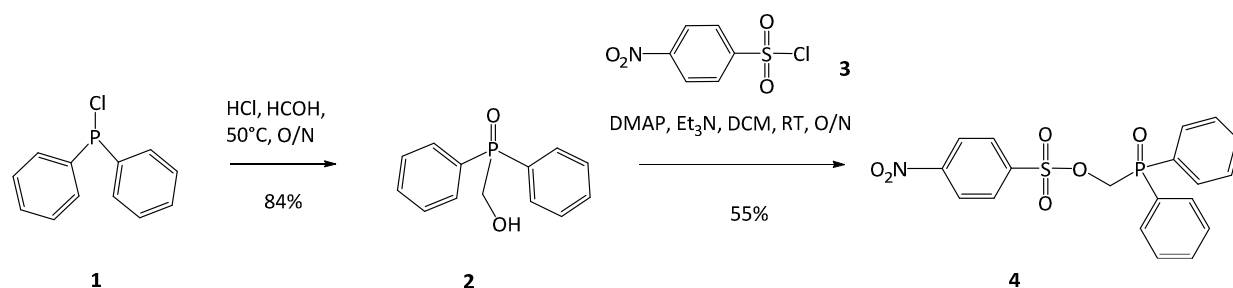
Scheme 2-6: *Alkylation precursor synthesis scheme*

The following step consisted of alkylation of adenine with the previously synthesised diphenylphosphine oxide **4**. NaH was used as a strong base to deprotonate the *N*-9 hydrogen of adenine. The nucleobase attacked **4** releasing the nitrobenzensulfonate. The desired compound **5** was obtained with a 58% yield. The reaction was performed in DMF to allow the purine to dissolve and to favour the S_N2-type mechanism. Adenine was mainly alkylated at the *N*-9 position and the minor *N*-7 isomer was removed by column chromatography after *N*-6 benzoyl protection. A comparison of the ^{13}C NMR values of **5** with literature values[10] confirmed that *N*-9 alkylation was obtained (Table 2-1), with position 4 being particularly diagnostic.

Table 2-1: Comparison of ^{13}C NMR values of 5 to literature values
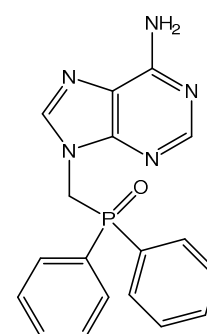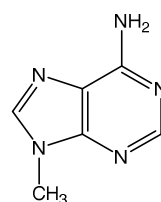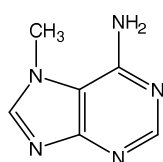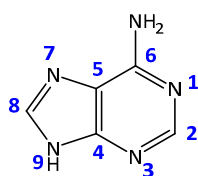
	N-7 Literature example[10]	*N*-9 Literature example[10]	**5**
C$_2$	152.3	152.5	152.8
C$_4$	159.8	149.9	149.9
C$_5$	111.7	118.7	129.1
C$_6$	151.9	155.9	155.3
C$_8$	145.9	141.4	140.8

To avoid side reactions during the coupling reaction with ferrocene, the primary amine of adenine had to be protected. Benzoyl chloride was chosen instead of the dibutylaminomethylene used by Dahl. Indeed, benzamide protecting groups are commonly

used in DNA synthesis to protect nucleosides; thus we investigated this way of protection bearing in mind the later tetra-substituted ferrocene synthesis. Following to the procedure reported by White,[11] benzoylation was performed in the presence of pyridine with benzoyl chloride overnight to give **6** in 77% yield after a basic work-up and purification on silica gel using 30% hexane in EtOAc.
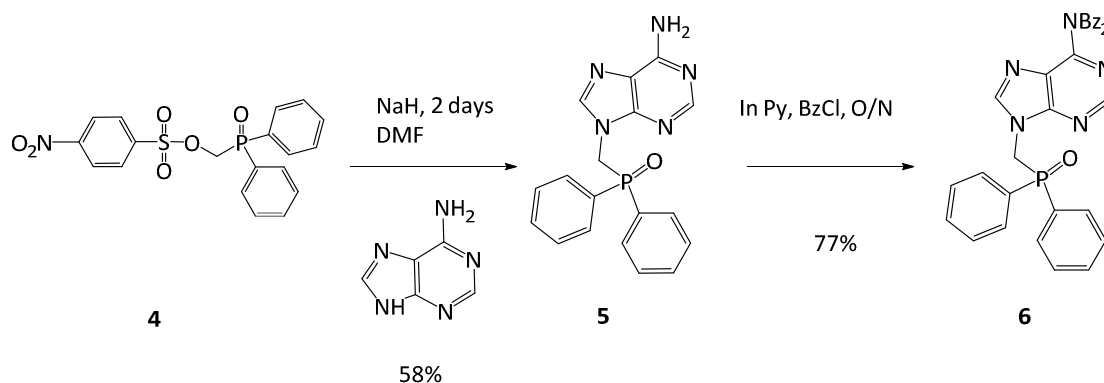
Scheme 2-7: *Alkylation and protection of adenine*

Given the reasonably good yields obtained with adenine compared to the results obtained by Dahl and coworkers[7], the same series of reactions were performed to alkylate and protect cytosine. Alkylation of cytosine was obtained in 61% yield and mono-protected with benzoyl in 72% yield. Interestingly in this case di-benzoylation was not observed according to the analysis of the proton and carbon NMR spectrums.
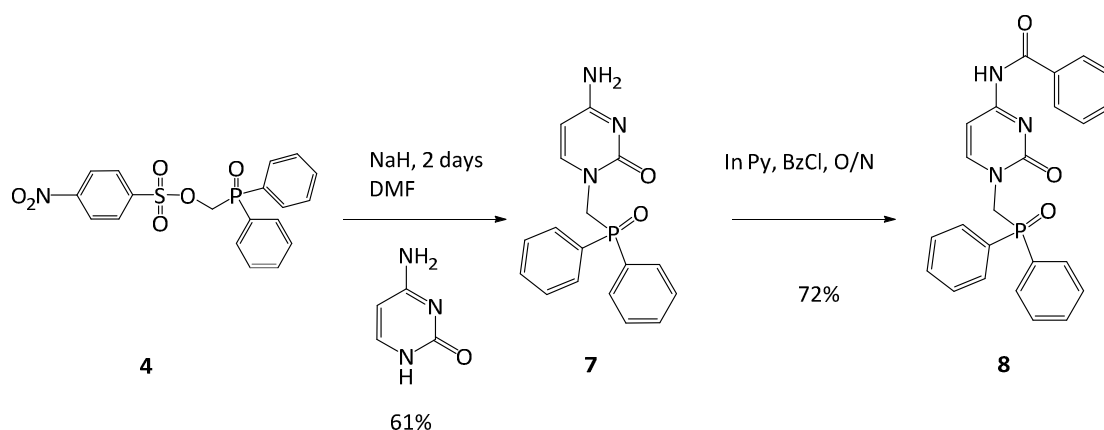
Scheme 2-8: *Cytosine alkylation and protection*

2.2.2.2 Horner-Wittig coupling

The other starting material needed for the coupling reaction was 1-1'-dicarboxaldehyde ferrocene **9**. It was synthesised following the procedure described by Balavoine *et al.* in 1991. [12] The first step involves metalation of ferrocene with *n*-butyllithium and tetramethylethylenediamine (TMEDA). Dimethyl formaldehyde then reacts as an electrophile with the dilithio-ferrocene-TMEDA complex to give the target compound **9** in 78% yield after an aqueous work-up and purification via flash column chromatography using 70% EtOAc in hexane. (Scheme 2-9)
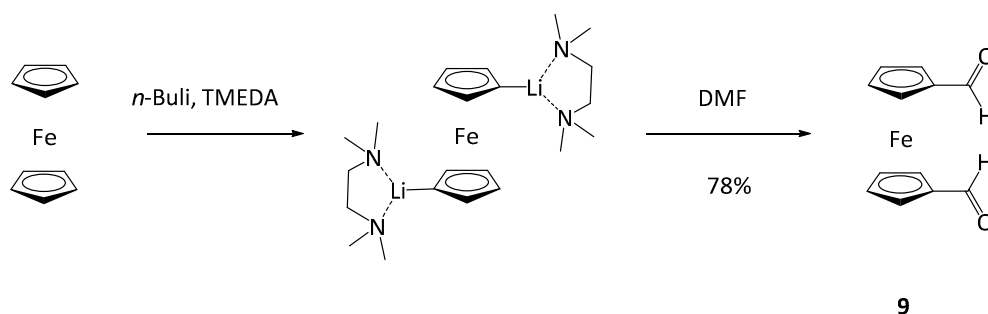
Scheme 2-9: *Synthesis of 1,1'-bis-dicarboxaldehyde ferrocene*

Ferrocene **9** was then reacted with adenine phosphine oxide **6** under Horner-Wittig conditions.
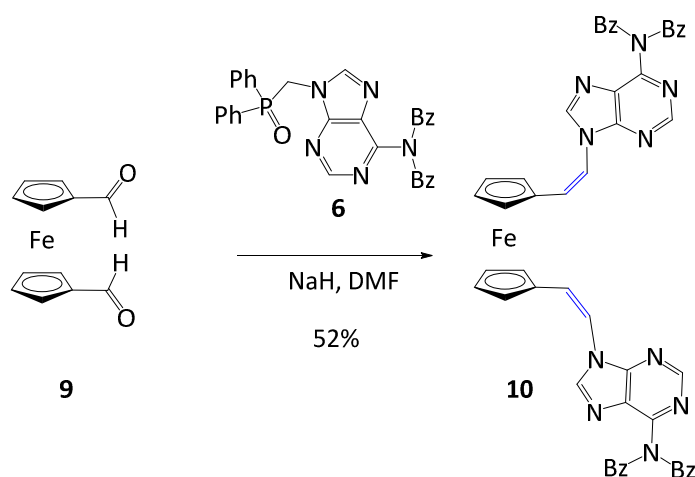
Scheme 2-10: *Horner-Wittig coupling with ferrocene carboxaldehyde and alkylated adenine.*

The reaction was quenched with a 1:1 mixture of EtOAc/Water and purified via flash chromatography with a 60% EtOAc/hexane mixture to give 1,1'-Bis-*N*-6-(dibenzoyladenine)ethenyl ferrocene **10** in 52% yield. Analysis of ^{1}H NMR shows two singlets at 8.75 and 8.09 integrating for the cyclic protons of the two adenines and two doublets at 6.84 and 6.39 ppm integrating for the four protons of double bonds. The vicinal CH=CH coupling constant value determined from the ^{1}H NMR spectrum were J_{HH} = 8.7 Hz, which is consistent with the formation of *Z*-isomer of the alkene[13] and agrees with the results obtained by Dahl. In their case, the reaction of *N*-6-(Dibutylaminomethylene)-9-(diphenylphosphorylmethyl) adenine and benzaldehyde gave a 2:7 mixture of *E:Z* isomers of the resulting alkene in 65% overall yield. Their results and our results are consistent with the previously developed theory on the Horner-Wittig mechanism involving unstabilized ylids with diphenylphosphine oxide.

Reduction of the double bonds and the deprotection of the protecting groups were investigated next as described below. (Scheme 2-11)
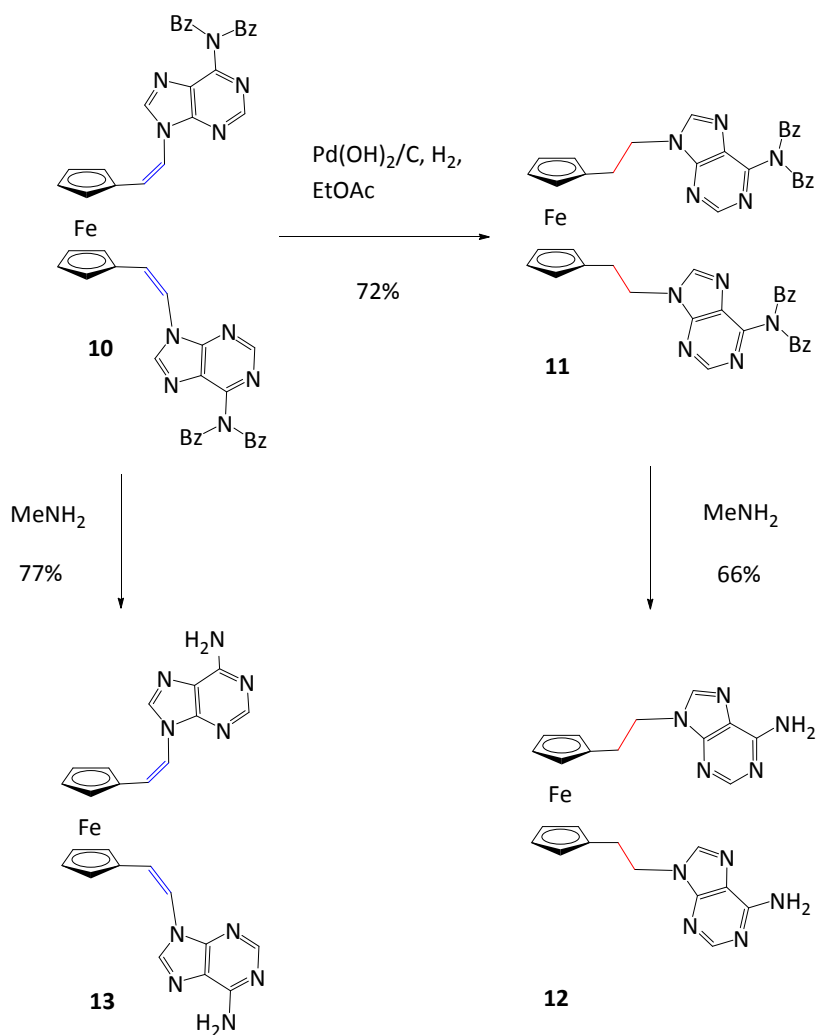
Scheme 2-11: *Hydrogenation of the unsaturated product of the Horner-Wittig reaction and debenzoylation of adenine.*

Hydrogenation of the unsaturated bonds of **10** was achieved in 72% yield with Pearlman's catalyst $Pd(OH)_2$/C (20%) using H_2 gas as source of hydrogen at normal atmospheric pressure (1 atm). The disappearance of the vicinal proton peaks in the proton NMR spectrum indicated that an overnight reaction was sufficient to obtain **11**. No undesired deprotection of adenine was observed. The overall yield of the coupling and the hydrogenation was 37%. Removal of the benzoyl protecting group was achieved with a methylamine solution giving **12** in 66% yield and **13** in 77% yield from compounds **11** and **10** respectively.

The same Horner-Wittig coupling reaction was then tried with alkylated cytosine **8** but unfortunately no reaction was observed. After stirring overnight, both starting materials were recovered but with a slight degradation of the phosphine oxide cytosine, probably due to oxidation (Scheme 2-12). The reaction was performed again in drier conditions but without success. The coupling reaction was then tried under Mitsunobu conditions and via a bromide substitution. This will be discussed in the next sections.
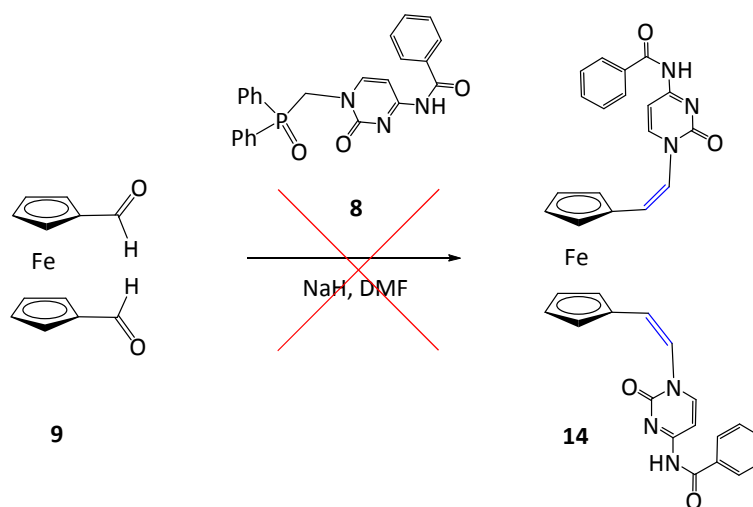
Scheme 2-12: *Horner-Wittig coupling with ferrocene carboxaldehyde and alkylated cytosine*

Compound **12** was recrystallized by slow evaporation from a DCM/MeOH solvent mixture to afford crystals suitable for X-Ray diffraction.
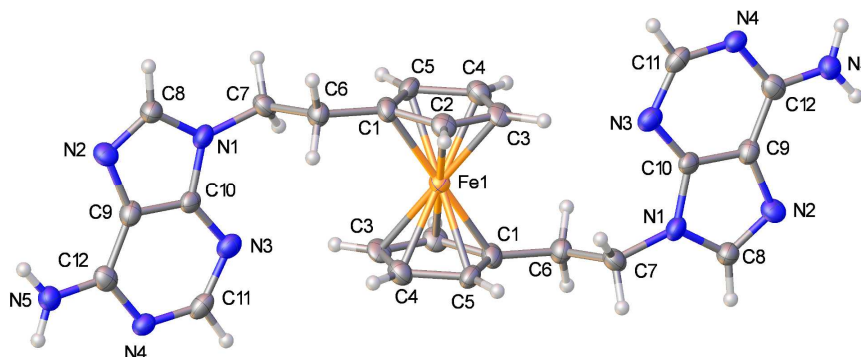
Figure 2-6: *Crystal structure of 12 with ellipsoids drawn at the 50 % probability level. The iron atom is located on an inversion centre such that only half of the molecule is crystallographically independent.*

The structure (Figure 2-6) reveals interesting features as well as providing proof of the success of the synthesis, confirming for example alkylation of adenine at the *N*-9 position and not at the *N*-7 position. This is of importance for the later coupling of adenine with the tetra-substituted ferrocenyl monomer. Indeed *N*-7 substitution would affect the ability of the monomer to form hydrogen bonds, which would disfavour any duplex formation. The iron atom of **12** is placed on an inversion centre of the molecule, which means that only half of the molecule is crystallographically unique and the two cyclopentadienyl rings are identical. The C6-C7 bond lengths confirmed the saturated nature of the linker with a characteristic length of 1.54 (Å). (Table 2-2)

Table 2-2: Selected bond lengths (Å) and angles (°) for 12

Bond lengths and angles (and their standard deviation)	12
C6–C7	1.536 ± 0.009
N2–C8	1.31 ± 0.001
N2–C9	1.415 ± 0.009
N5–C12	1.321 ± 0.009
C1–C6–C7	115.1 ± 0.6
C6–C7–N1	110.3 ± 0.6
C8–N2–C9	103.6 ± 0.6
N4–C12–N5	117.9 ± 0.7
C9–C12–N5	126.0 ± 0.7

The crystal structure also shows a Cp twist angle of 36°, and an axial positioning of the ferrocene substituents, giving a torsion angle of 180° between them (C6-C1-C1-C6). This

particular arrangement is due to the formation of intermolecular hydrogen bonds between the bases. This feature has already been described by Ganesh in the case of thymine and uracil.[1,2] The packing organisation is represented in Figure 2-7.
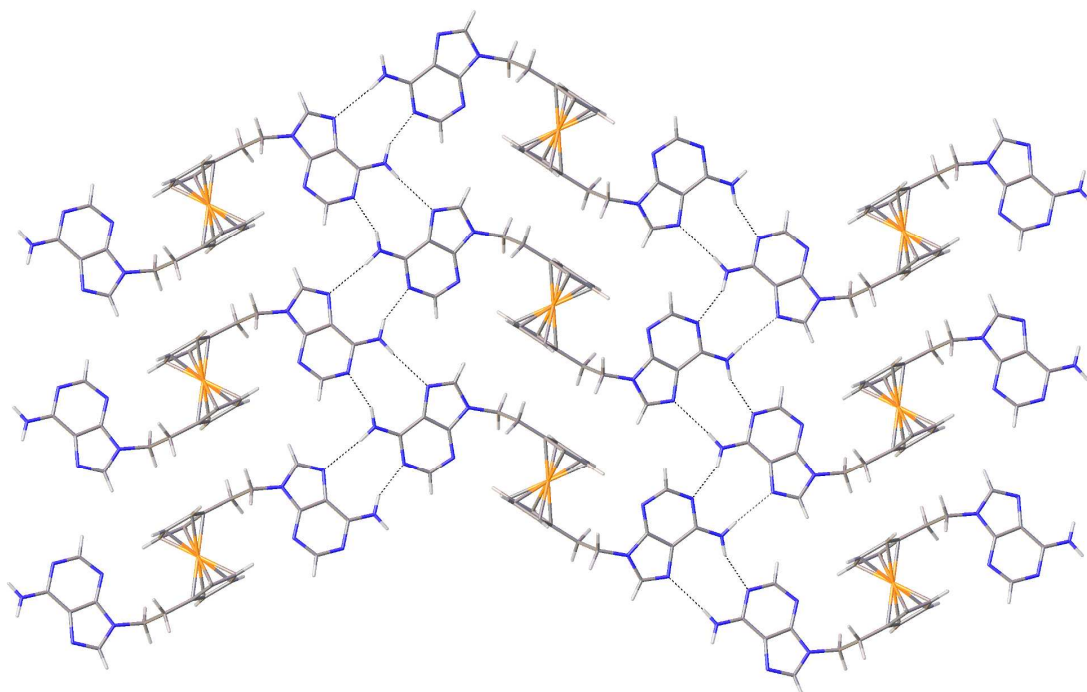
Figure 2-7: *Molecular packing diagram showing the H-bonded sheet formed by A:A base pairs of crystallographically independent molecules of 12.*

Compound **12** forms a sheet of hydrogen-bonded ribbons, with each adenine interacting with one another via two H-bonds coming from protons on the exo-amine acting as donors and two H-bonds coming from the nitrogens on the purine ring acting as acceptors. Hydrogen bonds lengths and angles are reported in Table 2-3. Only two are presented because of the symmetry of the molecule.

Table 2-3: *Detail of hydrogen bonding (Å) and (°) in crystalline structure of 12.*

Donor–H···Acceptor	d(D–H)	d(H···A)	d(D···A)	∠(DHA)
12: N5–H5A···N2	0.88	2.28	3.159 ± 0.008	175.3
12: N5–H5B···N4	0.88	2.02	2.850 ± 0.008	156.8

Even though the Horner-Wittig was a successful way to synthesise a new adenine-containing ferrocene,[14] the yield of the coupling reaction to form **10** was quite low and the overall number of steps was quite large. Furthermore no product was observed in the corresponding reaction with cytosine, therefore other routes were also explored. As mentioned earlier, the Mitsunobu reaction has been used to couple ferrocene to thymine and uracil via a 1- and 4-carbon linker[1] and was therefore considered to be an interesting alternative for improving the coupling reaction. The results of these studies are outlined below.

2.3   Coupling: Mitsunobu approach

The reaction of an alcohol and a nucleophile in the presence of diethyl azodicarboxylate (DEAD) or diisopropyl azodicarboxylate (DIAD) and triphenylphosphine is called the Mitsunobu reaction or sometimes DEADCAT reaction (DiEthyl AzoDiCarboxylate with Acid and Triphenylphosphine). The general mechanism can be explained in five steps, as shown in scheme 2-13. In the first step, triphenylphosphine attacks the N=N azodicarboxylate bond to form the corresponding nitrogen anion, which is stabilised by one of the ester groups. In the second step the lone pair on the carboxylate is delocalised onto the nitrogen, which is basic enough to deprotonate the alcohol. The third step is driven by the strong affinity of the oxygen towards the phosphorus. Indeed, the alkoxide immediately attacks the phosphorus leading to the formation of a second nitrogen anion and a phosphoryl derivative. The negative charge on the nitrogen is delocalised in the same way as the first. In the fourth step, the negatively charged nitrogen deprotonates the nucleophile, which attacks the

phosphorus derivative in the final fifth step. The result of this last step is the production of a reduced azodiester, a triphenylphosphine oxide, and the desired compound.
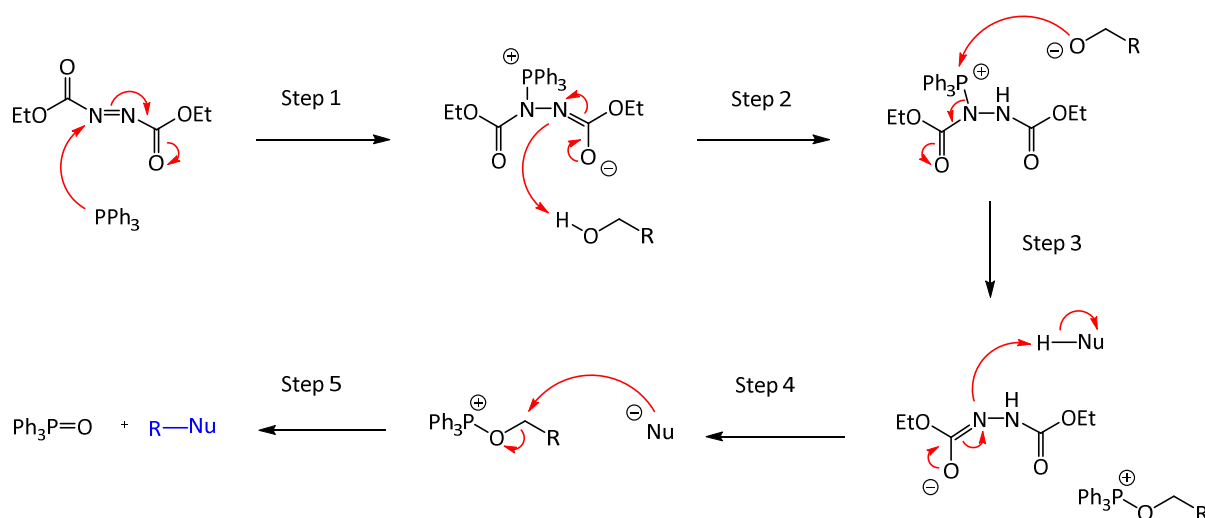
Scheme 2-13: *Mitsunobu reaction mechanism*

In the process of linking nucleobases to ferrocene via the Mitsunobu reaction, a ferrocenyl derivative acts as an electrophile and the nucleobase as the nucleophile. To play these roles, ferrocene was functionalised with an alcohol moiety and the nucleobases were protected as described in the following section.

2.3.1   Synthesis

2.3.1.1   Bis/Mono hydroxyl-Ferrocenyl precursor

Ferrocenyl alcohols have been the subjects of many synthetic investigations.[15] For example, in 2009, Swarts and coworkers reported the synthesis of a series of primary ferrocenyl alcohols with different carbon linker lengths by reduction of the corresponding ferrocenylcarboxylic acids **A**.[16] They also used the γ-ketoacid ferrocenylpropanoic acid **B** that was reduced with $AlCl_3/LiAlH_4$, the ester methyl 4-ferrocenylbutanoate **C** that was reduced with $LiAlH_4$ and the ferrocenylcarboxaldehyde **D** that was reduced with $NaBH_4$ (Scheme 2-14).
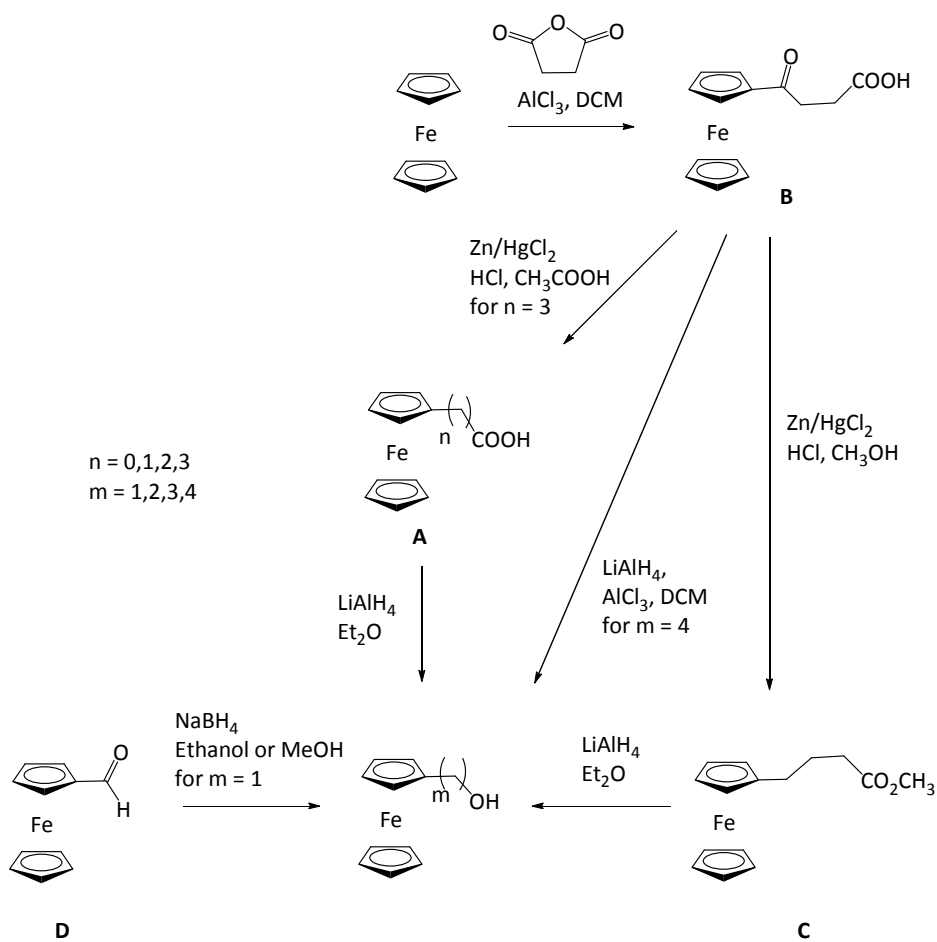
Scheme 2-14: *Synthetic routes to the different ferrocenyl alcohols by Swarts*

Another interesting approach was proposed by Barry and Nataro[17], who described a simple way to synthesise 1,1'-bis-(hydroxyethyl) ferrocene from the 1,1'-bis-vinyl ferrocene in 44% yield. The vinyl intermediate was obtained in 63% yield from 1,1'-dicarboxaldehyde ferrocene. (Scheme 2-15)
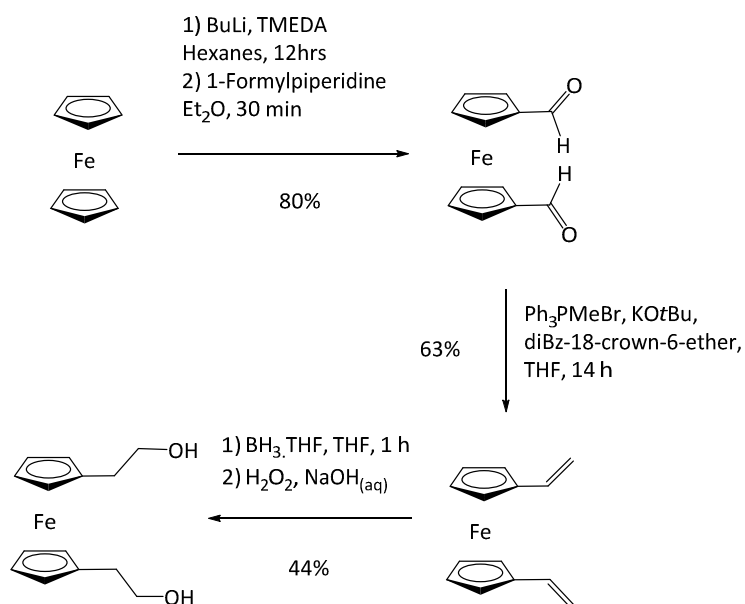
Scheme 2-15: *Synthetic route to the hydroxyethyl ferrocene by Nataro*

This pathway was followed to achieve the synthesis of 1,1'-bis-(2-hydroxyethyl) ferrocene and mono-(2-hydroxyethyl) ferrocene (Scheme 2-16). The first step after the formylation of ferrocene is a Wittig reaction. 1,1'-Dicarboxyaldehyde ferrocene was treated with triphenylmethylphosphonium bromide in the presence of potassium *tert*-butoxide in dry THF and reacted overnight. The reaction was catalysed by dibenzo-18-crown-6-ether, which possesses a strong binding affinity for potassium. 1,1'-Bis-vinyl ferrocene was obtained in 70% yield and vinyl ferrocene in 78% yield.
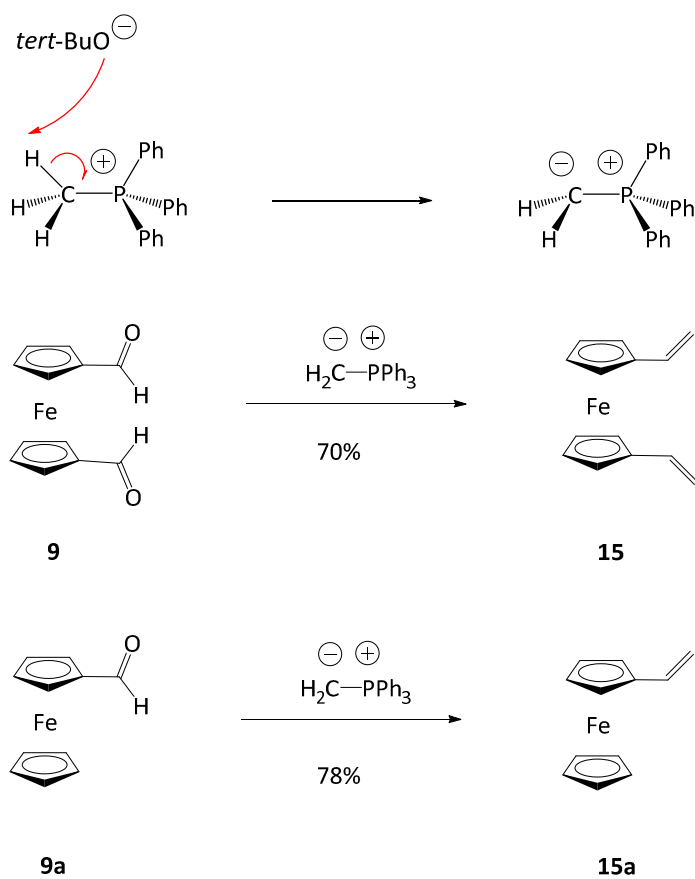
Scheme 2-16: *Formation of mono and bis-vinyl ferrocene via Wittig reaction*

The following step is the hydroboration-oxidation of 1,1-bis-vinyl ferrocene **15** that consisted of a two-step reaction that converted the alkene moiety of **15** and **15a** into the alcohol **16** and **16a**. (Scheme 2-17)
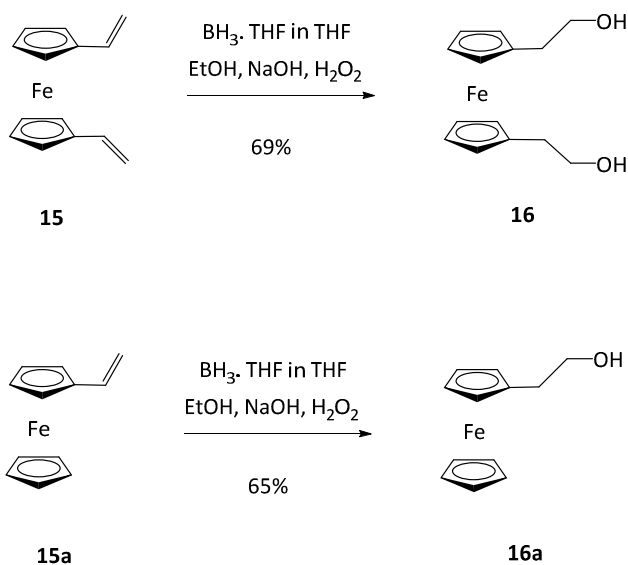
Scheme 2-17: *Hydroboration of bis-divinyl ferrocene*

The hydroboration step is an "*anti*-Markovnikov" type addition where the hydride attacks the more substituted carbon of the alkene or the more stable carbocation of the transition state. This regioselectivity is also due to the polarity of the B-H bond where the partial negative charge is located on the hydrogen. The hydroboration is *syn*-selective and proceeds via the formation of a four-membered ring transition state. The monoalkyl borane can undergo two more alkylations depending on its steric hindrance.

The oxidation part of the hydration of the vinyl derivative involves hydrogen peroxide that replaces the carbon-boron bond with a carbon-oxygen bond to give the alcohol. The peroxide anion reacts with the boron atom and the alkyl chain moves from the boron to the oxygen of the peroxide, releasing a hydroxide anion. The reaction usually occurs via the formation of a trialkyl borate. The final alcohol is then released from the alkylborate after reaction with hydroxide.

1,1'-Bis-(hydroxyethyl) ferrocene **16** and mono-(hydroxyethyl) ferrocene **16a** were accordingly synthesised in 69% yield and 65% yield respectively after extraction with DCM and purification via flash chromatography with a *3:7* EtOAc/hexane mixture. Analysis of both hydroxyethyl ferrocene ^{1}H NMRs showed the desapearance of the vinyl peaks at 5.0, 5.3 and 6.4 ppm and revealed the presence of peaks at 2.6 and 3.7 ppm corresponding to the CH_2. The obtention of the compounds were also confirmed by ^{13}C NMR and high resolution mass spectrometry.

2.3.1.2 Adenine, uracil and cytosine protection
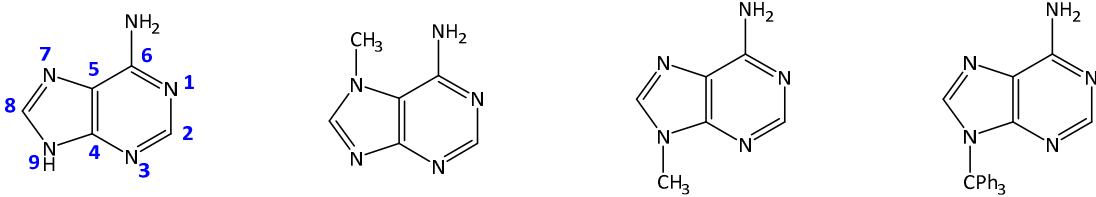
To be reliable reagents in the Mitsunobu coupling reaction, adenine and uracil had to be selectively protected. Protection of the *N*-6 primary amine of adenine, the *N*-3 of uracil and the *N*-4 of cytosine avoids potential side-reactions during the coupling. Benzoyl chloride was chosen as it had been previously investigated for the diphenylphosphine adenine **6**. Furthermore, in the Mitsunobu reaction, the nucleobases act as nucleophiles. To be able to play that role, the *N*-9 position in adenine and the *N*-1 in uracil and cytosine have to remain unprotected. Indeed, the reaction mechanism imposes a deprotonation of those nitrogens to enable nucleophilic attack of the alcohol.

To fulfil these conditions, a protection strategy for adenine was devised to avoid simultaneous protection of the *N*-6 and *N*-9 positions. To begin with, *N*-9 had to be protected via tritylation, followed by protection of the *N*-6 primary amine with benzoyl chloride. The trityl was then deprotected while the benzoyl remained. This strategy is based on the different acid-base sensitivity of trityl and benzoyl groups. Trityl is acid labile, whereas benzoyl is base labile.
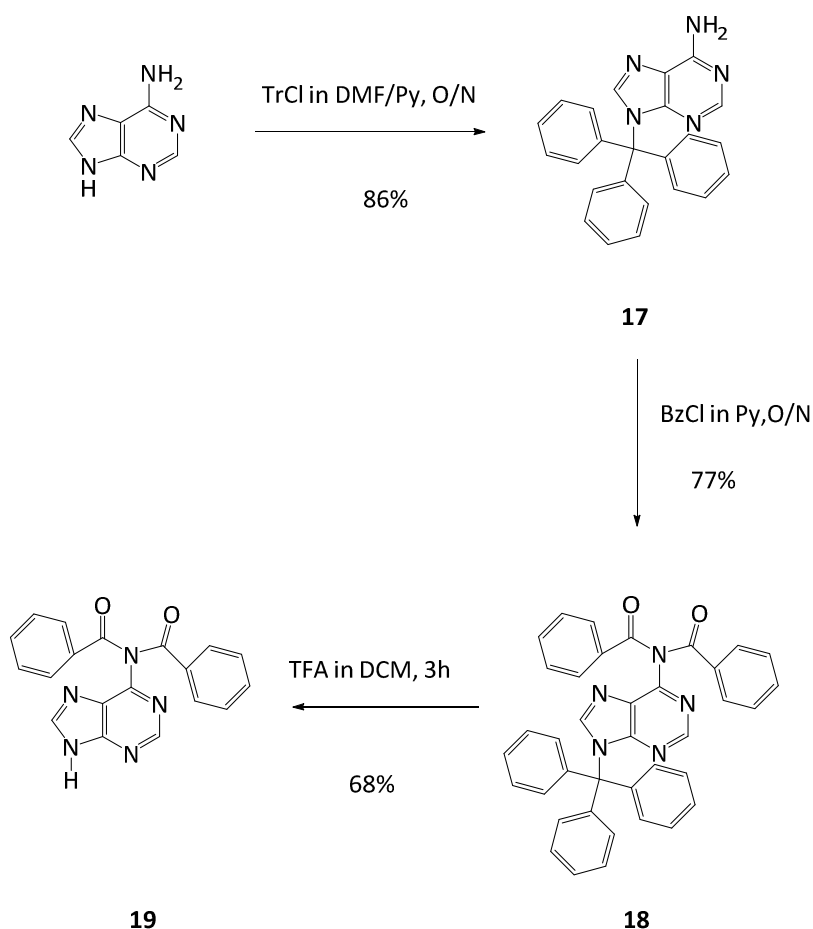
Scheme 2-18: Synthesis strategy to selectively protect adenine

The first step of the adenine protection was performed using trityl chloride in DMF/Py at room temperature overnight, as described by Hakimelahi *et al.*[18] Adenine is poorly soluble in the solvent mixture but its tritylation increases the solubility of the product. After overnight stirring, the solution was clear and the reaction was quenched with water. A quick extraction with ethyl acetate and a filtration was sufficient to obtain a very pure solid product that corresponded to the desired 9-trityladenine **17** in 86% yield. The ^{13}C NMR chemical shifts of **17** were consistent with a similar example found in the literature[10] to indicate alkylation of *N*-9 instead of *N*-7, as shown in Table 2-4.

Table 2-4: Comparison of ^{13}C NMR values of 17 to literature values

	N-7 Literature example[10]	N-9 Literature example[10]	17
C2	152.3	152.5	152.3
C4	159.8	149.9	151.4
C5	111.7	118.7	121.5
C6	151.9	155.9	155.8
C8	145.9	141.4	141.9

The second step consisted of benzoylation of the primary amine using benzoyl chloride as described previously. The fully protected adenine was synthesised in 77% yield. The last step consisted of deprotection of the trityl with a strong acid. As described by Fletcher[19] a classic and efficient way to deprotect the acid-labile trityl is to use trifluoroacetic acid (TFA) in DCM for 3 h. The compound was successfully synthesised in 68% yield.

With the idea of selectively protecting the N-3 and not the N-1 position, uracil was protected following the procedure described by Reese[20] who reacted it with a large excess of benzoyl chloride in acetonitrile/pyridine for 16 h. The crude was then filtered off and washed with acetonitrile. Reese obtained the N-1,N-3-dibenzoyluracil in 65% yield and then treated it with potassium carbonate in dioxane/water to remove the N-1 group and afford the N-3-benzoyluracil, also in 65% yield. However in our case, the crude was directly purified by column chromatography to directly access the mono-N-3 compound **20**. However **20** was

obtained in 25% yield instead of the 43% overall yield obtained by Reese.[20] The ^{1}H NMR signal for the NH at 11.6 ppm and the ^{13}C NMR signal of C_5 at 100.1 ppm reported by Reese,[20] agree with the values found for **20** and confirmed that the right compound had been synthesised.
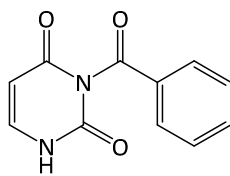
20

Figure 2-8: *N-3-benzoyluracil*

Mono-protection of cytosine was achieved using benzoyl chloride via the procedure described by Acevedo *et al.*[21] using 5 eq of benzoyl chloride followed by basic treatment with NaOH for 1 h. After an acid treatment with HCl, the compound was recrystallised from ethanol for 1 h. A white powder was collected after filtration in a 53% yield. Attempts to synthesise *N,N*-4-dibenzoylcytosine by adding 1 eq or 2.5 eq of benzoyl chloride to *N*-4-benzoylcytosine led to the protection of the *N*-1 position instead. Therefore it was decided to try the coupling with mono-benzoyl cytosine.
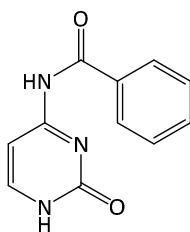
21

Figure 2-9: *N-4-benzoylcytosine*

2.3.1.3 Adenine/Uracil coupled with Bis/Mono hydroxyl ferrocenyl precursor

The investigation of the Mitsunobu coupling consisted of reacting both mono and bis-(hydroxyethyl) ferrocene **16a** and **16** with adenine **19**, uracil **20** and cytosine **21**. DEAD and DIAD were tried independently to get an idea of the best reagent to use. In each reaction, triphenylphosphine attacks azodicarboxylate, which deprotonates the ferrocene ethanol. The ferrocenyl ethoxide then attacks triphenylphosphine to form a triphenylphosphonate ferrocene. Finally, azodicarboxylate deprotonates the *N*-9 of adenine or the *N*-1 of uracil and cytosine, which attacks the ferrocene to form the final coupled compound. (Scheme 2-19)
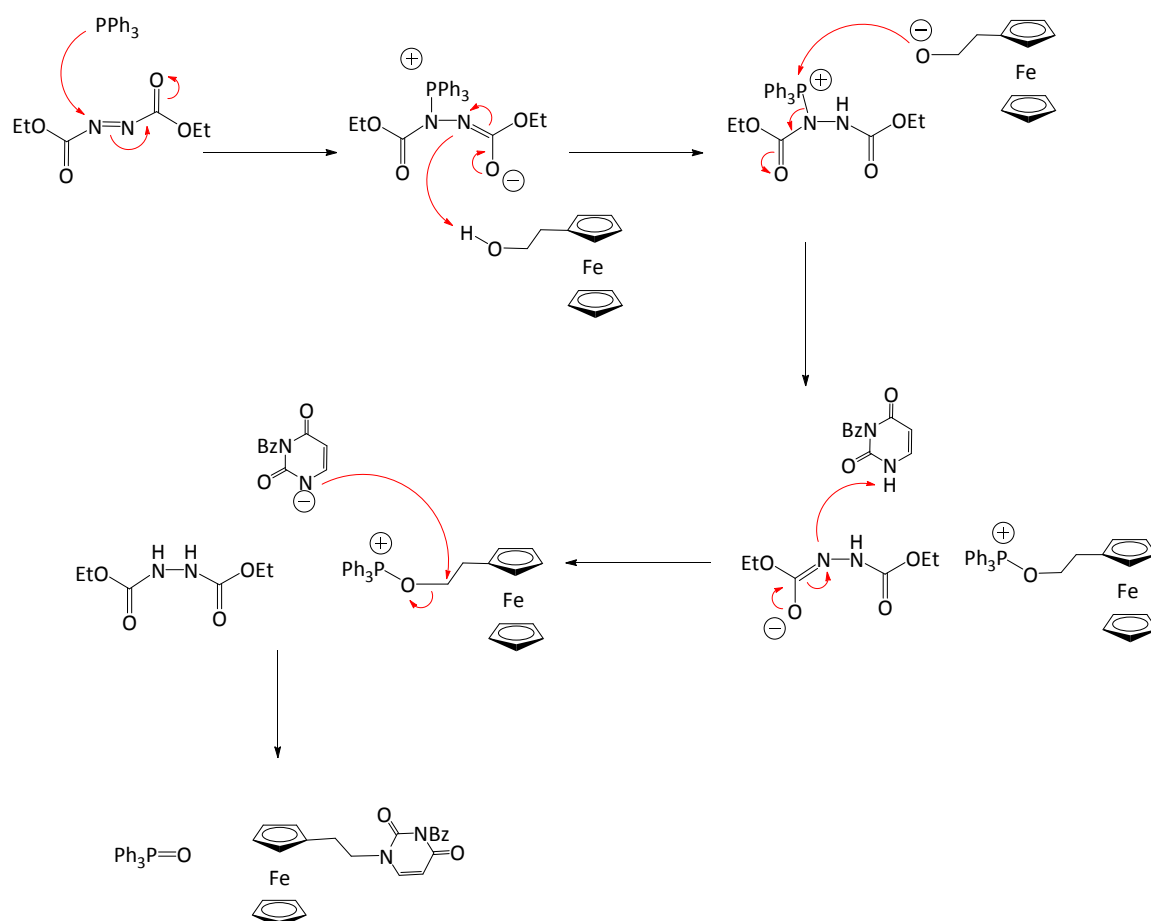
Scheme 2-19: *Mitsunobu mechanism of mono-substituted ferrocene uracil 24*

The reaction was first tried on mono-(hydroxyethyl) ferrocene **16a**. Two equivalents of each reagent (azodicarboxylate, Ph₃P and the nucleobase) were used for one equivalent of mono-

(hydroxyethyl) ferrocene. Adenine mono substituted ferrocene **22a** was obtained in 33% yield in presence of DEAD and the corresponding uracil derivative **24a** was obtained in 83% yield (Scheme 2-20). A better yield was obtained with uracil due to the use of DIAD instead of DEAD, which is less reactive. However adenine solubility in THF was not good, which could also explain the big difference of yield. The reaction was also tried with the cytosine derivative in the same conditions but only the mono substituted cytosine was obtained in very small amount, probably due to the lack of the nucleobase solubility in THF. The reaction was then tried in acetonitrile at 85˚C, but these changes did not improve the results.
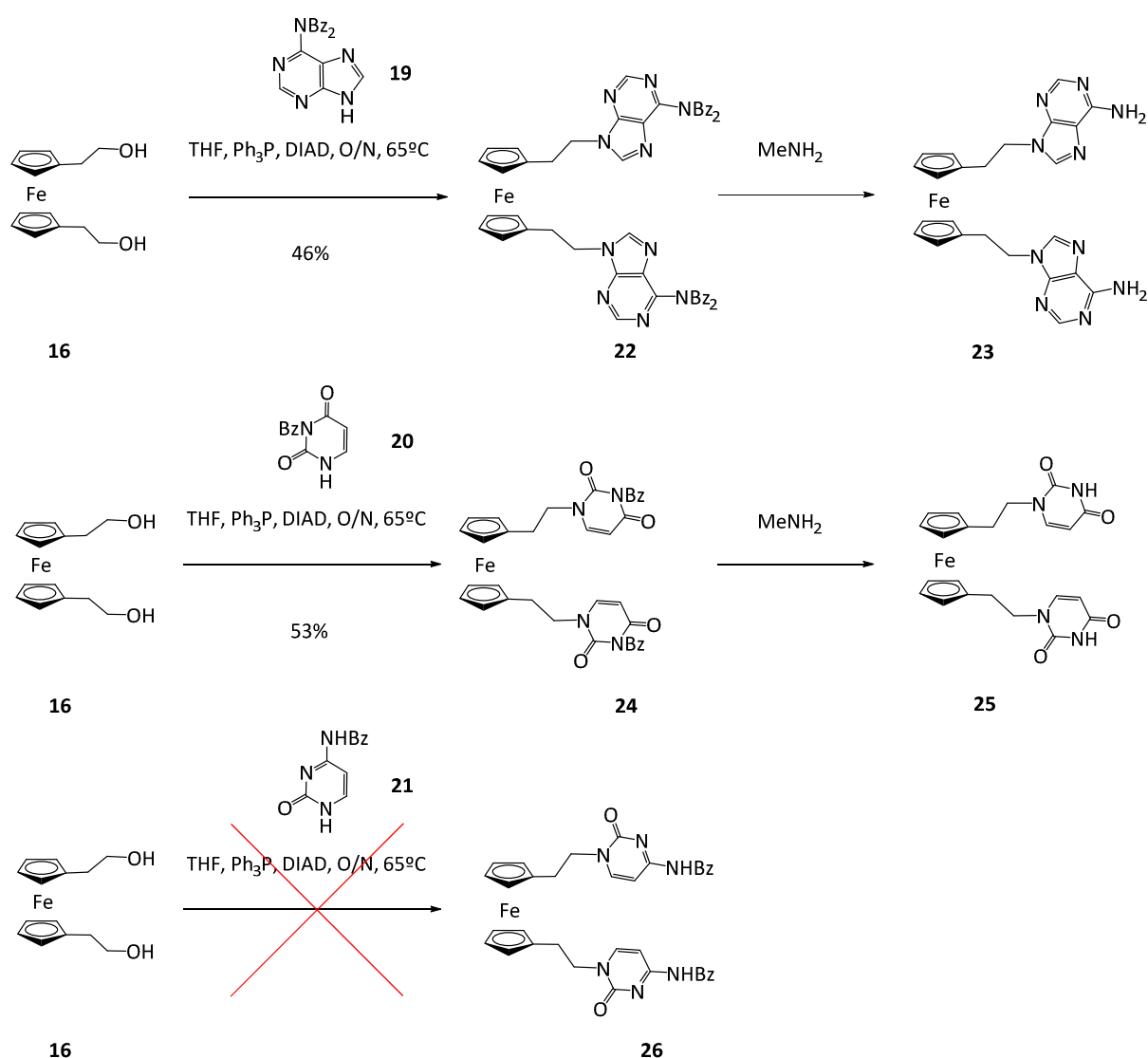
Scheme 2-20: *Coupling adenine, uracil and cytosine to mono-ethanol ferrocene under Mitsunobu conditions*

The deprotection of **22a** and **24a** was also investigated and performed in methylamine, giving 100% yield for the uracil derivative **25a** and 58% for the adenine derivative **23a**. Methylamine acts as a nucleophile towards the carbonyl function of the benzoyl, releasing the deprotected amine and *N*-methylbenzamide.

Coupling adenine **19**, uracil **20** and cytosine **21** to bis-(hydroxyethyl) ferrocene **16** was performed in the same way (Scheme 2-21) but in these cases, 3 eq of triphenylphosphine and DIAD and 2.6 eq of adenine or uracil were used for one equivalent of bis-(hydroxyethyl) ferrocene. The bis-coupled adenine ferrocene **22** was obtained in a 46% yield and the bis-coupled uracil ferrocene **24** in a 53% yield. Cytosine coupling was also tried but once again no reaction occurred for solubility reasons.
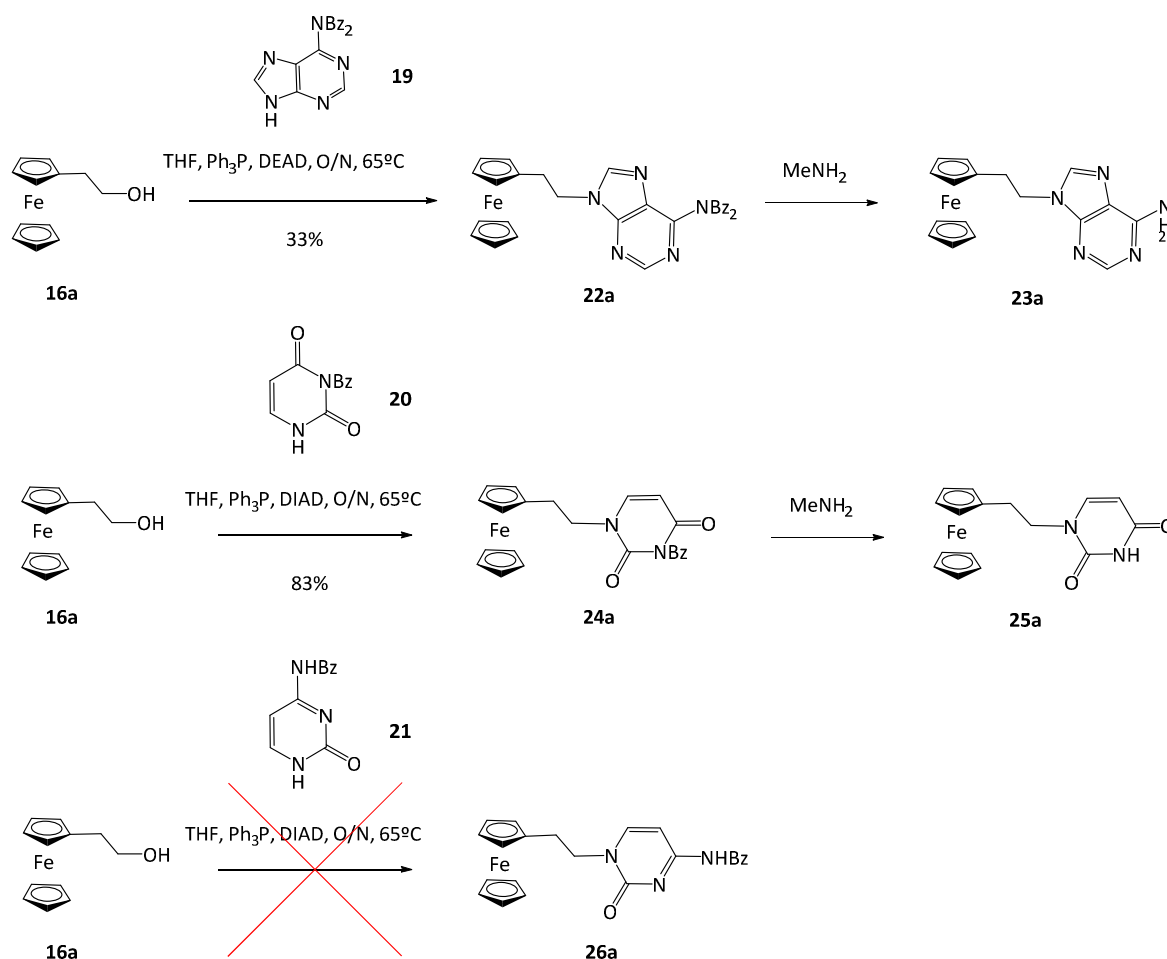
Scheme 2-21: *Coupling adenine and uracil to bis-ethanol ferrocene via Mitsunobu*

Only deprotection of **24** was tried because this reaction had already been investigated earlier with adenine. Compound **25** was recovered quantitatively as a yellow powder that could not be dissolved in the usual NMR solvents (CH_2Cl_2, MeOD, D_2O, DMSO or THF). However, the compound was characterised by mass spectrometry. An exact mass of 485.0888 m/z was found which correlated well with the calculated mass of 485.0872 (for M + Na^+). Furthermore IR spectroscopy showed peaks corresponding to the carbonyl of the urea moiety (stretching: 1744 cm^{-1}), the carbonyl (stretching: 1699 cm^{-1}) and the NH of the amide group (bending: 1550 cm^{-1}).

2.4   Cytosine coupling: Bromide substitution approach

The case of cytosine is interesting because of the low solubility of its derivatives in almost all types of solvent used in the laboratory. As previously seen, mono-protected cytosine was not soluble enough in THF to couple with ferrocene but a quick investigation revealed that DMF and DMSO could dissolve it. Therefore, to achieve the coupling of cytosine with ferrocene, a reaction using DMF or DMSO as main solvent had to be considered. In 1997, Howarth and Wakelin[22] reported the synthesis of a new type of PNA called α-PNA made of a backbone containing a series of homoserine derivatives linked together with glycine. The four canonical bases including cytosine had been attached to the backbone. The monomer was synthesised in three steps from the *N*-Boc-homoserine (Scheme 2-22). The carboxylic acid moiety was first esterified with methyl iodide to allow the conversion of the alcohol function to the corresponding bromide. This bromination involving NBS and triphenyl

phosphine will be described in more detail in the following section. Alkylation of the Cbz-cytosine to the PNA monomer was performed in DMF in a 61% yield.
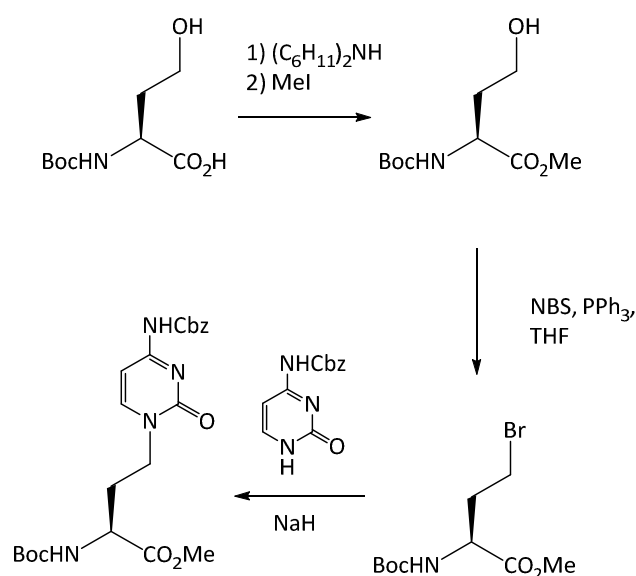
Scheme 2-22: *Cytosine coupling approach by Howard and Wakelin*

This coupling method was followed to link cytosine to a ferrocene bromide, as described below.

2.4.1 Synthesis

2.4.1.1 Mono/Bis-Bromo-ferrocenyl precursor

As mentioned above, synthesis of 1,1'-(bromoethyl) ferrocene was essential to study cytosine coupling. The bromination procedure used by Howarth and Wakelin[22] was also used by Tius and Fauq[23] in the total synthesis of the (+)-Desepoxyasperdiol, which is a synthetic precursor to the antitumor natural product Asperdiol. (Figure 2-10)

(+)-Desepoxyasperdiol   **Asperdiol**
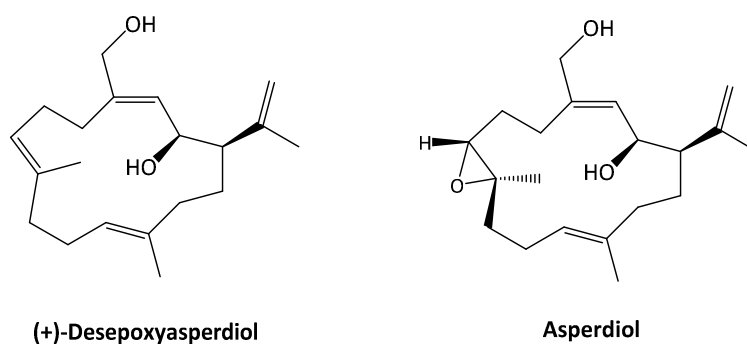
Figure 2-10: (+)-Desepoxyasperdiol precursor of Asperdiol

This procedure was tested on both mono and bis-(hydroxyethyl) ferrocene leading successfully to the corresponding bromides **27a** and **27** in yields of 91% and 97% yield respectively.
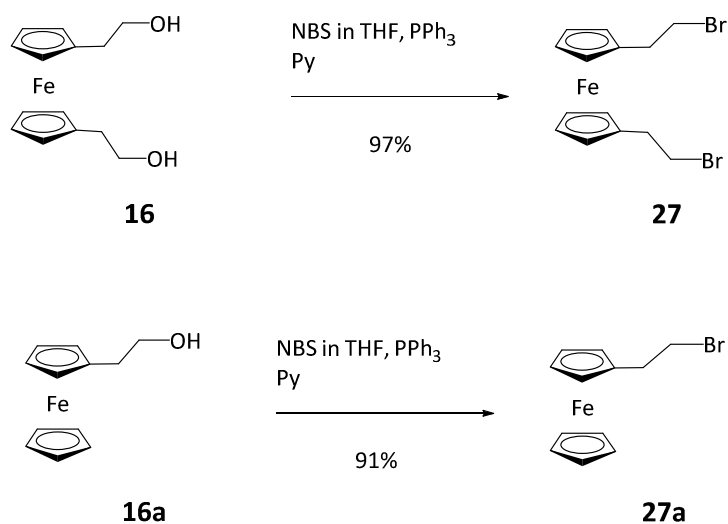
Scheme 2-23: Bromination of mono and bis-ethanol ferrocene

The mechanism is based on the activation of *N*-bromosuccinimide by triphenylphosphine releasing bromide ions.[24] In presence of pyridine, the bromide ion would replace the triphenylphosphonium formed with the alcohol, releasing **27a**, triphenylphosphine oxide and the succinimide. (Scheme 2-24)
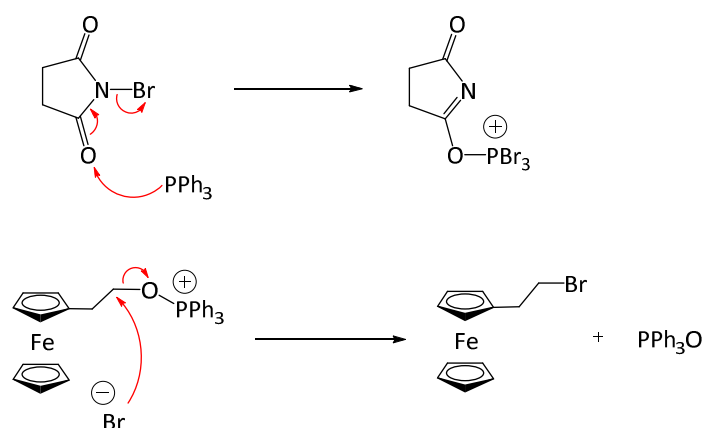
Scheme 2-24: *Mechanism of bromide ions production suggested by Trippett[24] and bromination mechanism of hydroxethyl ferrocene*

2.4.1.2 Bromide substitution coupling

The coupling reaction is based on a nucleophilic substitution of the bromide by a cytosine. It is reasonable to think that the substitution is of type 2 (S_N2) for the following reasons. First of all, the substrate is unhindered. Indeed, the reaction occurs in one step and the nucleophile needs space to replace the leaving group by breaking the bromide-carbon bond. Furthermore, bromide is a good leaving group. Cytosine is deprotonated by NaH to form the corresponding anion. The pyrimidine is then able to act attack the ferrocene bromide. DMF is polar and aprotic so favours the nucleophilic substitution towards S_N2.

According to Howarth and Wakelin,[22] the reaction was performed at room temperature. Unfortunately, repeating the same conditions with **27** only produced mono substituted cytosine in poor yield even after a reaction overnight. Therefore, to improve the efficiency of the reaction and to obtain the bis-coupled cytosine ferrocene **28**, the reaction was heated up to 50˚C.
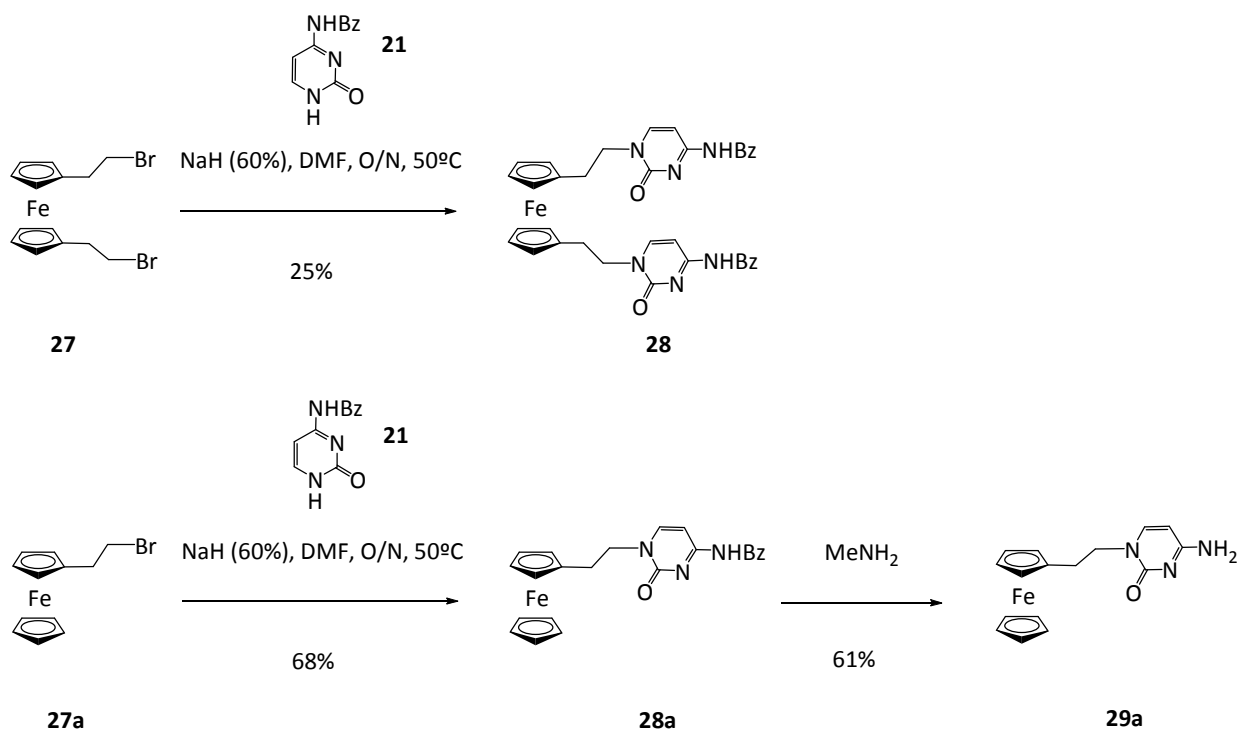
Scheme 2-25: *Coupling cytosine to mono and bis-bromoferrocene*

After an aqueous work-up and purification, **28a** and **28** were obtained in yields of 68% and 25% respectively. The debenzoylation of **24a** with methylamine in ethanol gave **29a** in 61% yield. The solubility of **28** was not good in $CDCl_3$ and two carbon peaks (C_2 and C_4) on its ^{13}C NMR spectrum were not observable. To overcome this problem, a few drops of MeOD were added to the NMR sample. As shown in Figure 2-11, the two carbons appear at 167 and 156 ppm.
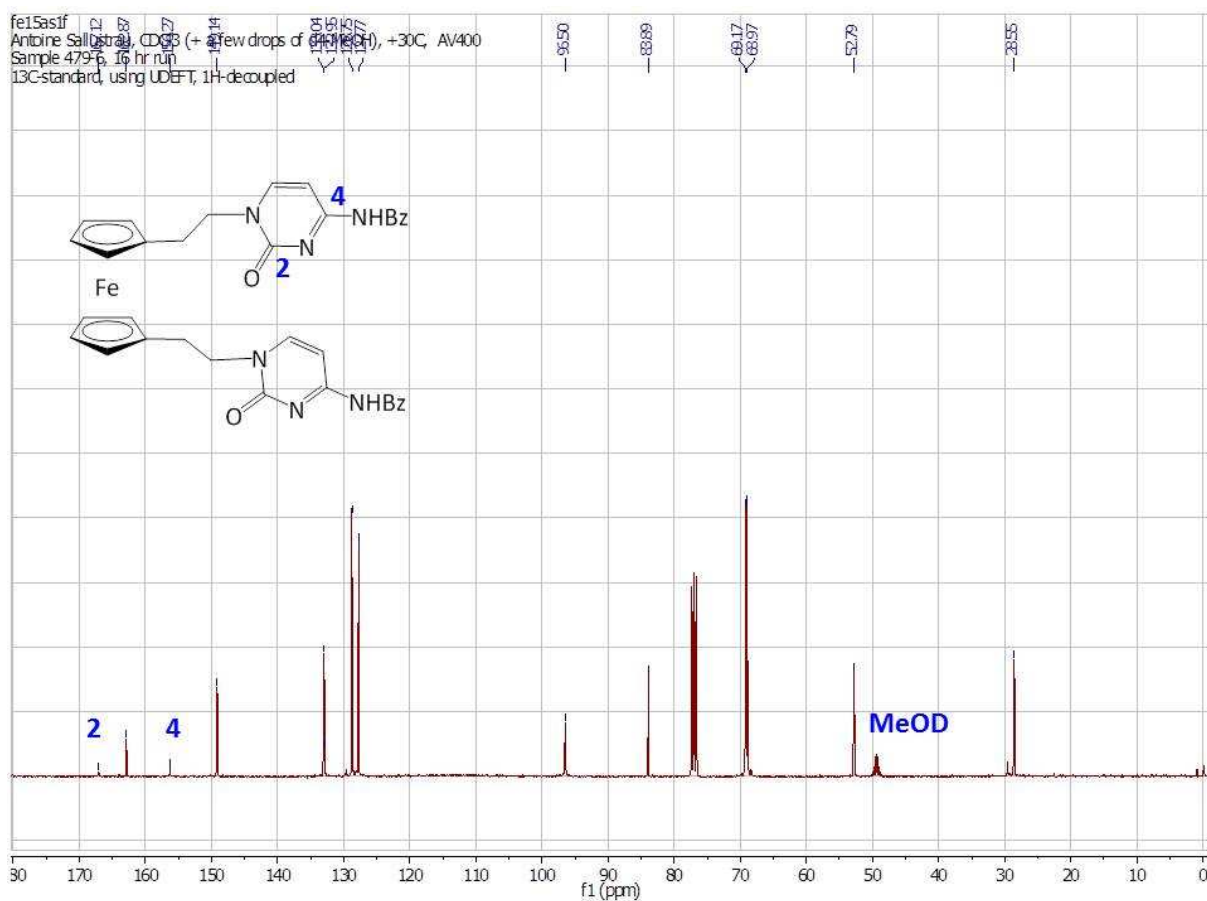
Figure 2-11: ^{13}C *NMR spectrum of 28 using Uniform Driven Equilibrium Fourier Transform (UDEFT)*

2.5 Electrochemistry

In order to obtain a better understanding of the electrochemical behaviour of substituted ferrocenes with adenine, uracil and cytosine, as well as the influence of the linker on the electrochemical response, cyclic voltammetry studies were performed on the following compounds. (Figure 2-12)
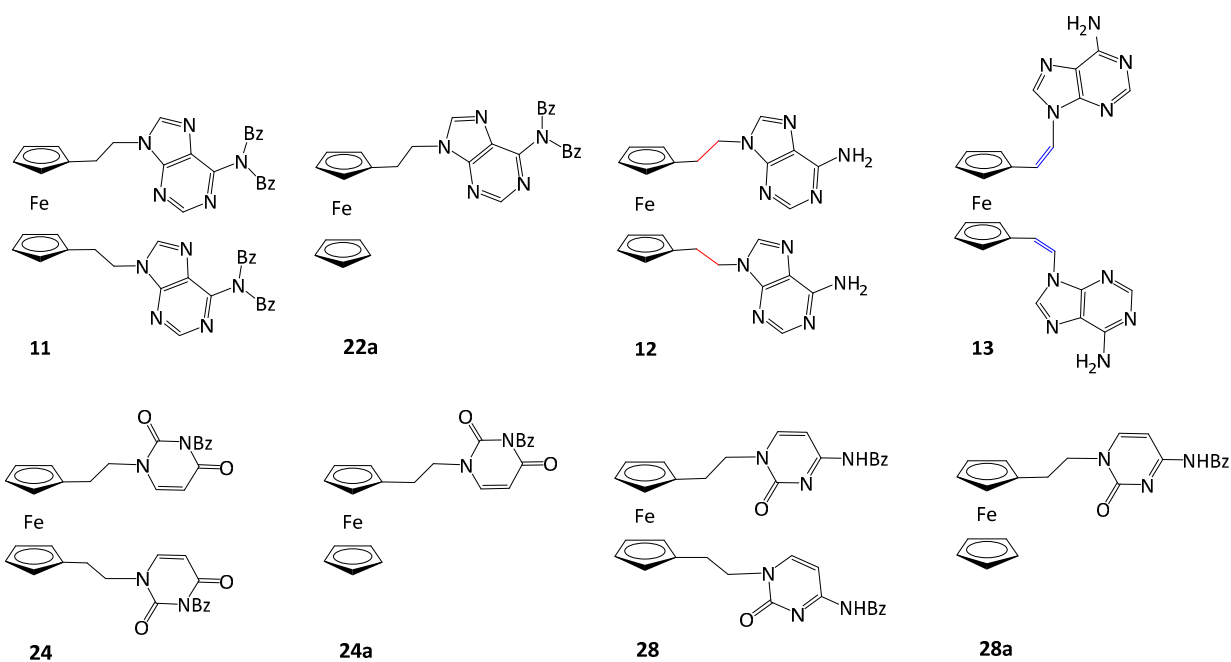
Figure 2-12: *Ferrocenyl compounds coupled with adenine, uracil and cytosine subjected to electrochemical studies*

Cyclic voltammetry is one of the most widely used electroanalytical methods to study electroactive species.[25] It brings qualitative information about redox mechanisms and offers a quick determination of electrode potentials. This is made possible via analysis of the voltammograms that are obtained by cyclically sweeping the potential between two defined values at a fixed rate. The potential is measured at the working electrode and the resulting current flows through a counter electrode. The electrode potential is measured relative to a reference electrode and the voltammogram is displayed as a function of current against potential. (Figure 2-13)
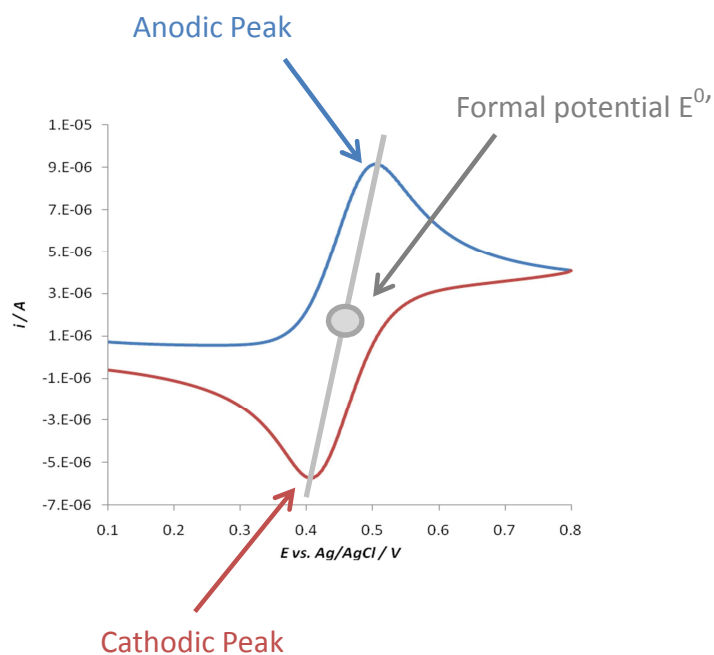
Figure 2-13: *Cyclic Voltammogram*

The redox properties of these compounds were investigated using a Pt working electrode, a Pt counter electrode and an Ag/AgCl reference electrode. Tetrabutylammonium hexafluorophosphate (0.1 M) was used as the supporting electrolyte in DCM and decamethylferrocene was used as an internal reference to be able to compare different ferrocenyl derivatives.

As shown in Figure 2-13, the anodic current (blue) increases due to oxidation of the redox-active species until all the starting material diffusing near the electrode surface have been oxidised. When the scan is reversed, the current switches to negative values and the cathodic current (red) corresponds to the reduction of the previously oxidised species at the electrode surface. Chemical irreversibility (i.e. reaction or decomposition) is characterised by a smaller or no return peak after oxidation or reduction. Furthermore, electrochemical reversibility is characterised in a number of ways:

- The ratio between current peaks is equal to one.

- The potential of oxidation and reduction peaks does not change with the scan rate.

- The potential difference between the anodic and cathodic peaks is 59 mV.

- A linear relationship between the peak current and the square root of the scan rate.

In the following, three factors are investigated via analysis of cyclic voltammograms: (1) The electrode potentials and their electrochemical reversibility; (2) the type and number of linker groups and (3) the type of nucleobase.

2.5.1   Influence of linker nature

The influence of the linker group was studied by comparing the effect of the saturated and unsaturated bonds on the electrode potentials of ferrocene of **12** and **13**. Cyclic voltammograms and electrode potentials of both compounds are presented in Figure 2-14 and Table 2-5.
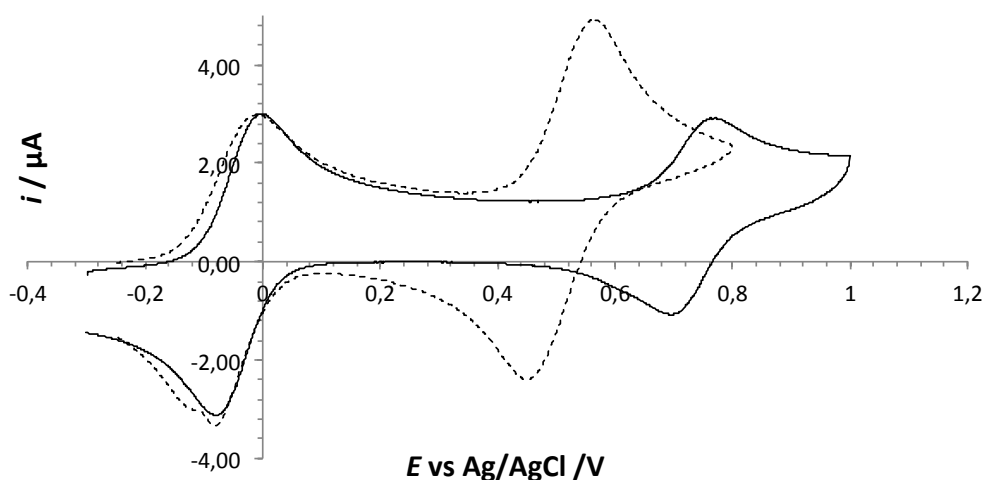
Figure 2-14: *Cyclic voltammograms of 12 (dotted line) and 13 (plain line) in DCM (scan rate = 500 mv.s^{-1}).*

Table 2-5: *Electrochemical potentials vs decamethylferrocene of 12 and 13 in DCM.*

	12	13
$E^{0'}$ (mV)	552	770

The nature of the linker between the base and the ferrocene has a significant effect on the electrode potential values. As can be seen on the graph, oxidation of **13,** which contains an unsaturated linker, is more difficult than **12**. In each case, the more electron-rich saturated linker lowers the ferrocene-centred redox couple. This results in the value for **13** being higher than **12** by 218 mV. Similar effects have been observed previously in related systems,[26] including adenine-based ferrocene derivatives[27] containing either a triple bond or a saturated linker. Both compounds **12** and **13** give linear current versus $v^{1/2}$ relationship with an intersection at zero as shown in Figure 2-15.
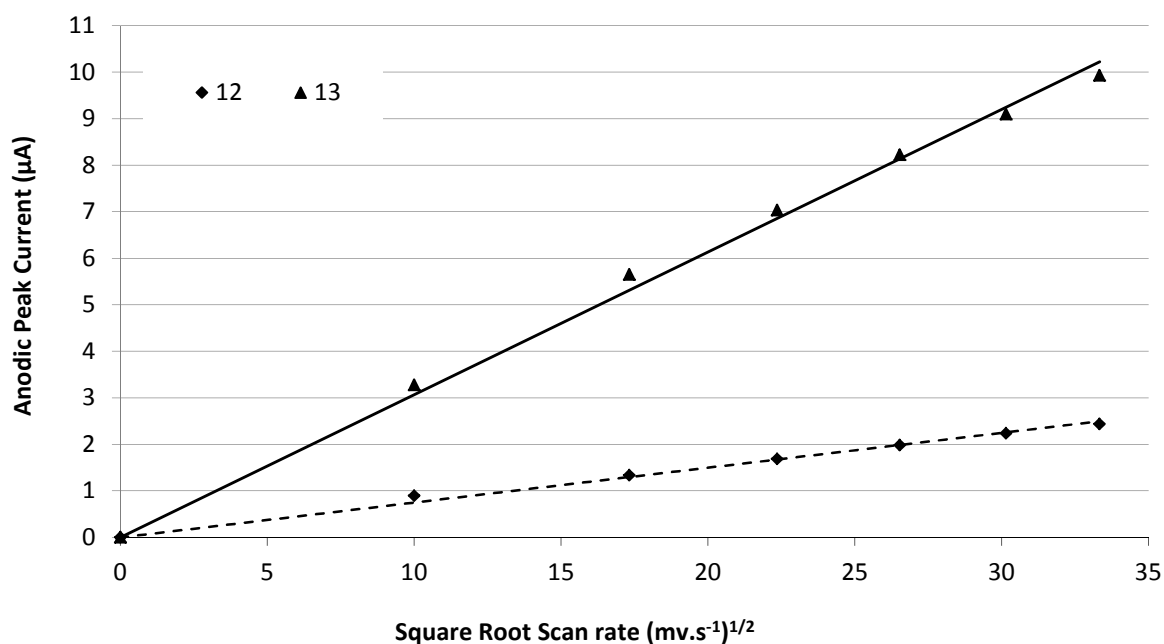
Figure 2-15: *Electrochemical reversibility of compounds 12 (dotted line) and 13 (plain line).*

2.5.2   Effect of the number of substituents on ferrocene

As described above, the nature of the linker (saturated or unsaturated) plays a significant role in the electrochemical behaviour of ferrocene. It is reasonable to assume that the electrochemical properties of ferrocene could also be affected by the way it is substituted in terms of number of substituents. Therefore, bis and mono substituted ferrocenes were compared. Three couples of compounds were studied: **11** and **22a** for adenine derivatives, **24** and **24a** for uracil derivatives, and **28** and **28a** for cytosine derivatives. Their cyclic voltammograms are shown in Figure 2-16.
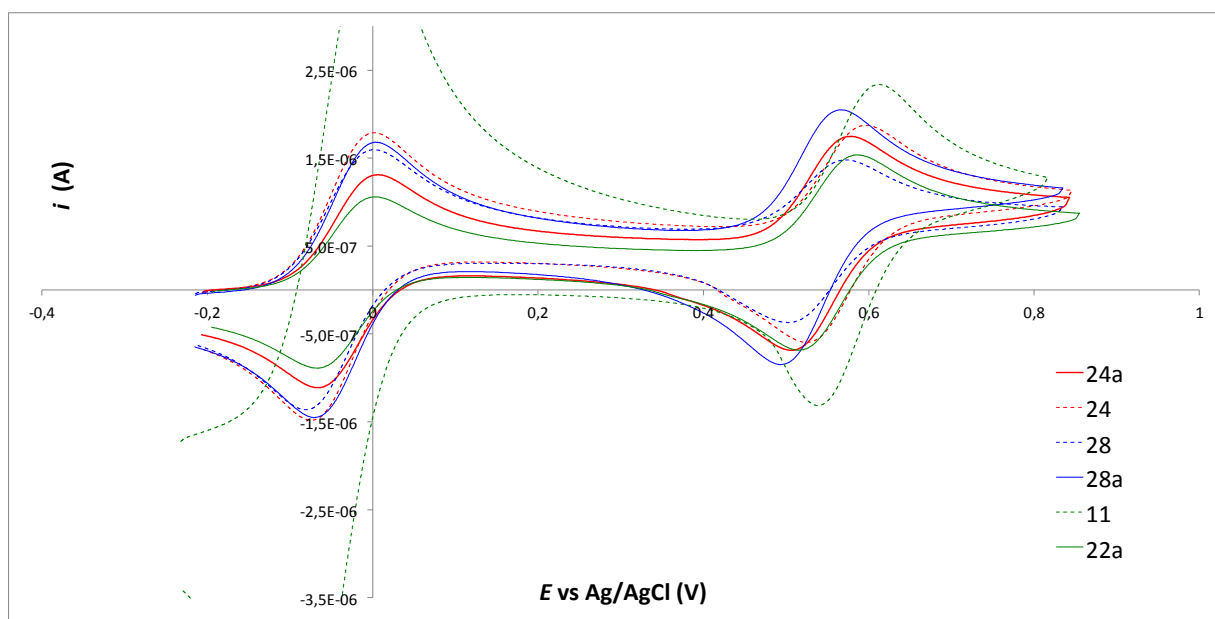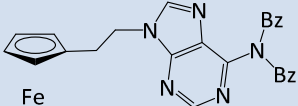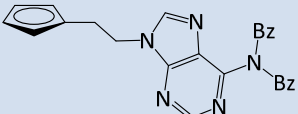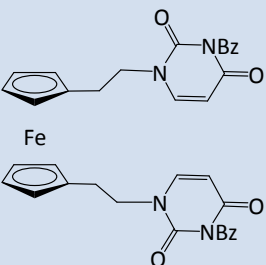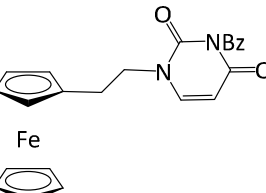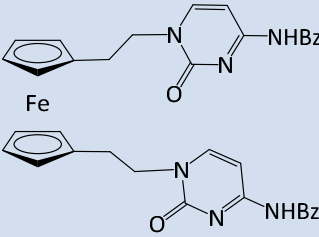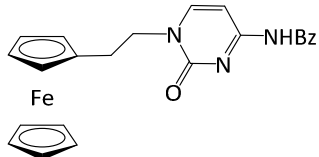
Figure 2-16: *Cyclic voltammogram of 11, 22a, 24, 24a, 28 and 28a (scan rate = 100 mv.s^{-1}) vs. decamethyl ferrocene.*

The graphs show oxidation and reduction peaks for adenine derivatives (Green), uracil derivatives (red) and cytosine derivatives (blue) at a scan rate of 100 mv.s^{-1}. Bis-ethylferrocenyl-adenine **11** shows a positive shift of 41 mV compared to its mono counterpart **22a**, **24** gave an electrode potential 23 mV higher than **24a** and **28** was 10 mV higher than **28a**. Therefore, these results indicated that bis-substituted ferrocenes **11**, **24** and **28** are more difficult to oxidise than their mono-substituted analogues **22a**, **24a** and **28a**. (Table 2-6)

Table 2-6: *Electrochemical potentials of mono and bis-ferrocene linked to adenine, uracil and cytosine. Electrode potentials, $E^{0'}$, where $E^{0'} = (Epa + Epc)/2$, are referenced to decamethylferrocene (ca. 1 mM), which was used as an internal reference. The confidence limit is ± 5 mV.*

Compounds		$E^{0'}$ (mV)
	11	624
	22a	583
	24	597
	24a	574
	28	573
	28a	563

As reported by Houlton and coworkers[3] in his publication about the synthesis and the redox properties of several ferrocenylmethyl nucleobases, nucleobases are playing a determinant role in the electrochemical behaviour of the ferrocenyl moiety. For example, he compared the electrode potentials of 9-ferrocenyl-methyladenine **A** with ferrocene using cyclic voltammetry. He noticed a potential increase of 90mV for the ferrocenyl-methyladenine **A** compared to ferrocene. He justified this result by the electron withdrawing effect of the nitrogen, which as a part of an aromatic system of adenine, is making oxidation of the ferrocenyl moiety more difficult to achieve. Furthermore, he demonstrated that additional withdrawing groups (chloride group) on the adenine could increase the redox potential by 100 mV for compounds such as 2-amino-6-chloro-9-ferrocenylmethylpurine **B** compared to ferrocene. Houlton also measured the electrochemical response of the 6-chloro-2-ferrocenylmethylaminopurine **C**, where the ferrocenyl moiety is link to a nitrogen atom that is not incorporated into the purine rings. This resulted in a negative shift of the formal electrode potential of 8 mV indicating that the ferrocenyl moiety is unaffected by the base. (Figure 2-17)

A +90 mV   **B** +100 mV   **C** -8 mV
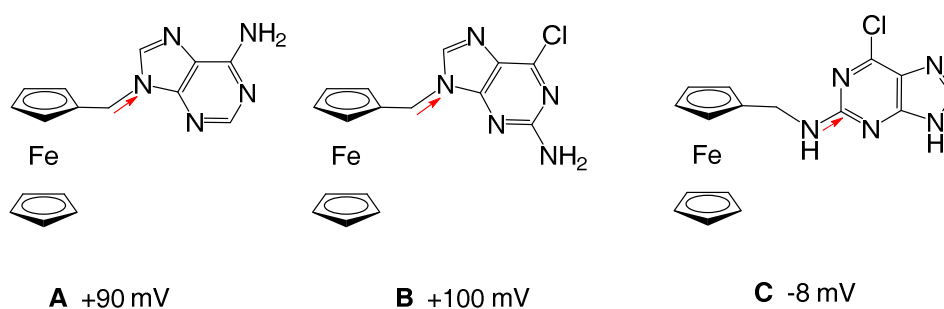
Figure 2-17: *Formal electrode potentials (vs. ferrocenium–ferrocene) for the ferrocenyl-methyladenine A and related derivatives B and C obtained from cyclic voltammetry (scan rate 500 mv.s^{-1})*

In view of these elements, it can be postulated that bis-substituted ferrocenyl derivative **11**, **24** and **28** are more difficult to oxidise than their mono counterparts **22a**, **24a** and **28a**

because they contain twice as much nucleobases and thus ferrocenyl moiety oxidation is made more difficult by the electron withdrawing effect of the two nucleobases.

Electrochemical reversibility of the six compounds was also determined. Their reversible linear profiles are presented in Figure 2-18.
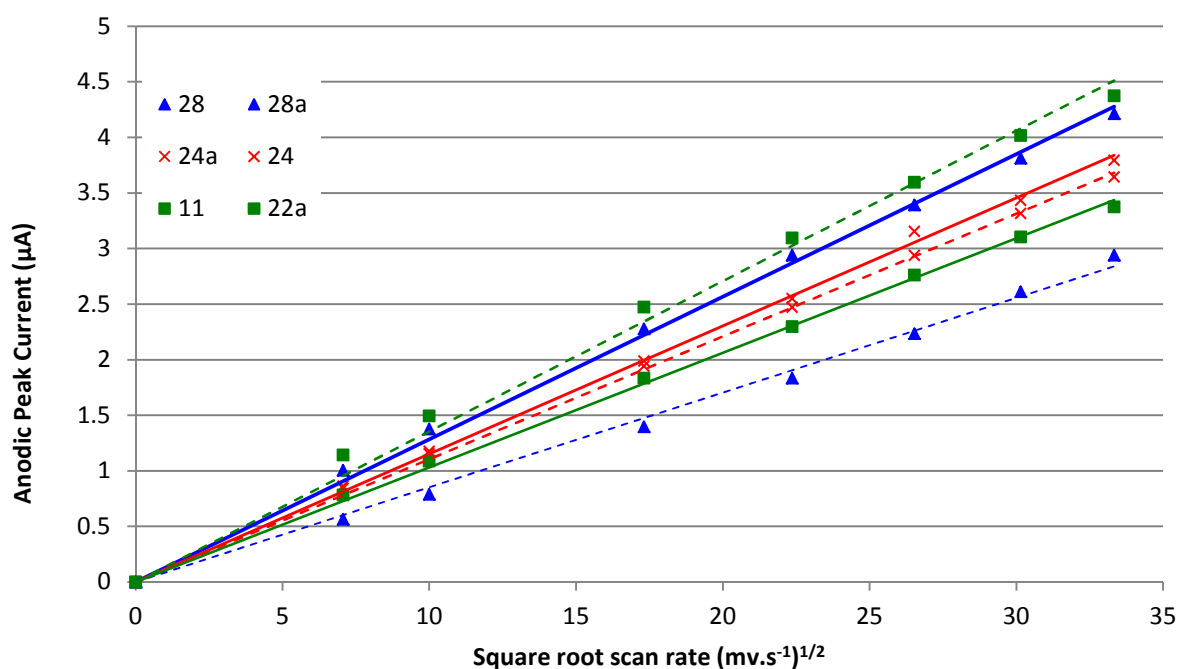
Figure 2-18: Electrochemical reversibility plots of 11, 22a, 24, 24a, 28 and 28a

2.5.3   Effect of the nucleobases

The influence of the type of nucleobase linked to ferrocene and their influence on the electrode potential was then investigated. As can be seen in Table 2-7, adenine ferrocenyl derivatives are the most difficult to oxidize, followed by uracil ferrocenyl derivative and finally cytosine ferrocenyl derivatives.

Table 2-7: *Effect of the type of nucleobase on the electrode potential of the ferrocenyl moiety. Electrode potentials, $E^{0'}$, where $E^{0'}= (Epa + Epc)/2$, are referenced to decamethylferrocene (ca. 1 mM), which was used as an internal reference. The confidence limit is ± 5 mV.*

	Adenine	Uracil	Cytosine
	11	**24**	**28**
$E^{0'}$ (mV)	624	597	573
	22a	**24a**	**28a**
$E^{0'}$ (mV)	583	574	563

Houlton compared the electron-withdrawing environment of adenine derivative **A** with the *N*-1 of cytosine derivative **D** and the *N*-3 of uracil derivative **E**.[3] In the cytosine derivative, the *N*-1 is adjacent to one carbonyl group (C_2) and one alkene moiety (C_6), and the formal potential of the compound was +74 mV compared to ferrocene. In the case of **E** where uracil is substituted at the *N*-3 position, the two carbonyls (C_2 and C_4) increase the electron withdrawing effect, resulting in a higher formal potential compared to ferrocene (+135 mV). (Figure 2-19)

A +90 mV   **D** +74 mV   **E** +135 mV
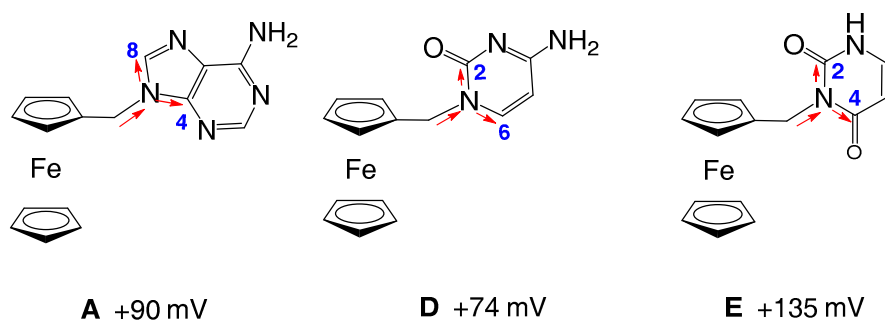
Figure 2-19: *Electron withdrawing effect of uracil, cytosine and adenine and their corresponding formal electrode potentials.*

The nucleobases in compound **A** and **D** are substituted at the same position as compounds **22a** and **28a** and give a very similar trend, with the adenine derivative having a slightly higher electrode potential. However the uracil derivatives **E** and **24a** are substituted differently, which explains the different trend for these compounds. Our studies show that when ferrocene is placed at the position where normally the sugar would be connected, adenine has a more powerful influence on the oxidation of the ferrocenyl moiety than pyrimidines due to the stronger electron-withdrawing environment of the *N*-9 nitrogen.

To conclude, our results are consistent with Houlton's conclusions on the importance of the electron-withdrawing effect of the nucleobases on the electrode potential of the ferrocenyl compounds. They also confirm the importance of the nature as well as the number of nucleobases on the electrochemical behaviour of these ferrocenyl derivatives.

2.6 Conclusion

In this chapter it has been demonstrated that it was possible to successfully attach ferrocene to adenine, uracil and cytosine via different coupling methods, including Horner-Wittig,

Mitsunobu and a bromide substitution. In the case of the bis-adeninyl ferrocene, the Mitsunobu coupling gave a better yield compared to the Horner-Wittig reaction. Cytosine was successfully coupled to ferrocene despite its poor solubility in most usual solvents. However, it would be interesting perform further investigations on this reaction to improve the coupling yield. Crystal structure analysis revealed interesting features such as the formation of elegant assemblies via hydrogen bonding for adenine-containing ferrocenes. Electrochemistry studies exhibit good electrochemical reversibility for the different ferrocene derivatives and demonstrate the importance of the nature of the linker as well as the nature and number of nucleobases on the redox properties.

These results aided our investigations on the synthesis of more complex tetra-substituted ferrocene monomers, with the aim of designing and creating novel types of nucleic acid analogues.

2.7 References

1. A. N. Patwa, S. Gupta, R. G. Gonnade, V. A. Kumar, M. M. Bhadbhade, and K. N. Ganesh, *J. Org. Chem.*, **2008**, *73*, 1508-1515.
2. A. N. Patwa, R. G. Gonnade, V. A. Kumar, M. M. Bhadbhade, K. N. Ganesh, *J. Org. Chem.*, **2010**, *75*, 8705-8108.
3. A. Houlton, C. J. Isaac, A. E. Gibson, B. R. Horrocks, W. Clegg, M. R. J. Elsegood, *J. Chem. Soc. Dalton Trans.*, **1999**, 3229-3234.
4. C. Price, M. Aslanoglu, C. J. Isaac, M. R. J. Elsegood, W. Clegg, B. R. Horrocks, A. Houlton, *J. Chem. Soc. Dalton Trans., 1996,* 4115-4120*.*
5. J. Kumar, C. S. Purohit, S. Verma, *Chem. Commun.*, **2008**, 2526-2528.
6. S. Verma, A. K. Mishra, J. Kumar, *Acc. Chem. Res.*, **2010**, *43*, 79-91.
7. T. Boesen, C. Madsen, U. Henriksen, O. Dahl, *J. Chem. Soc. Perkin Trans. 1*, **2000**, 2015-2021.
8. G. Wittig and G. Geissler, *Liebigs Ann.*, **1953**, *580*, 44-57.
9. R. S. Marmor and D. Seyferth*, J. Org. Chem.*, **1969**, *34*, 748-749.

10. M.-T. Chenon, R. J. Pugmire, D. M. Grant, R. P. Panzica, L. B. Townsend, *J. Am. Chem. Soc.*, **1975**, *97*, 4637-4636.

11. E. White, *Org. Synth.* **1973**, *5*, 336.

12. G. G. A. Balavoine, G. Doisneau and T. Fillebeen-Khan, *Journal of Organometallic Chemistry*, **1991**, *412*, 381-382.

13. M. Kaplus, *J. Am. Chem. Soc.*, **1963**, *85*, 2870-2871.

14. H. V. Nguyen, A. Sallustrau, L. Male, P. J. Thornton, and James H. R. Tucker, *Organometallics*, **2011**, *30*, 5284-5290.

15. D. R. Van Staveren and N. Metzler-Nolter, *Chem. Rev.*, **2004**, *104*, 5931-5985; V. Mamane, *Tetrahedron: Asymmetry*, **2010**, *21*, 1019-1029.

16. W. L. Davis, R. F. Shago, E. H. G. Langner, J. C. Swarts, *Polyhedron,* **2005**, *24*, 1611-1616.

17. K. P. Barry, and C. Nataro, *Inorganica Chimica Acta*, **2009**, *362*, 2068-2070.

18. G. H. Hakimelahi, T. W. Ly, A. A. Moosavi-Movahedi, M. L. Jain, M. Zakerinia, H. Davari, H.-C. Mei, T. Sambaiah, A. A. Moshfegh, S. Hakimelahi, *J. Med. Chem.*, **2001,** *44*, 3710-3720.

19. S. Fletcher, *Tetrahedron Letters*, **2010**, *51*, 2948-2950.

20. K. A. Cruickshank, J. Jiricny, C. B. Reese, *Tetrahedron Letters*, **1984**, *25*, 681-684.

21. Acevedo *et al.*, *US patent 5714606*, **1998**.

22. N. M. Howarth and L. P. G. Wakelin, *J. Org. Chem.*, **1997,** *62*, 5441-5450.

23. M. A. Tius and A. H. Fauq, *J. Am. Chem. Soc.***, 1986**, *108*, 1035-1039.

24. S. Trippett, *J. Chem. Soc.,* **1962***,* 2337.

25. J. Heinze, *Angew. Chem. Int. Ed. Engl.*, **1984**, *23*, 831-847.

26. J. D. Carr, S. J. Coles, M. B. Hursthouse, M. E. Light, J. H. R. Tucker, *Organometallics*, **2000**, *19*, 3312.

27. M. Hocek, P. Stepnicka, J. Ludvik, I. Cisarova, I. Votruba, D. Reha, P. Hobza, *Chem. Eur. J.*, **2004**, *10*, 2058.

CHAPTER 3: TETRA-SUBSTITUTED FERROCENE MONOMERS

3.1 Introduction

In the light of significant work on nucleic acid analogues developed over the past few decades, the Tucker group devised the notion of an organometallic version called ferrocene nucleic acid (FcNA), which is based on ferrocenes linked together via phosphodiester linkages. In order to make a version of FcNA shown in Figure 3-1, the synthesis of appropriate monomer units first had to be successfully achieved.
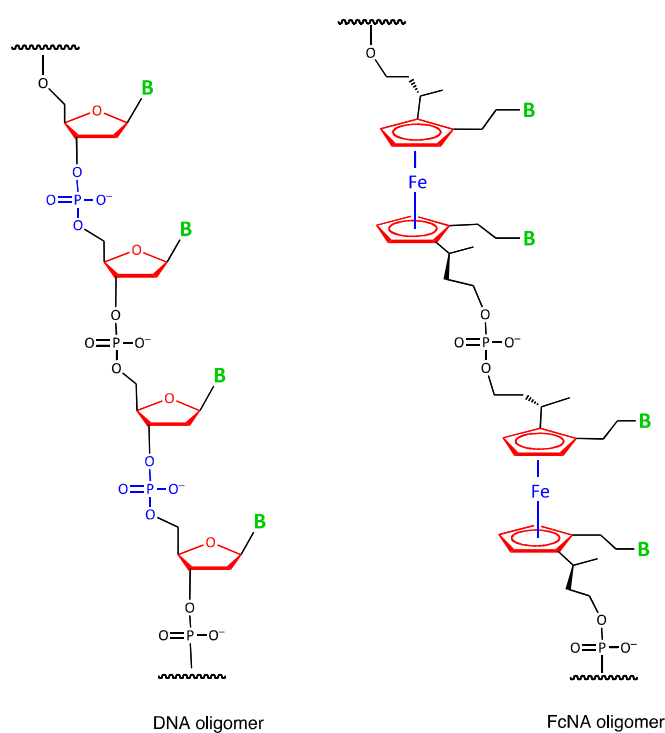
Figure 3-1: DNA and FcNA oligomer (B = Base)

Several factors were taken in account in the synthetic design of the monomer. First of all, a phosphoramidite version of the monomer was required so that the oligomer could be synthesised via automated nucleic acid synthesis. Consequently, each cyclopentadienyl ring

had to be substituted with a "phosphodiester-linker" containing one alcohol moiety. The Cp

rings were also to be substituted with an alkyl spacer group linked to nucleobases to allow

duplex formation via base pairing. Finally, the tetra-substituted ferrocene monomers would

have to be chirally pure, with the monomer units shown in Figure 3-1 each containing four

stereogenic elements.

The synthesis of the monomers can be divided into three sections. The goal of the first part

was to develop a tetra-substituted ferrocenyl precursor. In this step, central and planar

chirality were to be introduced, with C_2 symmetry retained to minimise potential side

reactions. The second part was to deal with construction of the three-carbon

"phosphodiester-linker" groups, consistent with the spacing previously seen in the

literature.[1] The third part was to be concerned with coupling ferrocene to nucleobases

adenine and uracil followed by deprotection.
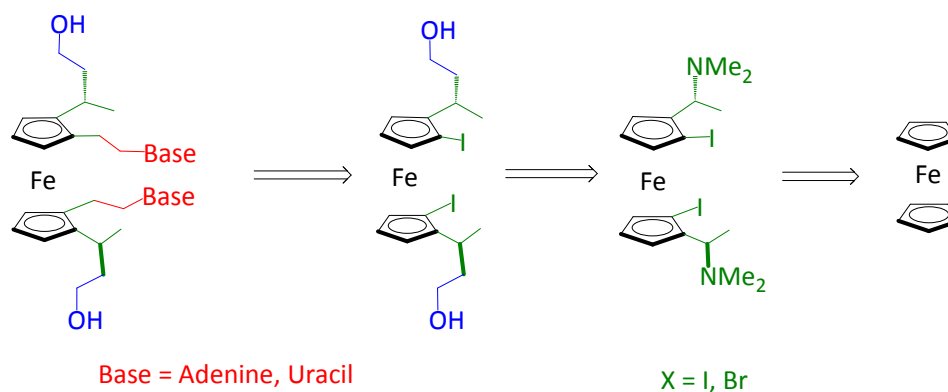
Scheme 3-1: *Retro-synthetic scheme of the synthesis of adenine and uracil tetra-substituted ferrocenyl monomers*

Two tetra-substituted ferrocenyl monomers were eventually synthesised to afford the

targeted diols. These diols were then to be primed for oligomerisation via phosphitylation

and tritylation. The first monomer is a tetra-substituted ferrocene coupled to adenine. Due

to synthetic difficulties encountered using the Horner-Wittig approach that had previously been successfully used to give the thymine target, developed in parallel in the group, a new route had to be investigated using Mitsunobu coupling. The second monomer is a tetra-substituted ferrocene coupled to uracil. This was also synthesised via the same Mitsunobu approach. This route builds on the successful attempts to make bis-functionalised ferrocenes as described in Chapter 2.

3.2   Part 1: Monomer precursor

The main goal of this part was to synthesize a common basic unit for the two tetra-substituted ferrocene monomers. Starting from ferrocene, the first key-step corresponded to the introduction of two specific chiral centres on the α-positions of the ferrocene. The second key-step involved the introduction of planar chirality via a halogen substitution on each Cp ring. (Scheme 3-2)
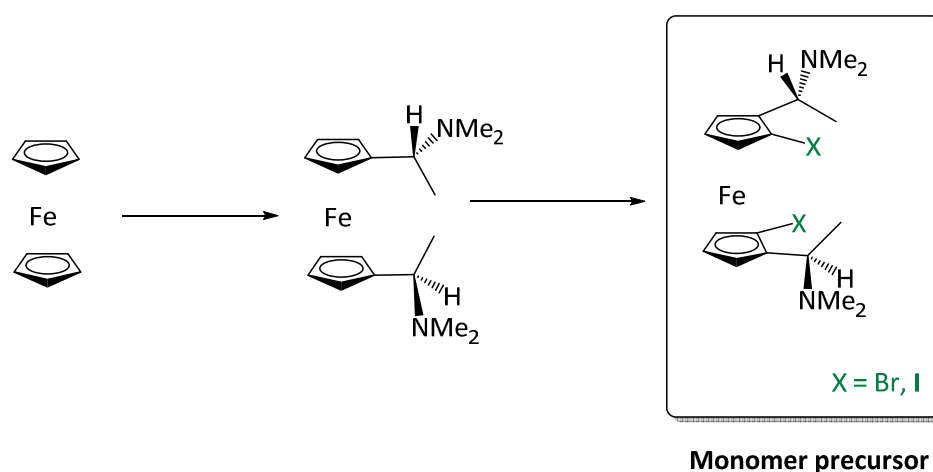
Scheme 3-2: *The two first key-steps for the synthesis of the precursor of the tetra-substituted ferrocenyl monomers*

This halogenation is actually based on a directed *ortho*-metallation involving a chiral dimethylamine ferrocene and a lithium base. The mechanism of this induced-halogenation is

based on interaction between lithium and the dimethyl amine group, as shown in Figure 3-2. The mono-substituted monomer instead of the bis-substituted monomer is shown for clarity purposes.
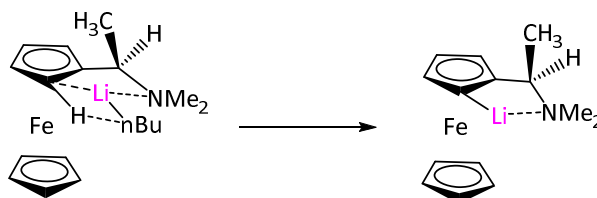
Figure 3-2: Ortho-lithiation of Ugi's amine

Ugi[2] explained that stereoselectivity of the *ortho*-metallation can be induced by a stereogenic chiral centre situated on the α-position of the ferrocene. In the case of a chiral *R*-α-*N,N*-dimethylaminoethyl ferrocene treated with *n*-BuLi, he showed that proton H^2 and H^5 were replaced by lithium with a 96:4 selectivity ratio. This ratio can be explained by the position of the methyl, which is slightly above the Cp ring when butyllithium is interacting with nitrogen. Indeed, this conformation is energetically lower than when the methyl is closer to the iron. Considering *R* configuration of the chiral centre, H^2 is more likely to be replaced by lithium than H^5, as shown in Scheme 3-3.
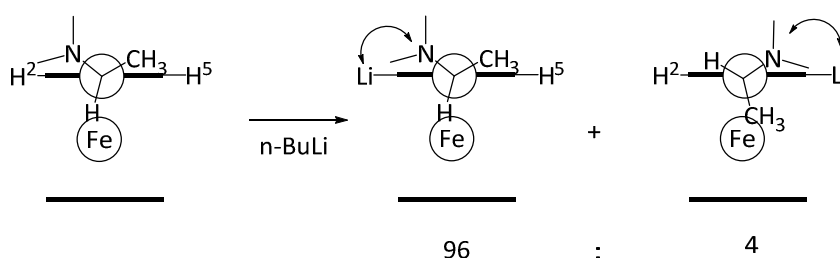
Scheme 3-3: Ugi's abstraction[2] of ortho-H on a mono substituted ferrocene

Butler[3] and Knochel[4] supported this theory via 2D-NMR and NOE (Nuclear Overhauser Effect) experiments. To conclude, the diastereoselectivity of this ortho-metallation is highly influenced by the configuration of the chiral centre and leads to a highly selective substitution.

As explained above, depending on the configuration of the stereogenic carbon centre, two ortho-positions could be considered for the introduction of the halogen: **a** and **b** giving respectively compounds **A** (R,R,S_p,S_p) and **B** (S,S,R_p,R_p). (Scheme 3-4)
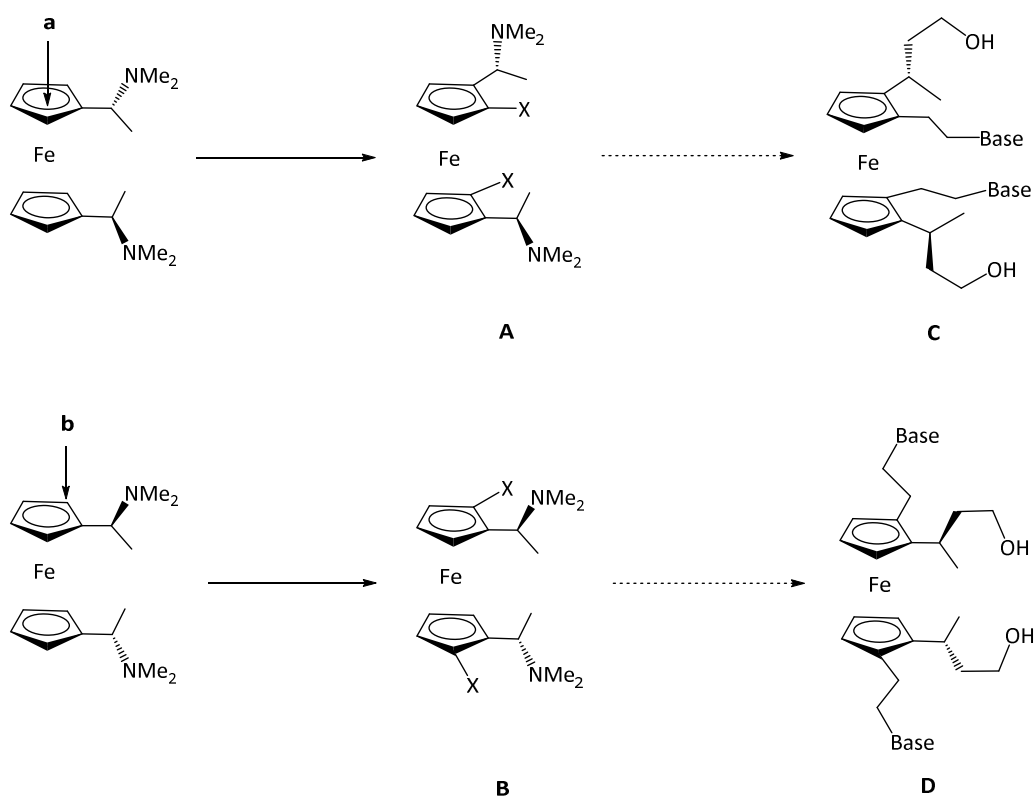
Scheme 3-4: *Introduction of the base linkers on the ortho-position*

A modelling study within the group indicated that either enantiomer (**C** or **D**) could be placed within a B-DNA duplex structure but enantiomer **C** gave the more stable duplex according to modelisation, consequently it was decided to start with the synthesis of **C**.

The monomer precursor was synthesised in five steps as summarised in Scheme 4. Ferrocene was first acylated and then reduced in order to obtain α-chiral diol **31**. Acetylation was followed by a nucleophilic substitution leading to the dimethylamine **33**. The dimethylamine ferrocene was then substituted at its *ortho* position to give **34**. Some of the mechanisms are discussed in the following sections.
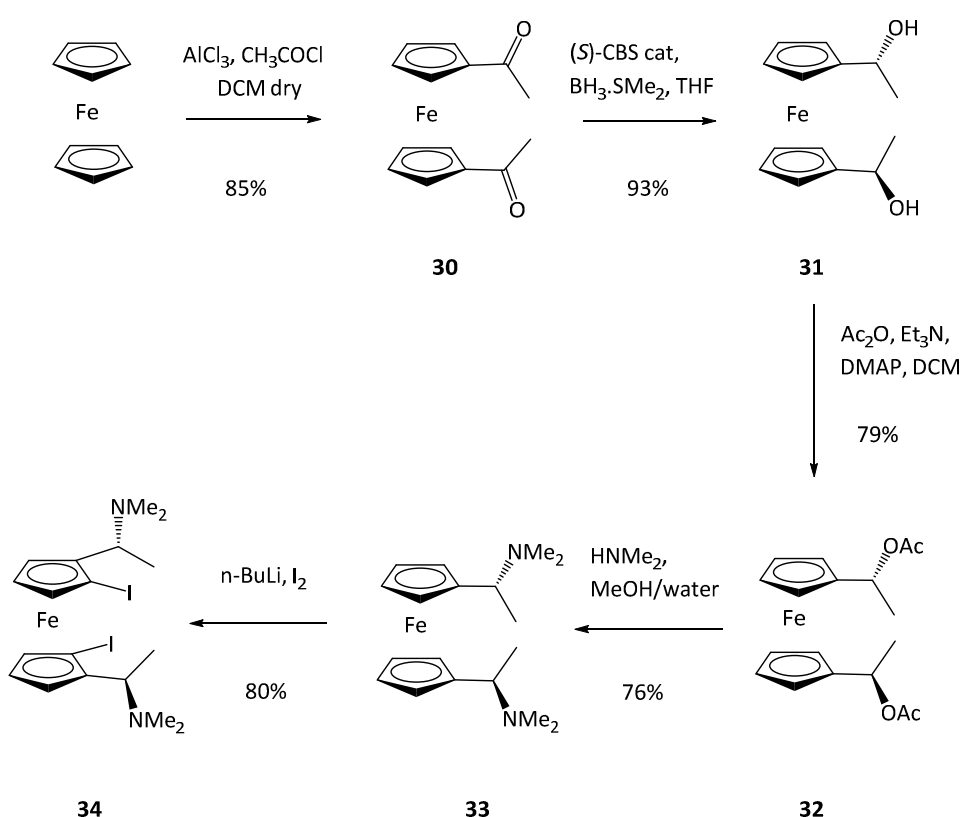
Scheme 3-5: *First part synthesis scheme*

3.2.1 Friedel-Crafts Acylation

Acylation was one of the first reactions performed on ferrocene after its discovery.[5] In the presence of aluminium chloride and acetyl chloride, ferrocene can be acylated in DCM to give 1,1'-diacetylferrocene. The mechanism is based on the Friedel-Crafts reaction, which

attaches electrophiles to aromatic rings. An acylium ion is formerly produced by the reaction of acetyl chloride with aluminium chloride, which acts as a Lewis acid. Ferrocene attacks the acylium producing the bis-ketone ferrocene and releasing HCl. Slightly more than one equivalent of the catalyst (aluminium chloride) is used per mole of reagent because the first mole of catalyst forms a complex with the carbonyl of the reagent. (Scheme 3-6)

Acylium ion

30
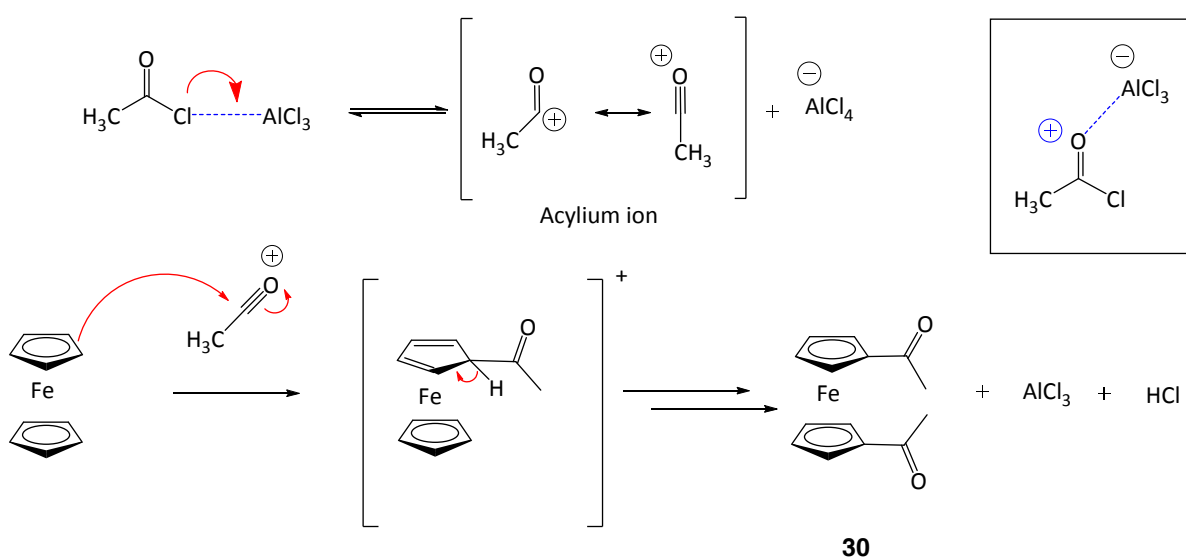
Scheme 3-6: Friedel-Crafts acylation

1,1'-Diacylferrocene **30** was obtained via this method in a yield of 85%. ^{13}C NMR shows a peak at 177 ppm characteristic of the ketone carbonyl.

1.1.1 Enantioselective reduction of ketone

Reduction of ketones consists of addition of two hydrogens to the carbon-oxygen bond of the carbonyl, leading to the formation of an alcohol. This is usually done via a strong reducing agent such as lithium aluminium hydride or sodium borohydride. Non-symmetrical ketones are prochiral and depending on which face of the carbonyl is attacked, two enantiomers can be obtained (*R* or *S*). In the case of reduction with LiAlH$_4$ or NaBH$_4$, there is

no distinction between the two faces for the attack of the hydrogen, which leads to a racemic product. Interest in enantioselective reduction of ketones led to the development of chiral reducing agents that could direct the reduction towards a specific enantiomer. In the 1980's, Itsuno and his group[6,7] reported the enantioselective reduction of achiral ketones using a chiral amino-alcohol (S-Valinol) in presence of BH_3.THF (Scheme 3-7). Further developments with this approach improved the enantioselectivity of the reduction. It was only with the work of Corey, Bakshi and Shibata[8,9] that the mechanism of this reaction was clarified. It goes through the formation of a chiral oxazaborolidine by reaction of the tertiary amino alcohol (valinol derivative) with BH_3.
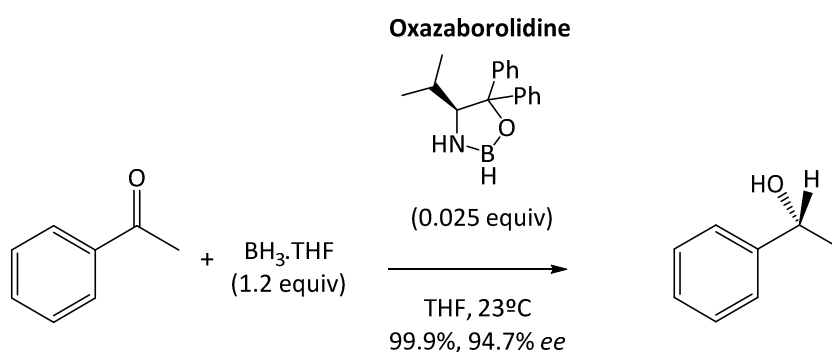
Scheme 3-7: *Enantioselective reduction of ketone via oxazaborolidine*

Corey *et al.* found out that the Corey-Bakshi-Shibata catalyst, inspired by Itsuno's oxazaborolidine, gave much better results towards the enantioselective reduction of ketones. (Scheme 3-8)
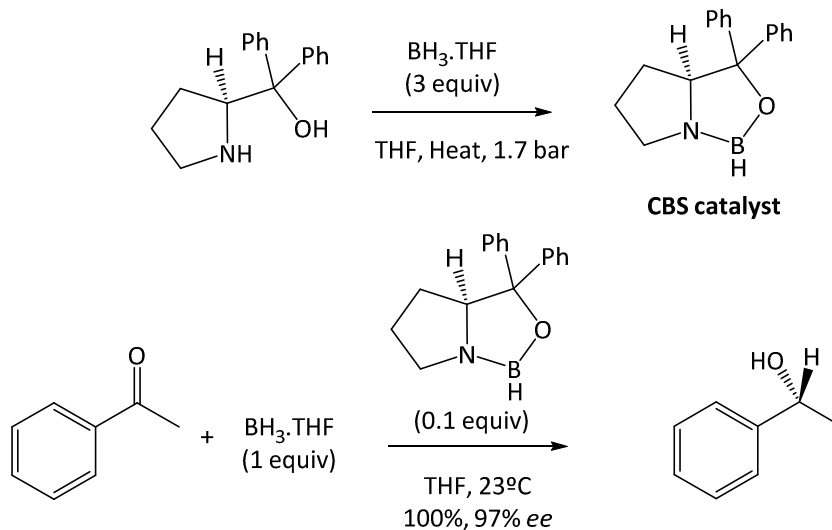
Scheme 3-8: *CBS enantioselective reducing agent developed by Corey et al.*

To further understand the stereochemistry of the reaction, Corey *et al.* developed a mechanistic model represented in Scheme 3-9. [10]
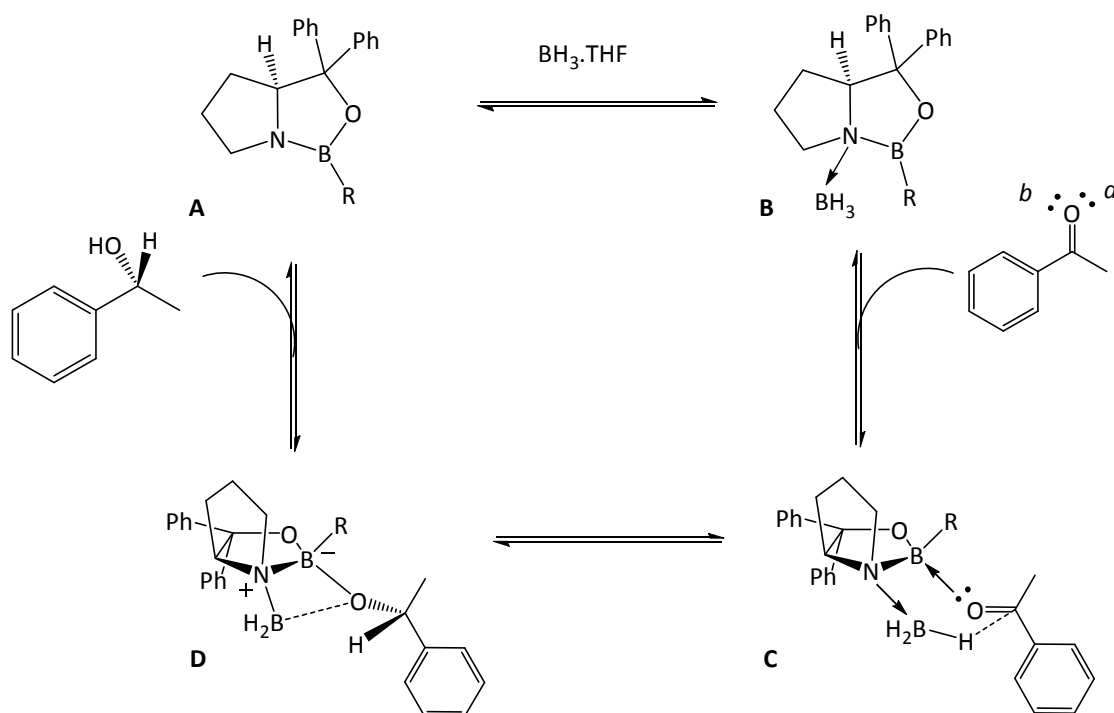
Scheme 3-9: *Mechanistic model proposed by Corey for the enantioselective reduction of ketone by CBS catalyst*

The first step of the reaction is the coordination of BH_3 to the nitrogen of the oxazaborolidine **A** to form complex **B**. This activates BH_3 as a hydride donor and activates the Lewis acidity of the heterocyclic boron atom. Both activated sites enhance binding to the ketone. To minimise steric interactions, the ketone binds complex **B** by the less hindered electron pair of the oxygen (a) in syn-configuration towards BH_3 with the phenyl group being in pseudo equatorial position, forming a six-member ring transition state. The reduction occurs via hydrogen transfer, forming a chair or a boat transition state. The catalyst is then regenerated by cyclo-elimination.

The CBS catalyst has demonstrated its efficiency through numerous applications over the last decades and was consequently chosen for the reduction of 1,1'-diacylferrocene **30** following the procedure developed by Schwink and Knochel[4] . The (*S*)-isomer of the catalyst was used in the presence of borane dimethylsulfide (BMS) to give the desired (*R,R*) diastereoisomer **31**, in 93% yield. (Scheme 3-10)
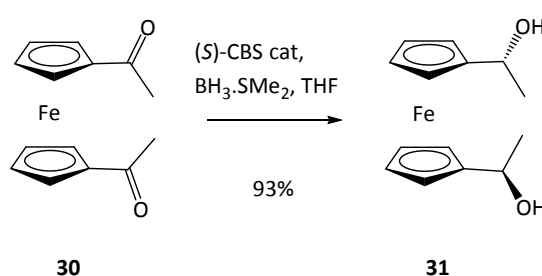
***Scheme 3-10:** Ketone reduction using (S)-CBS catalyst*

The ^{1}H NMR of **31** gives a quadruplet at 4.68 ppm that integrates for 2H, corresponding to the two protons of the chiral carbons of **31**. The singlet at 4.34 ppm also integrates for 2H

and corresponds to the two alcohol protons. Its ^{13}C NMR spectrum confirmed the disappearance of the carbonyl peak.

1.1.2 Acetylation

Since Ugi's work in 1970,[2,11] it has become well established that the α-chiral primary alcohol on ferrocenes can be substituted with various nucleophiles with retention of configuration. Schwink and Knochel[4] described interesting acetylation examples involving bis-α-chiral hydroxyferrocenyl systems as well as their ruthenocene analogues. Using Knochel's procedure, acetic anhydride was added to a solution of **31** in DCM followed by DMAP and triethylamine. The acetic anhydride is activated by DMAP releasing acetic acid. Then **31** attacks the activated carbonyl to give the protonated form of the final acetyl derivative (*R,R*)-1,1'-bis(α-acetoxyethyl)ferrocene **32.** The acetic acid deprotonate it and react finally with Et3N to form the corresponding salt. (Scheme 3-11)
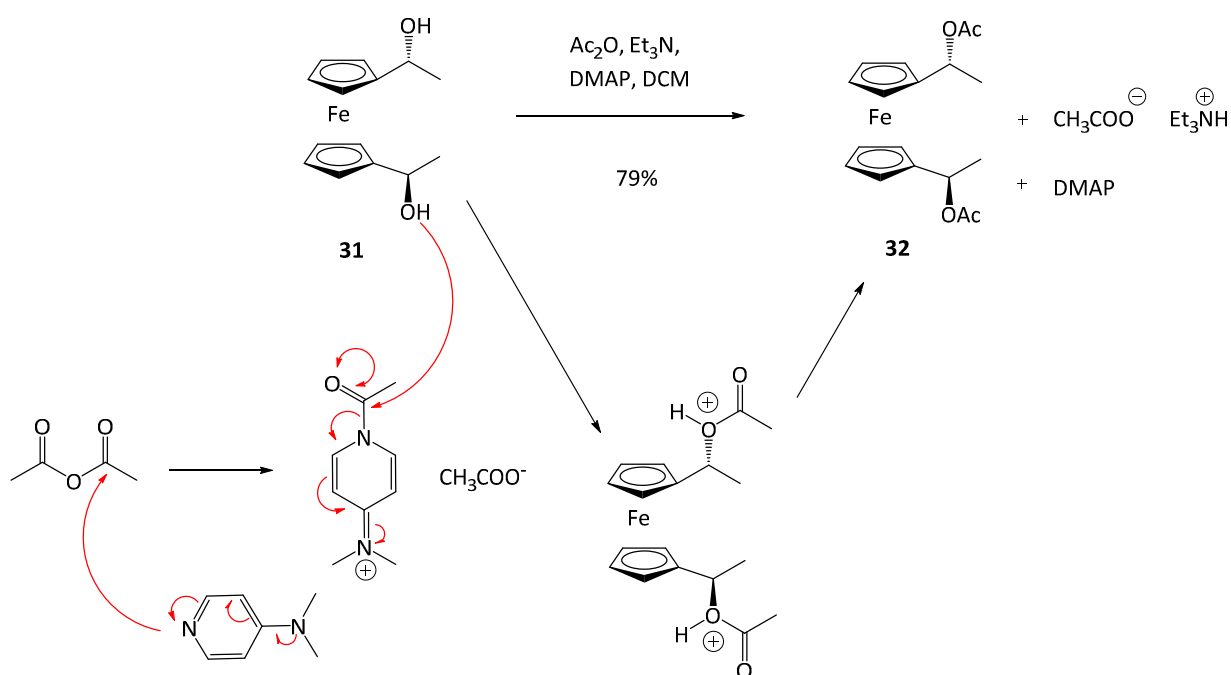
Scheme 3-11: *Acetylation step*

An attempt at purification of the crude product on silica or alumina led to partial degradation of **32**. To overcome this problem, 1% of TEA was added to the eluent to neutralise the silica and improve purification. The ^{1}H NMR spectrum of **32** shows a characteristic singlet at 2.05 ppm integrating for 6H and corresponding to the methyl of the acetyl group of **32**. Analysis of the proton decoupled ^{13}C NMR spectrum shows a carbonyl peak at 170.44 ppm.

1.1.3   Dimethylamine substitution

The reaction involved in this step is a S$_N$1-type substitution involving an α-ferrocenyl carbenium intermediate as described by Ugi[9]. Ferrocene can in fact stabilise a positive charge in the vicinal position of a side chain. This has been justified by iron participation[12] or iron hyperconjugation[13] involving an HOMO-LUMO interaction between d orbitals of the iron and the p orbital of the carbocation. The mechanism of the reaction is based on the departure of the leaving group to give the carbocation. The positive charged is then stabilised, possibly by electronic participation of the iron,[12] as shown in Scheme 3-12. The nucleophilic substitution occurs with retention of configuration via attack on the carbenium on the exo-side.
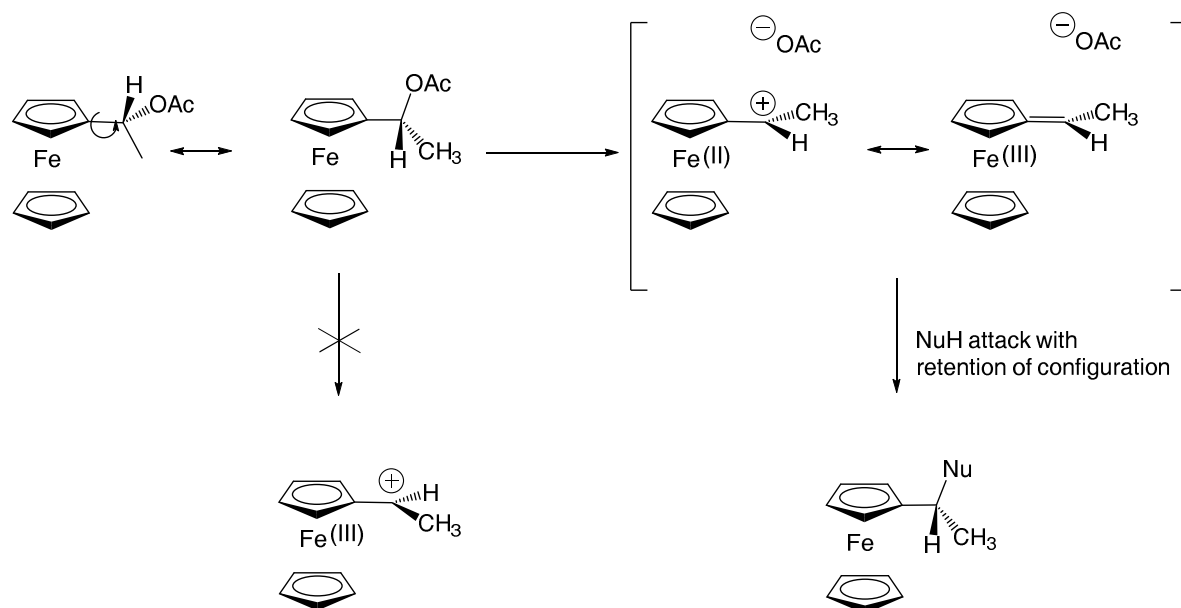
Scheme 3-12: *Carbenium intermediate and nucleophilic attack with retention of configuration*

Schwink and Knochel[4] reported this reaction in methanol/water and obtained the (*R,R*)-1,1'-bis(α-*N*,*N*-dimethylaminoethyl)ferrocene **33** with a yield of 91% and 98% retention of configuration. (Scheme 3-13)
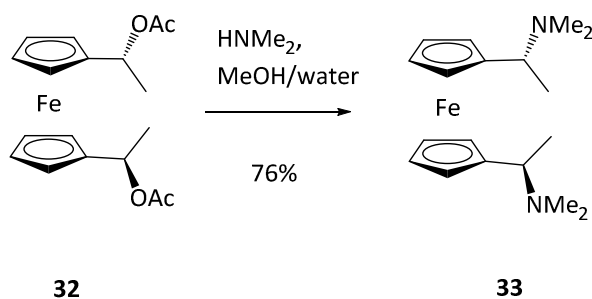
Scheme 3-13: *Dimethylamine substitution*

Following the same procedure, (*R,R*)-**33** was obtained in 76% yield. Its ^{1}H NMR spectrum showed a singlet at 1.98 ppm integrating for 12H and corresponding to the four methyl

groups on the two amines. Analysis of the proton decoupled ^{13}C NMR spectrum revealed the disappearance of the carbonyl peak.

1.1.4 Directed ortho-halogenation

The main challenge of this reaction was to attach a halogen at the right position to obtain the desired nucleobase linkers. One of the most efficient ways[14] to prepare enantiopure planar chiral ferrocenes involves a directed *ortho*-metallation described by Ugi, as previously mentioned (introduction of Part 1). The *ortho*-halogenation involves *ortho*-lithiation in position 1 of the ferrocene using *n*-BuLi followed by lithium-halogen exchange that leads to the 1,1'-(dimethylaminoethyl)-2,2'-dihalogeno ferrocene **34**. (Scheme 3-14)
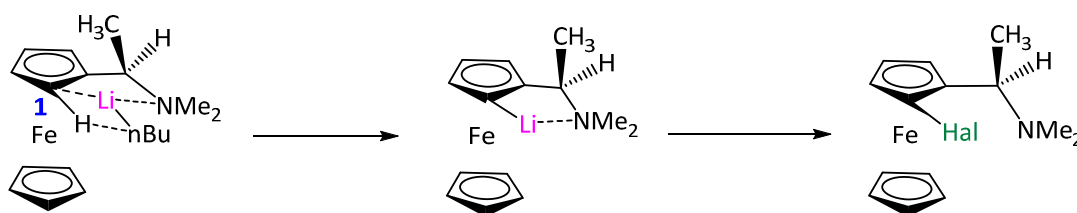
Scheme 3-14: Ortho-halogenation via lithium-halogen exchange in position 1

As described in Scheme 3-15, three mechanisms have been put forward to explain the lithium-halogen exchange:[15] a) "Four-centred transition state model"; b) radical transfer between lithium and halogen leading to an exchange of substituents; c) formation of an "ate" complex intermediate, leading to the nucleophilic substitution of the lithium by the halogen.
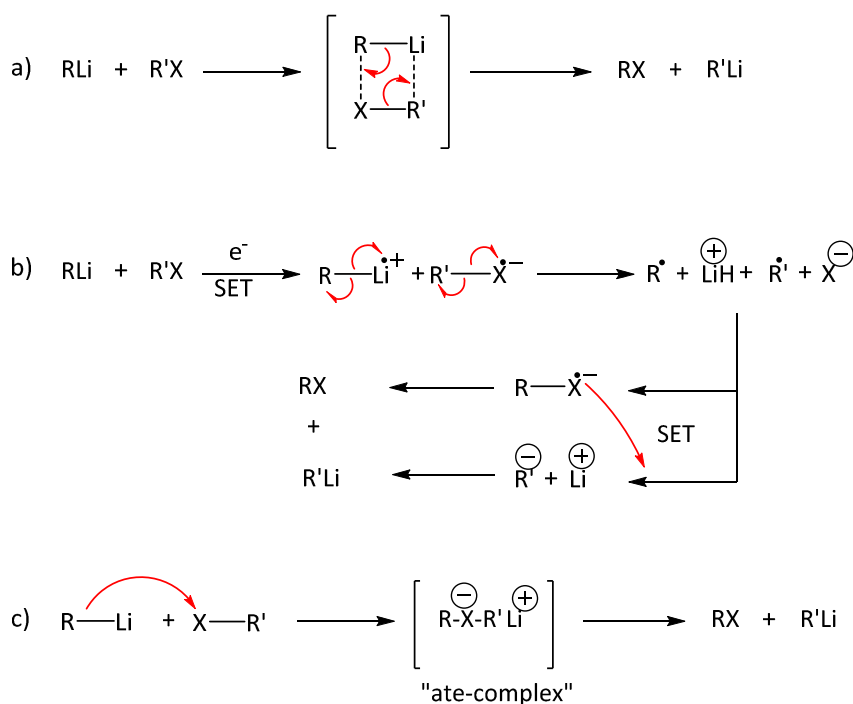
Scheme 3-15: *Three possible lithium-halogen exchange mechanisms*

Kang *et al.*[16] reported bromide substitution on a dimethylaminopropyl ferrocene with 1,2-dibromotetrachloroethane as a halogen source. They obtained a single diastereoisomer of the dibromoferrocene with retention of configuration in 84% yield. Based on this procedure, only lithium-bromide and lithium-iodide exchange were investigated. Indeed, organic fluoride and organic chloride are known to not undergo metal-halogen exchange as shown by Gilman.[17]
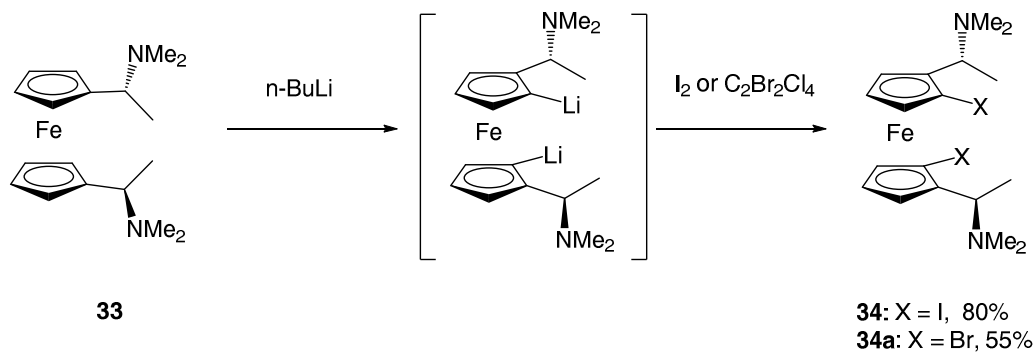
Scheme 3-16: *Ortho-metallation of (R,R)-1,1'-bis-(α-dimethylaminoethyl)ferrocene.*

Halogenation with iodine was achieved in 80% yield (**34**) compared to 55% with $C_2Br_2Cl_4$ (**34a**). As shown by Gilman[18], the halide exchange rate is faster with iodide, which could explain the difference in yields. Iodine was therefore chosen as t he suitable halogen for future reactions. ^{1}H NMR analysis revealed the ferrocene protons integrating for 6H instead of 8H, proving disubstitution on each Cp ring. Analysis of the proton decoupled ^{13}C NMR spectrum gave a peak at 88.22 ppm corresponding to the *ipso* carbon bonded to bromide and 90.8 ppm for the *ipso* carbon attached to iodine, confirming halogenation in each case.
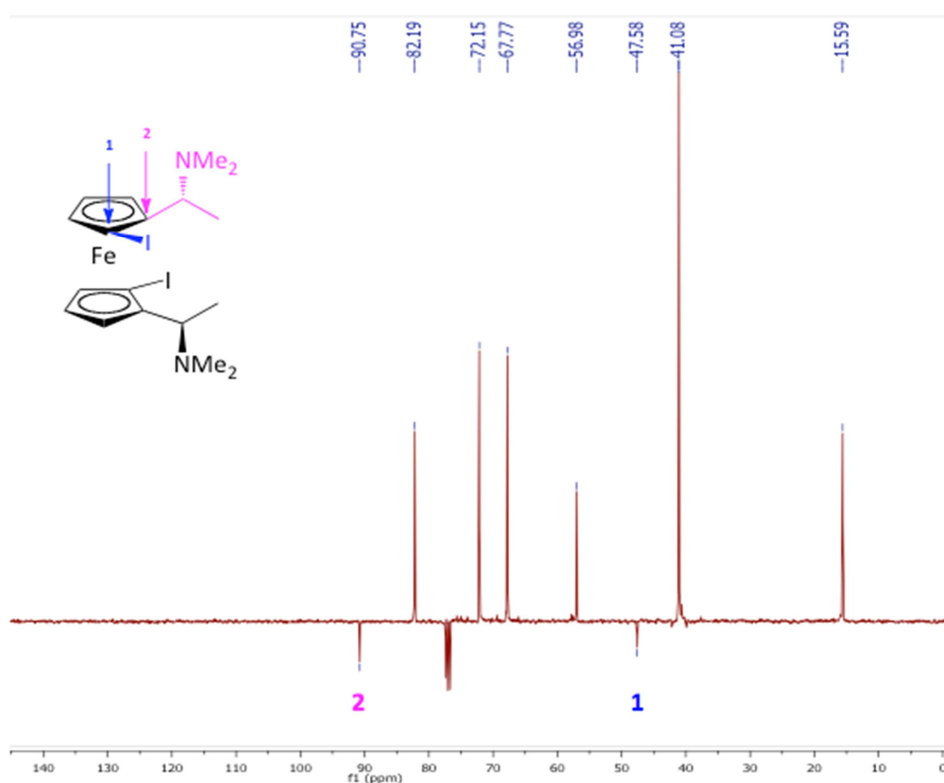
Figure 3-3: *Proton decoupled Pendant ^{13}C NMR spectrum of 34 in CDCl$_3$*

With the introduction of planar chirality, the configuration of compounds **34** and **34a** were assigned (*R,R,S$_p$,S$_p$*) as presented in Figure 3-4.

Central chirality

34 *(R,R)*   34a *(R,R)*

Planar chirality
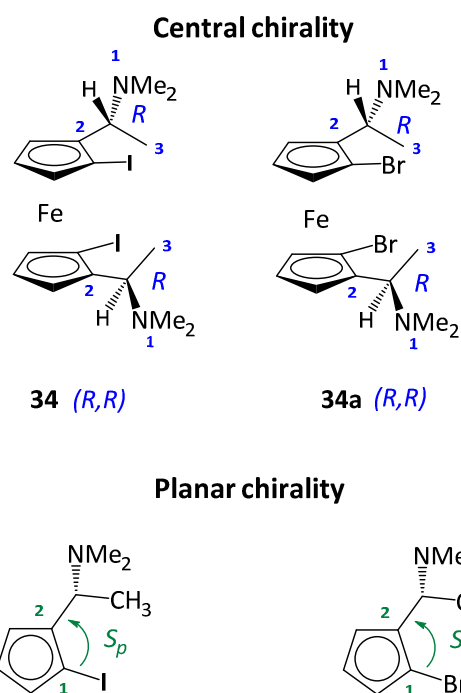
Figure 3-4: *Chirality determination of 34 and 34a*

To check the enantiopurity at this stage of the synthesis, the specific optical rotation of **34** and its corresponding isomer was measured in DCM with a polarimeter: $[\alpha]_D$ (c = 0.0053 g/mL) = +178.8 and the opposite enantiomer synthesised by Dr. Nguyen, postdoc in the Tucker group, gave $[\alpha]_D$ (c = 0.0054 g/mL) = -192.5. Considering the 0.5% instrumental error of the polarimeter on the optical rotation displayed, the two absolute values are similar, suggesting a good enantiomeric ratio in favour of **34**. Chiral analysis using chiral high-performance liquid chromatography (HPLC) was then performed to prove enantiopurity. It revealed a single peak at 4.6 min using 10% IPA in hexane as eluent mixture. Using peak areas for the two enantiomers, the enantiomeric excess ratio was calculated as >99.9% for the (R,R,S_p,S_p) enantiomer. The chiral HPLC graphs are shown in the appendix. (Figure 7-5, 7-6 and 7-7)

To conclude, compound **34**, the precursor to linker elongation and nucleobase coupling, was successfully synthesised. HPLC demonstrated that **34** was synthesised in high chiral purity.

3.3   Part 2: Linker extension

The second part of the synthesis was focused on the extension of the three-carbon "phosphodiester-linker" of the tetra-substituted ferrocenyl precursor. A six-step route was investigated, going through acetylation and reduction, methoxylation, formation of an ester using silyl enol ether, ester reduction and finally protection of the alcohol via benzylation. A summary of the synthesis is shown in Scheme 3-17.
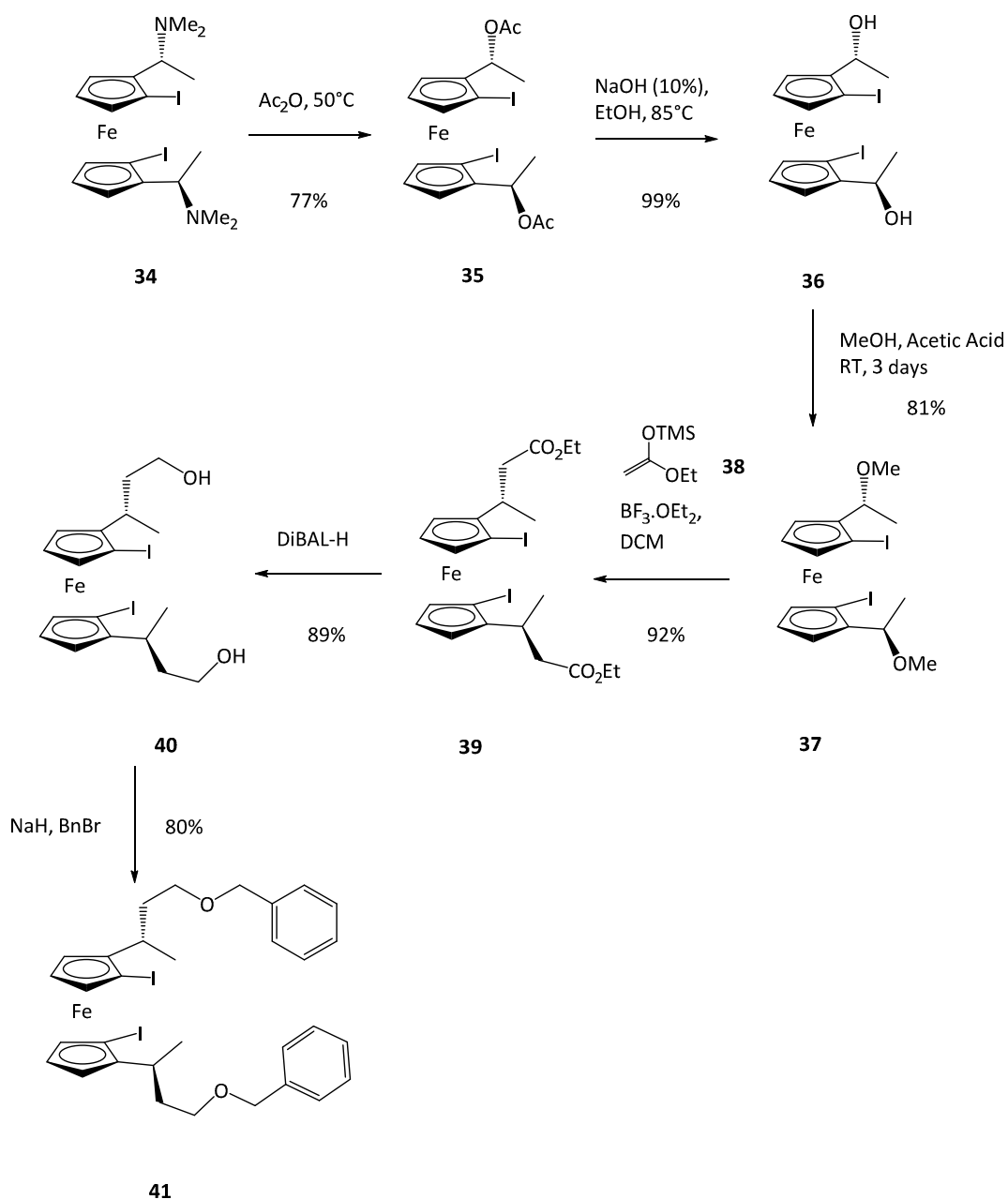
Scheme 3-17: *Linker extension synthesis*

3.3.1   Acetylation and reduction

In the context of studying the influence of a ferrocenyl diphosphine on the palladium-catalysed asymmetric alkylation of diphenylpropenyl acetate, Kang and coworkers[19] reported acetylation of dibromo-dimethylamine ferrocene using acid anhydride at 70°C for 10 h in 85% yield, followed by reduction using KOH, leading to the corresponding alcohol with complete retention of configuration in 99% yield. Following Kang's procedure, the acetylation was performed on **34** at 50 °C for 2 h instead of 10 h at 70°C to avoid degradation. The desired iodine derivative (R,R,S_p,S_p)-**35** was obtained in 77% yield. Analysis of the proton NMR spectrum of the acetate gave a singlet at 2.04 ppm, which integrated for 6H corresponding to the methyls groups of the acetate. However **35** was not stable, so its hydrolysis was done straight away after purification. The reduction was then performed in ethanol by heating at 85 °C for 15 min. After quenching the reaction with water and extraction with DCM, the crude product was checked by ^{1}H NMR spectroscopy and the resulting spectrum was very clean. The crude was purified on silica gel column to eliminate all eventual traces of salts formed during the reaction. The methyls signal had disappeared and a new broad singlet at 2.5 ppm integrating for 2H was assigned to the hydroxyl protons. The reduction gave (R,R,S_p,S_p)-**36** in 99% yield. (Scheme 3-18)
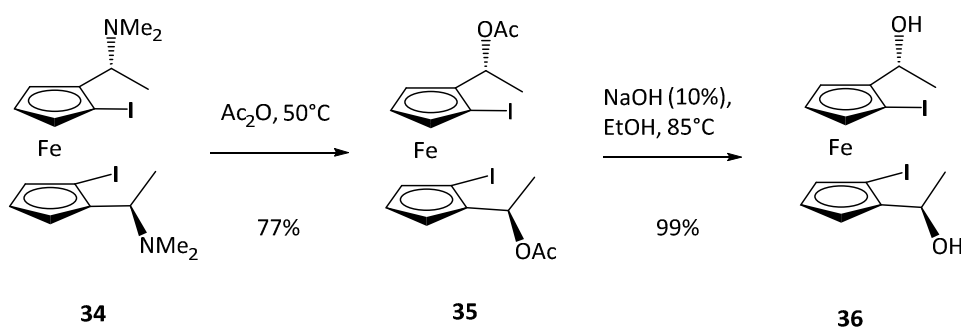
Scheme 3-18: *Acetylation and reduction from the diaminoferrocene*

Both reactions occur via the previously described S_N1-type mechanism involving the ferrocene carbenium intermediate stabilised by electronic interaction with the iron. Optical rotation was determined and gave $[\alpha]_D$ (c = 0.0061 g/mL, DCM) = +95.0 for **36** and $[\alpha]_D$ (c = 0.0060/mL g, DCM)= -92.0 for the opposite enantiomer also synthesised by Dr. Nguyen. Chiral HPLC was performed on the acetate **35** and the alcohol **36** to confirm the enantiopurity over these two steps. Both compounds were eluted with 10% IPA in hexane. **35** gave a peak at 18.4 min, giving an enantiomeric excess ratio of 99% and **36** at 28.8 min, giving an enantiomeric excess ratio of >99.9%. The chiral HPLC graphs are shown in the appendix. (Figure 7-8, 7-9 and 7-10)

3.3.2   Methanolysis and esterification

Locke *et al.*[20] synthesised a C_2 symmetric ferrocenophane via Friedel-Crafts cyclisation (Figure 3-9) via methoxylation and esterification of a bis-benzyloxy ferrocene.
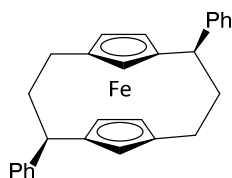
Figure 3-5: *Ferrocenophane*

Methoxylation gave a relatively low yield of 42% in the presence of a 9:1 methanol/acetic acid mixture stirred overnight. The following esterification was performed using a silyl enol ether and $BF_3.OEt_2$ and gave a 98% yield with 92% *ee* for the diester. (Scheme 3-19)
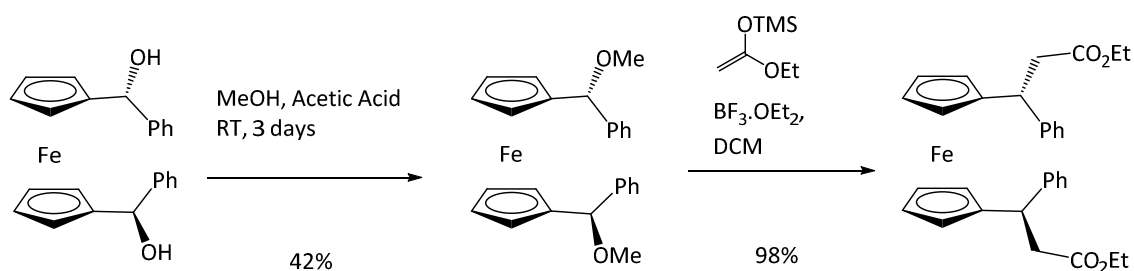
Scheme 3-19: Methoxylation and esterification by Lock, Richards and coworkers[20]

The same synthesis scheme was therefore followed for the synthesis of **39**. Methoxylation of

(*R,R,S$_p$,S$_p$*)-**36** was performed keeping the 9:1 methanol/acetic acid conditions but running

the reaction for three days, leading to a two-fold improvement in the yield of product

(*R,R,S$_p$,S$_p$*)-**37** (81%). The optical rotation of the compound was measured, giving $[\alpha]_D$ (c =

0.0054 g/mL, DCM) = +149.6 for **37** and $[\alpha]_D$ (c = 0.0054 g/mL, DCM) = -155.6 for the

corresponding enantiomer synthesised by Dr. Nguyen. For the esterification of **37**, it was

necessary to synthesize one essential reagent: silyl enol ether **38**. Silyl enol ether is usually

prepared from ketones using a strong base and trimethylsilyl chloride (TMSCl). Fukuzumi and

co-workers[21] described its synthesis from ethyl acetate using diisopropylamine, *n*-BuLi and

trimethylsilyl chloride for the enolate protection, as shown in Scheme 3-20.
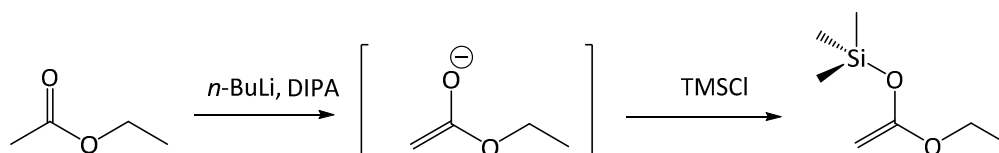
Scheme 3-20: Silyl enol ether synthesis

The same procedure was followed and the crude was purified on a Kugelrohr at 50 °C under

vacuum. Analysis of the ^{1}H NMR spectrum revealed the presence of ethyl acetate and

hexane. The boiling points of the silyl enol ether and these solvents are quite close, making the distillation step difficult.

The formation of the ester was attempted anyway following the method used by Richards and coworkers in 1994.[22] Richards *et al.* investigated the reaction with different types of silyl enol ethers and stabilised or unstabilised α-carbenium ferrocenes. They prepared carbenium ions via addition of HBF_4 on a mono (α-hydroxyethyl)-ferrocene that they reacted with a series of silyl enol ethers in the presence of $BF_3.OEt_2$, leading to the corresponding esters (Scheme 3-21). They showed that the success of the reaction did not depend on the relative stability of the carbenium and proceeded with retention of configuration.
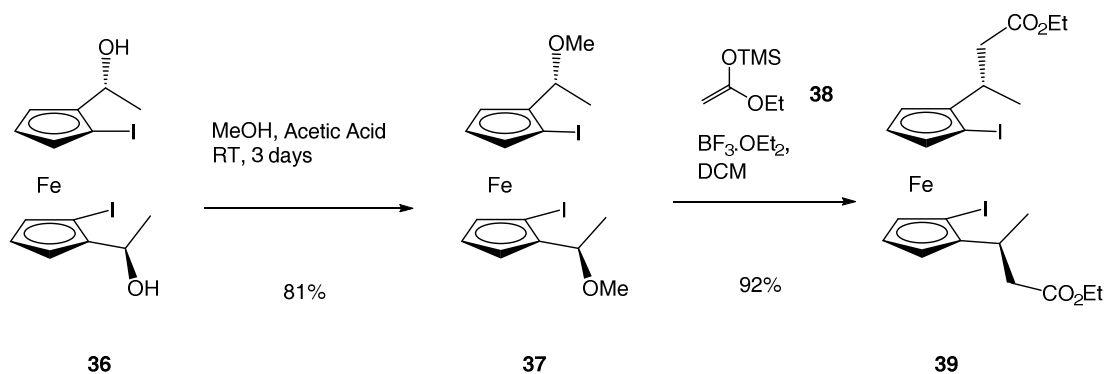
Scheme 3-21: *Extension of a three carbons chain by esterification*

Esterification of **37** adds two more carbons to the linker chain via nucleophilic attack of the enol ether on the ferrocenyl carbenium. It is worth pointing out that the absolute configuration of the two centrally chiral carbons during this step as shown in Figure 3-6.

Central chirality

37 *(R,R)*   39 *(S,S)*
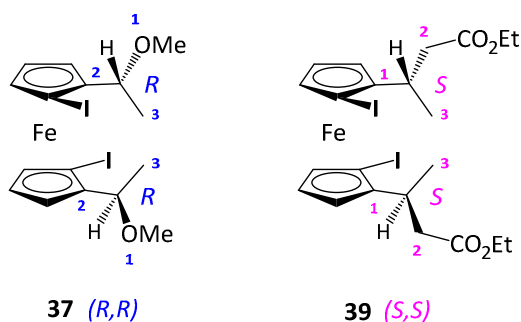
Planar chirality
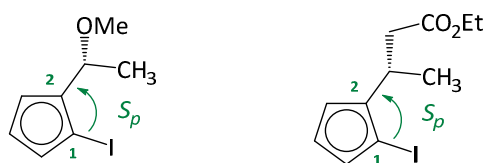
Figure 3-6: *Chirality assignment of 37 and 39*

The reaction was done with a considerable excess of silyl enol ether (> 4 fold) to take into account the ethyl acetate impurity. However, the product (S,S,S_p,S_p)-**39** was obtained in the high yield of 92%. The optical rotation of the compound was measured giving $[\alpha]_D$ (c = 0.0066 g/mL, DCM) = +123.0 and $[\alpha]_D$ (c = 0.006 g/mL, DCM) = -112.6 for the opposite enantiomer. The absolute optical values of the two enantiomers are slightly different but chiral HPLC clearly showed an enantiomeric excess >99.9%, with one single peak obtained at 22.7 min with 5% IPA in hexane (Figure 7-11, 7-12 and 7-13). A lower percentage of IPA was used compared to previous compounds due to the higher hydrophilicity brought by the ester groups and the use of an OD column instead of an AD column. The chiral HPLC graphs are shown in the appendix. (Figure 7-11, 7-12 and 7-13)

The (*S,S,S$_p$,S$_p$*) configuration of the chiral centre of **39** was proven by X-ray analysis of crystals grown from the slow evaporation of DCM. (Figure 3-7)
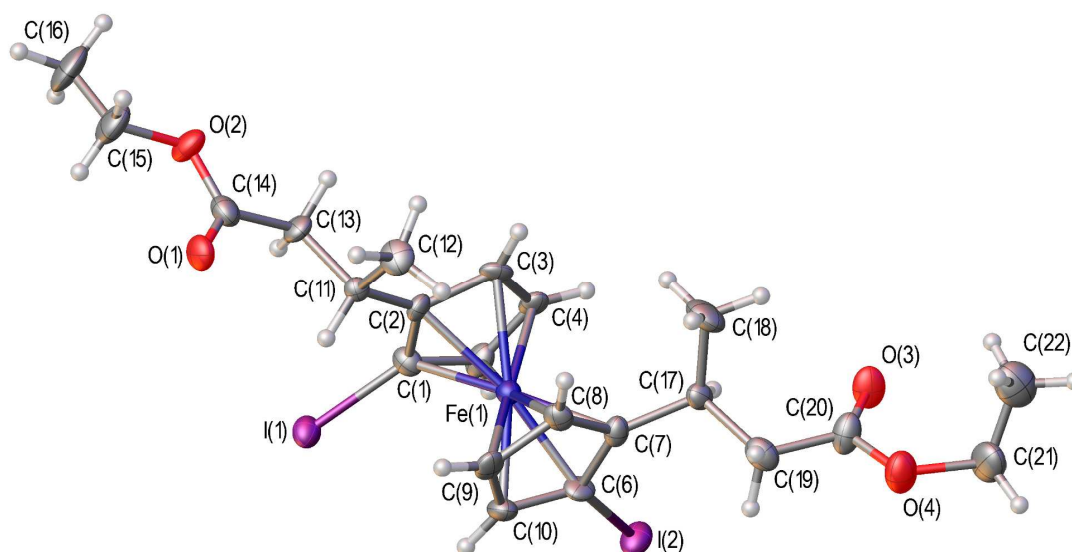
Figure 3-7: *Crystal structure of 39 with ellipsoids drawn at the 50% probability level.*

The structure gave two crystallographically independent molecules but only one is shown for clarity. Furthermore the methyl group C(16) (73%) /C(16') (27%) of the ester group of the second molecule is disordered over two positions and the minor positions have been omitted, again for clarity (Figure 6-2). Of interest is the presence of two intramolecular and one intermolecular halogen bonds shown in table 3-1.

Table 3-1: *Halogen bonds for 39 in (Å)*

Donnor...Acceptor	d(D...A)
I(101)...O(101)	3.08 ± 0.01
I(101)...O(01')	3.04 ± 0.02
I(102)...O(1)	3.263 ± 0.06

3.3.3 Ester reduction

Among many other examples of ester reduction, Brisset[65] used LiAlH$_4$ to reduce 1,1'-bis-[(2-ethyloxycarbonyl)ethyl]-ferrocene in diethyl ether under reflux for 1 h. The corresponding alcohol was obtained in 75% yield. (Scheme 3-22)
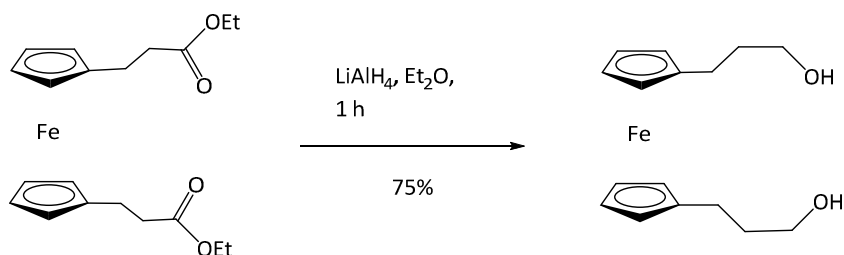
Scheme 3-22: *Brisset's ester reduction*

Under similar reaction conditions, reduction of **39** gave **40** in 70% yield after an overnight reaction, followed by a laborious Fieser work-up for larger scales. Fieser work-up consists in adding successively n mL of water, n mL of NaOH (15%) and $3n$ mL of water for every n g of LiAlH$_4$ used. Although the reaction was successful and gave a decent yield, **39** was also treated with DIBAL-H as a trial. (Scheme 3-23)
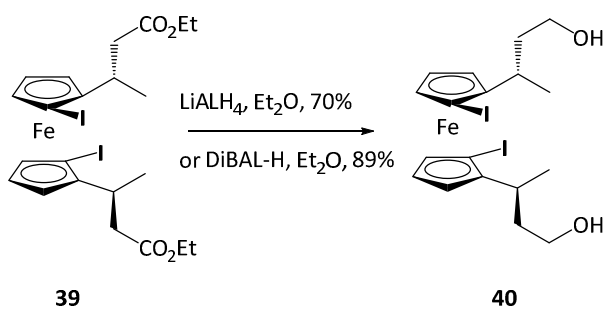
Scheme 3-23: *Ester reduction using DIBAL-H*

DIBAL-H is a weak reducing agent and is usually known to reduce esters to the corresponding aldehydes at low temperature with 1 equivalent of DIBAL per ester. It was decided to perform the reaction in diethyl ether for 1 h at room temperature using an excess

of DIBAL-H (3 equivalent per ester groups). The reaction was quenched with ethyl acetate and sodium potassium tartrate (Rochelle's salt), extracted with diethyl ether and washed with brine. Rochelle's salt is an excellent the aluminium ligand that breaks up the aluminium emulsion after quenching. The final compound (S,S,S_p,S_p)-**40** was obtained in 89% yield after purification. Chiral HPLC was conducted and as shown in Figure 3-14, **40** showed a single peak at 48.9 min in a 10% IPA in hexane eluent mixture. Indicating the formation of the pure enantiomer (S,S,S_p,S_p) (ca. 99.9% *ee*) and full retention of configuration for this step. The chiral HPLC graphs are shown in the appendix. (Figure 7-14, 7-15 and 7-16)

3.3.4 Benzylation

To avoid side-reactions during the nucleobase coupling reaction, the hydroxyl groups of the phosphodiester linkers had to be protected. The Horner-Wittig coupling reaction leads to the formation of a double bond that can be reduced via hydrogenation on Pd(OH)$_2$/C. Interestingly, benzyl groups are sensitive to hydrogenation. Therefore, using benzyl as a protecting group gave an opportunity to reduce the unsaturated bond and deprotect the alcohol moiety at the same time in the last step of the synthesis.

NaH was used to deprotonate **40** in DMF and benzyl chloride was added to enable nucleophilic substitution by the alkoxide. The bis-protected alcohol (S,S,S_p,S_p)-**41** was obtained in 80% yield. However, even after an overnight reflux, the reaction was not complete and some starting material and mono-substituted alcohol remained.
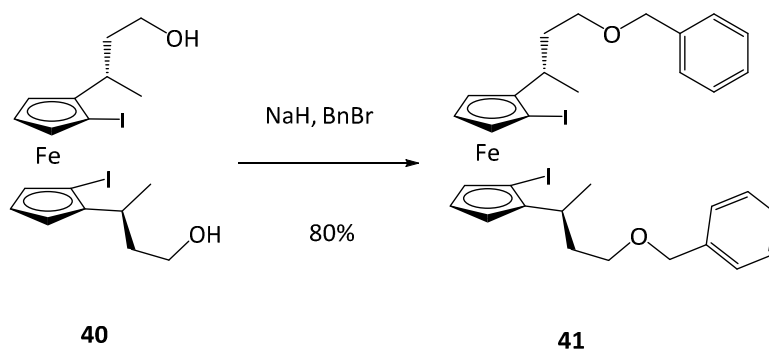
Scheme 3-24: *Benzylation*

To conclude this part of the synthesis, the extension of the phosphodiester-linkers was successfully achieved in six steps showing relatively good yields in a stereospecific manner as demonstrated by HPLC. The next part presents the different coupling methods used to attach adenine and uracil to the tetra-substituted ferrocene.

3.4   Part 3: Nucleobase coupling

3.4.1   Horner-Wittig approach

3.4.1.1   Formylation

Based on previous studies carried out on mono and bis-substituted ferrocenes, the Horner-Wittig coupling of tetra-substituted ferrocenes with adenine was investigated. To be able to perform the coupling, first formylation of the tetra-substituted diiodo ferrocene **41** had to be achieved. The formylation of ferrocene is a two-step reaction. The first step is a halogen-lithium exchange, as described earlier in the directed *ortho*-metallation step. The second part of the reaction is a lithium-formaldehyde exchange leading to the formation of the aldehyde.
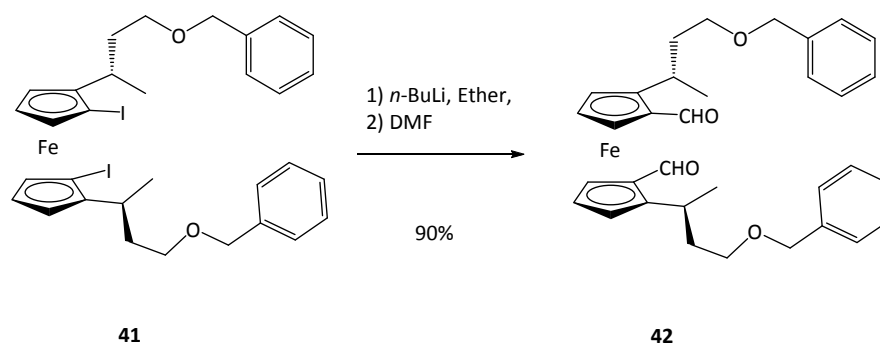
Scheme 3-25: Formylation of 41 to give aldehyde 42

The lithium-iodide exchange was performed in diethyl ether in presence of *n*-BuLi at -78°C (Scheme 3-25). When the dilithio-ferrocene was formed, DMF was added to form a dark-red solution of the corresponding aldehyde. After purification to remove a small amount of mono-aldehyde, (*S,S,S$_p$,S$_p$*)-**42** was obtained in 90% yield. The aldehyde protons appeared on the ^{1}H NMR spectrum as a singlet at 10.04 ppm, integrating for 2H. Analysis of the proton decoupled ^{13}C NMR spectrum confirmed the success of the reaction, with a characteristic peak for the carbon of the aldehyde at 193.1 ppm and a shift downfield of the *ipso* carbon linked to the aldehyde from 46.7 (C-I) to 77.7 ppm (C-CHO).

3.4.1.2 Horner-Wittig coupling with adenine

Horner-Wittig coupling was performed following the procedure previously described (Chapter 2). The diphenylphosphine oxide of dibenzoylated adenine **6** was reacted with NaH to form the ylid to attack the bis-aldehyde ferrocene **42**. (Scheme 3-26)
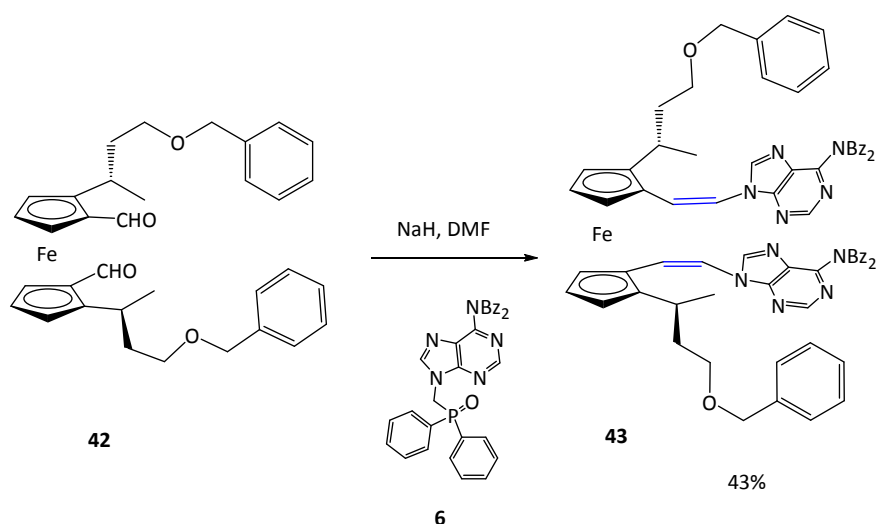
Scheme 3-26: *Horner-Wittig coupling of tetra-substituted ferrocene aldehyde 42 with adenine 6*

After purification, three fractions were collected. The first and major fraction corresponded to the *Z* isomer of (*S,S,R$_p$,R$_p$*)-**43** and was obtained in 43% yield. Analysis of the ^{1}H NMR spectrum gave the vicinal CH=CH coupling constant value J_{HH} = 8.8 Hz, which corresponds to *cis*-isomer of the alkene (Figure 3-8). The second fraction yielded the mono-substituted gave a singlet at ca 9 ppm integrating for 1H corresponding to an aldehyde proton and two other singlets at ca 8.6 ppm and 8.7 ppm. Each of these integrated for 1H and corresponded to the vicinal protons of the solitary adenine attached to the ferrocene. The last fraction corresponded to the starting material.
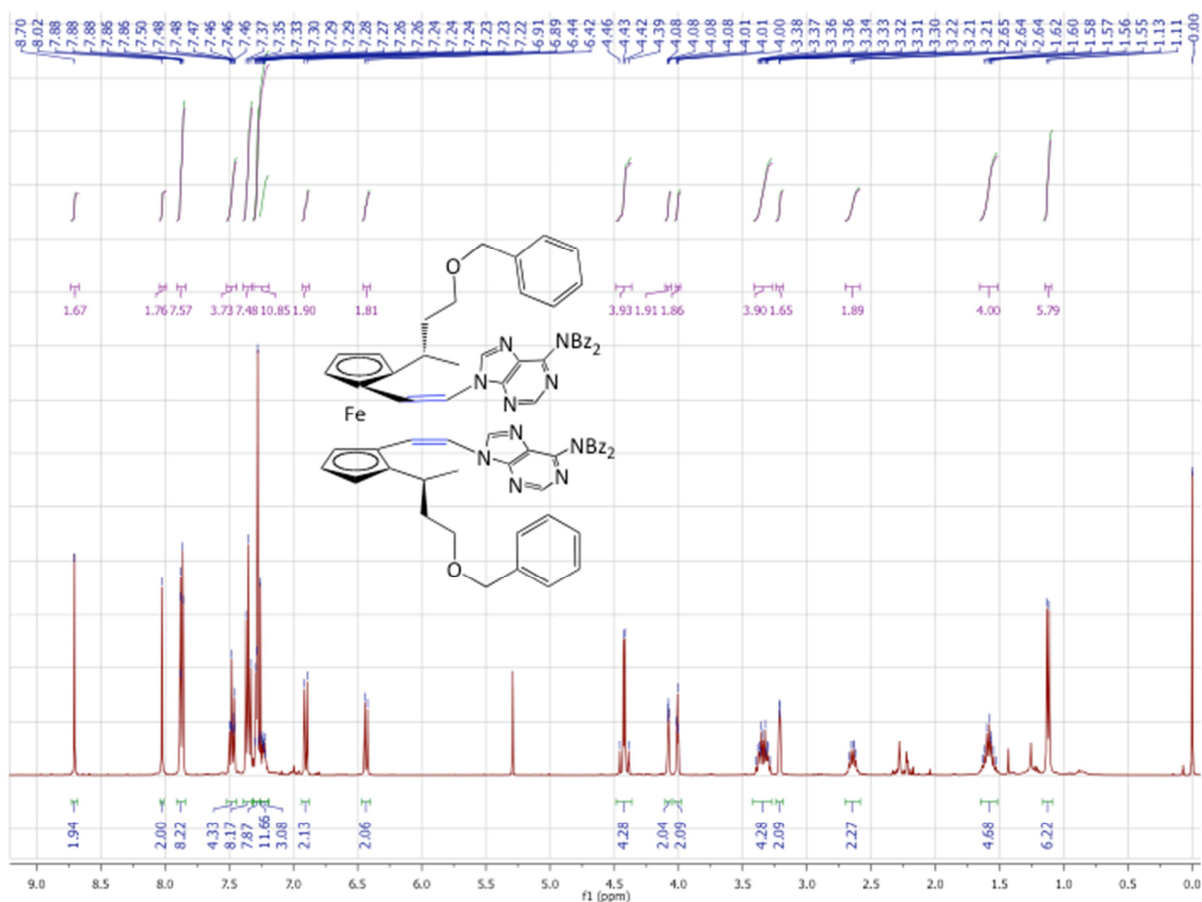
Figure 3-8: *^{1}H NMR spectrum of **43** in CDCl$_3$*

3.4.1.3 Hydrogenation

Hydrogenation consists of the addition of H$_2$ to a compound containing a multiple bond in presence of a catalyst. The catalysts used can be divided in two classes: heterogeneous and homogeneous. Heterogeneous catalysts such as palladium on charcoal (Pd/C) or Raney Nickel are insoluble in the reaction solvent. Homogenous catalysts are soluble in the reaction medium. In this step, only heterogeneous catalysts were used since they are easily separable from reaction mixtures.

Most catalytic reductions of unsaturated bonds involve a *syn* addition of hydrogen to the less-hindered face of the bond. The mechanism is not completely understood but the

generally accepted mechanism is a two-step process (Scheme 3-27). Firstly, the compound is adsorbed on the surface of the catalyst on the less-hindered face of the bond. Hydrogen atoms are then successively transferred to the compound to give the final reduced compound. In the specific case of hydrogenolysis of O-benzyls, which corresponds to the hydrogenation of a C-O bond, affinity of oxygen for the metal promotes the rupture of the bond. Numerous methods of hydrogenolysis have been reported affording debenzylation[23] in very good yields.
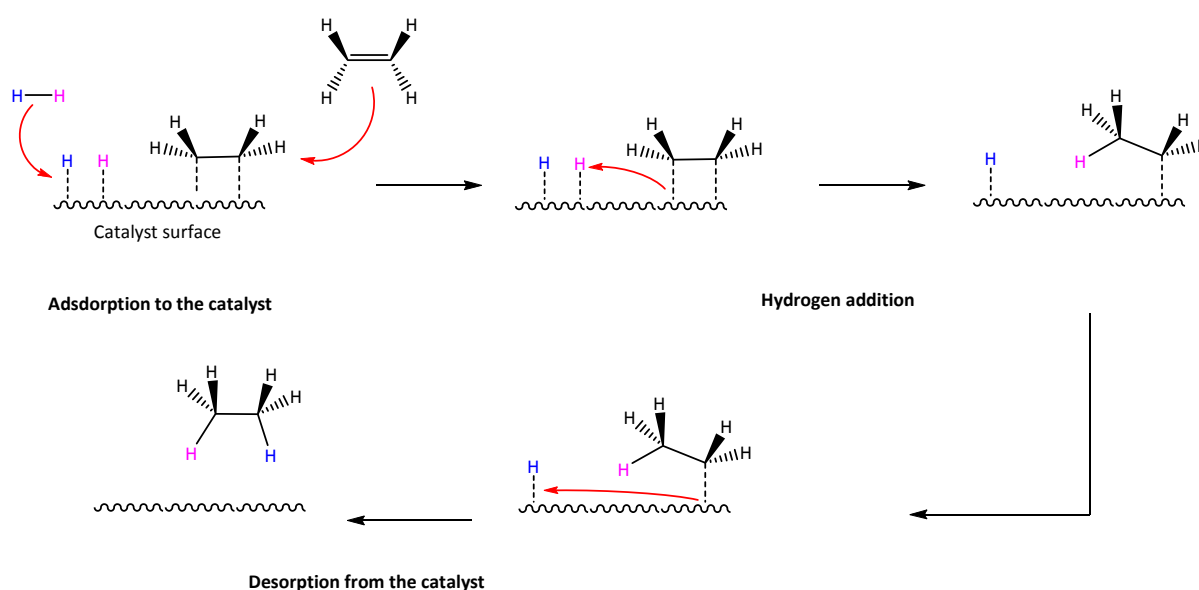
Scheme 3-27: *Hydrogenation via Heterogeneous catalysis*

In the case of the tetra-substituted ferrocene **43**, hydrogenation was meant to reduce the double bond formed after Horner-Wittig coupling and to deprotect benzyl groups at the same time. Based on Brisset's procedure[64] described in chapter 1, the reaction was set up in ethyl acetate, in presence of Pearlman's catalyst and a balloon of hydrogen. Unfortunately the reaction did not proceed well in either the reduction of the double bond or the full deprotection of the alcohol groups. The hydrogen source, pressure of hydrogen gas, solvent,

temperature and reaction time were all then varied in an attempt to obtain the desired

compound as shown in Table 3-2, however none were successful.

*Table 3-2: Different hydrogenation conditions towards reduction and deprotection of **43***

Catalyst (2eq)	H$_2$ source	Pressure (1 atm unless specified)	Solvent	T (°C)	t (days)	Results
Pd(OH)$_2$/C	H$_{2\,gas}$	Balloon	EtOAc	RT	2	Mono deprotection Partial deprotection of Bz
Pd(OH)$_2$/C	H$_{2\,gas}$	Balloon	EtOH MeOH	35	2	Mono deprotection Partial deprotection of Bz
Pd(OH)$_2$/C	H$_{2\,gas}$	Balloon	MeOH	35 50	3	Mono deprotection Partial deprotection of Bz
Pd(OH)$_2$/C	H$_{2\,gas}$	Balloon	EtOH	75	3	Degradation
Pd(OH)$_2$/C	Cyclohexene	Balloon	EtOAc	RT	3	Mono deprotection Partial deprotection of Bz
Pd(OH)$_2$/C	H$_{2\,gas}$	Pressure Reactor (1 to 4 atm)	EtOH EtOAc	RT 37 70	3	Mono deprotection Deprotection of Bz

The double bond environment is quite bulky and it is known that hydrogenation is sensitive

to steric hindrance. This could explain why the reduction of the double bond did not occur.

However, this assumption cannot readily explain why hydrogenolysis of benzyls also did not

occur. It is possible that this was caused by an interaction between the catalyst and the first

deprotected alcohol. To get a better understanding and to improve the reaction, stepwise

reduction and deprotection was investigated independently, first on the double bond alone

and then on the benzyl using the dibenzyl-diiodo-ferrocene **41**. To selectively reduce the

double bond without removing the benzyl groups, sodium borohydride in the presence of

acid acetic and Pd catalyst were used in isopropanol, according to Tran's procedure.[24]

Several other solvents such as THF and acetonitrile were also tried in order to improve the

solubility of **43**. However in all cases, only a partial deprotection of the alcohol was observed instead of the double bond reduction. To investigate hydrogenolysis the benzyl groups in compound **41**, three methods were tried as presented in Table 3-3. Once again the results were not satisfactory with no or low yields of the desired product. Interestingly the analogous reaction with the less hindered thymine substituent was found to proceed cleanly.[25]

Table 3-3: Deprotection conditions via hydrogenation of 41

Catalyst (2eq)	H_2 source	Solvent	T (°C)	t (days)	Results
Pd(OH)$_2$/C	H_2	EtOAc (+ Acetic acid)[26]	RT	O/N	No deprotection
Pd(OH)$_2$/C	Cyclohexene	Ethanol	75	O/N	No deprotection
Ni Raney[27]	H_2	Ethanol	RT	2 days	Fully debenzylation (minor fraction) 15% Partial deprotection (minor fraction) 28% No deprotection (major fraction) 57%

These investigations of hydrogenation and hydrogenolysis are not comprehensive enough to give a clear explanation as to why both reactions did not work. However, it is possible that steric hindrance was a likely cause of the failure of hydrogenation of the double bond. Therefore, another synthetic route was investigated to avoid formation of a double bond. The new route involved a change of protecting group, with Mitsunobu coupling leading directly to the formation of a saturated bond, as described below.

3.4.2 Mitsunobu approach

The first part of the new synthetic route consisted of developing a suitable tetra-substituted ferrocene precursor for the Mitsunobu coupling, which was previously investigated on bis-substituted systems, as described in Chapter 2. This precursor had to contain two protected

alcohols that would go on to provide the phosphodiester linkers and two hydroxyethyl linkers that would react with the nucleobases during the coupling.

3.4.2.1 Protection of alcohols

As previously described, benzyls were difficult to cleave on hindered ferrocenes via hydrogenation. Consequently, an investigation of alternative protecting groups was carried out. Silyl ethers are frequently used as protecting groups for alcohols. Indeed, their reactivity can be adjusted by modifying the substituents linked to the silicon atom. Among the numerous different silyl groups, reactivity towards acid treatment increases with substitution as follows: TMS (1) < TES (64) < TBDMS (20,000) < TIPS (700,000) < TBDPS (5,000,000), as it does with basic treatment as follows: TMS (1) < TES (10-100) < TBDMS - TBDPS (20,000) < TIPS (100,000). TMS is too sensitive to acidic and basic conditions and would be susceptible to cleavage during Mitsunobu coupling. It is likely that TBDMS would be cleaved in the presence of lithium during the formylation reaction or even later during the borohydration-oxidation. TBDPS is a very stable group under acidic and basic conditions and can be readily removed with TBAF.[28] For these reasons, the TBDPS protecting group seemed to be the most promising and was consequently chosen for the protection.
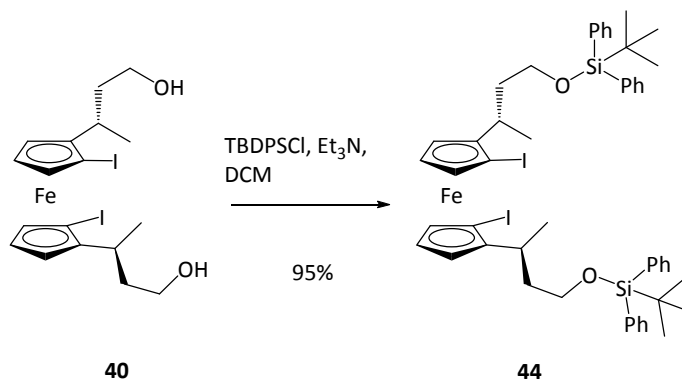
Scheme 3-28: *Hydroxyl protection with TBDPS*

Following the procedure reported by Hanessian and Lavalee[28] in 1975, diol **40** was treated with TEA, TBDPSCl and DMAP in DCM overnight to give (*S,S,S$_p$,S$_p$*)-**44** in 95% yield (Scheme 3-28). The presence of silyl groups was highlighted by ^{1}H NMR analysis, showing three characteristic peaks. Two multiplets at 7.67 and 7.4 ppm, integrating respectively for 8H and 12H, corresponded to the phenyl substituents and the *tert*-butyl substituent was characterised by a singlet at 1.05 ppm, integrating for 18H (Figure 3-9). Analysis of the proton decoupled ^{13}C NMR spectrum and high-resolution mass spectrometry confirmed that the protection had been successful.
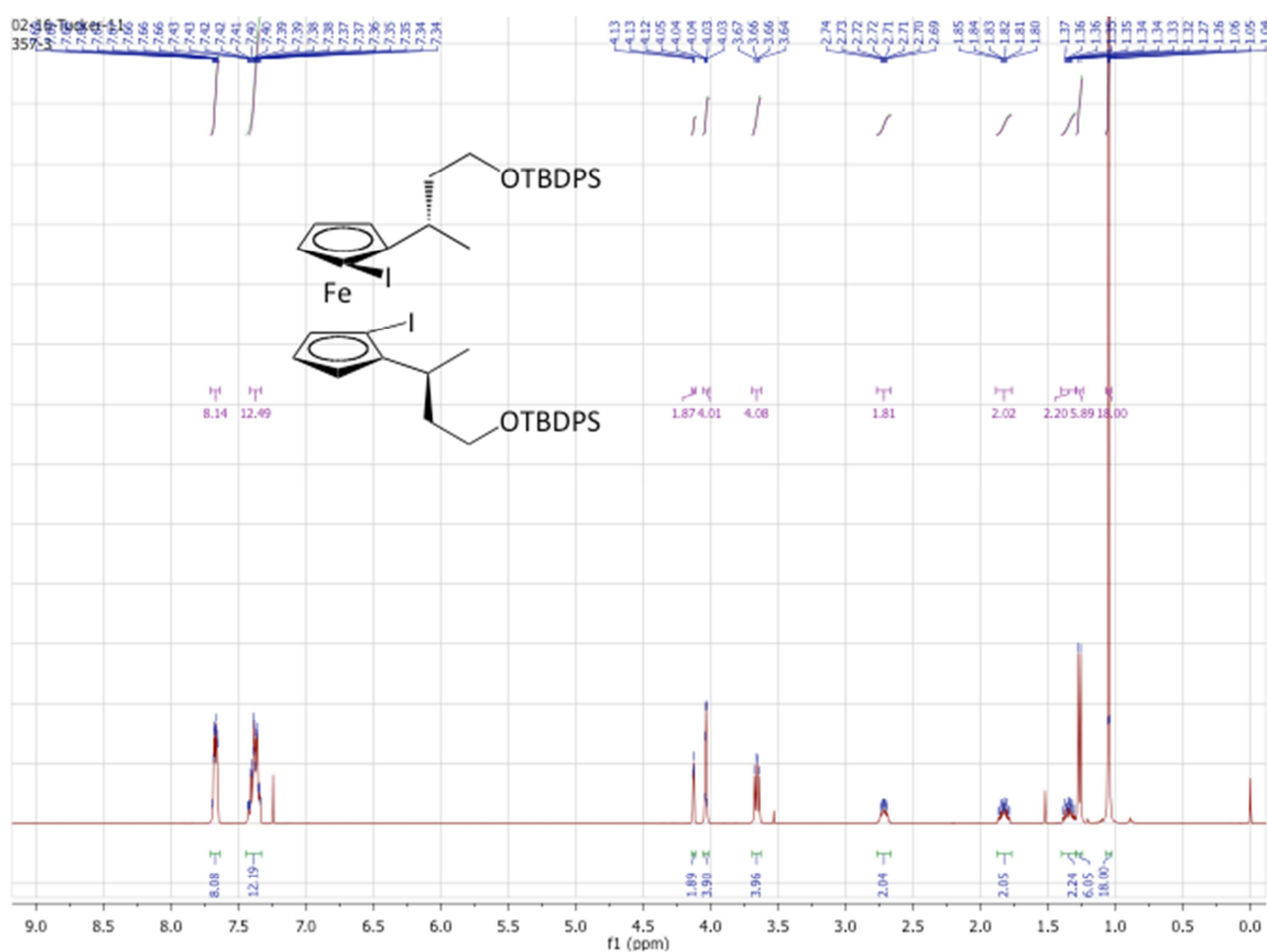
Figure 3-9: [1]*H NMR spectrum of 44 in CDCl$_3$*

3.4.2.2 Synthesis of hydroxyethyl linkers

The synthesis of suitable linkers for the coupling reaction with adenine and uracil followed the same route as that described for the bis-susbtituted systems (Chapter 2). To begin with, formylation of **44** was performed using the same conditions previously developed for the dibenzyl diiodo ferrocene **41**. The dialdehyde (S,S,S_p,S_p)-**45** was obtained in 78% yield and was then subjected to a Wittig reaction in presence of triphenylmethyl phosphonium bromide and *tert*-butoxide in THF to give (S,S,R_p,R_p)-**46** in 98% yield. During this step, the planar configuration changed due to the lower priority order of the vinyl chain compared to the phosphodiester-linker chain as shown in Figure 3-10. The configuration is now (S,S,R_p,R_p).

Planar chirality
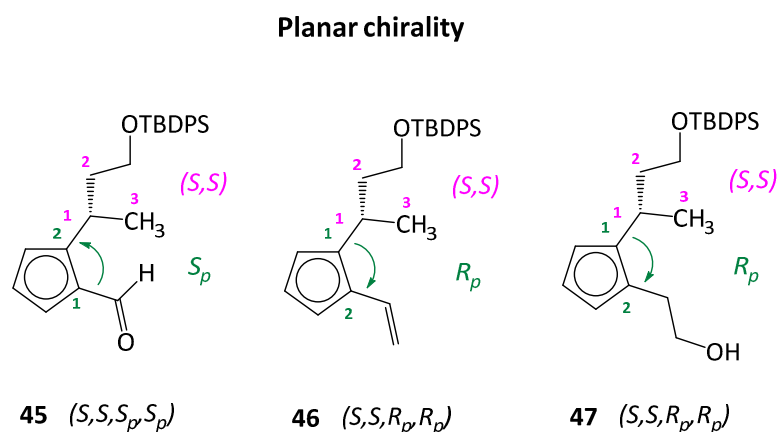
Figure 3-10: *Stereochemistry of 45, 46 and 47*

Hydroboration of the bis-divinyl ferrocene in presence of a borane tetrahydrofurane solution and hydrogen peroxide led to the synthesis of the bis-dihydroxyethyl ferrocene **47** in 78% yield as shown in Scheme 3-29.
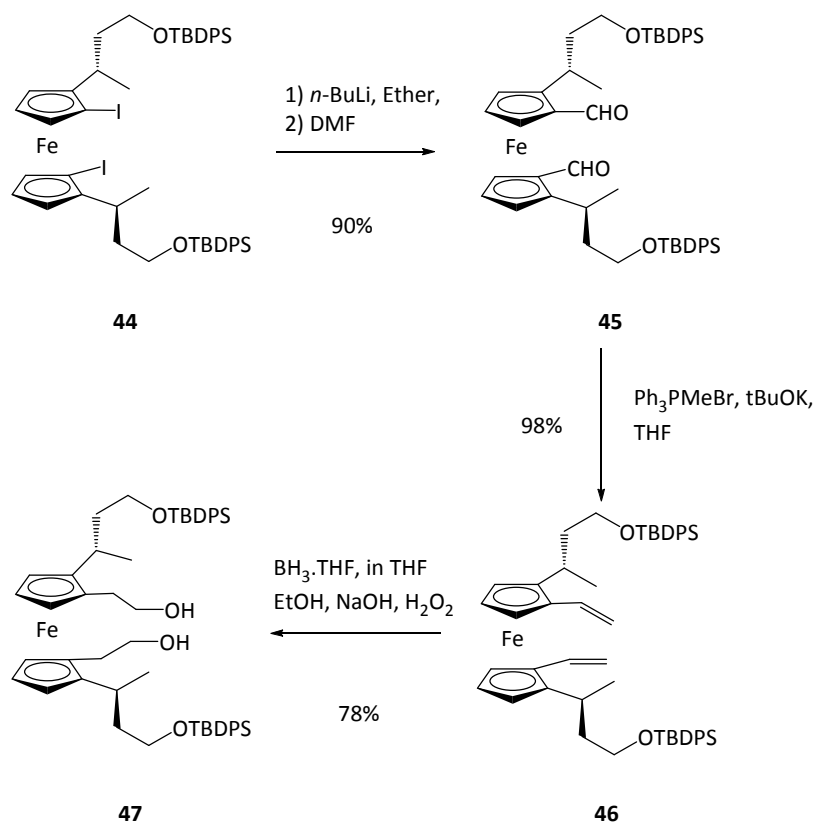
Scheme 3-29: *New route synthesis to Mitsunobu coupling*

Each compound was characterised by ^{1}H NMR, ^{13}C NMR, mass spectrometry, IR and melting point. To check for retention of configuration over these three steps, chiral HPLC was conducted on compound **47**. As shown in the figure below, **47** gave only one single peak at 53.1 min corresponding to the single enantiomer (S,S,R_p,R_p). A less polar eluent mixture (2.5% IPA in hexane) was used to obtain a good separation peak although the resolution of the peak was not optimal. Increasing the elution rate improved the resolution but reduced the separation between the peaks. Changing the column from AD to OD did not bring any improvements. The chiral HPLC graphs are shown in the appendix. (Figure 7-17, 7-18 and 7-19)

Crystals of **47** grown from the slow evaporation of an EtOAc/Hexane mixture were subjected to X-ray analysis. (Figure 3-11)
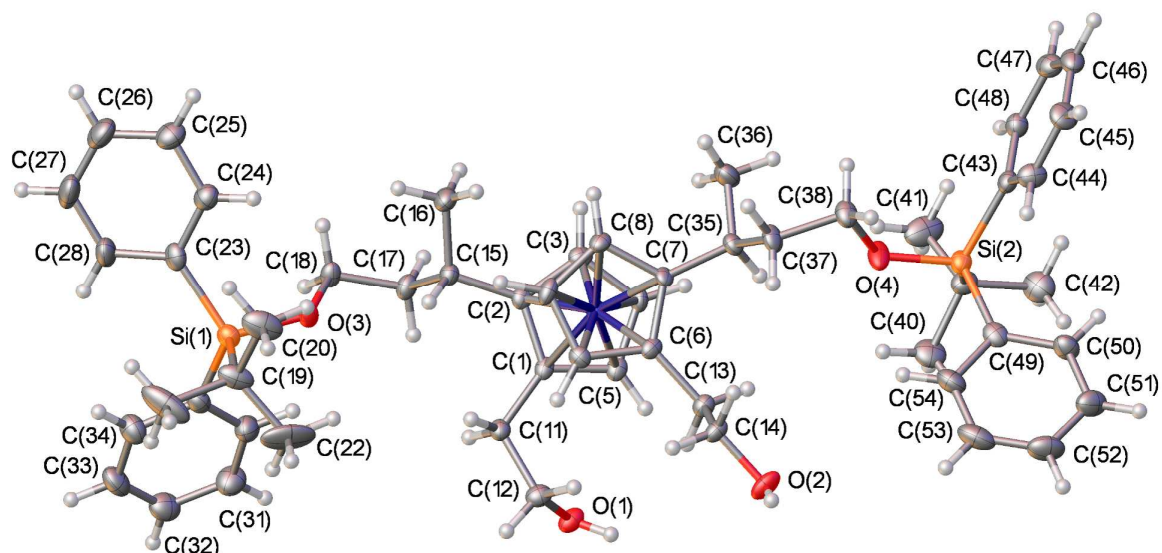
Figure 3-11: *Crystalline structure of one of the two crystallographically independent molecules of 47 with absolute stereochemistry (S,S,$_p$R,$_p$R) and with ellipsoids drawn at the 50 % probability level.*

The structure contains two crystallographically independent molecules, with matching stereochemistry and molecular geometry being the same within experimental error. Only one is shown for clarity. The structure confirmed the expected stereochemistry of the four stereogenic centres (S,S,R_p,R_p) and also revealed the presence of four hydrogen bonds between the two molecules as shown in Table 3-4.

Table 3-4: *Hydrogen bonds for 47 (Å and °)*

Donnor-H...Acceptor	d(D-H)	d(H...A)	d(D...A)	<(DHA)
O(2)-H(2A)...O(102)	0.84	1.95	2.774 ± 0.004	168.1
O(4)-H(4A)...O(2)	0.84	1.98	2.821 ± 0.004	177.8
O(102)-H(12G)...O(104)	0.84	1.96	2.786 ± 0.004	166.0
O(104)-H(14E)...O(4)	0.84	1.90	2.728 ± 0.004	170.0

3.4.2.3 Mitsunobu coupling with adenine and uracil

The Mitsunobu reaction was used to couple adenine **19** and uracil **20** to the tetra-substituted bis-dihydroxyethyl ferrocene **47**. The conditions developed for the bis-disubstituted ferrocene were followed for both couplings. The targets (S,S,R_p,R_p)-**48** and (S,S,R_p,R_p)-**49** were obtained in 52% and 75% yield respectively. However, instead of the expected dibenzoylated adenine compound, ^{1}H NMR of **48** revealed a mono deprotection of adenine, which partially explained the lower yield for this compound. Furthermore, the reaction did not go to completion and some starting material remained. Longer reaction times gave full debenzoylation of adenine that could cause side-reactions during the coupling steps in the automated oligomer synthesis; this is why the reaction was stirred for only two hours.

Notwithstanding the issues discussed above, uracil coupling is still more efficient than adenine coupling. As a purine, adenine is bigger than uracil and contains two benzoyl protecting groups as opposed to one for uracil. Consequently, adenine could have more difficulty accessing the ferrocene, causing a further drop in yield. (Scheme 3-30)
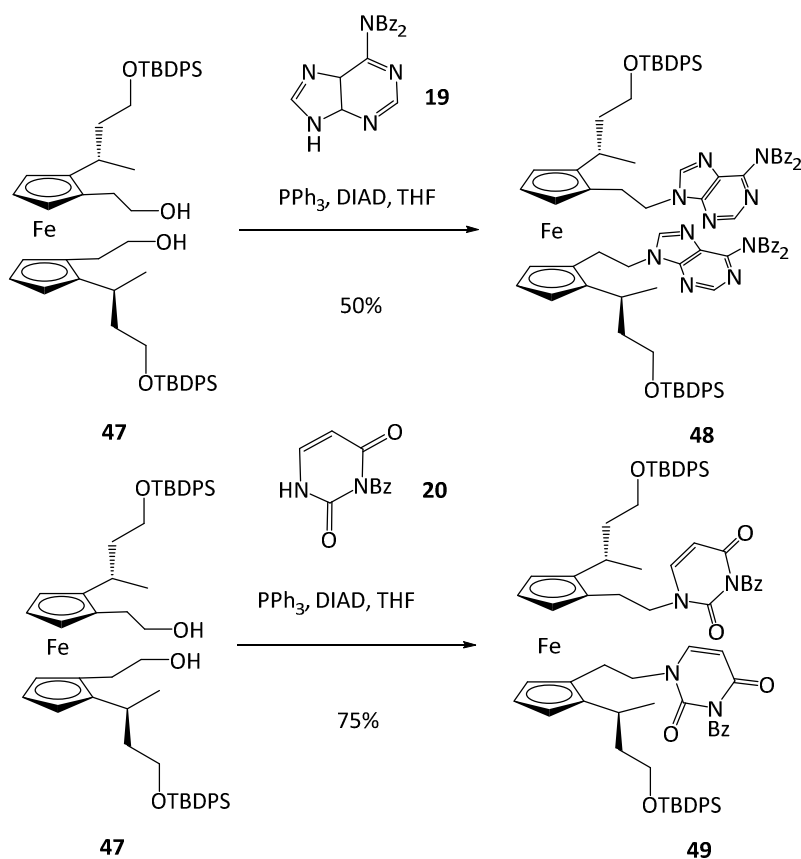
Scheme 3-30: *Synthesis of 48 and 49 via a Mitsunobu coupling with adenine and uracil*

Chiral HPLC on the ferrocene nucleobases **48** and **49** was tried using both AD and OD columns and each column was used with different eluent mixtures but no resolved peaks were ever observed, although the other enantiomer has not been synthesised yet. The optical rotation of the two compounds were measured $[\alpha]_D$ (c = 0.0066 g/mL, DCM) = -25.1 for **48** and $[\alpha]_D$ (c = 0.0066 g/mL, DCM) = +9.5 for **49**. Although the stereoselectivity should not be affected by this step, further investigations on determination of enantiopurity should be conducted in the future.

3.4.2.4 Silyl deprotection

The last step of the synthesis consisted of the deprotection of the TBDPS groups. Fluorides

are normally used to achieve the deprotection since the Si-F bond is much stronger than Si-O

bond. Following the procedure described by Hanessian and Lavallee[28], a solution of TBAF in

THF was used to deprotect **49** to give (S,S,R_p,R_p)-**51** in quite a low yield of 34%. The poor

yield of the reaction was mainly due to purification difficulties encountered. Indeed, TBAF

impurities remained even after water work-up and column. The long butyl chains help to

solubilise the salt in organic solvents such as DCM and MeOH that were used as purification

eluents. TBAF impurities were finally removed via many NH_4Cl washes followed by

extractions with ethyl acetate. **48** was deprotected using a crystalline form of TBAF instead

of a solution of TBAF leading to (S,S,R_p,R_p)-**50** in 92% yield. (Scheme 3-31)
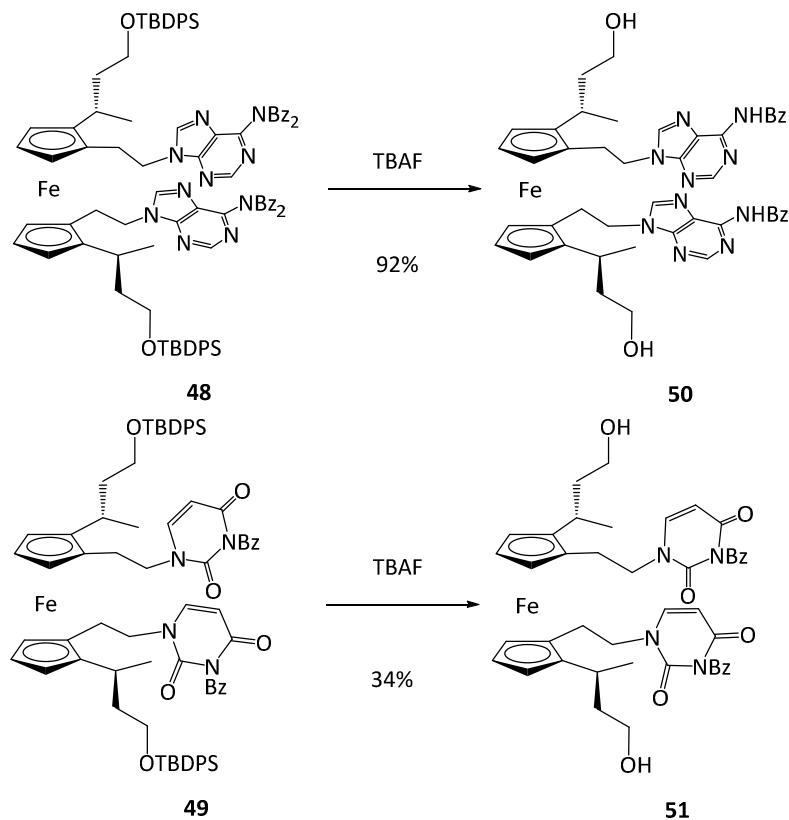
Scheme 3-31: *TBAF deprotection of tetra-substituted ferrocene adenine and uracil 48 and 49*

Crystals structure of (*S,S,R$_p$,R$_p$*)-**51** grown by the slow evaporation of a DCM solution were found to be suitable for X-ray analysis. (Figure 3-22)
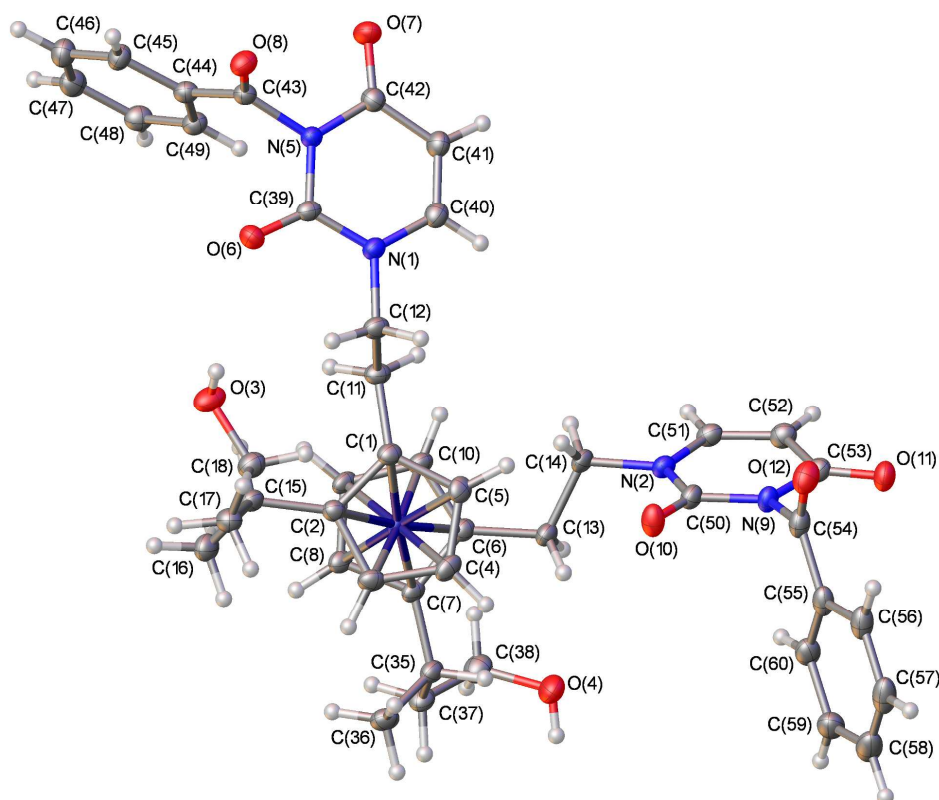
Figure 3-12: *Crystalline structure of 51 with ellipsoids drawn at the 50 % probability level. A molecule of deuterated chloroform has been omitted for clarity.*

The structure confirms the configuration of the compound with the expected absolute stereochemistry of the four stereogenic centres (*S,S,R$_p$,R$_p$*) observed. In addition and reveal the presence of two intermolecular and intramolecular hydrogen bonds were observed, as reported Table 3-5.

Table 3-5: *Hydrogen bonds for 51 (Å and °)*

Donnor-H...Acceptor	d(D-H)	d(H...A)	d(D...A)	<(DHA)
O(4)-H(4)...O(11)	0.84	2.03	2.848 ± 0.003	164.8
O(3)-H(3A)...O(4)	0.84	1.98	2.814 ± 0.003	169.3

A comparison of the geometry of compounds **47** and **51** in the region of the added uracil is given in Table 3-6.

Table 3-6: *A comparison of bond lengths (Å), bond angles (°) and torsion angles (°) in compounds 47 and 51. Ct(1)/Ct(101) is the centroid of the cyclopentadienyl ring C(1)-C(5)/C(101)-C(105) while Ct(2)/Ct(102) is the centroid of C(6)-C(10)/C(106)-C(110).*

	47 (Molecule 1 / Molecule 2)	51
C(1)-C(11) / C(101)-C(111)	1.505 ± 0.005 / 1.501 ± 0.004	1.504 ± 0.003
C(11)-C(12) / C(111)-C(112)	1.512 ± 0.004 / 1.522 ± 0.004	1.519 ± 0.003
C(12)-[O(1)/N(1)] / C(112)-O(101)	1.439 ± 0.004 / 1.432 ± 0.004	1.475 ± 0.003
C(1)-C(11)-C(12) / C(101)-C(111)-C(112)	114.9 ± 0.003 / 109.2 ± 0.003	114.2 ± 0.002
C(11)-C(12)-[O(1)/N(1)] / C(111)-C(112)-O(101)	110.6 ± 0.003 / 109.7 ± 0.003	109.5 ± 0.002
C(1)-Ct(1)-Ct(2)-C(9) / C(101)-Ct(101)-Ct(102)-C(109)	-64 / -64	-41
C(1)-Ct(1)-Ct(2)-C(10) / C(101)-Ct(101)-Ct(102)-C(110)	8 / 8	31

While the bond lengths and angles show no unexpected differences between the structures, it can be seen that the cyclopentadienyl rings of the ferrocene units are in an almost fully eclipsed confirmation in **47** (for eclipsed confirmation expected C(1)-Ct(1)-Ct(2)-C(9)/C(101)-Ct(101)-Ct(102)-C(109) torsion is -72**°** and expected C(1)-Ct(1)-Ct(2)-C(10)/C(101)-Ct(101)-Ct(102)-C(110) torsion is 0**°**) while in **51** the rings are in an almost fully staggered confirmation (for a staggered confirmation the expected C(1)-Ct(1)-Ct(2)-[C(9)/C(10)]/C(101)-Ct(101)-Ct(102)-[C(109)/C(110] torsion is 36**°**).

3.4.2.5 Bromine substitution with Cytosine

Preliminary work was carried on the coupling of cytosine with a tetra-substituted ferrocenyl bromide using the same method investigated in Chapter 2 with bis-substituted ferrocenyl derivatives. First, bromination of diol **47** was investigated. Compound **52** was obtained in 97% yield in presence of 5.6 eq of triphenylphosphine, 6 equivalents of NBS and 2.4 eq of pyridine in DCM. (Scheme 3-32)
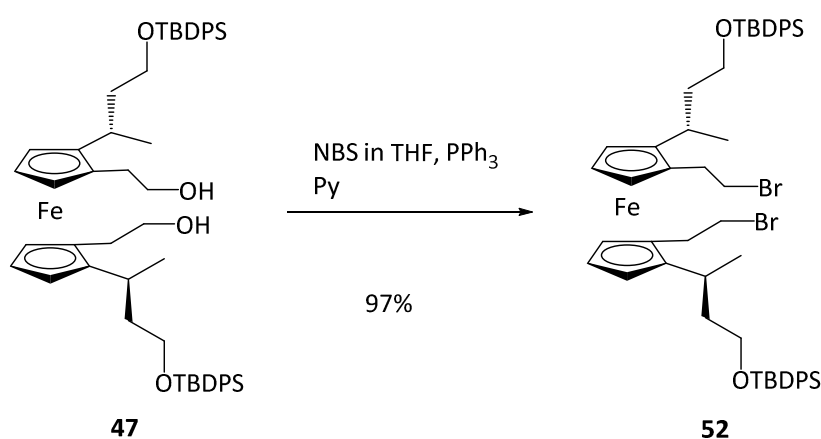
Scheme 3-32: *Bromination of tetra-substituted ferrocene*

Following the successful synthesis of **52**, its coupling with *N*-6-benzoyl cytosine was then investigated following the procedure developed earlier in Chapter 2. Using three equivalents of cytosine and NaH, *N*-6-benzoyl cytosine was then successfully coupled to tetra-substituted ferrocene **47** to give **53** as confirmed by ^{1}H, ^{13}C NMR and high resolution mass spectrometry. As already mentioned in the case of the bis-(bromoethyl) ferrocene, the reaction was not complete. The reaction gave **53** in a low yield of 16%. The reaction should be reinvestigated to improve this yield, which could be a starting point for future work. (Scheme 3-33)
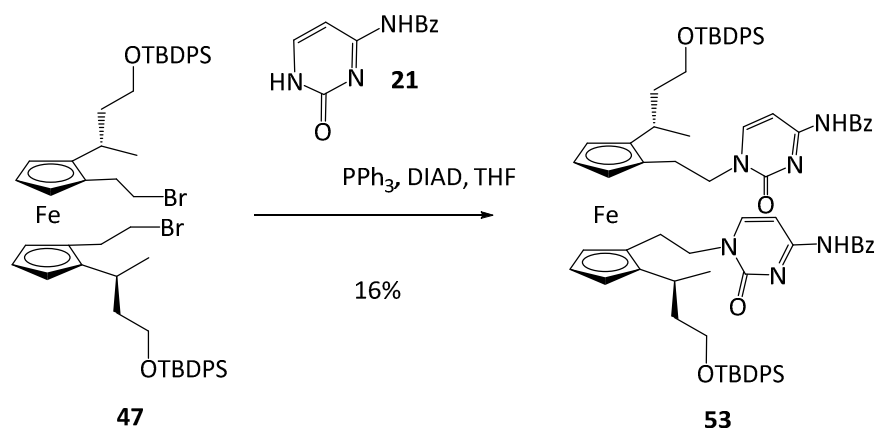
Scheme 3-33: *Cytosine coupling via Bromide substitution*

3.5 Conclusion

In this chapter, the synthesis of two tetra-substituted bis adenine/uracil/cytosine ferrocene derivatives have been investigated. To start with, the 1,1'-(α-dimethylaminoethyl)-2,2'-diiodo ferrocene as common precursor of both monomers was synthesised via introduction of central chirality followed by planar chirality. The results confirmed that the chiral centre α to the ferrocene induced diastereoselectivity in the *ortho*-halogenation as described by Ugi. Then a series of nucleophilic substitutions have been carried out to achieve the synthesis of a three-carbon phosphodiester-linker chain. All these reactions were accomplished with configuration retention via formation of an iron-stabilised carbenium ferrocene intermediate. After a formylation, the tetra-substituted ferrocene was attached to adenine via Horner-Wittig coupling. Unfortunately, the later reduction/deprotection of the unsaturated benzoylated monomer could not be achieved for steric reasons.

A new route was then investigated involving a new protecting group and a new coupling method. TBDPS was chosen as suitable protecting group before developing hydroxyl alkyl chains from iodine that were coupled to adenine and uracil via the Mitsunobu reaction. Both

compounds were deprotected via fluoride treatment leading to the synthesis of the two targeted adenine and uracil FcNA monomers. The tetra-substituted ferrocenyl monomer was also coupled to cytosine via a bromide substitution but in poor yields. Future work would consist of a reinvestigation of this coupling reaction to improve the efficiency of the reaction. An interesting alternative would be to attempt full protection of the exo-amine of cytosine leading to an improvement of its solubility in THF and then the coupling under Mitsunobu conditions. Further investigations on the preparation of the monomers for the automated oligonucleotide synthesis should also be conducted. The preparation of the monomers would consist of the tritylation and the phosphitylation of the two primary alcohols of the monomers as described in Scheme 3-34.
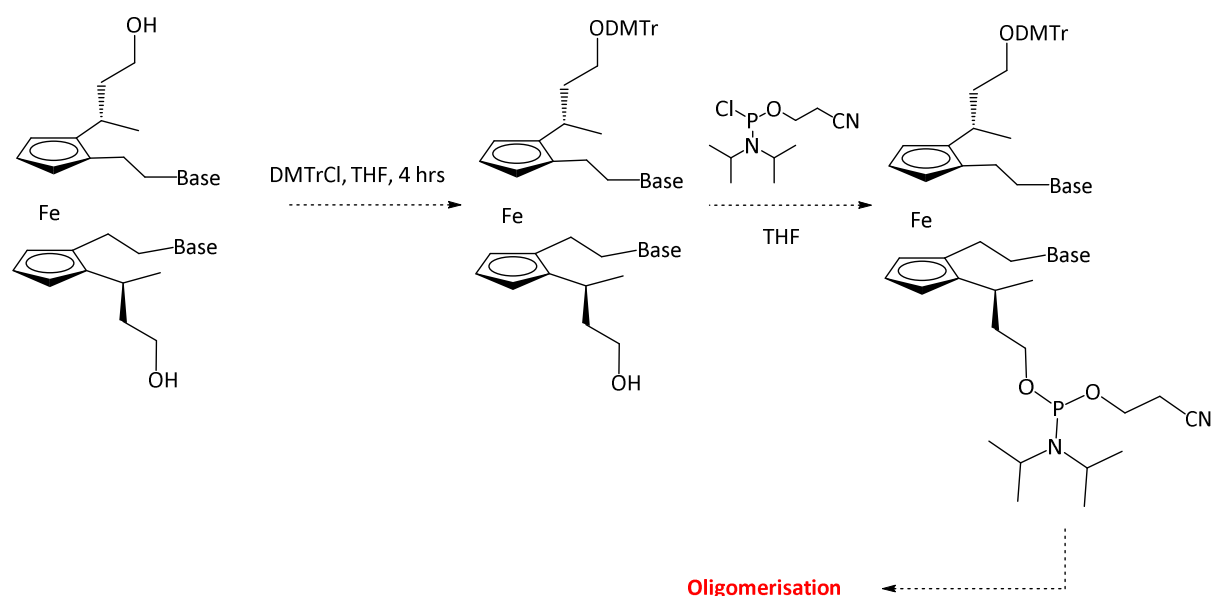
Scheme 3-34: *Tritylation and phosphitylation of the ferrocenyl monomers for their oligomerisation*

As previously described by Brisset[64] and Ihara[65] in chapter 1, DMTrCl was successfully used in presence of DMAP for the tritylation of one of the alcohol of a bis-hydroxyl-ferrocene. They

also reported the use of a chloro(diisopropylamine)(b-cyanoethoxy)phosphine in presence of

DIPEA for the phosphitylation of the second hydroxyl.
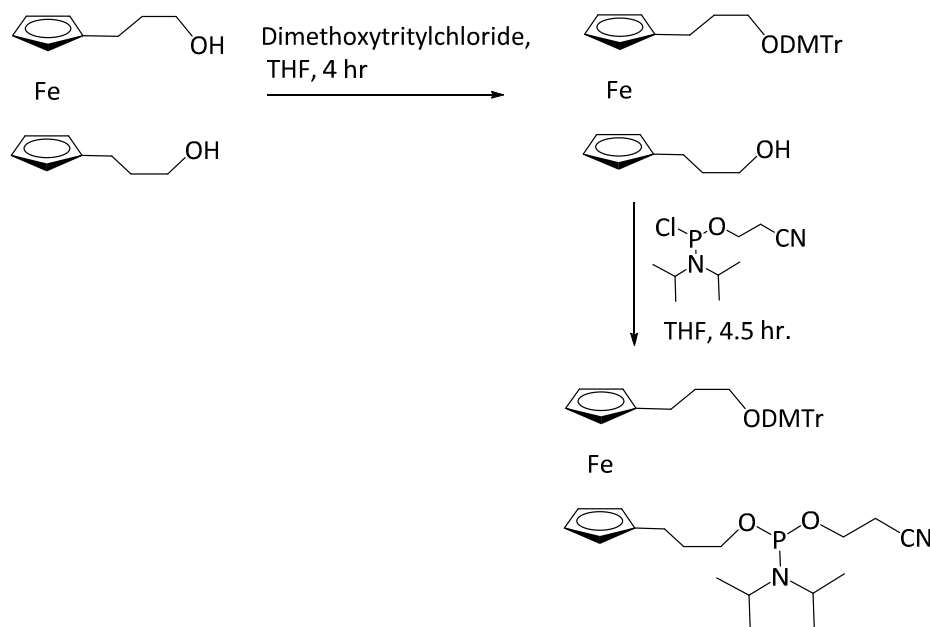
Scheme 3-35*: Tritylation and phosphitylation of bis-hydroxy-ferrocene*

3.6 References

1.   G. Chatelain, H. Brisset, C. Chaix, *New J. Chem.*, **2009**, *33*, 1139-1147.
2.   G. W. Gokel, D. Marquarding, I. Ugi, *J. Org. Chem.,* **1972,** *37*, 3052-305
3.   I. R. Butler, W. R. Cullen, F. G. Herring, N. R. Jagannath, *Can. J. Chem.*, **1986**, *64*, 667-669.
4.   L. Schwink and P. Knochel, *Chem. Eur. J.*, **1998**, *4*, 950-968.
5.   R. B. Woodward, M. Rosenblum, M. C. Whiting, *J. Am. Chem. Soc.*, **1952**, *74*, 3458-3459; P. J. Graham and G. M. Whiteman*, U.S. Pat. 2859233*, **1958**.
6.   A. Hirao, S. Itsuno, S. Nakahama, N. Yamazaki, *J. Chem. Soc. Chem. Commun.,* **1981**, 315-317.
7.   S. Itsuno, K. Ito, A. Hirao, S. Nakahama, *J. Chem. Soc. Chem. Comm.*, **1983**, 469-470.
8.   E. J. Corey, R. K. Bakshi, S. Shibata, C-P. Chen, V. K. Singh, *J. Am. Chem. Soc.,* **1987**, *109,* 7926-7927.
9.   E. J. Corey, R. K. Bakshi, S. Shibata, *J. Am. Chem. Soc.,* **1987**, *109,* 5553-5554.
10. E. J. Corey and C. J. Helal, *Angew. Chem. Int. Ed.,* **1998**, *37*, 1986-2012.

11. G. Gokel, P. Hoffmann, H. Klusacek, D. Marquarding, E. Ruch, I. Ugi, *Angew. Chem. Int. Ed. Engl.*, **1970**, *9*, 64-65.

12. M. Cais, J. J. Dannenberg, A. Eisenstadt, M. J. Levenberg, J. H. Richards, *Tetrahedron Lett.*, **1966**, 1695-1701

13. a) J. C. Ware and T. G. Traylor, *Tetrahedron Lett.,* **1966**, 1295. b) T. G. Traylor and J. C. Ware, *J. Am. Chem. Soc.,* **1967**, *89*, 2304-2316. c) J. D. Fitz-Patrick, L. Watts, and R. Pettit, *Tetrahedron Lett.,* **1966**, 1299.

14. O. Riant, O. Samuel, T. Flessner, S. Taudien, H. B. Kagan, *J. Org. Chem.*, **1997**, *62*, 6733-6745.

15. For literature review: W. F. Bailey and J. J. Patricia, *J. Organomet. Chem.*, **1988**, *352*, 1-46.

16. J. Kang, J. H. Lee, K. Soo Im, *J. Molecul. Catalysis A: Chemical*, **2003**, *196*, 55-63.

17. H. Gilman and F.W. Moore, *J. Chem. Soc.*, **1940**, *62*, 1843.

18. W. Langham, R.Q. Brewster, H. Gilman, *J. Am. Chem. Soc.*, **1941**, *63*, 545-549.

19. J. Kang, J. Hee Lee, J. Sun Choi, *Tetrahedron: Asymmetry*, **2001**, *12*, 33-35.

20. a) A. J. Locke, C. J. Richards, D. E. Hibbs, M.B. Hursthouse, *Tetrahedron: Asymmetry,* **1997**, *8*, 3383-3386; b) A. J. Locke and C. J. Richards, *Tetrahedron Lett.,* **1996**, *37*, 7861-7864.

21. K. Mikami, S. Matsumoto, A. Ishida, S. Takamuku, T. Suenobu, S. Fukuzumi, *J. Am. Chem. Soc.,* **1995**, *117*, 11134-11141.

22. C. J. Richards, D. Hibbs, M. B. Hursthouse, *Tetrahedron Lett.,* **1994**, *35*, 4215-4218.

23. C. H. Heathcock and R. Ratcliffe, *J. Am. Chem. Soc.*, **1971**, *93*, 1746-1757.

24. A. T. Tran, V. A. Huynh, E. M. Friz, S. K. Whitney, D. B. Corde, *Tetrahedron Lett.*, **2009**, *50*, 1817-1819.

25. H. V. Nguyen, Z. Y. Zhao, A. Sallustrau, S. L. Horswell, L. Male, A. Mulas, J. H. R. Tucker, *Chem. Commun.*, **2012**, *48*, 12165-12167.

26. A. Csámpai, A. Z. Györfi, G. I. Túrós, P. Sohár, *Journal of Organometallic Chemistry*, **2009**, *694*, 3667-3673.

27. K. Horita, T. Yoshioka, T. Tanaka, Y. Oikawa and A. Yonemitsu, *Tetrahedron*, **1986**, *42*, 3021-3028.

28. S. Hanessian and P. Lavallee, *Can. J. Chem.*, **1975**, *53*, 2975-2977; S. K. Chaudhary and O. Hernandez, *Tetrahedron Letters*, **1979**, *20*, 99-102; Y. Guindon, C. Yoakim, M. A. Bernstein, and H. E. Morton, *Tetrahedron Letters*, **1985**, *26*, 1185-1188.

CHAPTER 4: FERRONUCLEOBASES AS POTENTIAL DRUGS

4.1 Introduction

4.1.1 Drug discovery

Medicinal chemistry has been practised for several thousand years. Mankind has always tried to treat and cure the diseases it has been affected by as a part of its survival.[1] The beginning of drug discovery used to be based on plants and used to be empirical, which meant that people knew the beneficial or toxic effect of a substance without understanding the scientific reasons behind it. With the development of scientific and technological progress, scientists have been able to synthesise substances with predictable and controllable effects. Nowadays, drug discovery is the one of the most commun process by which a new drug is put on the market.

The development of a drug goes through four major steps of research to finally end with the commercialisation of the drug.[2] The first step corresponds to the synthesis of the drug candidate usually initiated by academic research, which is then tested *in vitro* via a sequence of defined experiments called drug screening. Following the evaluation of the drug activity on cells, the drug is tested on animal models and submitted to three phases of the clinical testing, which consist of evaluating the efficiency and the toxicity of the drug on humans. The last phase of the development is the commercialisation of the drug on the market and the monitoring of its side effects on the global population. (Figure 4-1)

| In vitro studies | Animal testing | Clinical testing | | Marketing |
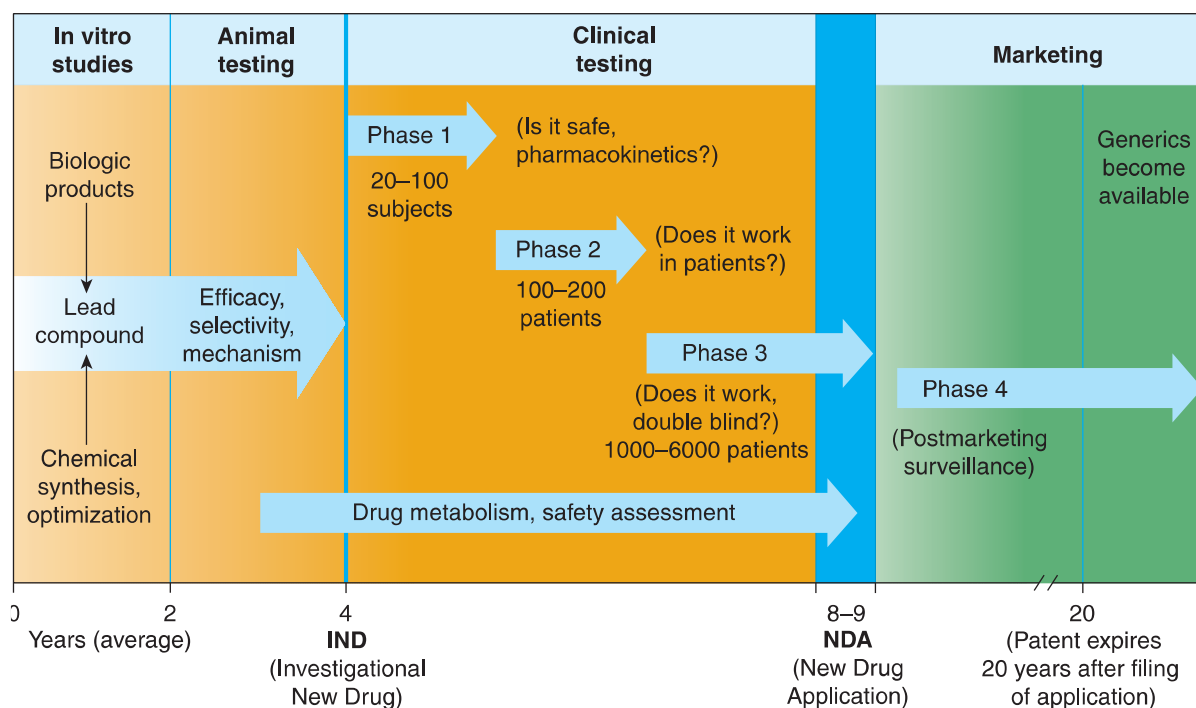
Figure 4-1: The different stage of drug development

In the first stages of drug discovery, the candidate is subjected to pharmacological tests to model the influence of the drug on the organism. Pharmacological studies consist of studying the substances interactions with living organisms through chemical processes by interaction with regulatory molecules (Proteins, DNA). The studies are based on pharmacokinetics and pharmacodynamics. As described by Benet[3] "Pharmacokinetics may be simply defined as what the body does to the drug, as opposed to pharmacodynamics which may be defined as what the drug does to the body." To model and simplify the many different processes happening between an organism and a drug, the ADME model[4] is known to give a good approximation to these processes. ADME stands for absorption, distribution, metabolism and excretion. The absorption stage takes in account the different processes responsible for the penetration of the substance into blood circulation. The second stage corresponds to the distribution of the substance through the body, followed by the

metabolism stage corresponding to the bio-transformation of the substance in the body. The later process activates or inactivates the substance, which provokes biological effects and responses from the organism, both described by pharmacodynamics. The excretion stage consists of the elimination of the substance by the body. (Figure 4-2)
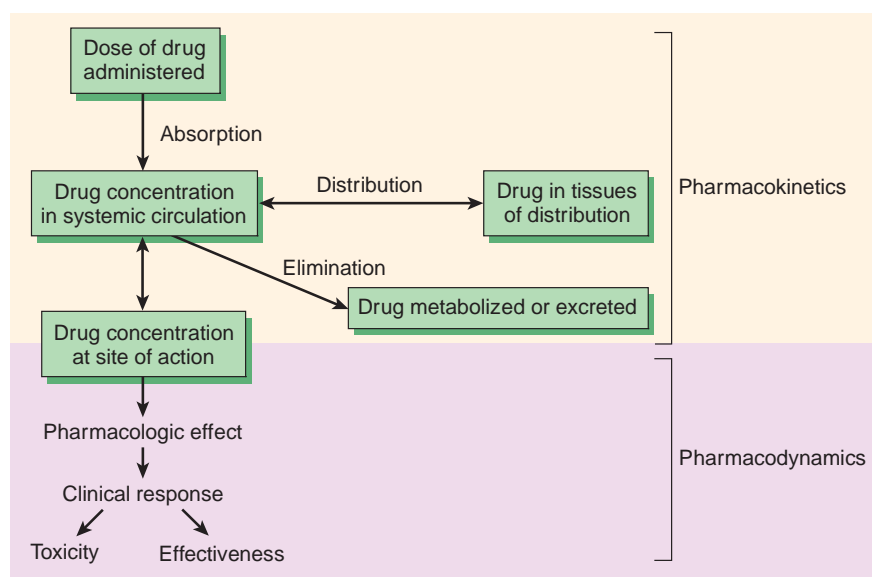
Figure 4-2: *The different stages of pharmacokinetics and pharmacodynamics.*

Prior to these pharmacological studies, the drug candidate is submitted to studies based on cell-based assays in order to evaluate its potency, which means the amount of compound needed to produce an effect with a defined intensity. A highly potent drug induces an intense response at low concentrations, whereas a drug with low potency produces a small response at high concentrations. The potency is usually expressed by the EC_{50} value. EC_{50} is the half maximal effective concentration and corresponds to the concentration at which the drug produces 50% of its maximal possible effect on a target or a biological process. The lower the EC_{50} is, the less the amount of the drug is needed to produce 50% effect on the target and higher is the potency. EC_{50} is obtained from a dose-response curve, which

represents the concentration of a drug as a function of the response of an organism (Cell). (Figure 4-3)
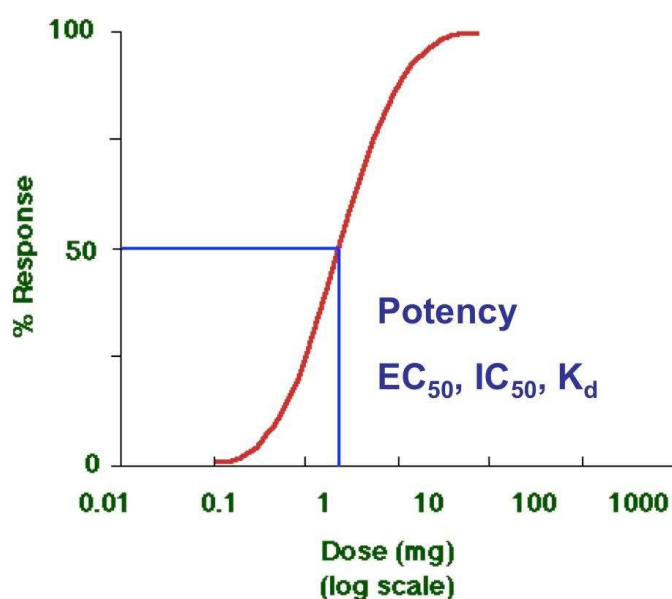
Figure 4-3: *Dose-response curve with EC$_{50}$ and IC$_{50}$ as the concentration of a drug that produces respectively 50% of activation and inhibition on biological response*

The dose-response relationship also gives the half maximal inhibitory concentration (IC$_{50}$), which is comparable to EC$_{50}$, in that it corresponds to the concentration of the drug required for 50% inhibition of a biological process *in vitro*. The two values allow an understanding of the activity and the efficiency of a drug on a target. Another important way to screen the activity of a substance is to study its cytotoxicity, which is by definition the ability of this compound to induce cell death. Cytotoxicity tests usually measure cell apoptosis and cell necrosis as a consequence of the activity of the substance and therefore give an idea of how efficient a drug is. The cytotoxicity is evaluated via the determination of CC$_{50}$ and MCC, which are both related to IC$_{50}$ but are more specific parameters. CC$_{50}$ corresponds to the cytotoxic concentration required to reduce cell growth by 50%, which means that the number of cells is reduced by 50% compared to the control cells and the MCC corresponds

to the minimum cytotoxic concentration that causes a microscopically detectable alteration of cell morphology leading to a detachment of the cells from the support.

Different assays have been developed, which are of importance for the determination of these indicators of the product biological activity. Some of them are presented in the following section.

4.1.1.1 Assays

The evaluation of drug activity is usually obtained via cell-based assays that probe mitochondrial function (MTT, MTS), the uptake of a dye by dead cells after failure of a cell permeability barrier (Trypan blue) and other parameters such as morphological modifications (CPE assay) or cell replication (BrdU assay). A brief description of these different assays is developed in the following.

One of the most common assays to test cytotoxicity is the MTT assay,[5,6] which is a colorimetric assay that measures the ability of the cell to survive, grow and multiply. Only in living cells, MTT is reduced by mitochondrial dehydrogenase into an insoluble dark purple product called MTT-formazan (Scheme 4-1). MTT-formazan is then solubilised with an organic solvent and measured via spectrophotometry. The amount of MTT-formazan dye is directly proportional to the number of living cells, and therefore the assay enables a direct measure of the viability of the cells after treatment with the drug.
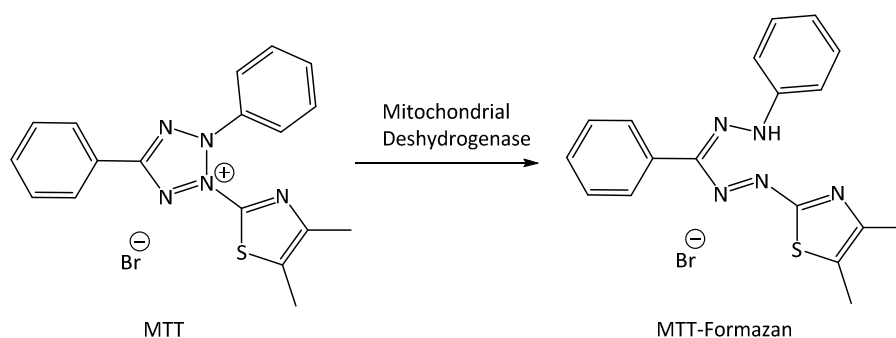
Scheme 4-1: *MTT reduction to formazan*

However, the assay has its limitations. For example, Johno *et al.*[7] showed that pH could affect the outcome of the assay and the absorbance of the MTT-formazan decreases in a pH-dependent manner but without affecting the cell viability.

Other assays using an identical process of assessment of living cells have been developed, that use MMT derivatives such as XTT[8] or MTS.[9] These derivatives have reduced forms that are soluble in the culture media and are not toxic, so it is possible to reuse the cells for further investigations. The MTS assay also involves an electron-coupling reagent called phenazine methosulfate (PMS) (Scheme 4-2). After the protonation of PNS, it reduces MTS to MTS-formazan, which is directly detectable in the buffer, avoiding the intermittent step of solubilisation required in the MTT assay.
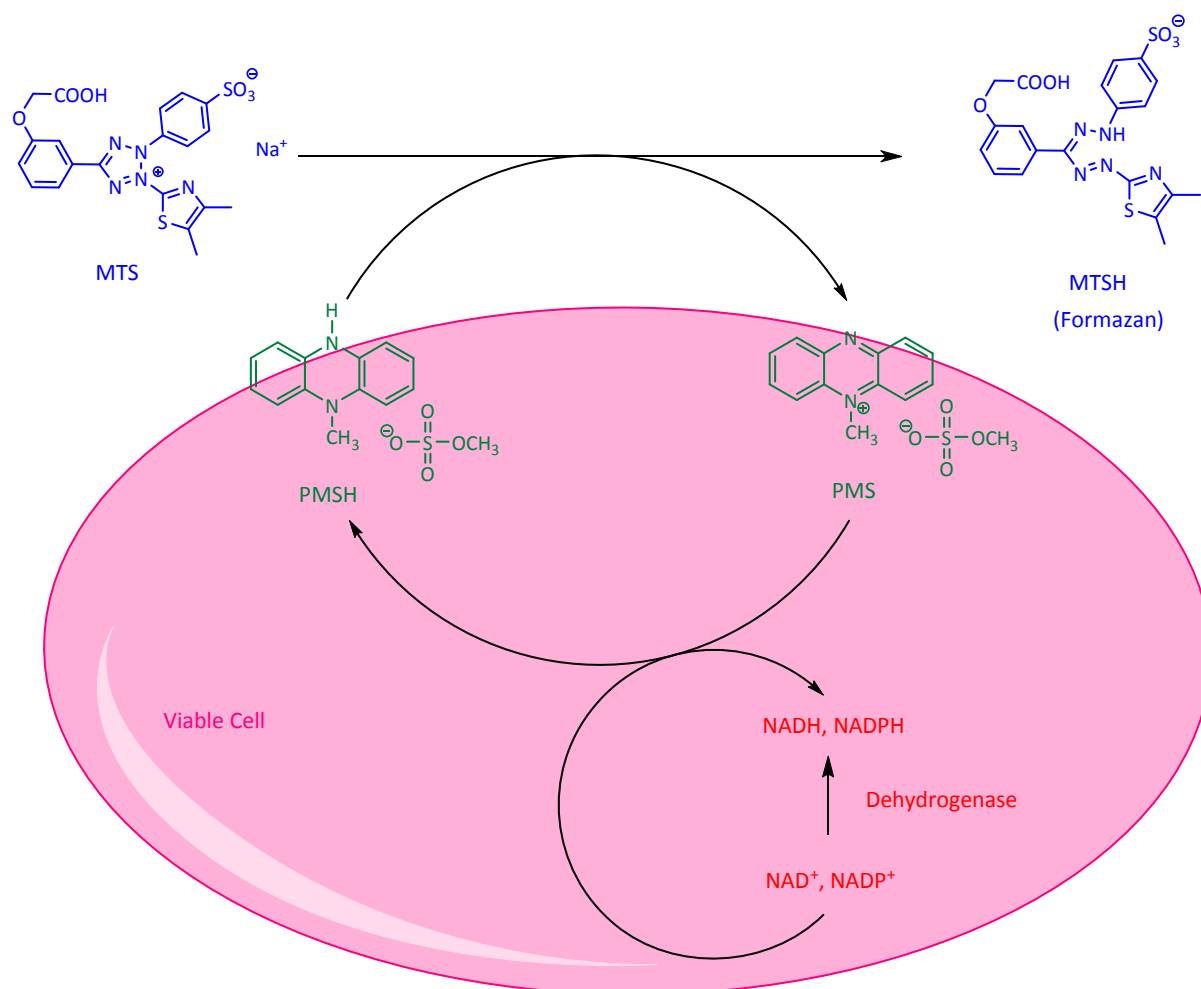
Scheme 4-2: *Dehydrogenase reduction of MTS to MTSH (formazan) via PMS*

This assay allows a quantitative evaluation of the cytotoxicity of the compound and is usually combined with a cell morphology assay giving a more qualitative evaluation of the cytotoxicity. A common morphological assay is the cytopathic effect assay (CPE),[10] which consists of evaluating the ability of the drug to prevent a virus from causing viral cytopathic effects in cells. Cytopathic effects, detected using inverted light microscopy, are morphological modifications of the cells caused by a viral infection. The antiviral activity of the drug consequently measures via the inhibitory concentration (IC_{50}) that reduces the cytopathic effects caused by the virus by 50%.

Another colorimetric assay designed to measure cell viability is the Trypan blue exclusion assay[11], which colours dead cells blue. Therefore, this assay also allows an evaluation of the cytotoxicity activity of the test drug.
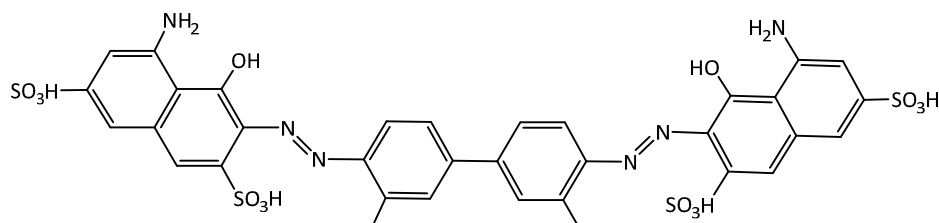
Figure 4-4: *Trypan blue*

Viable cells are impermeable to trypan blue but when their membrane is damaged, the dye is taken up by dead cells so living cells appear clear and dead cells are stained in blue. However this method does not differentiate the apoptotic cells and the necrotic cells.

Other types of cytotoxic assays have also been developed such as the genotoxicity BrdU assay, which measures cell proliferation. It involves the thymidine analogue BrdU (Figure 4-5), which is incorporated at a specific stage of cell division (Phase S).
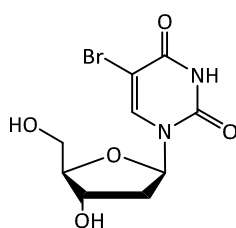
Figure 4-5: *BrdU as a thymidine analogue*

BrdU replaces thymidine during replication of DNA and fluorescent antibodies are used to recognise the bromide derivative of thymidine after denaturation of DNA. This assay is

therefore useful for giving information on the ability of the drug to reduce cell proliferation for example.

4.1.2 Inorganic compounds as drugs

In the 1960's, a pivotal discovery propelled inorganic chemistry towards medicinal applications with the reports by Rosenberg on the antitumor properties of cisplatin (Figure 4-6). [12,13]
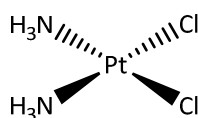
Figure 4-6: *Cisplatin*

In a cellular environment, one of the chloride ligands of cisplatin is replaced by a water ligand leading to the $[PtCl(H_2O)(NH_3)_2]^+$, which readily binds to DNA nucleobases and preferably to adjacent guanines. Upon loss of a second chloride, which inhibits cell division, DNA repair mechanisms are not able to counter the effect of this adduct on DNA, which induces cell death as a result. Cisplatin has proven to be effective against many different types of cancer including testicular, ovarian or lymphomas.[14] Consequently it has become a reference standard for tumour treatment and platinum complexes have been the objects of active research as potential antitumor drugs for the past 30 years. Nevertheless, only two other relative compounds have been authorised for clinical use: carboplatin and oxaliplatin. (Figure 4-7)
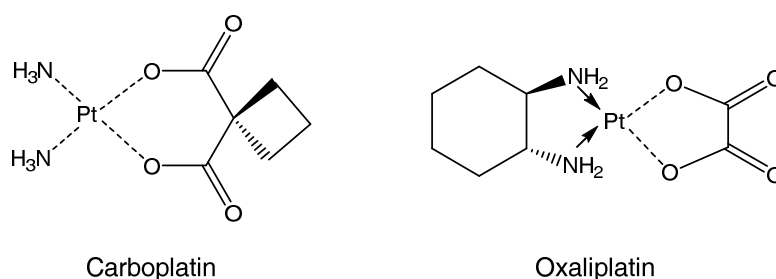
Figure 4-7: *Carboplatin and Oxaliplatin structures*

However these platinum complexes show significant limitations. Severe toxic side effects such as nephrotoxicity, cell resistance and some limited activity against certain types of cancer have led to investigations to find new inorganic drugs, including those containing organometallic moieties as outlined below.

4.1.3 Bioorganometallic compounds as drugs

Organometallic complexes are attracting increasing academic interest in the field of medicinal chemistry.[15] Ferrocene, which is the most common and popular representative of the metallocene family, is lipophilic, which helps penetration of cell membrane, and stable in biological environments and shows no toxic effects.[16] The ready functionalisation of ferrocene can further improve or change these properties and ferrocenyl derivatives are known to give interesting biological activities such as antitumor,[17,18] or cytotoxic effects.[19] In the 1970's, Edwards *et al.* reported the synthesis of a series of β-lactamase inhibitors containing ferrocene such as ferrocenyl-penicillins and ferrocenyl-cephalosporins to overcome penicillin and cephalosporin resistances,[20] which are antibiotics used against syphilis and other infectious diseases.

Ferrocenyl-penicillins   Ferrocenyl-cephalosporins
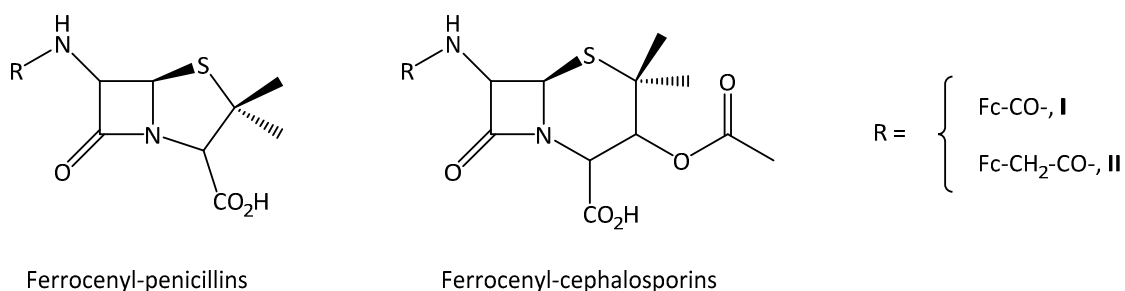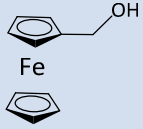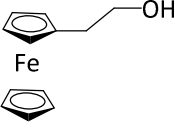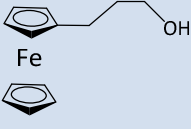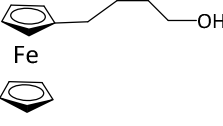
Figure 4-8: *Ferrocenyl-penicillins and ferrocenyl-cephalosporins developed by Edwards*

No antibiotic effect was observed for compound **I** (Figure 8) but when ferrocene was separated from the β-lactamase ring via a methylene space linker (**II**) antibiotic activity was comparable to benzypenicillin. Edward's work was the starting point for a large number of studies involving ferrocene in the design of potential organometallic drugs. For example, ferrocenyl derivatives such as ferrocenyl acetic acid have shown to be active against human andenocarcinoma, squamous cell carcinoma and large cell carcinoma of the lung, when it is used at high concentration (100 µg.mL^{-1}) via a human tumor clonogenic assay.[21] The clonogenic assay is used to evaluate the efficiency of a drug on survival and proliferation of cells. It consists of treating the cells, allowing them to grow and determining the percentage of cells that survived. Swarts *et al.* tested cytotoxicity of hydroxyl-ferrocenes on HeLa cells via a MTT assay and showed an interesting structure-activity relationship.[22] (Table 4-1)

Table 4-1: *EC$_{50}$ values of hydroxyl-ferrocenes with different side chain length by Swarts*

Compounds	IC$_{50}$ (µM)
	>100
	35.0
	17.0
	5.7

The data in Table 4-1 shows, the longer the side chain, the higher the cytotoxicity of the compounds. The ferrocenylbutanol (IC$_{50}$ = 5.2 µM) was almost 20 times more effective than the ferrocenyl methanol (IC$_{50}$ = 100 µM) for killing HeLa cells but not as active as cisplatin (IC$_{50}$ = 1.3 µM) under the same conditions. It has been also been reported that the antitumor activity of ferrocenyl compounds is related to the oxidation state of the iron of their ferrocenyl moiety. According to Orsella *et al.*,[23] the activity comes from the production of oxygen active radicals via enzymatic oxidation of Fe(II) to the ferrocenium form Fe(III). The ferrocenium ions interact with water and oxygen to form OH$^{\bullet}$ radicals that break DNA molecules, leading to cell death.

Based on the idea of "bio-isoterism", which corresponds to the principle of exchanging a group by another with similar chemical or biological properties, Jaouen[24] developed Ferrocifen, which is active as an antitumor compound against breast cancer, and Biot

developed ferroquine[25], which is an antimalarial compound. These two compounds are two recent examples of potential new organometallic drugs involving ferrocene. (Figure 4-9)

Tamoxifen (R = H)
Hydroxytamoxyfen (R = OH)

Hydroxyferrocifen

Chloroquine
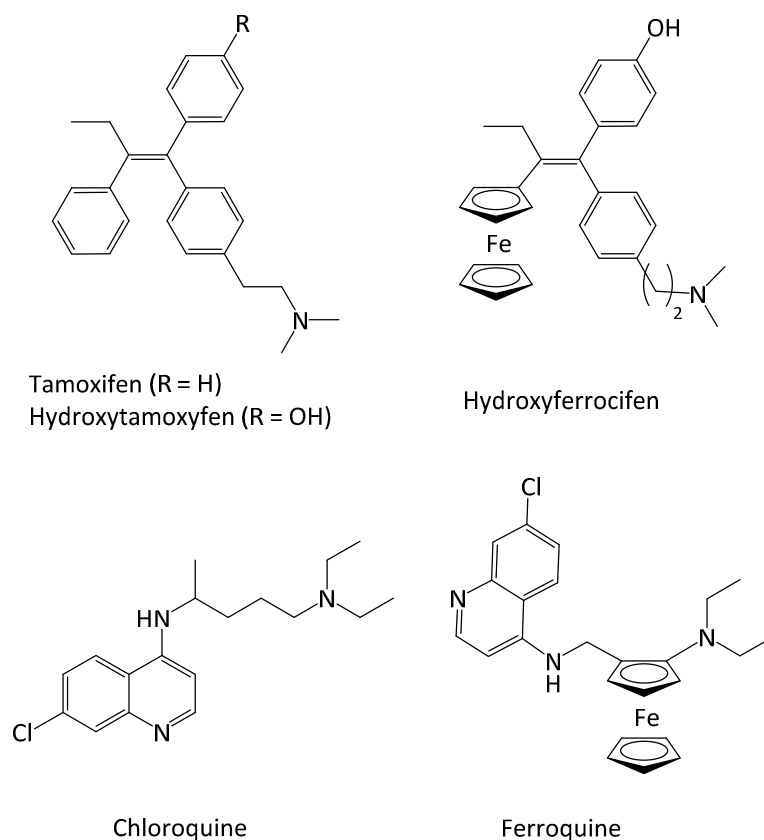
Ferroquine

Figure 4-9: *Chemical structure of tamoxifen, hydroxytamoxifen, chloroquine and their corresponding ferrocenyl drugs ferrocifen, hydroxyferrocifen and ferroquine*

In 2010 in the UK, around 50,000 women were diagnosed with breast cancer.[26] Unfortunately it is the most common cancer in UK and one of the most fatal of female cancers. Most breast tumour growths are linked to the presence of α-ERs (Estrogen Receptors) that are activated by the estrogen hormone. After many metabolic steps, interaction of estrogen with the receptors leads to cell proliferation. Tamoxifen is the standard treatment against hormone-dependent tumours (ER+) but it does not act directly on the receptors as it has a low affinity for the targeted receptor (ER). It has to be converted into the active antagonist hydroxytamoxifen by cytochrome P450 in the liver, whose anti-

proliferative activity comes from its competitive binding to ER receptor, leading to a repression of DNA transcription in cancer cells.[27] The limitations of this treatment are the low efficiency of the drug towards non-hormone-dependent tumours (ER-) and cell resistance against tamoxifen. (Figure 4-10)

Estrogen receptor-positive breast cancer

Estrogen

Tamoxifen inhibits

Estrogen receptor

Cell proliferation
• Controlled by estrogen
• Inhibited by tamoxifen

Estrogen receptor-negative breast cancer

Cell proliferation
• Not controlled by estrogen
• Not inhibited by tamoxifen

Artwork by Jeanne Kelly © 2010.
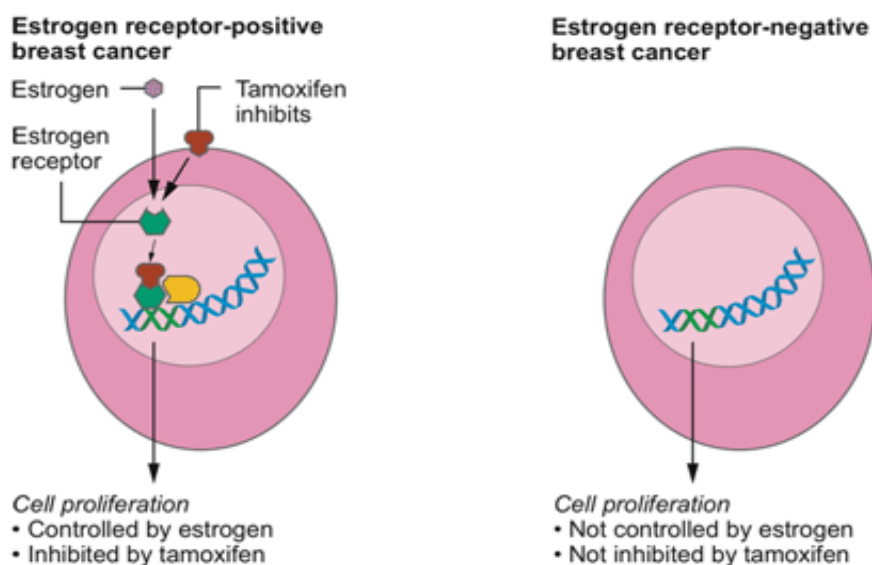
***Figure 4-10:** Estrogen receptor-positive and negative cancer mechanisms[28]*

To overcome these problems, Jaouen *et al.* developed hydroxyferrocifen by replacing the β-phenyl group of hydroxytamoxifen by a ferrocenyl moiety. Indeed, this drug revealed significant antiproliferatives effects on both ER+ and ER- receptors. As previously explained, the ferrocenyl moiety is involved in the formation of radicals that play a significant role in the activity of the drug in parallel of its binding mode of action.[29] This alternative activity of the ferrocenyl group was highlighted by related work on the ruthenium analogue of ferrocifen (Figure 4-11), which showed similar effects with ER+ cell lines but was inactive with ER- cell lines.

M = Fe, Ru
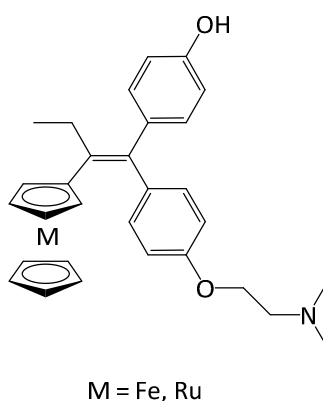
Figure 4-11: *Ruthenocifen, the ruthenium analogue of ferrocifen*

Jaouen explained that ruthenocene and ferrocene are similar in size and shape, but differ by their electrochemical behaviour. Ruthenocene is harder to oxidise and more importantly the resulting electron transfer is not reversible, unlike its ferrocene analogue.[30] This is a possible reason why ruthenocene does not allow formation of radicals and does not have any effects on ER- cells.

Using the same kind of bio-isoteric approach but towards bacterial agents, Biot *et al.*[23] replaced a part of chloroquine, one of the principal treatments against malaria, with a ferrocenyl group. Malaria affects about 300 million of people per year, via the transmission of the parasite *plasmodium falciparum* by the bite of a mosquito. Chloroquine and quinine have been used widely against the disease but the parasite developed strong resistance against these treatments. Consequently, the development of new anti-malarial alternatives has been the subject of intense research over the past few decades.[31] Unlike chloroquine, ferroquine does not seem to induce cell resistance and recently went through phase II of clinical trials as a potential efficient antimalarial drug.[14] The ferrocenyl enhanced lipophilicity and redox activity was used to explain the improved results.

In the light of these inspiring works, our group decided to investigate analogues of the previously synthesised FcNA monomers as potential antitumor or antiviral drugs.

4.2 Aim

Intensive research over the past 30 years on the structural modification of nucleosides has promoted the development of nucleoside analogues as potential drugs. Modification of the nucleobase or the sugar itself has resulted in antiviral drugs such as Acyclovir,[32] Brivudine[33] and Cidofovir[32] and antitumor drugs such as Fluorouracil (5-FU).[34] (Figure 4-12)

Brivudine   Acyclovir   Fluorouracil
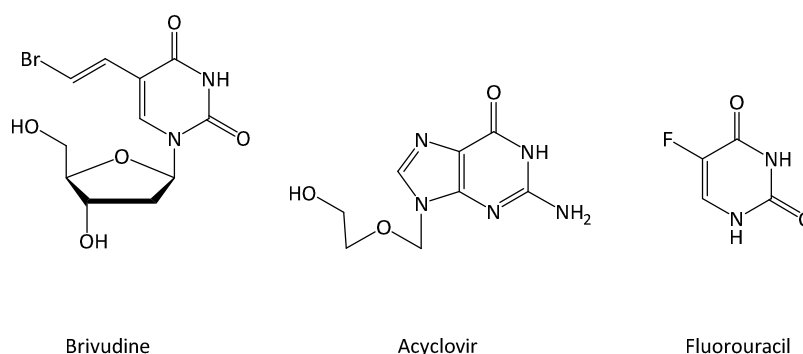
Figure 4-12: Three nucleosides analogues

Brivudine is an antiviral thymidine analogue used as a powerful inhibitor of Herpes Simplex Virus (HSV-1 and HSV-2) and the vesicular stomatitis virus (VZV). In fact it was first synthesised at the University of Birmingham in the 1980's by A. S. Jones *et al.*[35] Its mechanism of action is based on its incorporation into viral DNA and blocking DNA polymerase in DNA replication. The compound is activated after phosphorylation via the viral thymidine kinase (TK), which is a phosphotransferase enzyme that is also found in most living cells. The enzyme can be found in two forms, TK1 and TK2 and can be used as cell proliferation marker or as a way to identify a mechanism of action for drug candidates. As a

similar example of antiviral drug, Acyclovir is an acyclic analogue of guanosine, which is also used against Herpes Simplex virus and VZV. Its mechanism of action is comparable to Brivudine mechanism by its incorporation in viral DNA. Cidofovir, on the other hand is an analogue of cytosine as shown in Figure 4-13. It is used against CMV by preventing viral replication and transcription. It works similarly to Brivudine in that it inhibits DNA replication via its incorporation into DNA by viral DNA polymerase. However, unlike Brivudine or Acyclovir, it does not need to be activated via a viral kinase to be activated, but still needs to be phosphorylated.
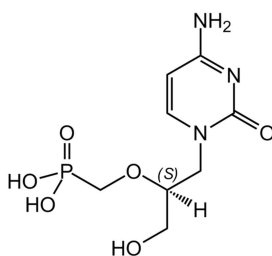
Figure 4-13: *Cidofovir*

5-FU is an analogue of uracil used as an antitumor drug. Uracil is important for the synthesis of RNAs and is the principal source of thymidine triphosphate (TTP), which is incorporated into DNA after its synthesis by *Thymidine synthase*. 5-FU acts as a direct competitive inhibitor of the thymidine synthase and blocks the synthesis of TPP and DNA synthesis, leading to cell death. It also intercalates into RNA leading to mistakes in transcription.
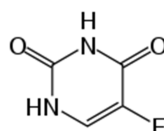
Figure 4-14: *5-Fluorouracil*

As explained by Romeo,[36] nucleoside analogues showing antiviral or antitumor activities present three significant structural features (Scheme 4-3): a) the hydroxyl group (Red), to allow phosphorylation by kinases in biological environment, b) the nucleobase (Green) to allow its direct interaction with the target via hydrogen bonds, and c) the spacer (Blue) between the hydroxyl and the nucleobase for orientating both groups in the right position. The FcNA monomers previously described in Chapter 3 appeared to loosely fit the criteria (Scheme 4-3). Therefore the target FEN-T, containing just one base and one hydroxyl group, was designed and synthesised within the group following the same synthetic route developed for FcNA-Adenine, FcNA-Uracil and FcNA-Thymine.
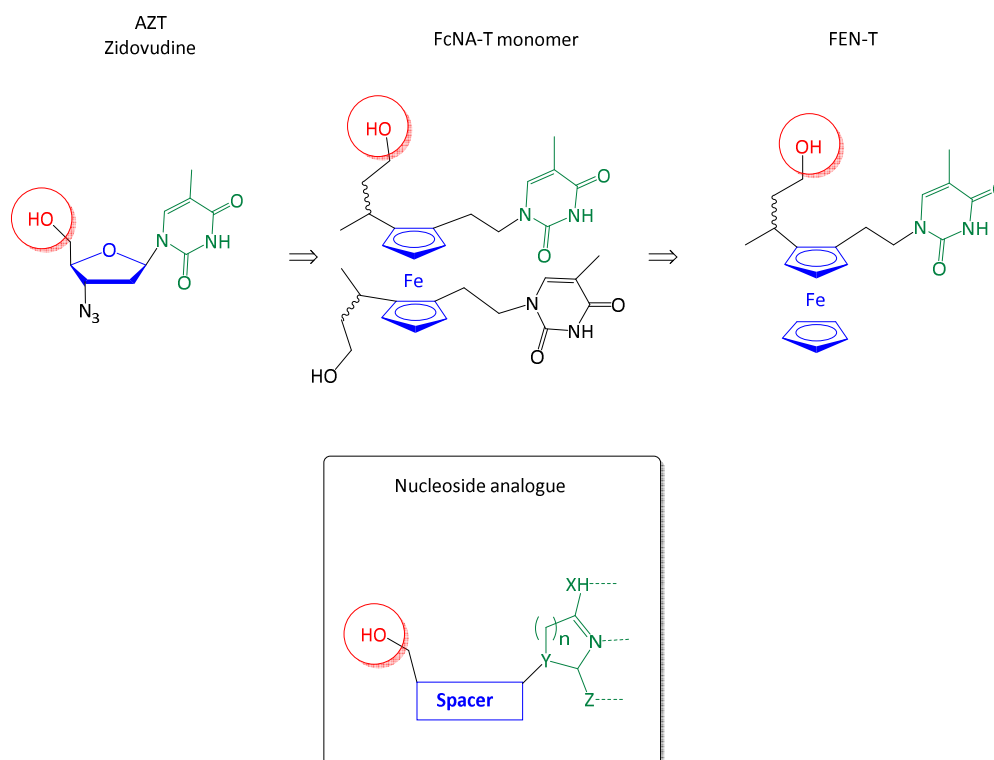
Scheme 4-3: *Structural similarities between AZT and FcNA-T that led to the design of FEN-T*

The bio-activity of FEN-T was then tested in collaboration with the Laboratory of Virology and Chemotherapy in Leuven, Belgium, for preliminary pharmacological studies and was also studied in collaboration with researchers in LES (Biosciences) and MDS (Schools of Immunity

and Infection and Cancer Sciences) at the University of Birmingham. Encouraged by the promising results of FEN-T that are presented later on in this chapter, it was decided to extend the synthesis to analogues involving other nucleobases. The synthesis of the new ferronucleobases FEN-Adenine and FEN-Cytosine is detailed in the next section. (Figure 4-15)
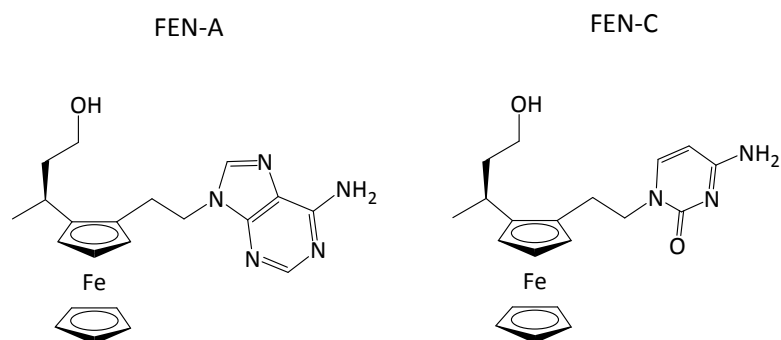
Figure 4-15: Targets: Ferronucleobases containing adenine and cytosine

4.3 Synthesis of ferronucleobases as potential drugs

The synthesis of the ferronucleobases followed the previous synthetic route developed for FcNA monomers in Chapter 3 and goes through the same mechanisms but in this case only one Cp ring of the ferrocene was substituted. The synthesis was divided into three major steps. The first part consisted of the synthesis of disubstituted iodo-dimethylamine-ferrocene, followed by the extension of the methyl-propanol arm via nucleophilic substitutions. In the final part of the synthesis, thymine was coupled to ferrocene via Mitsunobu coupling reaction after developing the two-carbon alkyl chain.

4.3.1 Part 1: Precursor synthesis

The Friedel-Craft acylation of ferrocene gave the mono-substituted ferrocene ketone in good yields, which was then subjected to enantioselective reduction using (*S*)-CBS catalyst to give

the chiral hydroxyl (*R*)-**55** in 85% yield. Acetylation of the alcohol using acetic anhydride, TEA and DMAP in DCM gave mono-acetyl (*R*)-**56** in 86% yield. In the next two steps leading to the disubstituted iodo-dimethylamine ferrocene (*R*,*S*$_p$)-**58**, two side-reactions were encountered, as shown in Scheme 4-4.
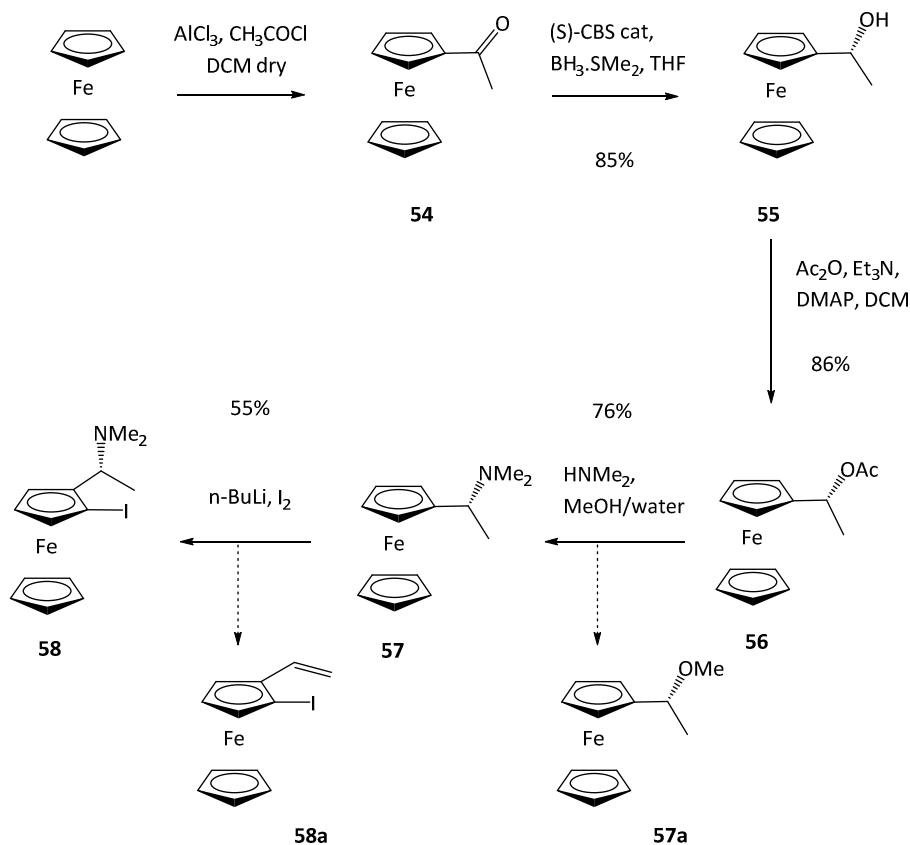
Scheme 4-4: *First part of the synthesis*

The nucleophile substitution of acetate **56** in presence of dimethylamine in MeOH/H$_2$O gave dimethylamine (*R*)-**57** in 76% yield. In parallel, a side-reaction formed the methoxy derivative **57a**. This side-reaction has already been described by Schwink and Knochel[37], who highlighted the strong influence of the solvent on the substitution reaction by comparison of two solvent systems: THF/H$_2$O and MeOH/H$_2$O. The targeted compound **A** was obtained quantitatively in THF/H$_2$O but the same reaction in MeOH/H$_2$O gave exclusively the methoxy derivative **B** (Scheme 4-5).[37]
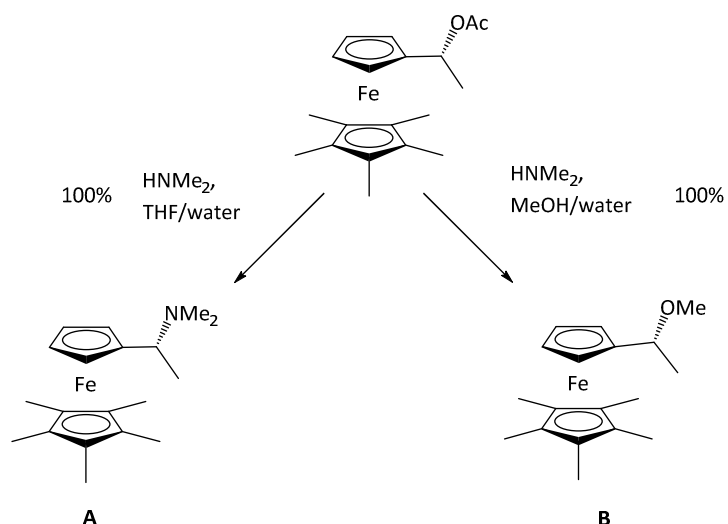
Scheme 4-5: *Influence of the medium on the substitution reaction by Knochel*

The result was explained by a combination of two factors. The first one is the parallel methanolysis reaction competing with the dimethylamine substitution. Methanol (solvent) is in excess compared to the dimethylamine reagent and therefore it displaces the reaction equilibrium towards formation of **B** via a thermodynamic process. The second factor is the ability of the electron-rich pentamethylferrocenyl moiety to stabilise the formation of the ferrocenyl carbenium ion.

In the case of **56**, the competing methanolysis reaction could be significantly reduced using a smaller volume of solvent and a larger excess of dimethylamine. The ability of the ferrocene to stabilise the carbenium is weaker than the pentamethylcylopentadienyl moiety and therefore the equilibrium towards the formation of **57** is favoured under these conditions. (Scheme 4-6)
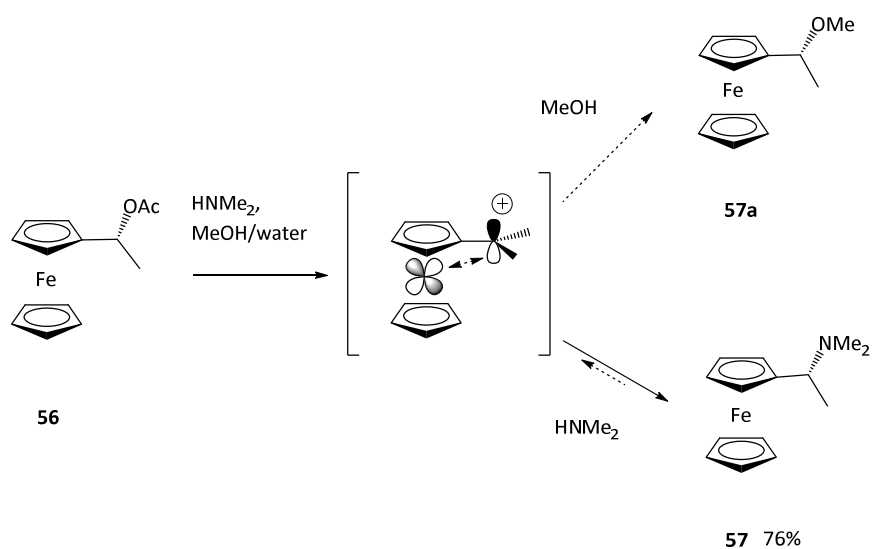
Scheme 4-6: *Side reaction process during dimethylamine substitution*

The following directed *ortho*-metallation of **57** with iodine gave (*R,S$_p$*)-**58** in a yield of 55%, which is lower than the 80% yield obtained with the bis-dimethylamine ferrocene **33**. (Scheme 4-7)
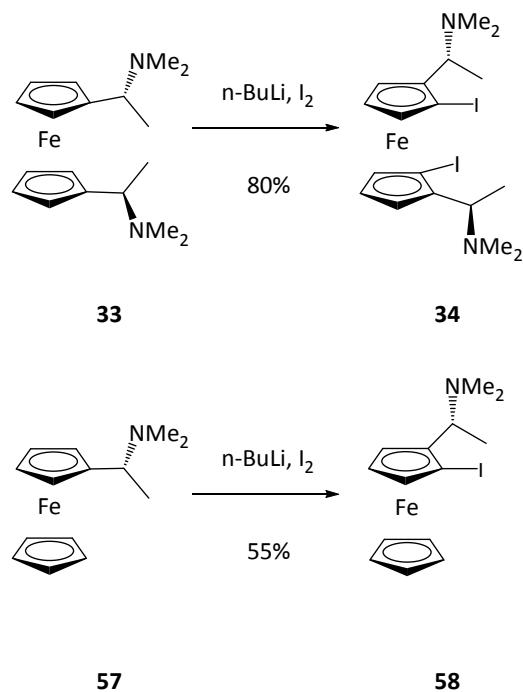
Scheme 4-7: *Ortho-halogenation of bis and mono-substituted ferrocene 33 and 57*

The low yield is due to a competing elimination reaction leading to the formation of vinyl (S_p)-**58a** as shown in Scheme 4-8. Several factors favoured elimination of dimethylamine: a) *n*-BuLi is a very strong base and is able to deprotonate the methyl at the β position of the dimethylamine; b) the carbenium formed is stabilised by the electron-rich ferrocenyl moiety and d) the reaction is performed in aprotic solvents (Et$_2$O, THF) that tend to promote eliminations. Another factor plays an important role in favouring the elimination: temperature. In the second part of the procedure, addition of iodine was performed at -78°C and the temperature was progressively raised up to room-temperature to bring lithium-halogen exchange to completion. Unfortunately, increasing the temperature would also favour elimination processes leading to the formation of **58a**. The optimisation of the reaction was therefore a compromise between completing the lithium-halogen exchange and the limiting elimination process.
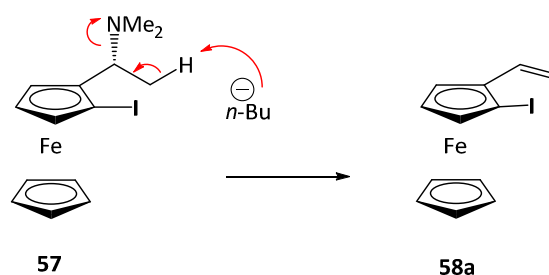
Scheme 4-8: *Elimination process during ortho-metallation of 57*

The synthesis of the iodo-dimethylamine-ferrocene **58** was then followed by the extension of the methylpropanol arm, as described in the following section.

4.3.2   Part 2: Hydroxyl arm extension

The development of the hydroxyl arm of the ferronucleobase involves six steps from the iodo-dimethylamine to the silylated-hydroxyl following the route previously adopted for FcNA monomers. (Scheme 4-9)
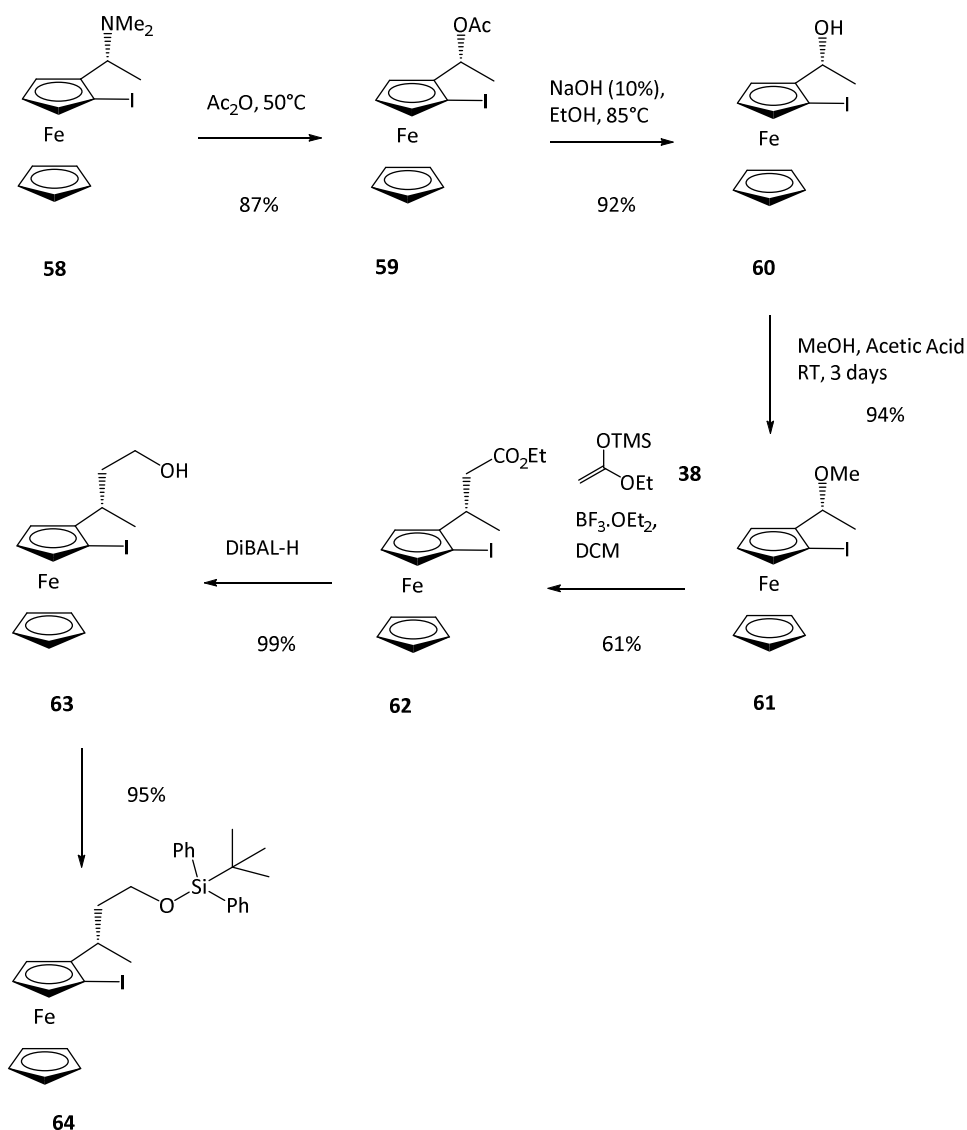
Scheme 4-9: *Extension of hydroxyl part of the ferronucleobase*

The di-substituted iodo-dimethylamine ferrocene (*R,S$_p$*)-**58** was acetylated with acetic anhydride at 50 ˚C for 2 h to give the acetate (*R,S$_p$*)-**59** in 87% yield. The latter was

hydrolysed with sodium hydroxide to give (R,S_p)-**60**, which was then methoxylated under acidic conditions to give (R,S_p)-**61**. Both reactions proceeded in very high yields. Formation of ester **61** via the vinylethoxytrimethylsylane with $BF_3.OEt_2$ acting as a promotor for the nucleophilic attack of the vinylethoxytrimethylsylane **38** on the ferrocene carbenium, gave (S,S_p)-**62** in 61% yield. Reduction via DIBAL-H gave (S,S_p)-**63** almost quantitatively, which was followed by protection of the hydroxyl group with TBDPSCl, giving (S,S_p)-**64** in 95% yield.

4.3.3 Part 3: Extension of three carbon linker

The synthesis of the ferrocenyl precursor required for the nucleobase coupling step was straightforward. The three steps from the iodide derivative **64** led to the synthesis of the desired two-carbon linker alcohol **67** as shown in Scheme 4-10.
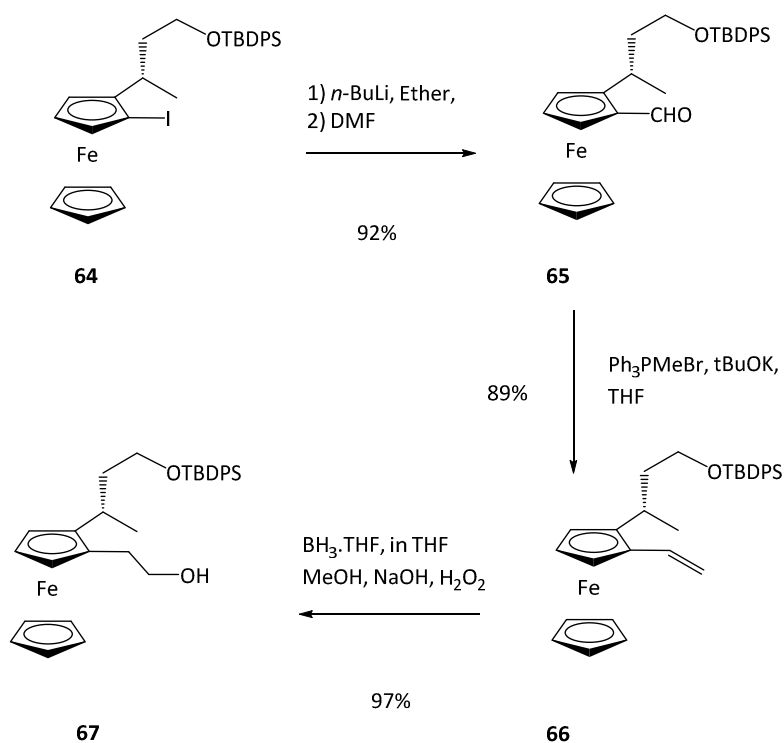
Scheme 4-10: *Third part of the synthesis*

The lithiation of (S,S_p)-**64** in presence of *n*-BuLi in ether was followed by addition of DMF to give (S,S_p)-**65** in 92% yield. Wittig reaction on the aldehyde gave the vinyl derivative (S,R_p)-**66** in 89% yield and a change in the planar chirality configuration, according to Cahn-Ingold-Prelog rules. The alcohol (S,R_p)-**67** was obtained after hydroboration-oxidation of the vinyl (S,R_p)-**66** in 97% yield (Scheme 4-10). The enantiopurity of the synthesis was checked using chiral HPLC on compound **67**. As shown in Figure 7-20, **67** gave a peak at 16.8 min corresponding to the (S,R_p) enantiomer and a second smaller peak at 14.4 min corresponding to the other enantiomer (R,S_p). However, the calculated enantiomeric excess of 96.6% was considered good enough to go on with the synthesis. The chiral HPLC graphs are shown in the appendix. (Figure 7-20, 7-21 and 7-22)

4.3.4 Part 4: Nucleobase coupling

Adenine and cytosine were linked to the di-substituted ferrocene via two different paths. As previously developed in Chapter 2 and 3, adenine was coupled via a Mitsunobu reaction and cytosine via a bromide substitution.

4.3.4.1 Adenine coupling

Coupling (S,R_p)-**67** with the protected adenine **19** was achieved in THF in presence of DIAD at 65˚C. The disubstituted ferrocenyl (S,R_p)-**68** was obtained in 72% yield, which was then deprotected with TBAF to give (S,R_p)-**69** in 80% yield followed by a debenzoylation with methylamine to give the target FEN-A (S,R_p)-**70** in 73% yield. (Scheme 4-11)
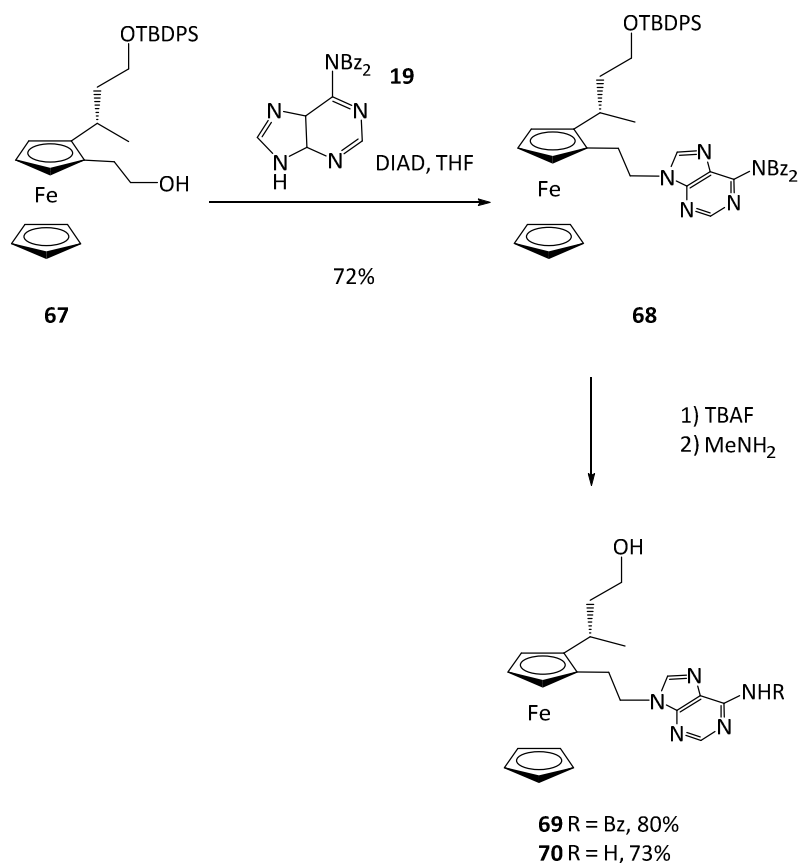
Scheme 4-11: *Adenine coupling and deprotection of the FEN-A*

4.3.4.2 Cytosine coupling
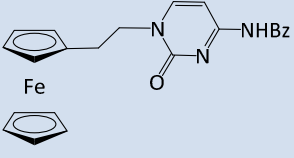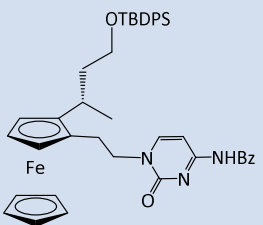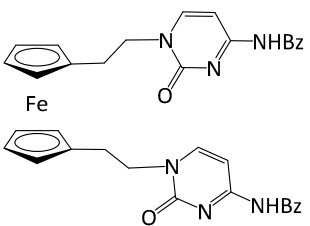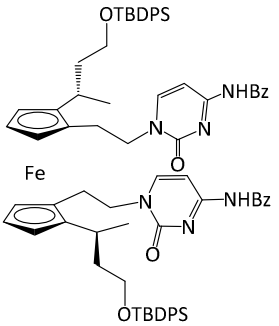
Cytosine coupling was performed on the bromide derivative (S,R_p)-**71** obtained from bromination of (S,R_p)-**67** in 84% yield using NBS in presence of triphenylphosphine and pyridine. The coupling with the protected cytosine **21** was carried out in DMF at 50°C in presence of NaH to give (S,R_p)-**72** in 60% yield. TBDPS deprotection of the coupled ferrocene with TBAF led to (S,R_p)-**73** in 93% and the final debenzoylation of the nucleobases using methylamine gave the target FEN-C (S,R_p)-**74** in 97% yield. (Scheme 4-12)
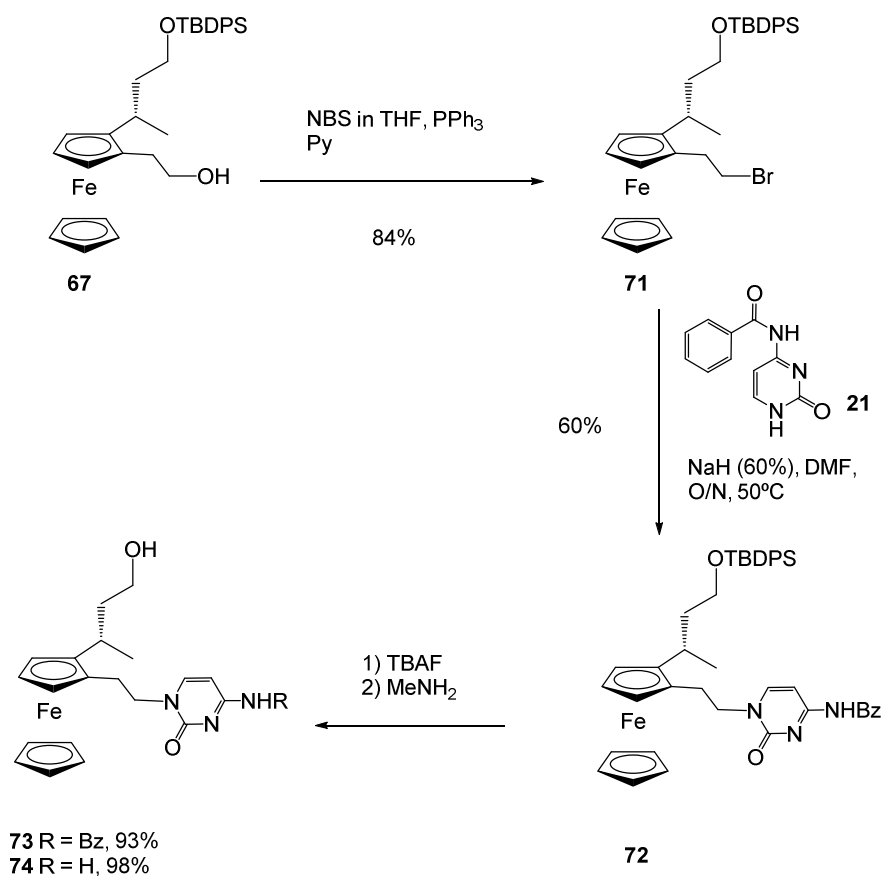
Scheme 4-12: *Cytosine coupling and deprotection*

It is interesting to compare the yields of various cytosine derivatives synthesised as part of this thesis (Table 4-2). It appears that steric hindrance plays a significant role in the efficiency of the nucleophilic substitution. Substitution of one Cp only (**28a** and **72**) is much easier than bis-substitution (**28** and **53**).

Table 4-2: *Ferrocenyl cytosine derivatives*

Compound	Yield	Compound	Yield
	68%		60%
	25%		16%

In conclusion, the two targets, FEN-A and FEN-C, were successfully synthesised via the same synthetic route developed for the tetra-substituted ferrocenyl derivatives, although side-reactions reduced the efficiency of two steps in the synthesis. FEN-T, FEN-A and other derivatives are currently undergoing cell line tests to investigate potential antitumor or antiviral activities. Preliminary results are described below.

4.4 Biological results

The biological studies conducted in the laboratories of Leuven and Birmingham consisted of evaluating the biological activity of FEN-T, FEN-A and some of their derivatives (Figure 4-18). The drug screening was conducted towards various infectious diseases such as hepatitis, AIDS, influenza virus (H1N1, H3N2), viccinia virus (VV), vesicular stomatitis virus (VSV),

herpes (HSV-1, 2) and against cancer cells. MTS, BrdU, AMES and adenylate assays were performed on different types of cells, including human embryonic lung cells (HEL), Madin-Darby canine kidney epithelial Cells (MDCK), murine leukemia cells (L1210), human T-lymphocyte cells (CEM), human cervix carcinoma cells (HeLa), Crandell-Rees Feline Kidney cells (CRFK) and Vero cells.
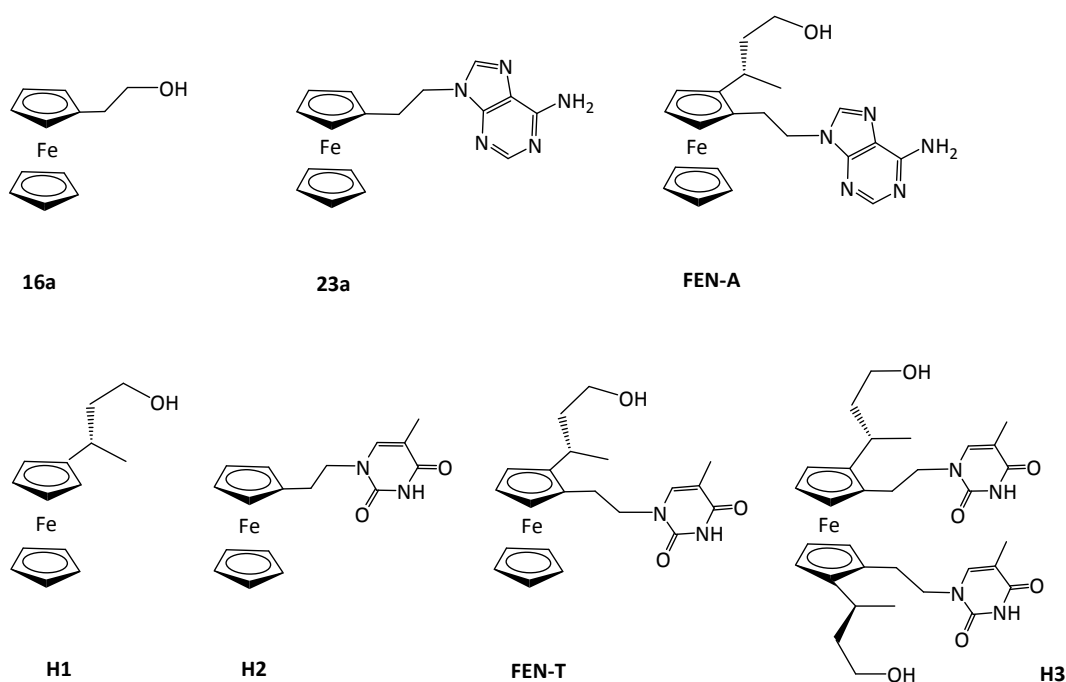
Figure 4-16: *Targets*

The activity of these drug candidates was investigated to get a better understanding of the influence of the different moieties of the main target (FEN-T) on its biological activity.

4.4.1   Antiviral activity

The first results reported by the laboratory of virology of Leuven have indicated that FEN-T is quite a toxic compound against the majority of the cells tested but shows interesting antiviral activities against Herpes virus such as HSV-1, HSV-2, HSV-1 (HSV-1 TK⁻ KOS ACV), VV and vesicular stomatitis virus in HEL cells. FEN-T activity seems to be comparable to known

clinical drugs such as Brivudine (BVDU) and Cidofovir (HPMPC) used as positive controls. (Table 4-3)

Table 4-3: *FEN-T antiviral activity against Herpes virus compared to Brivudine*

	MMC (µM)		EC_{50} (µM)	
	HSV-1	HSV-2	HSV-1	HSV-2
FEN-T	244		2.4	2.4
Brivudine	250		0.02	183
Cidofovir	250		2	2

These results indicated that FEN-T is highly toxic in most the cell tested (HeLa, CRFK, Vero cells, MDCK) with MCC values of 9.88 µM compared with the 100-250 µM for certain commercially available drugs (Ribavirine, DHPA, DS 5000). Unfortunately, this appears to make FEN-T too cytotoxic and not specific enough to offer good antiviral activity. However, FEN-T did give a MMC value of 244 µM comparable to Brivudine cytotoxic activity (> 250 µM) on HEL cells infected with HSV-1 or HSV-2. It was though that FEN-T was less cytotoxic due to these being monolayer confluent HEL cells. Under these conditions, these cells are not in a growth phase and are therefore less susceptible to the cytotoxic effect of the compound than rapidly proliferating CEM or MT-4 cells. An encouraging result under these conditions is that FEN-T gave a better EC_{50} value than Brivudine towards HSV-2 with EC_{50s} of 2.4 µM for FEN-T, against 183 µM for Brivudine. Furthermore, FEN-T shows comparable antiviral activity to Cidofovir against HSV-1 and 2 with 2.4 µM for FEN-T against 2 µM for Cidofovir.

FEN-T also gives competitive activities towards other viruses such as vaccinia virus (VV) and vesicular stomatitis virus (VSV). With a similar minimum cytotoxic concentration to the other drugs, the antiviral activity of FEN-T against VSV is better than Brivudine but not against VV as shown in Table 4-4. Furthermore, Cidofovir gives better results than FEN-T against VV but not against VSV.

Table 4-4: *FEN-T antiviral activity against vaccinia virus (VV) and vesicular stomatitis virus (VSV) compared to Brivudine and Cidofovir.*

	MCC (µM)		EC$_{50}$ (µM)	
	VV	VSV	VV	VSV
FEN-T	244	21.6	48	
Brivudine	250	10	250	
Cidofovir	250	17	250	
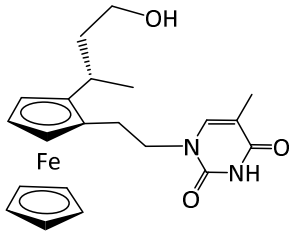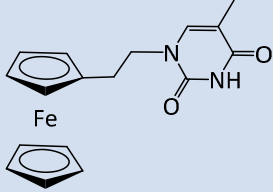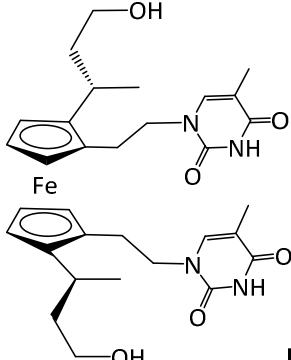
To conclude, the preliminary results indicate that FEN-T is generally highly cytotoxic for a range of cell lines but without significant activity at subtoxic concentrations. However, on non-rapidly dividing cell lines the compound appears to inhibit herpes viruses 1 and 2 and the vesicular stomatitis virus. Furthermore, its antiviral activity can be similar or even better than certain commercial drugs such as Brivudine or Cidofovir. These results are promising and will be the subject of further investigations in the future.

4.4.2 Antitumor activity

Leuven and Birmingham laboratories worked in parallel to investigate the antitumor activity of FEN-T and FEN-A as well as some of their derivatives as presented in Figure 4-18. In Leuven, an investigation of the thymine compounds and their controls was carried out on the proliferation of murine leukemia cells (L1210), human cervix carcinoma cells (HeLa) and non-cancerous human T-lymphocyte cells (CEM). Cisplatin was used as a positive control to compare activities.

As shown in Table 4-5, FEN-T showed to be the most promising candidate, giving the lowest IC_{50} against the three cell lines and shows higher cytotoxicity than cisplatin on L1210 cells with an IC_{50} of 0.78 µM compared to 1 µM for cisplatin. Interestingly FEN-T shows a comparable activity to cisplatin on the non-cancerous CEM, with an IC_{50} of 0.9 µM. However, the compound is not as active as cisplatin on HeLa cells. These results also highlighted the importance of the alcohol group with **16a** being 15 times more toxic than the control (**H2**), but less active than FEN-T.

Table 4-5: *Antitumoral activity of FEN-T and some of its analogues compared to cisplatin antitumoral activity*

	IC$_{50}$ (µM)		
	L1210	CEM	HeLa
FEN-T	*0.78*	*0.9*	2.7
Cisplatin	*1*	*0.9*	1.2
16a	25	43	52
H2	417	592	509
H3	99	149	100

Studies were also carried out on three oesophageal cancer cell lines in the School of Biosciences at the University of Birmingham. The results were broadly similar. The cell viability studies (MTT) showed that two oesophageal cancer cell lines (OE 19 and 21) were susceptible to FEN-T, FEN-A and to the other compounds to varying degrees, with preliminary results indicating FEN-T to be as active as cisplatin. Interestingly not all the cell lines tested were susceptible, with OE 33 being resistant. Once again the combination of the hydroxyl group and the nucleobase was important, with FEN-T being the most active , followed by FEN-A.

The potential mutagenicity of the compounds was evaluated via the AMES assay. It consists of using genetically modified bacteria (salmonella) that are unable to synthesise histidine. In the case of the substance induced mutations, the cell regains its ability to live without the help of growing factors such as histidine, which can be synthesised again by the cell. Preliminary AMES test data were encouraging in that they showed all the compounds to be negative.

In vitro assays of cellular viability (MTT assay) and cell proliferation (BrdU assay) were also performed on three colorectal cancer cell lines (HT29, RKO and SW480) in the School of Cancer Sciences. The commercial nucleosidic anticancer agent fluorouracil (5-FU) was included as a positive control. As shown in Figure 4-19, the study compares the results obtained with the targets and 5-FU on the proliferation and the viability of collateral cancer cells after 48h of exposition. Once again, it shows that compounds FEN-A and FEN-T are the most promising compounds, giving a high potential of activity as anti-neoplastic agents in terms of effect on cellular proliferation in comparison with 5-FU.
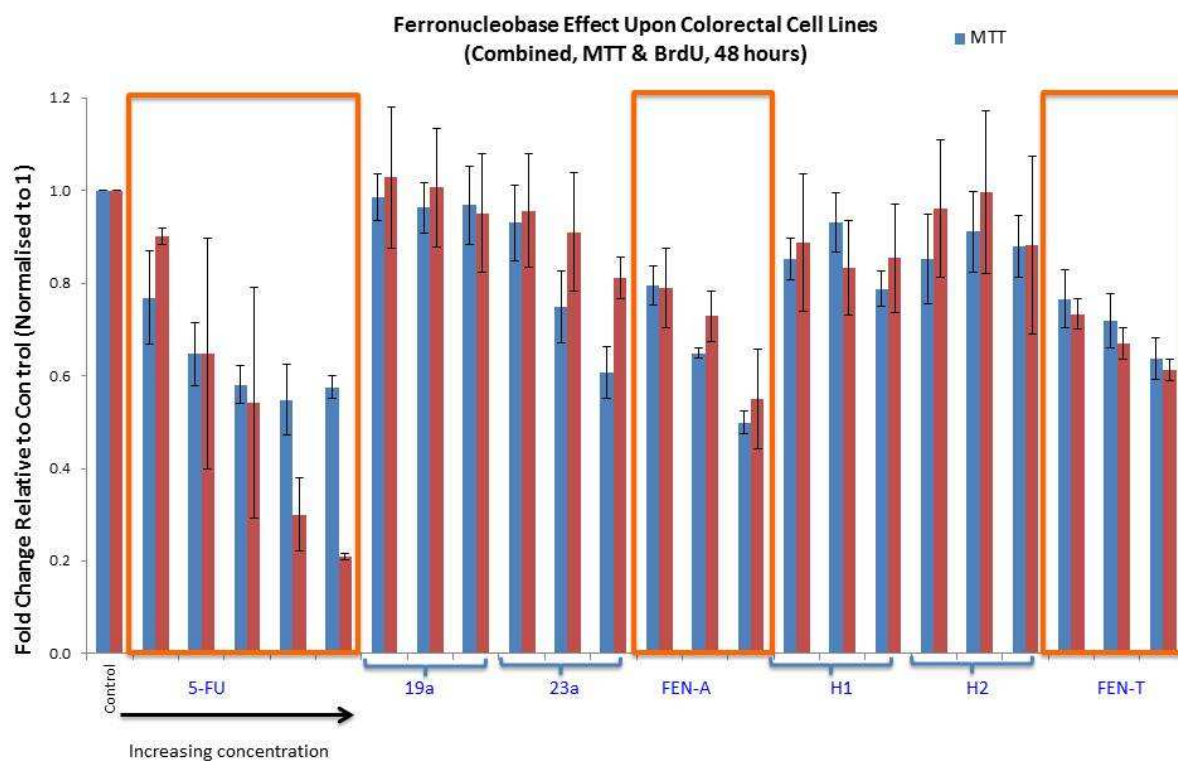
Figure 4-17: *MTT and BrdU assays for the evaluation of antitumoral activity of FEN-A and FEN-T compared to 5-FU*

The data again indicate that the compounds containing both a nucleobase and an alcohol group are the most active, suggesting they play a role in hindering cell proliferation by inhibiting DNA synthesis.

4.5 Conclusion

These preliminary results demonstrate the potential antiviral activity of ferronucleobases, with FEN-T giving activities comparable to commercial drugs such as Brivudine and Cidofovir. Several of these compounds in particular those containing both a nucleobase and an alcohol group, appear to play a role in hindering cell proliferation by inhibiting DNA synthesis. However, the cytotoxicity of these compounds is an issue, which may preclude their use as antiviral agents. However, this cytotoxicity is advantageous when considering antitumor activity. Promising results have been obtained that are comparable to 5-FU, which is an anticancer drug that inhibits DNA synthesis rather like the antiviral drugs. However for these compounds to be effective, selectivity towards cancer cell lines over non-cancerous ones needs to be addressed and studied in more detail.

4.6 References

1. R. Porter, *The greatest benefit to mankind: A medical history of humanity* (The Norton history of science), **1999**.
2. Bertram G. Katzung in *Introduction* in B. G. Katzung, S. B. Masters, A. J. Trevor, *Basic and clinical pharmacology (12th edition),* **2012.**
3. L. Z. Benet in M. G. Horning, J. Mitchell, *Drug metabolism and drug toxicity*, **1984**.
4. H. E. Selick, A. P. Beresford, M. H. Tarbit, *Drug Discovery Today*, **2002**, *7*, 755-756.
5. U. Landegren, *J. Immunol. Methods,* **1984**, *67*, 379-388.
6. F. Denizot and R. Lang, *Journal of Immunological Methods,* **1986***, 89,* 271-277.
7. J. A. Plumb, R. Milroy, S. B. Kaye, *Cancer Res.*, **1989**, *49*, 4435-4440.
8. D. A. Scudiere, R. H. Shoemaker, K. D. Paul, A. Monks, S. Tierney, T. H. Nofziger, M. J. Currens, D. Seniff, M. R. Boyd, *Cancer Res*, **1988**, *48*, 4827-4833.
9. D. D. Dunigan, S. B. Waters, T. C Owen, *BioTechniques*, **1995**, *19*, 640-649.
10. D. F. Smee, A. C. Morrison, D. L. Barnard, R. W. Sidwell, *Journal of Virological Methods*, **2002**, *106*, 71-79.
11. G. S. A. Longo-Sorbello, G. Saydam, D. Banerjee, J. R. Bertino, chapter 38 : Cytotoxicity and Cell Growth Assays in *Cell Biology, A Laboratory Handbook, 4-Volume* (3rd Edition), **2006**.

12. B. Rosenberg, L. VanCamp, T. Krigas, *Nature*, **1965**, *205*, 698.
13. B. Rosenberg, L. VanCamp, J. E. Tronsko, V. H. Mansour, *Nature*, **1969**, *222*, 385-386.
14. E. Wong and C. M. Giandomenico, *Chem. Rev.*, **1999**, *99*, 2451-2466.
15. G. Gasser and N. Metzler-Nolte, *Curr. Opinion Chem. Biol.*, **2012**, *16*, 84-91.
16. K. Dombrowski, W. Baldwin, J. E. Sheats, *J. Organomet. Chem.*, **1986**, *302*, 281-306.
17. G. Gasser, I. Ott, and N. Metzler-Nolte*, J. Med. Chem.*, **2011**, *54*, 3-25.
18. M. F. Fouda, M. M. Abd-Elzaher, R. A. Abdelsamaia, A. A. Labib, *Appl. Organometal. Chem.*, **2007**, *21*, 613-625.
19. P. Meunier, I. Ouattara, B. Gautheron, J. Tirouflet, D. Camboli, J. Besancon, *Eur. J. Med. Chem.*, **1991**, *26*, 351-362.
20. E. I. Edwards, R. Epton, G. Marr, *J. Organomet. Chem.,* **1976**, *107*, 351-357; E. I. Edwards, R. Epton, G. Marr*, J. Organomet. Chem.*, **1979**, *168*, 259-272.
21. E. W. Neuse and F. Kansawa, *Appl. Organomet. Chem.*, **1990**, *4*, 19-26.
22. R. F. Shago, J. C. Swarts, E. Kreft, C. E. J. Van Rensburg, *Anticancer Research*, **2007**, *27*, 3431-3434.
23. D. Osella, M. Ferrali, P. Zanello, F. Laschi, M. Fontani, C. Nervi, G. Cavigiolio, *Inorg Chim Acta*, **2000**, *306*, 42-48.
24. A. Vessieres, S. Top, W. Beck, E. Hillard, G. Jaouen, *Dalton Trans.*, **2006**, 529-540.
25. D. Dive and C. Biot, *Chem. Med. Chem.*, **2008**, *3*, 383-391.
26. http://www.cancerresearchuk.org/cancer-info/cancerstats/types/breast, **10/2013**
27. A. K. Shiau, D. Barstad, P. M. Lorisa, L. Cheng, P. J. Kushner, D. A. Agard, G. L. Greene, *Cell*, **1998**, *95*, 927-937.
28. http://www.cancer.gov/cancertopics/understandingcancer/estrogenreceptors/AllPages, **10/2013**.
29. D. Hamels, P. M. Dansette, E. A. Hillard, S. Top, A. Vessieres, P. Herson, G. Jaouen, D. Mansuy, *Angew. Chem. Int. Ed.*, **2009**, *48*, 9124-9126.
30. E. Hillard, A. Vessieres, L. Thouin, G. Jaouen, C. Amatore, *Angew. Chem.*, **2006**, *118*, 291-296; *Angew. Chem. Int. Ed.*, **2006**, *45*, 285-290.
31. M. Patra, G. Gasser, N. Metzler-Nolte, *Dalton Trans.*, **2012**, *41*, 6350-6358.
32. H. Schaeffer, S. Gurwara, R. Vince, S. Bittner, *Journal of Medicinal Chemistry,* **1971**, *14*, 367-369.
33. E. De Clercq, *Nature*, **2004**, *6*, 704-720.
34. C. Heidelberg, N. K. Chaudhuri, P. Danneberg, D. Mooren, L. Griesbach, R. Duschinsky, R. J. Schnitzer, E. Pleven, J. Scheiner, *Nature,* **1957***, 179*, 663-666.
35. R. T. Walker, A. S. Jones, E. De Clercq, J. Descamps, H. S. Allaudeen, J. W. Kozarich, *Nucleic Acids Symp Ser.*, **1980**, *8*, 95-102.
36. G. Romeo, U. Chiacchio, A. Corsaro, P. Merino, *Chem. Rev.*, **2010**, *110*, 3337-3370.
37. L. Schwink and P. Knochel, *Chem. Eur. J.*, **1998**, *4*, 950-968.

CHAPTER 5: CONCLUSIONS AND FUTURE WORK

All along the development of this thesis, investigations on linking ferrocenyl derivatives with different nucleobases have been carried out. The main goal of this work at the outset was to synthesise nucleoside analogues containing ferrocene that could form metal containing nucleic acids. In order to achieve this goal, preliminary studies on bis-substituted ferrocenes were first of all carried out to investigate how ferrocene could be coupled to adenine, but also to uracil and cytosine. Further studies showed how the type and number of linkers as well as the type of nucleobases affects the electrochemical properties. The synthesis of the bis-substituted systems was then used to inform the systems of the tetra-substituted monomers that were required for FcNA synthesis. Routes for retaining chirality pure monomer units have now been established. Now that the monomers have been successfully made, future work will be directed towards their oligomerisation on an automated DNA synthesiser (Figure 5-1) and the formation of the corresponding duplexes will then be investigated.
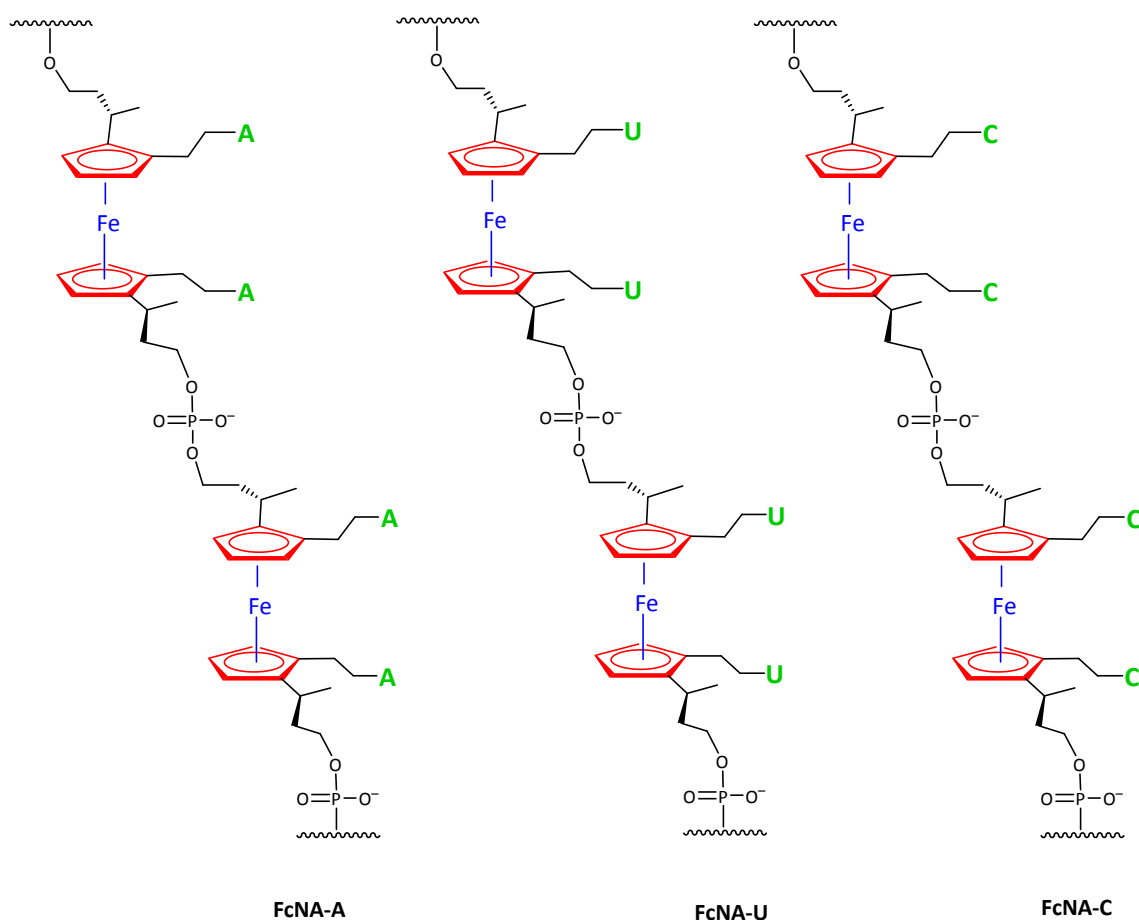
***Figure 5-1:** Oligomerisation of the three synthesised monomers FcNA-A, FcNA-U and FcNA-C*

This work can also be considered as a starting point for further studies towards the development of other type of FcNAs monomers and FENs for biological activity. Different parameters can be considered such as the linker length between the ferrocenyl moiety and the nucleobase. For example, FcNAs monomers with three-carbons linker could be made by using the tetra-substituted bis-aldehyde ferrocene and a triethyl phosphonoacetate coupled via the Wittig reaction, followed by the hydrogenation of the corresponding double bond. The ester groups would then be reduced using LiAlH$_4$ and nucleobases would be coupled to the corresponding alcohol via a Mitsunobu reaction as shown in Scheme 5-1.
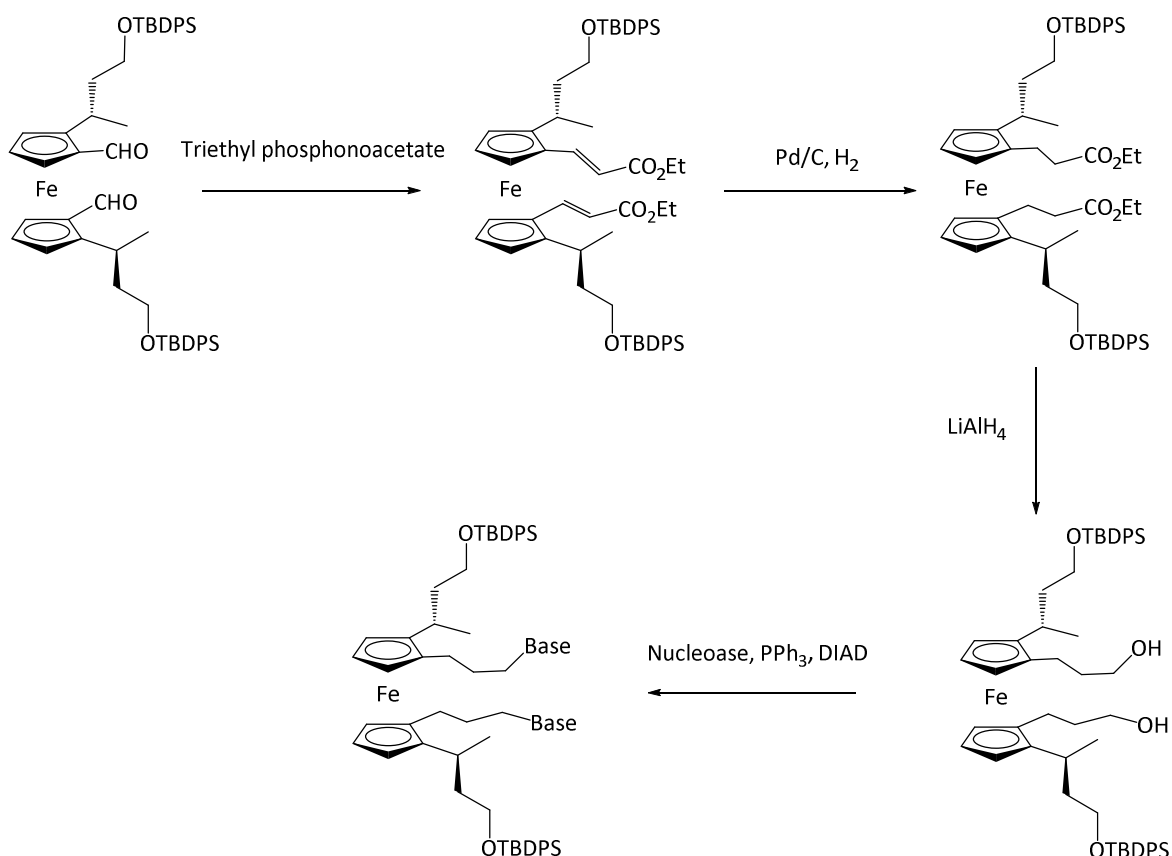
Scheme 5-1: *Synthetic route for the synthesis of a FcNA monomer with a three-carbon linker to the nucleobase.*

It would also be interesting to investigate the synthesis of the ferrocenyl nucleic analogue containing guanine (FcNA-G). Due to the low solubility of the nucleobase in usual organic solvents, a derivative of guanine such as the 2-amino-chloropurine could be considered for the coupling reaction with the ferrocenyl moiety. As previously described by Fletcher in 2009,[1] the purine derivative would then be converted into the natural guanine to obtain the final desired target as shown in Scheme 5-2.
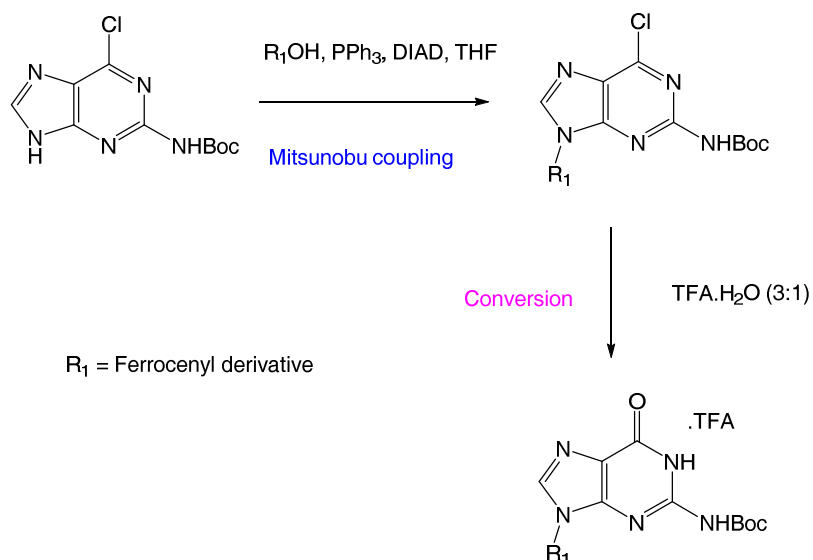
Scheme 5-2: *Synthetic route for the guanine coupling with ferrocenyl derivatives based on the work of Fletcher[2]*

Finally, routes to FcNA and FEN derivatives with only planar chirality should also be considered to evaluate the importance of chirality on the FcNA oligomer properties and the FEN biological activity. All these future studies should open the door to many new perspectives on the use of ferrocene in the bioorganometallic field.

5.1 References

1. C. Smit, M. W. Fraaije, and A. J. Minnaard, *J. Org. Chem.*, **2008**, *73*, 9482-9485.
2. S. Fletcher, V. M. Shahani, P. T. Gunning, *Tetrahedron Lett.*, **2009**, *50*, 4258-4261.

CHAPTER 6: EXPERIMENTAL

6.1   Synthesis

All the products were used as received from Sigma-Aldrich, TCI, and Fisher Scientific. All the solvents were used as received from Fischer and Sigma-Aldrich. Dry solvents were collected from a Solvent Purification System. Thin layer chromatography were visualised under UV-light and flash chromatography were performed on silica 60 with the specified eluent. Routine ^{1}H NMR were recorded at 300 MHz on a Bruker AVIII300 or at 400 MHz on a Bruker AVIII400 spectrometer equipped with a 5 mm probe. ^{13}C NMR and 2D NMR spectra (COSY, HSQC) were recorded at 101 MHz on a Bruker AVIII400 spectrometer. ^{31}P NMR were recorded at 122 MHz on a Bruker AVIII300. All the spectra were recorded at 298 K. Chemical shifts (δ) are expressed in parts per million (ppm) to higher frequency compared to the methyls signal of trimethylsilane and the coupling constants (J) are expressed in Hertz (Hz). Data were processed using Bruker Topspin version 2.1 (300 and 400 MHz) and Mestrenova Light version 5.2.5. HRES MS were performed on a Waters/Micromass spectrometer using the ES+ method. Optical rotations were determined via a PolAAr 2001 digital polarimeter using a cell with a volume of 1 mL and a length of 0.25 dm. The polarimeter presents a instrumental error on the displayed optical angles of 0.5%.

6.1.1. (Hydroxymethyl)diphenylphosphine oxide **2**[9]
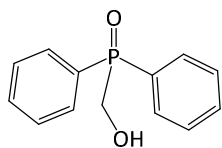
In a 100 mL schlenk tube, 16 mL of conc. HCL was added slowly to diphenylphosphine chloride (1.68 mL, 9.06 mmol) followed by addition of 16 mL of HCOH (37% in water). The mixture was then heated up to 50°C and stirred overnight. The pale yellow mixture was then neutralised with 400 mL of saturated $NaHCO_3$, extracted with DCM, dried on $NaSO_4$ and evaporated. A white powder was obtained (1.756 g, 84%). ^{1}H NMR (400 MHz, $CDCl_3$) δ 7.79 – 7.71 (m, 4H), 7.54 – 7.48 (m, 2H), 7.43 (td, J = 7.6, 2.8 Hz, 4H), 4.40 (s, 2H). ^{13}C NMR (101 MHz, $CDCl_3$) δ 132.13 (Ph), 131.44 (Ph), 131.35 (Ph), 130.98 (ipso Ph), 130.02 (ipso Ph), 128.71 (Ph), 128.60 (Ph), 61.62 (CH_2), 60.79 (CH_2). MS (ES) (m/z) calcd for $C_{13}H_{13}O_2PNa$ 255.0551, found 255.0553. IR (cm^{-1}): 3202 br (OH), 3080 (=CH), 2899 (CH_2), 2817 (CH_2), 1151 (P=O), 690 (C=C). Mp 136 °C - 138 °C.

6.1.2. (Diphenylphosphoryl)methyl 4-nitrobenzenesulfonate **4**[7]
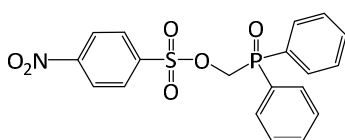
The (hydroxymethyl)diphenylphosphine oxide **2** (1.5 g, 6.5 mmol) was dissolved 15 mL of DCM. Nitrobenzylsufonate chloride (1.432 g, 6.5 mmol) was added to the mixture followed by TEA (1.35 mL, 9.7 mmol) and DMAP (0.079 g, 0.65 mmol). The reaction was stirred overnight under argon at room temperature. The crude was quenched with 10 mL of $NaHCO_3$, extracted with DCM and dried over Na_2SO_4. Solvent was evaporated and the crude was purified via flash column chromatography (Gradient: 60% EtOAc in hexane to 100% EtOAc) to yield product. A white solid was obtained (1.489 g, 55%). ^{1}H NMR (400 MHz, $CDCl_3$) δ 8.32 – 8.26 (d, J = 6.2 Hz, 2H), 7.95 – 7.89 (d, J = 6.2 Hz, 2H), 7.76 – 7.68 (m, 4H), 7.66 – 7.59 (m, 2H), 7.53 – 7.48 (m, 4H), 4.75 (d, J = 6.2 Hz, 2H). ^{13}C NMR (101 MHz, $CDCl_3$) δ 150.90

(ipso Ph), 140.32 (ipso Ph), 133.10 (Ph), 131.46 (Ph), 131.37 (Ph), 129.42 (Ph), 129.21 (ipso

Ph), 129.06 (Ph), 128.94 (Ph), 128.17 (ipso Ph), 124.47 (Ph), 66.26 (CH_2), 65.47 (CH_2). MS (ES)

(m/z) calcd for $C_{19}H_{16}NO_6PSNa$ 440.0334, found 440.0333. IR (cm^{-1}): 3061, 2941 (CH_2), 1609

(NO_2), 1538 (NO_2), 1371, 1085, 820 (CH=CH), 736. Mp 156 °C - 158 °C. Characterisation data

is in agreement with the literature data.

6.1.3. *N*-9-((Diphenylphosphoryl)methyl)-adenine **5**[7]
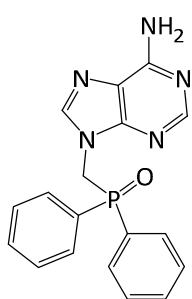
Adenine (0.486 g, 3.6 mmol) was added in one portion to a solution of NaH

(0.202 g, 5.04 mmol) dissolved in 20 mL of DMF. After being stirred for 3 h

at room temperature, (diphenylphosphoryl)methyl 4-nitrobenzene

sulfonate **4** (1.5 g, 3.6 mmol) previously dissolved in 10 mL of DMF are

added to the mixture. After 2 days of stirring, the reaction was quenched with EtOH and the

solvents were removed *in vacuo* and the crude was filtered and washed with an EtOH/EtOAc

mix. The crude was purified via flash column chromatography (5% MeOH, 5% TEA in EtOAc)

to yield product (0.669 g, 53%). ^{1}H NMR (400 MHz, CDCl$_3$) δ 8.26 (s, 1H), 8.25 (s, 1H), 7.86 –

7.73 (m, 4H), 7.58 – 7.49 (m, 2H), 7.47 – 7.42 (m, 4H), 5.71 (s, 2H), 5.05 (d, *J* = 6.3 Hz, 2H). [13]C

NMR (101 MHz, CDCl$_3$) δ 155.33 (ipso adenine), 152.85 (CH adenine), 149.95 (ipso adenine),

140.81 (CH adenine), 132.84 (Ph), 131.16 (Ph), 131.06 (Ph), 129.61 (ipso Ph), 129.09 (ipso

adenine), 128.99 (Ph), 128.87 (Ph), 43.26 (CH_2), 42.54 (CH_2). ^{31}P NMR (122 MHz, CDCl$_3$) δ

27.48.

6.1.4. *N,N*-6-Dibenzoyl-*N*-9-((diphenylphosphoryl)methyl)-adenine **6**
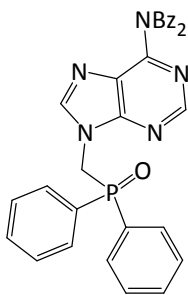
To a solution of **5** (0.100 g, 0.286 mmol) in Pyridine (4 mL) at 0 °C, was added 132 μL of benzoyl chloride. The solution was stirred for 5 min. The mixture was then warmed up to room temperature overnight. The pyridine was removed using high vacuum, the residue was dissolved in DCM, washed with 5% NaHCO$_3$, dried on Na$_2$SO$_4$ and evaporated. The crude was purified via flash column chromatography packed with 30% hexane in EtOAc. A first gradient of EtOAc was applied (70% to 100% in hexane) to the column followed by a second gradient of MeOH (2% to 10 % MeOH in EtOAc). A white foam was obtained (0.124 g, 78%). ^{1}H-NMR (400 MHz, CDCl$_3$) δ 8.49 (s, 1H), 8.46 (s, 1H), 7.85 – 7.78 (m, 4H), 7.78 – 7.71 (m, 4H), 7.58 – 7.51 (m, 2H), 7.49 – 7.42 (m, 6H), 7.34 – 7.32 (m, 4H), 5.08 (d, *J* = 6.2 Hz, 2H). ^{13}C NMR (101 MHz, CDCl$_3$) δ 172.14 (C=O), 153.04 (ipso adenine), 151.88 (CH adenine), 151.74 (ipso adenine), 145.06 (CH adenine), 134.06 (ipso Bz), 133.02 (Bz), 131.14 (Ph), 129.41 (Bz), 129.09 (Ph), 128.97 (Bz), 128.64 (Ph), 128.21 (ipso Ph), 126.54 (ipso adenine), 43.80 (CH$_2$), 43.09 (CH$_2$). ^{31}P NMR (122 MHz, CDCl$_3$) δ 26.75. MS (ES) (m/z) calcd for C$_{32}$H$_{24}$N$_5$O$_3$PNa 580.15, found 580.1511. IR (cm^{-1}): 3059 (=CH), 2975, 2924 (CH$_2$), 1696 (C=O), 1597, 1577, 1234, 1120, 692 (C=C). Mp 108 °C - 110 °C.

6.1.5. *N*-1-((Diphenylphosphoryl)methyl)-cytosine **7**[7]
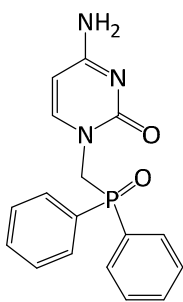
NaH (0.129 g, 5.38 mmol) was dissolved 20 mL of DMF. Cytosine (0.427 g, 3.84 mmol) was added in one portion and stirred under argon at room temperature for four hours. **4** (1.6 g, 3.84 mmol) previously dissolved in 10 mL of DMF, was then slowly added to the reaction at room temperature. After two days, the solvent was evaporated and the crude was purified via flash column chromatography (5% MeOH, 5% TEA in DCM) to yield product. A white solid was obtained (0.831 g, 61%). MS (ES) (m/z) calcd for $C_{17}H_{17}N_3O_2P$ 326.1058, found 326.1056 (M^+ + H). IR (cm^{-1}): 3339 (NH), 3210 (NH), 3054 (=CH), 2988 (CH_2), 2925 (CH_2), 1665 (C=C), 1624 (C=O), 1498, 1371 (CH_2), 1261 (CN), 1175 (P=O), 712 (NH_2), 691 (C=C). Mp 134 °C -136 °C.

6.1.6. *N*-4-Benzoyl-*N*-1-((diphenylphosphoryl)methyl)-cytosine **8**
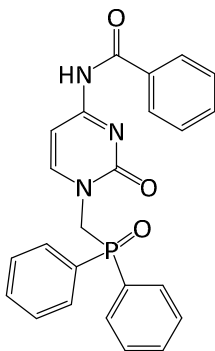
7 (0.4 g, 1.23 mmol) was dissolved in 15 mL of pyridine. Benzoyl chloride (0.856 mL, 7.37 mmol) was added at 0 °C, stirred for 15 min and then warmed up to room temperature overnight under argon. After evaporation of pyridine, the residue was purified via flash column chromatography (3% MeOH in DCM) to yield product. A white solid was obtained (0.382 g, 72%). ^{1}H NMR (400 MHz, CDCl$_3$) δ 8.79 (s, 1H), 8.34 (d, *J* = 7.4 Hz, 1H), 7.88 – 7.82 (m, 6H), 7.63 – 7.54 (m, 3H), 7.53 – 7.45 (m, 7H), 4.96 (d, *J* = 6.3 Hz, 2H). ^{13}C NMR (101 MHz, CDCl$_3$) δ 162.18 (C=O), 149.19 (CH Cytosine), 133.18 (Bz), 132.87 (Ph), 131.21 (Bz), 131.12 (Ph), 129.76 (ipso Bz), 129.04 (Bz), 128.99 (Ph), 128.92 (Bz), 128.75 (ipso Ph), 127.59 (Ph), 97.23 (CH cytosine), 46.73 (CH_2), 46.02 (CH_2). MS (ES) (m/z) calcd for $C_{24}H_{21}N_3O_3P$

430.1321, found 430.1318 ($M^+ + H$). IR (cm^{-1}): 3210 (NH), 3061 (=CH), 2988 (CH_2), 2925 (CH_2), 1675 (C=C), 1621 (C=O), 1477, 1347, 1239 (CN), 1167 (P=O), 693. Mp degrades at 178 °C.

6.1.7. 1,1'-Bis-dicarboxaldehyde-ferrocene 9[12]
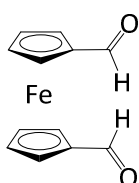
In a 50 mL schlenk flask, ferrocene (2 g, 10.75 mmol) was partially dissolved in Et_2O under argon. After addition of TMEDA (3.845 mL, 25.8 mmol), the mixture went to dark orange. The reaction was stirred for 5 min and 11.18 mL of n-BuLi (27.9 mmol) was added to the mixture at room temperature. After overnight stirring, the mixture was cooled down to -78°C and DMF (2.749 mL, 35.5 mmol) was added drop wise. After 10 min, the reaction was warmed up to room temperature and stirred for 1.5 h. The reaction was then quenched with water/Brine and extracted with DCM. The organic layers were combined, dried over $MgSO_4$ and concentrated. The crude was purified via flash column chromatography (70% EtOAc in hexane) to yield a red foam (2.05 g, 78%). ^{1}H NMR (400 MHz, Chloroform-d) δ 9.95 (s, 2H), 4.89 (t, J = 2.0 Hz, 4H), 4.70 – 4.64 (m, 4H). ^{13}C NMR (101 MHz, $CDCl_3$) δ 192.84 (C=O), 80.27 (ipso Cp), 77.32 (Fc), 74.19 (Fc), 70.86 (Fc). Mp 152 °C - 154 °C. Characterisation data is in agreement with the literature data.

6.1.8. 1,1'-Bis-[(*Z*)-2-((*N,N*-6-dibenzoyl)-adenin-9-yl))ethylenyl]-ferrocene **10**
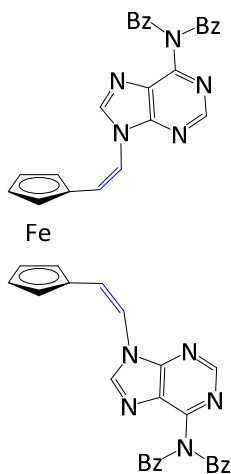
800 mg of **6** (1.43 mmol) were dissolved in 6 mL of pyridine. The solution was evaporated using high vacuum. The residue was then dissolved in 6 mL of DMF under Argon. After 5 min of stirring, 36 mg of sodium hydride 95% (1.505 mmol) were added in one portion at room temperature. The mixture was stirred at room temperature for 2 h. Then the bis-carboxaldehyde **9** (0.116 g, 0.478 mmol) previously dissolved in 5 mL of DMF was added at room temperature. After overnight stirring, the reaction was quenched with water/EtOAc (1/1) (20 mL) at 0 °C and extracted with Et$_2$O. The organic layers were combined, dried over Na$_2$SO$_4$ and concentrated. The crude was purified via flash column chromatography packed with 60% EtOAc in hexane. The purification involved a gradient from 60% to 100% of EtOAc. An orange foam was obtained (0.084 g, 32%). ^{1}H-NMR (400 MHz, CDCl$_3$) δ 8.75 (s, 2H), 8.09 (s, 2H), 7.89 (d, *J* = 7.1 Hz, 8H), 7.50 (t, *J* = 7.5 Hz, 4H), 7.37 (t, *J* = 7.7 Hz, 8H), 6.84 (d, *J* = 8.7 Hz, 2H), 6.39 (d, *J* = 8.7 Hz, 2H), 4.20 − 4.17 (t, *J* = 1.9 Hz, 4H), 3.85 (t, *J* = 1.9 Hz, 4H). ^{13}C NMR (101 MHz, CDCl$_3$) δ 172.25 (C=O), 152.99 (ipso adenine), 152.81 (CH adenine), 152.00 (ipso adenine), 144.29 (CH adenine), 134.16 (ipso Bz), 132.97 (Bz), 129.46 (Bz), 128.68 (Bz), 127.06 (ipso Bz), 126.29 (CH vinyl), 116.15 (CH vinyl), 77.67 (ipso Cp), 71.44 (Fc), 70.43 (Fc). MS (ES) (m/z) calcd for C$_{52}$H$_{36}$FeN$_{10}$O$_4$^{56}FeNa 943.22, found 943.2198. IR (cm^{-1}): 3063, 2923 (CH$_2$), 2853 (CH$_2$), 1697 (C=O), 1596, 1572, 1229. Mp 106 °C - 108 °C.

6.1.9. 1,1'-Bis-[2-((*N,N*-6-dibenzoyl)-adenin-9-yl)ethyl]-ferrocene **11**
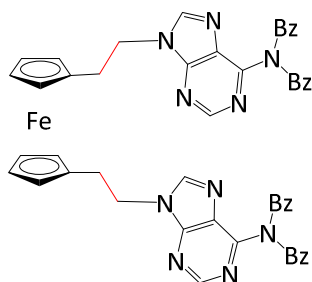
The bis-protected adenine ferrocenyl **10** (0.092 g, 0.099 mmol) was dissolved in 3 mL of EtOAc. 80.7 mg of pearlman's catalyst (Pd/(OH)$_2$) (2eq) were added to the solution. A balloon of H$_2$ was plugged to the flask and the mixture was stirred overnight at room temperature. The reaction was stopped and filtered through a pad of celite. The crude was purified via flash column chromatography (30% hexane in EtOAc). A yellow solid was obtained (0.064 g, 72%). ^{1}H-NMR (400 MHz, CDCl$_3$) δ 8.70 (s, 2H), 7.85 (d, *J* = 7.1 Hz, 8H), 7.76 (s, 2H), 7.49 (t, *J* = 7.5 Hz, 4H), 7.36 (t, *J* = 7.8 Hz, 8H), 4.34 (t, *J* = 6.9 Hz, 4H), 4.06 – 4.02 (t, *J* = 1.8 Hz, 4H), 3.82 (t, *J* = 1.8 Hz, 4H), 2.88 (t, *J* = 6.8 Hz, 4H). ^{13}C NMR (101 MHz, CDCl$_3$) δ 172.26 (C=O), 153.07 (ipso adenine), 152.10 (CH adenine), 151.67 (ipso adenine), 145.13 (CH adenine), 134.18 (ipso Bz), 132.89 (Bz), 129.44 (Bz), 128.65 (Bz), 127.48 (ipso adenine), 83.71 (ipso Cp), 69.14 (Fc), 68.93 (Fc), 45.70 (CH$_2$), 30.13 (CH$_2$). MS (ES) (m/z) calcd for C$_{52}$H$_{40}$N$_{10}$O$_4$^{56}FeNa 947.25, found 947.2469. IR (cm^{-1}): 3104, 1651 (C=O), 1605, 1522 (amide). Mp decomposed at 176 °C - 178 °C.

Mitsunobu coupling: 1,1'-bis-[2-((*N,N*-6-dibenzoyl)-adenin-9-yl)ethyl]-ferrocene **22**
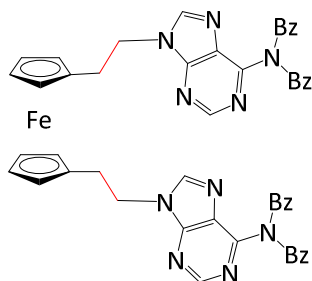
In a 50 mL schlenk tube, triphenylphosphine (0.861 g, 2.188 mmol) and the *N,N*-6-benzoyl-adenine **19** (0.651 g, 1.896 mmol) were dissolved in dry THF and stirred for 10 min at room temperature. **16** (0.200 g, 0.729 mmol) was then added to the mixture pre-dissolved in 5 mL of dry THF. The schlenk tube was then covered with foil and DIAD (0.476 mL, 2.188 mmol) was added at room temperature before the mixture was warmed up to 65 °C for 2 h. The reaction was evaporated, extracted with EtOAc, washed with brine followed

by water and dried over Na_2SO_4, solvent removed *in vacuo* and purified via flash column chromatography (2% MeOH in DCM) to yield product (0.311 g, 46%). (Data cf **11**)

6.1.10. 1,1'-Bis-[2-(adenin-9-yl)ethyl]-ferrocene **12**
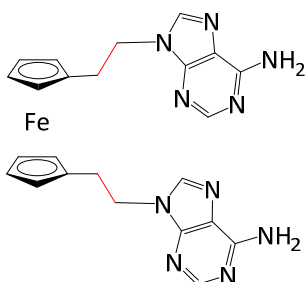
The bis-protected adenine ferrocenyl **11** (0.055 g, 0.0595 mmol) was dissolved in 1 mL of methylamine. The mixture was stirred at room temperature for half an hour under argon. The methylamine was evaporated. The crude was purified via flash column chromatography (10% MeOH in DCM). A yellow solid was obtained (0.020 g, 66%). ^{1}H-NMR (300 MHz, DMSO-d6) δ 8.15 (s, 2H), 8.02 (s, 2H), 7.17 (s, 4H), 4.28 (t, *J* = 7.4 Hz, 4H), 4.05 (t, *J* = 1.7, 4H), 4.01 (t, *J* = 1.6, 4H), 2.84 (t, *J* = 7.4 Hz, 4H). ^{13}C NMR (75 MHz, DMSO-d6) δ 156.38 (ipso adenine), 152.81 (CH adenine), 149.92 (ipso adenine), 141.22 (CH adenine), 119.25 (ipso adenine), 84.99 (ipso Cp), 69.00 (Fc), 68.55 (Fc), 44.40 (CH_2), 29.67 (CH_2). MS (ES) (m/z) calcd for $C_{24}H_{25}N_{10}{}^{56}Fe^+$ 509.16, found 509.1638 (M^+ + H^+). IR (cm^{-1}): 3109 (NH_2), 2924 (CH_2), 2852 (CH_2), 1659 (imine), 1598, 1571, 1305. Mp decomposed at 284 °C - 286 °C.

6.1.11. 1,1'-Bis-[(*Z*)-2-(adenin-9-yl))ethylenyl]-ferrocene **13**
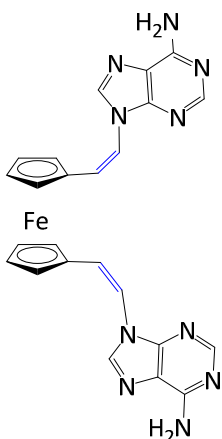
The bis-protected adenine ferrocenyl **10** (0.031 g, 0.034 mmol) was dissolved in 1 mL of methylamine. The mixture was stirred at room temperature for half an hour under argon. The methylamine was evaporated. The crude was purified via flash column chromatography (10% MeOH in DCM). An orange solid was obtained (0.013 g, 77%). [1]H

NMR (300 MHz, DMSO-d6) δ 8.16 (s, 2H), 8.00 (s, 2H), 7.33 (s, 4H), 6.78 (d, J = 8.5 Hz, 2H),

6.50 (d, J = 8.6 Hz, 2H), 4.21 − 4.09 (t, J = 1.8 Hz, 4H), 3.86 − 3.69 (t, J = 1.8 Hz, 4H). ^{13}C NMR

(75 MHz, DMSO-d6) δ 156.51 (ipso adenine), 153.50 (CH adenine), 150.00 (ipso adenine),

140.27 (CH adenine), 127.74 (CH vinyl), 118.82 (ipso adenine), 117.63 (CH vinyl), 78.43 (ipso

Cp), 71.16 (Fc), 70.46 (Fc). MS (ES) (m/z) calcd for $C_{24}H_{20}N_{10}{}^{56}FeNa$ 527.11, found 527.1138.

IR (cm^{-1}): 3303 (NH$_2$), 3122, 1670 (imine), 1645, 1595, 1572. Mp decomposed at 256 °C - 258

°C.

6.1.12. 1,1'-Bis-vinyl-ferrocene **15**[17]
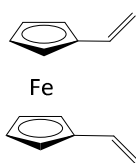
In a 100 mL schlenk tube, trimethylmethylphosphonium bromide (5.587 g,

15.64 mmol), potassium tert-butoxide (1.75 g, 15.64 mmol) and a catalytic

amount of dibenzo-18-crown-6-ether were dissolved in 14 mL of dry THF. The

mixture was stirred for 30 min and 1,1'-bis-dicarboxaldehyde ferrocene **9** (1.893 g, 7.82

mmol) previously dissolved in 28 mL of dry THF was added. The reaction was stirred

overnight at room temperature, quenched with water and extracted with Et$_2$O (20 mL). The

combined ethereal fractions were dried over Na$_2$SO$_4$, solvent removed *in vacuo* and purified

via flash column chromatography (40% EtOAc in hexane) to yield product (1.307 g, 70%). [1]H

NMR (400 MHz, CDCl$_3$) δ 6.36 (dd, J = 17.5, 10.7 Hz, 2H), 5.29 (dd, J = 17.5, 1.6 Hz, 2H), 5.06

(dd, J = 10.8, 1.6 Hz, 2H), 4.24 (t, J = 1.9 Hz, 4H), 4.16 (t, J = 1.9 Hz, 4H). ^{13}C NMR (101 MHz,

CDCl$_3$) δ 134.07 (CH vinyl), 111.23 (CH$_2$ vinyl), 84.15 (ipso Cp), 69.88 (Cp), 67.90 (Cp). MS (ES)

(m/z) calcd for $C_{14}H_{14}{}^{56}Fe$ 238.0445, found 238.0438. IR (cm^{-1}): 3077 (=C-H), 3009 (CH$_2$), 2978

(CH$_2$), 2915 (CH$_2$), 1631 (C=C), 994 (-CH=CH2), 893 (C=C), 817 (C=C), 726 (CH Ar). Mp 48 °C -

50 °C. Characterisation data is in agreement with the literature data.

6.1.13. Vinyl-ferrocene **15a**
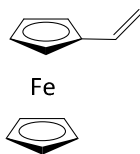
In 50 mL schlenk tube, trimethylmethylphosphonium bromide (1.836 g, 5.14 mmol), potassium tert-butoxide (0.577 g, 5.14 mmol) and a catalytic amount of dibenzo-18-crown-6-ether were dissolved in 15 mL of dry THF. The mixture was stirred for 30 min and carboxaldehydeferrocene **9a** (1 g, 4.67 mmol) previously dissolved in 10 mL of dry THF was added. The reaction was stirred overnight at room temperature, quenched with water and extracted with Et_2O (10 mL). The combined ethereal fractions were dried over $MgSO_4$, solvent removed *in vacuo* and purified via flash column chromatography (40% EtOAc in hexane) to yield product (0.768 g, 78%). ^{1}H NMR (400 MHz, $CDCl_3$) δ 6.45 (dd, J = 17.5, 10.7 Hz, 1H), 5.33 (dd, J = 17.4, 1.6 Hz, 1H), 5.02 (dd, J = 10.7, 1.6 Hz, 1H), 4.35 (t, J = 1.8 Hz, 2H), 4.20 (t, J = 1.9 Hz, 2H), 4.10 (s, 5H). ^{13}C NMR (101 MHz, $CDCl_3$) δ 134.65 (CH vinyl), 111.05 (CH_2 vinyl), 83.56 (ipso Cp), 69.21 (Fc), 68.66 (Fc), 66.66 (Fc). MS (ES) (m/z) calcd for $C_{12}H_{12}{}^{56}Fe$ 212.0288, found 212.0275. IR (cm^{-1}): 3082 (=C-H), 3006 (CH_2), 2993 (CH_2), 2851 (CH_2), 1623 (C=C), 1408 (C=CH_2), 998 (-CH=CH_2), 895, 822 (C=C), 726 (CH Ar). Mp 50 °C - 52 °C.

6.1.14. 1,1'-Bis-hydroxypropyl-ferrocene **16**[17]
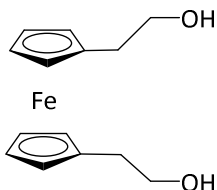
In 100 mL schlenk tube, **15** (0.252 g, 1.058 mmol) was dissolved in 15 mL of dry THF.BH_3 in THF (6.01 mL, 0.634 mmol) was then added drop wise at room temperature and stirred for 2 h. 7.15 mL of EtOH, 7.15 mL of NaOH (3M) and 5.29 mL of H_2O_2 (30%) were then successively added to the reaction and stirred for 1 h at room temperature. The reaction was extracted with DCM,

washed with brine and dried over Na_2SO_4, solvent removed *in vacuo* and purified via flash

column chromatography (70% EtOAc in hexane) to yield product (0.200 g, 69%). ^{1}H NMR

(400 MHz, CDCl$_3$) δ 4.05 (s, 8H), 3.69 (t, *J* = 6.6 Hz, 4H), 2.56 (t, *J* = 6.6 Hz, 4H), 2.04 (s, 2H).

^{13}C NMR (101 MHz, CDCl$_3$) δ 84.99 (ipso Cp), 69.16 (Fc), 68.41 (Fc), 63.48 (CH$_2$), 32.65 (CH$_2$).

MS (ES) (m/z) calcd for $C_{14}H_{18}O_2{}^{56}FeNa$ 297.0554, found 297.0558. IR (cm^{-1}): 3249 (OH), 3092

(=C-H), 2924 (CH$_2$), 2883 (CH$_2$), 2847 (CH$_2$), 1468 (CH$_2$), 1053 (OH), 805 (C=C). Mp 40 °C - 42

°C. Characterisation data is in agreement with the literature data.

6.1.15. 1-Hydroxypropyl-ferrocene **16a**[16]
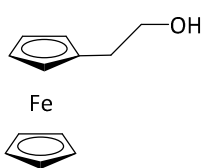
In 200 mL schlenk tube, **15a** (0.600 g, 3.1 mmol) was dissolved in 30 mL of

dry THF. BH$_3$,THF (17.62 mL, 9.3 mmol) was then added drop wise at room

temperature and stirred for 2 h. 10.45 mL of EtOH, 10.45 mL of NaOH (3M)

and 7.74 mL of H$_2$O$_2$ (30%) were then successively added to the reaction and stirred for 1 h

at room temperature. The reaction was extracted with DCM, washed with brine and dried

over MgSO$_4$, solvent removed *in vacuo* and purified via flash column chromatography (30%

EtOAc in hexane) to yield product (0.554 g, 65%). ^{1}H NMR (400 MHz, CDCl$_3$) δ 4.15 − 4.09 (m,

7H), 4.10 (d, *J* = 1.8 Hz, 2H), 3.73 (t, *J* = 6.2 Hz, 2H), 2.60 (t, *J* = 6.5 Hz, 2H), 1.64 − 1.54 (m,

1H). ^{13}C NMR (101 MHz, CDCl$_3$) δ 84.77 (ipso Cp), 68.60 (Fc), 68.42 (Fc), 67.67 (Fc), 63.49

(CH$_2$), 32.82 (CH$_2$). MS (ES) (m/z) calcd for $C_{12}H_{14}O{}^{56}Fe$ 230.0394, found 230.0398. IR (cm^{-1}):

3220 (OH), 3082 (=C-H), 2948 (CH$_2$), 2906 (CH$_2$), 2868 (CH$_2$), 1341 (OH), 1053 (C-OH), 805

(CH=CH), 721 (CH Ar). Mp 41 °C - 42 °C. Characterisation data is in agreement with the

literature data.

6.1.16. *N*-9-Trityl-adenine **17**[18,19]
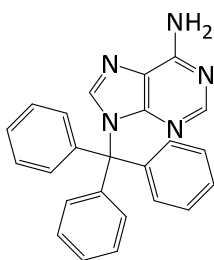
Adenine (2.5 g, 18.5 mmol) was dissolved in a mixture of 15 mL and 30 mL of DMF and Pyridine respectively. The mixture was stirred at room temperature for 10 min under argon. Tritylmethyl chloride (5.157 g, 18.5 mmol) was added to the suspension. The reaction was stirred overnight under argon. The reaction was quenched with 100 mL of EtOAc and 50 mL of water. The organic layer was washed five times with water. Filtration of the organic layer led to a colourless precipitate corresponding to the desired compound (6 g, 86%). ^{1}H NMR (400 MHz, CDCl$_3$) δ 7.99 (s, 1H), 7.68 (s, 1H), 7.25 – 7.23 (m, 9H), 7.12 – 7.07 (m, 6H), 5.73 (s, 2H). ^{13}C NMR (101 MHz, CDCl$_3$) δ 155.75 (ipso adenine), 152.34 (CH adenine), 151.40 (ipso adenine), 141.93 (CH adenine), 141.33 (ipso Ph), 129.79 (Ph), 128.06 (Ph), 127.91 (Ph), 121.17 (ipso adenine), 75.80 (ipso Tr). MS (ES) (m/z) calcd for C$_{24}$H$_{19}$N$_5$Na 400.1538, found 400.1537. IR (cm^{-1}): 3302 (NH$_2$), 3137 (NH$_2$), 3027 (=CH), 1666 (C=C), 1650 (NH$_2$), 1598 (NH$_2$), 1565 (C-C), 1445, 747 (CH Ar), 696 (C=C). Mp 258 °C - 262 °C. Characterisation data is in agreement with the literature data.

6.1.17. *N,N*-6-Dibenzoyl-N-9-trityl-adenine **18**
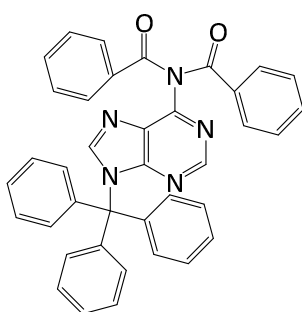
17 (1.197 g, 3.17 mmol) was dissolved in 60 mL of pyridine. The solution should turn to clear. Benzoyl chloride (0.919 mL, 7.93 mmol) was added at 0 °C, stirred for 15 min and then warmed up to room temperature overnight under argon. After evaporation of pyridine, the residue was dissolved in DCM and washed with water

and brine. The crude was purified via flash column chromatography (30% EtOAc in hexane) to yield product. A white foam was obtained (1.438 g, 77%). ^{1}H NMR (400 MHz, CDCl$_3$) δ 8.40 (s, 1H), 8.03 (s, 1H), 7.84 – 7.78 (m, 4H), 7.49 – 7.43 (m, 2H), 7.35 – 7.26 (m, 9H + 4H), 7.16 – 7.10 (m, 6H). ^{13}C NMR (101 MHz, CDCl$_3$) δ 172.29 (C=O), 154.44 (ipso adenine), 152.19 (ipso adenine), 151.70 (CH adenine), 146.25 (CH adenine), 140.76 (ipso Ph), 134.29 (ipso Bz), 132.88 (Bz), 129.64 (Ph), 129.41 (Bz), 129.02 (ipso adenine), 128.58 (Bz), 128.19 (Ph). MS (ES) (m/z) calcd for C$_{38}$H$_{27}$N$_5$O$_2$Na 608.2062, found 608.2064. IR (cm^{-1}): 3071 (=CH), 1699 (C=O), 1595 (amide), 1567 (C=N), 1446, 1385 (Cq), 1177, 1073, 693 (C=C). Mp 104 °C - 108 °C.

6.1.18. *N,N*-6-Dibenzoyl-adenine **19**
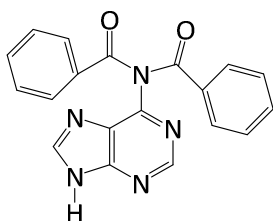
18 (3 g, 5.12 mmol) was dissolved in 15 mL of DCM under argon. TFA (0.592 mL, 7.68 mmol) was added at 0 °C, stirred for 3 h and then warmed up to room temperature overnight under argon. After evaporation of TFA and co-evaporation with CHCl$_3$, the crude was purified via flash column chromatography (2% MeOH in DCM) to yield product. A white foam was obtained (1.198 g, 68%). ^{1}H NMR (400 MHz, CDCl$_3$) δ 11.79 (s, 1H), 8.65 (s, 1H), 8.27 (s, 1H), 7.82 – 7.78 (m, 4H), 7.46 – 7.41 (m, 2H), 7.32 – 7.27 (m, 4H). ^{13}C NMR (101 MHz, CDCl$_3$) δ 172.31 (C=O), 154.86 (ipso adenine), 151.91 (CH adenine), 150.70 (ipso adenine), 144.27 (CH adenine), 133.85 (ipso Bz), 133.20 (Bz), 129.35 (Bz), 128.79 (Bz), 125.12 (ipso adenine). MS (ES) (m/z) calcd for C$_{19}$H$_{14}$N$_5$O$_2$ 344.1147, found 344.1131. IR (cm^{-1}): 3069 (=CH), 1691 (C=O), 1580 (NH), 1399, 1230, 1175, 1074, 693 (C=C). Mp 98 °C - 100 °C.

6.1.19. *N*-3-Benzoyluracil **20**[20]
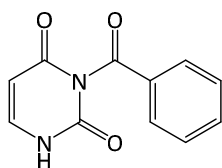
Uracil (3 g, 26.76 mmol) was dissolved in 33 mL of a mixture of acetonitrile and Pyridine with a 5/2 ratio. Benzoyl chloride (6.819 mL, 58.8 mmol) was added (turn to purple) and stirred overnight under argon at room temperature. The crude was then filtered off and washed with acetonitrile. Solvent was evaporated and the crude was purified via flash column chromatography (2% MeOH in DCM with a gradient of MeOH from 2% to 5%) to yield product. A white solid was obtained (1.437 g, 25%). Rf (9/1 DCM/MeOH) = 0.33. ^{1}H NMR (400 MHz, DMSO-d6) δ 11.61 (s, 1H), 7.99 – 7.93 (d, *J* = 7.0 Hz, 2H), 7.78 (d, *J* = 7.5 Hz, 1H), 7.67 (d, *J* = 7.8 Hz, 1H), 7.61 – 7.58 (t, *J* = 7.3 Hz, 2H), 5.75 (d, *J* = 7.7 Hz, 1H). ^{13}C NMR (101 MHz, DMSO) δ 169.96 (C=O Bz), 162.87 (C=O uracil), 150.01 (C=O uracil), 143.27 (CH uracil), 135.35 (Bz), 131.28 (ipso Bz), 130.15 (Bz), 129.44 (Bz), 100.04 (CH uracil). MS (ES) (m/z) calcd for $C_{11}H_8N_2O_3Na$ 239.0433, found 239.0434. IR (cm^{-1}): 3218 (NH), 3178 (NH), 3083 (=CH), 1745 (C=O), 1703 (amide/urea), 1648 (amide), 1625 (C=N), 1595 (NH), 1414, 782 (CH Ar Bz), 693 (C=C). Mp 149 °C - 150 °C. Characterisation data is in agreement with the literature data.

6.1.20. *N*-4-Benzoyl cytosine **21**[21]
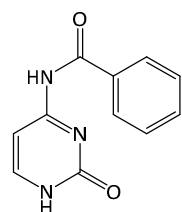
Cytosine was co-evaporated with pyridine and suspended in 67.5 mL of pyridine. 15.66 mL of benzoyl chloride were added drop wise and the reaction was stirred overnight at room temperature. 13.5 mL of water were added and the solvent was evaporated. The residue was then dissolved in 189 mL of water containing 14.85 g of NaOH. The mixture was stirred for one hour after complete dissolution. HCl was then added in order to obtain a pH=4. A White precipitate was

collected and boiled in 270 mL of EtOH and cooled to room temperature and filtered. [1]H

NMR (300 MHz, DMSO-d6) δ 11.68 (s, 1H), 11.14 (s, 1H), 8.02 (d, *J* = 7.2 Hz 2H), 7.98 − 7.88

(m, 1H), 7.63 (d, *J* = 7.0 Hz, 1H), 7.51 (t, *J* = 7.9 Hz, 2H), 7.22 (s, 1H). MS (ES) (m/z) calcd for

$C_{11}H_9N_3O_2Na$ 238.0592, found 238.0581. IR (cm^{-1}): 3225 (amide), 3156 (amide), 3062 (=CH

Fc), 2604 ($^+$NHBz), 1693 (amide/urea), 1621 (NH), 1460 (C=N), 1242, 812 (CH Ar), 701 (C=C).

Mp degrades at >300˚C.

6.1.21. 1-[2-((*N,N*-6-Dibenzoyl)-adenin-9-yl)ethyl]-ferrocene **22a**
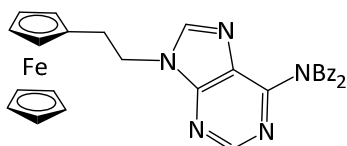
In a 50 mL schlenk tube, triphenylphosphine (0.383 g, 1.46

mmol) and the *N,N*-6-dibenzoyl-adenine **19** (0.500 g, 1.46

mmol) were dissolved in dry THF and stirred for 10 min at room

temperature. **16a** (0.2 g, 0.729 mmol) was dissolved in 7 mL of dry THF and added to the

mixture. The schlenk tube was then covered with foil and DIAD (0.240 mL, 1.176 mmol) was

added at room temperature before the mixture was warmed up to 65 °C for 2 h. The

reaction was evaporated, extracted with EtOAc, washed with brine followed by water and

dried over Na_2SO_4, solvent removed *in vacuo* and purified via flash column chromatography

(40% EtOAc in hexane) to yield product (0.134 g, 33%). ^{1}H NMR (400 MHz, CDCl$_3$) δ 8.69 (s,

1H), 7.86 (d, *J* = 7.0 Hz, 4H), 7.76 (s, 1H), 7.48 (t, *J* = 7.5 Hz, 2H), 7.34 (t, *J* = 7.8 Hz, 4H), 4.34

(t, *J* = 7.0 Hz, 2H), 4.11 (s, 5H), 4.06 (t, *J* = 1.8 Hz, 2H), 3.86 (t, *J* = 1.8 Hz, 2H), 2.90 (t, *J* = 7.0

Hz, 2H). ^{13}C NMR (101 MHz, CDCl$_3$) δ 172.26 (C=O Bz), 153.13 (ipso adenine), 152.07 (CH

adenine), 151.64 (ipso adenine), 145.18 (CH adenine), 134.19 (ipso Bz), 132.87 (Bz), 129.44

(Bz), 128.64 (Bz), 127.54 (ipso adenine), 83.42 (ipso Cp), 68.69 (Fc), 68.16 (Fc), 45.69 (CH$_2$),

30.36 (CH$_2$). MS (ES) (m/z) calcd for $C_{31}H_{25}N_5O_2$[56]Fe 555.1358, found 555.1354. IR (cm^{-1}):

3087 (=CH Fc), 2926 (CH$_2$), 2926 (CH$_2$), 2856 (CH$_2$), 1696 (C=O), 1598 (amide Bz), 1574 (NH$_2$), 1448 (CH$_2$), 1235, 830 (CH Ar), 692 (C=C). Mp 82 °C - 84 °C.

6.1.22. 1-[2-(Adenin-9-yl)ethyl]-ferrocene 23a
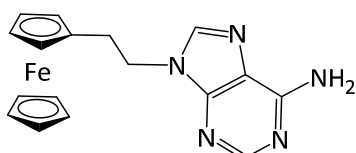
The bis-protected adenine ferrocenyl **22a** (0.055 g, 0.1 mmol) was dissolved in 3 mL of methylamine. The mixture was stirred at room temperature for half an hour under argon. The methylamine was then evaporated. The crude was purified on a silica gel chromatographic column with a 95/5 DCM/MeOH mix solvent. A yellow solid was obtained (0.019 g, 58%). ^{1}H NMR (400 MHz, DMSO-d6) δ 8.17 (s, 1H), 8.05 (s, 1H), 7.17 (s, 2H), 4.31 (dd, J = 8.2, 6.8 Hz, 2H), 4.15 (s, 5H), 4.08 – 4.02 (m, 4H), 2.85 (t, J = 7.5 Hz, 2H). ^{13}C NMR (101 MHz, DMSO-d6) δ 155.89 (ipso adenine), 152.35 (CH adenine), 149.40 (ipso adenine), 140.76 (CH adenine), 118.73 (ipso adenine), 84.39 (ipso Cp), 69.00 (Fc), 68.55 (Fc), 43.75 (CH$_2$), 29.34 (CH$_2$). MS (ES) (m/z) calcd for C$_{17}$H$_{18}$N$_5$^{56}Fe 348.0912, found 348.0920 (M$^+$ + H$^+$). IR (cm^{-1}): 3399 (NH$_2$), 3316 (NH$_2$), 3084 (=CH Fc), 2980 (CH$_2$), 2931 (CH$_2$), 2907 (CH$_2$), 1653 (C=C), 1596 (NH$_2$), 1435 (CH$_2$), 1245, 797 (CH Ar). Mp degrades at 142 °C.

6.1.23. 1-[2-((N-3-Benzoyl)-uracil-1-yl)ethyl]-ferrocene 24a
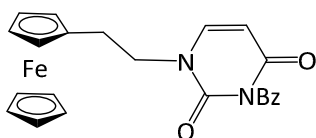
In a 50 mL schlenk tube, triphenylphosphine (0.570 g, 2.173 mmol) and the *N*-3-benzoyl-uracil **20** (0.469 g, 2.173 mmol) were dissolved in 15 mL of dry THF and stirred for 10 min at room temperature. **16a** (0.250 g, 1.087 mmol) was then added to the mixture pre-dissolved in 5 mL of dry THF. The schlenk tube was then covered with foil and DIAD (0.508 mL, 2.312

mmol) was added at room temperature before the mixture was warmed up to 65 °C for 2 h.

The reaction was evaporated, extracted with EtOAc, washed with brine followed by water

and dried over Na_2SO_4, solvent removed *in vacuo* and purified via flash column

chromatography (40% EtOAc in hexane) to yield product (0.388 g, 83%). ^{1}H NMR (400 MHz,

$CDCl_3$) δ 7.92 (d, *J* = 7.1 Hz, 2H), 7.66 (t, *J* = 7.4 Hz, 1H), 7.51 (dd, *J* = 8.3, 7.4 Hz, 2H), 6.93 (d, *J*

= 8.0 Hz, 1H), 5.65 (d, *J* = 8.0 Hz, 1H), 4.13 (s, 5H+2H), 4.04 (t, *J* = 1.8 Hz, 2H), 3.84 (t, *J* = 7.0

Hz, 2H), 2.76 (t, *J* = 7.0 Hz, 2H). ^{13}C NMR (101 MHz, $CDCl_3$) δ 168.83 (C=O Bz), 162.51 (C=O),

149.62 (C=O), 144.57 (CH uracil), 135.08 (Bz), 131.51 (ipso Bz), 130.48 (Bz), 129.16 (Bz),

101.42 (CH uracil), 83.25 (ipso Cp), 68.75 (Fc), 68.46 (Fc), 68.17 (Fc), 50.80 (CH_2), 29.10 (CH_2).

MS (ES) (m/z) calcd for $C_{23}H_{20}N_2O_3{}^{56}FeNa$ 451.0721, found 451.0717. IR (cm^{-1}): 3086 (=CH

Fc), 2964 (CH_2), 2932 (CH_2), 1733 (cyclic ketone), 1702 (C=O), 1653 (amide/urea), 1597

(amide), 1441 (CH_2), 1342, 1256, 1175, 809 (CH Ar), 682 (C=C). Mp 130 °C - 132 °C.

6.1.24. 1,1'-Bis-[2-((*N*-3-benzoyl)-uracil-1-yl)ethyl]-ferrocene **24**
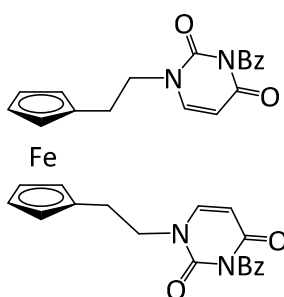
In a 50 mL schlenk tube, triphenylphosphine (0.574 g, 2.188 mmol)

and the *N*-3-benzoyl-uracil **20** (0.410 g, 1.896 mmol) were dissolved

in 10 mL of dry THF and stirred for 10 min at room temperature. **16**

(0.200 g, 0.729 mmol) was then added to the mixture pre-dissolved

in 5 mL of dry THF. The schlenk tube was then covered with foil and

DIAD (0.476 mL, 2.328 mmol) was added at room temperature before the mixture was

warmed up to 65 °C for 2 h. The reaction was evaporated, extracted with EtOAc, washed

with brine followed by water and dried over Na_2SO_4, solvent removed *in vacuo*. The residue

was dissolved in DCM and filtrated to yield product (0.260 g, 53%). ^{1}H NMR (400 MHz, $CDCl_3$)

δ 7.92 (d, *J* = 7.1 Hz, 4H), 7.66 (t, *J* = 7.4 Hz, 2H), 7.51 (t, *J* = 7.8 Hz, 4H), 6.94 (d, *J* = 8.0 Hz,

2H), 5.65 (d, *J* = 8.0 Hz, 2H), 4.11 (t, *J* = 1.8 Hz, 4H), 4.00 (t, *J* = 1.8 Hz, 4H), 3.83 (t, *J* = 7.0 Hz,

4H), 2.73 (t, *J* = 7.0 Hz, 4H). ^{13}C NMR (101 MHz, CDCl$_3$) δ 168.85 (C=O Bz), 162.46 (C=O),

149.65 (C=O), 144.51 (CH uracil), 135.15 (Bz), 131.44 (ipso Bz), 130.49 (Bz), 129.20 (Bz),

101.57 (CH uracil), 83.65 (ipso Cp), 69.21 (Fc), 69.08 (Fc), 50.71 (CH$_2$), 28.75 (CH$_2$). MS (ES)

(m/z) calcd for C$_{36}$H$_{30}$N$_4$O$_6$^{56}FeNa 693.1412, found 693.1416 (M$^+$ + Na$^+$). IR (cm^{-1}): 3096 (=CH

Fc), 2976 (CH$_2$), 2933 (CH$_2$), 2872 (CH$_2$), 1724 (C=O), 1597 (Amide bz), 1461 (CH$_2$), 1173, 821

(CH Ar). Mp 179 °C - 180 °C.

6.1.25. 1-[2-(Uracil-1-yl)ethyl]-ferrocene **25a**
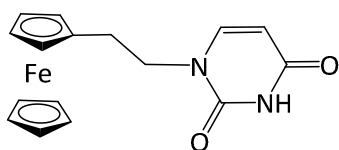
The mono-protected uracil ferrocenyl **24a** (0.1 g, 0.234 mmol)

was dissolved in 4 mL of methylamine. The mixture was stirred

at room temperature for half an hour under argon. The

methylamine was evaporated and the residue was purified on a silica gel chromatographic

column with a 98/2 DCM/MeOH mix solvent. A yellow solid was obtained (0.076 g, 100%). ^{1}H

NMR (400 MHz, CDCl$_3$) δ 8.56 (s, 1H), 6.79 (d, *J* = 7.9 Hz, 1H), 5.54 (d, *J* = 7.8 Hz, 1H), 4.13 (s,

4H), 4.10 (t, *J* = 1.8 Hz, 2H), 4.02 (t, *J* = 1.9 Hz, 2H), 3.80 (t, *J* = 6.8 Hz, 2H), 2.74 (t, *J* = 6.8 Hz,

2H). ^{13}C NMR (101 MHz, CDCl$_3$) δ 163.42 (C=O), 150.46 (C=O), 144.99 (CH uracil), 101.36 (CH

uracil), 83.42 (ipso Cp), 68.72 (Fc), 68.49 (Fc), 68.14 (Fc), 50.75 (CH$_2$), 29.21 (CH$_2$). MS (ES)

(m/z) calcd for C$_{16}$H$_{16}$N$_2$O$_2$^{56}FeNa 347.0459, found 347.0457. IR (cm^{-1}): 3323 (NH), 3086 (=CH

Fc), 2980 (CH$_2$), 2802 (CH$_2$), 1744 (cyclic ketone), 1700 (C=O), 1647 (amide/urea), 1550 (NH),

1344, 1176, 803 (CH Ar), 695 (C=C). Mp degrades at 158°C - 160 °C.

6.1.26. 1,1'-Bis-[2-(uracil-1-yl)ethyl]-ferrocene **25**
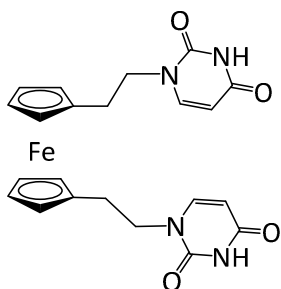
The 1,1'-bis-benzoyl-uracil ferrocene **24** (0.1 g, 0.149 mmol) was dissolved in 4 mL of methylamine. The mixture was stirred at room temperature for half an hour under argon. The methylamine was evaporated. The crude was filtered and washed with DCM. A yellow solid was obtained (0.069 g, 100%). The compound was not soluble in DMSO. MS (ES) (m/z) calcd for $C_{22}H_{22}N_4O_4{}^{56}FeNa$ 485.0888, found 485.0872 (M$^+$ + Na$^+$). IR (cm^{-1}): 3323 (NH), 3084 (=CH Fc), 2981 (CH$_2$), 2934 (CH$_2$), 2802 (CH$_2$), 1744 (Cyclic ketone), 1699 (C=O), 1658 (amide/Urea), 1602 (NH), 1550 (amide), 1343, 807 (C=C), 684 (C=C). Mp degrades at 178 °C.

6.1.27. 1,1'-Bis-(2-(bromo)ethyl)-ferrocene **27**
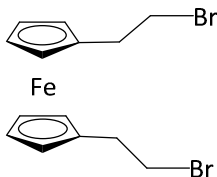
In a 50 mL schlenk tube, NBS (0.195 g, 1.094 mmol) was suspended in dry DCM. A DCM solution of triphenylphosphine (0.268 g, 1.021 mmol) was added drop wise to it. The resulting orange mixture was stirred for 5 min before addition of 0.043 mL (0.437 mmol) of pyridine. The mixture went black. **16** (0.05 g, 0.182 mmol) dissolved in 1 mL of dry DCM was added to the mixture. After overnight reaction, the solvent was removed *in vacuo* and the crude was purified via flash column chromatography (10% EtOAc in hexane) to yield product (0.450 g, 97%). ^{1}H NMR (400 MHz, CDCl$_3$) δ 4.07 (s, 8H), 3.41 (t, *J* = 7.7 Hz, 4H), 2.88 (t, *J* = 7.6 Hz, 4H). ^{13}C NMR (101 MHz, CDCl$_3$) δ 85.65 (ipso Cp), 69.01 (Fc), 68.55 (Fc), 33.48 (CH$_2$), 32.52 (CH$_2$). MS (ES) (m/z) calcd for $C_{14}H_{16}{}^{56}Fe^{79}Br_2$ 399.8948, found 399.8946. IR (cm^{-1}): 3067 (=C-H), 3002 (CH$_2$), 2964 (CH$_2$), 2930 (CH$_2$), 2854 (CH$_2$), 1432 (CH$_2$), 822 (-CH=CH$_2$), 693 (CH Ar). Mp 52 °C - 54 °C.

6.1.28. 1-(2-(Bromo)ethyl)-ferrocene **27a**
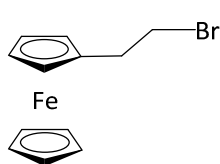
In a 50 mL schlenk tube, NBS (0.487 g, 2.735 mmol) was suspended in 9 mL of dry DCM. A 3 mL DCM solution of triphenylphosphine (0.669 g, 2.553 mmol) was added drop wise to it. The resulting orange mixture was stirred for 5 min before addition of 0.215 mL (2.188 mmol) of pyridine. The mixture goes brown. **16a** (0.250 g, 0.911 mmol) dissolved in 3 mL of dry DCM was added to the mixture. After overnight reaction, the solvent was removed *in vacuo* and the crude was purified via flash column chromatography (60% Et$_2$O in hexane) to yield product (0.244 g, 91%). ^{1}H NMR (300 MHz, Chloroform-d) δ 4.13 (s, 5H+2H), 4.11 – 4.09 (m, 2H), 3.43 (dd, J = 8.1, 7.3 Hz, 2H), 2.90 (t, J = 7.7 Hz, 2H). ^{13}C NMR (101 MHz, CDCl$_3$) δ 85.52 (ipso Cp), 68.64 (Fc), 68.30 (Fc), 67.69 (Fc), 33.66 (CH$_2$), 32.44 (CH$_2$). MS (ES) (m/z) calcd for C$_{12}$H$_{13}$^{56}Fe^{79}Br 291.9550, found 291.9557. IR (cm^{-1}): 3092 (=C-H), 2971 (CH$_2$), 2909 (CH$_2$), 2853 (CH$_2$), 1466 (CH$_2$), 1441 (CH$_2$), 1103, 806 (CH=CH), 714 (CH Ar). Mp 65 - 66 °C.

6.1.29. 1-[2-((*N*-4-Benzoyl)-cytosin-1-yl)ethyl]-ferrocene **28a**
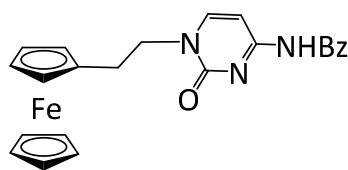
In a 50 mL schlenk tube, the *N*-3-benzoyl-cytosine **21** (0.165 g, 0.768 mmol) was stirred vigorously in 6 mL of dry DMF and NaH (0.0184 g, 0.768 mmol) were added to the suspension in one portion. After hydrogen production has stopped, **27a** (0.150 g, 0.512 mmol) was added to the mixture pre-dissolved in 3 mL of dry DMF. The reaction was stirred overnight. The reaction was evaporated, extracted with EtOAc, washed with brine followed by water and dried over Na$_2$SO$_4$, solvent removed *in vacuo* and purified via flash column chromatography (2% MeOH in DCM) to yield product (0.154 g, 68%). ^{1}H NMR (300 MHz, CDCl$_3$) δ 8.62 (s, 1H),

7.89 (d, J = 7.3 Hz, 2H), 7.62 (t, J = 7.4 Hz, 1H), 7.52 (t, J = 7.7 Hz, 2H), 7.34 − 7.28 (m, 1H),

7.22 (d, J = 7.1 Hz, 1H), 4.12 (s, 5H), 4.09 (t, J = 1.8 Hz, 2H), 3.97 (t, J = 1.9 Hz, 2H+2H), 2.85 (t,

J = 6.6 Hz, 2H). ^{13}C NMR (101 MHz, CDCl$_3$ + MeOD) δ 166.94 (C=O), 162.81 (C=O), 156.31 (C-

N), 149.13 (CH cytosine), 132.91 (Bz), 128.70 (Bz), 127.72 (Bz), 96.38 (CH cytosine), 83.51

(ipso Cp), 68.60 (Fc), 68.43 (Fc), 68.02 (Fc), 52.83 (CH$_2$), 28.80 (CH$_2$). MS (ES) (m/z) calcd for

C$_{23}$H$_{22}$N$_3$O$_2$^{56}Fe 428.1061, found 428.1059. IR (cm^{-1}): 3229 (NH), 3089 (=CH Ar), 2945 (CH$_2$),

2914 (CH$_2$), 2852 (CH$_2$), 1692 (C=O), 1647 (amide/urea), 1611 (NH), 1552 (amide), 1485

(C=N), 1427 (CH$_2$), 1359, 808 (CH Ar), 686 (C=C). Mp degrades at 184 °C.

6.1.30. 1,1'-Bis-[2-((N-4-benzoyl)-cytosin-1-yl)ethyl]-ferrocene **28**
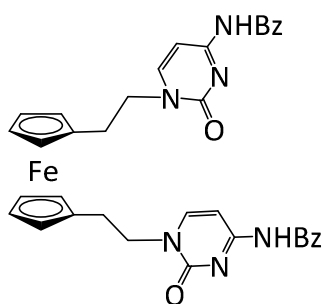
In a 50 mL schlenk tube, the N-4-benzoyl-cytosine **21** (0.157 g, 0.730 mmol) was stirred vigorously in 6 mL of dry DMF and NaH (0.0175 g, 0.730 mmol) was added to the suspension in one portion. After hydrogen production stopped, **27** (0.097 g, 0.240 mmol) was added to the mixture pre-dissolved in 2 mL of dry DMF. The reaction was stirred overnight at 50 °C. The reaction was evaporated, extracted

with EtOAc, washed with brine followed by water and dried over Na$_2$SO$_4$, solvent removed *in*

vacuo and purified via flash column chromatography (2% MeOH in DCM) to yield product

(0.039 g, 25%). ^{1}H NMR (400 MHz, CDCl$_3$) δ 8.58 (s, 2H), 7.88 (d, J = 7.6 Hz, 4H), 7.62 (t, J =7.5

Hz, 2H), 7.52 (dd, J = 8.4, 7.0 Hz, 4H), 7.35 (s, 2H), 7.23 (d, J = 7.2 Hz, 2H), 4.06 (t, J = 1.8 Hz,

4H), 3.99 − 3.92 (m, 4H+4H), 2.81 (t, J = 6.7 Hz, 4H). ^{13}C NMR (101 MHz, CDCl$_3$ + MeOD) δ

167.12 (C=O Bz), 162.87 (C=O), 156.27 (C-N), 149.14 (CH cytosine), 132.95 (Bz), 128.75 (Bz),

127.77 (Bz), 96.50 (CH cytosine), 83.89 (ipso Cp), 69.17 (Fc), 68.97 (Fc), 52.79 (CH$_2$), 28.55

(CH$_2$). MS (ES) (m/z) calcd for C$_{36}$H$_{32}$N$_6$O$_4$^{56}FeNa 691.1732, found 691.1739. IR (cm^{-1}): 3240 (NH), 3083 (=CH Fc), 2920 (CH$_2$), 2856 (CH$_2$), 1744 (cyclic ketone), 1692 (C=O), 1650 (amide/urea), 1613 (NH), 1485 (C=N), 1428 (CH$_2$), 1359, 786 (CH Ar), 685 (C=C). Mp degrades at 162 °C.

6.1.31. 1-[2-(Cytosin-1-yl)ethyl]-ferrocene **29a**
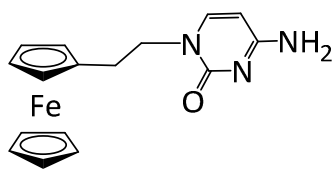
28a (0.040 g, 0.0936 mmol) was dissolved in 1 mL of methylamine. The mixture was stirred at room temperature for half an hour under argon. The methylamine was evaporated. The crude was purified on a silica gel chromatographic column (10% MeOH in DCM). A yellow solid was obtained (0.020 g, 61%). ^{1}H NMR (400 MHz, DMSO-d6) δ 7.44 (d, *J* = 7.1 Hz, 1H), 6.94 (s, 2H), 5.57 (d, *J* = 7.1 Hz, 1H), 4.17 (s, 5H), 4.08 (s, 4H), 3.78 (t, *J* = 7.6 Hz, 2H), 2.58 (t, *J* = 7.5 Hz, 2H). ^{13}C NMR (101 MHz, DMSO-d6) δ 165.90 (C=O), 155.63 (C-N), 146.02 (CH cytosine), 92.80 (CH cytosine), 84.72 (ipso Cp), 68.34 (Fc), 67.83 (Fc), 67.08 (Fc), 49.64 (CH$_2$), 28.45 (CH$_2$). MS (ES) (m/z) calcd for C$_{16}$H$_{17}$N$_3$O$_2$^{56}FeNa 346.0619, found 346.0625. IR (cm^{-1}): 3345 (NH), 3289 (NH), 3091 (=CH Fc), 2958 (CH$_2$), 2916 (CH$_2$), 2853 (CH$_2$), 1744 (Cyclic ketone), 1697 (C=O), 1657 (amide/urea), 1619 (NH), 1475 (C=N), 1434 (CH$_2$), 1385, 790 (CH Ar), 681 (C=C). Mp degrades at 184 °C.

6.1.32. 1,1'-Bis-acetyl-ferrocene **30**[5]
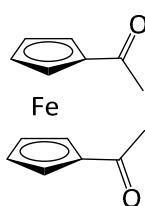
The acetyl chloride (10.58 mL, 149 mmol) was added to a suspension of aluminium (III) chloride (17.63 g, 132 mmol) in DCM at 0 °C. The ferrocene (10 g, 53.7 mmol) in DCM was then added drop wise within 20 min. The reaction was stirred for 2 h and warmed at room temperature. When the reaction was complete, the reaction was quenched by drop wise addition of ice-cold water at 0 °C. The mixture was then diluted with DCM, washed carefully (gas evolution) (2 x) with saturated aqueous K_2CO_3 and brine. The crude was dried on Mg_2SO_4 and evaporated. The crude was purified via flash column chromatography (25% EtOAc in hexane) to yield yellow-orange solid (12.38 g, 85%). ^{1}H NMR (400 MHz, Chloroform-d) δ 4.77 (s, 4H), 4.51 (s, 4H), 2.36 (s, 6H). ^{13}C NMR (101 MHz, CDCl$_3$) δ 201.11 (C=O), 80.68 (ipso Cp), 73.60 (Fc), 70.96 (Fc), 27.64 (CH$_3$). MS (ES) (m/z) calcd for $C_{14}H_{14}O_2{}^{56}$FeNa 293.0239, found 293.0241. IR (cm^{-1}): 3087 (=CH Ar), 1654 (C=O), 1373 (CH$_3$), 1353, 824 (C=C). Characterisation data is in agreement with the literature data.

6.1.33. (*R,R*)-1,1'-Bis-(α-hydroxyethyl)-ferrocene **31**[4]
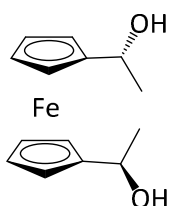
A solution of (*S*)-CBS (5 g, 18 mmol) in THF was cooled down to 0 °C under argon. To this solution, BH$_3$.SMe$_2$ (30 mL) was added in two steps. First 8.5 mL was added to the mixture in order to create the catalyst system. The solution was stirred for 5-10 min. Then 21.5 mL of BH$_3$.SMe$_2$ was added simultaneously with a solution of 1,1-diacyl ferrocene **30** (8.12 g, 30 mmol) in THF (150 mL) drop wise using a cannula. After 30 min of stirring at 0 °C, the excess of BH$_3$.SMe$_2$ was quenched by drop wise addition of MeOH (40 mL, gas evolution). The crude was poured into 300 mL of NH$_4{}^+$Cl$^-$, washed with ether, water, brine and dried on Na$_2$SO$_4$. The crude was

purified via flash column chromatography (75% Et_2O in hexane). A yellow-orange solid was obtained (7.56 g, 93%). ^{1}H NMR (400 MHz, Chloroform-d) δ 4.66 (q, *J* = 6.4 Hz, 2H), 4.32 (t, *J* = 3.4 Hz, 2H), 4.19 (t, *J* = 1.9 Hz, 4H), 4.20 – 4.18 (m, 2H), 4.15 – 4.12 (m, 2H), 1.39 (d, *J* = 6.4 Hz, 6H). ^{13}C NMR (101 MHz, CDCl3) δ 95.20 (ipso Cp), 67.67 (Fc), 67.56 (Fc), 66.14 (Fc), 65.99 (Fc), 65.62 (CH*), 25.63 (CH_3). MS (ES) (m/z) calcd for $C_{14}H_{18}O_2{}^{56}FeNa$ 297.0550, found 297.0554. $[\alpha]_D$ (c = 0.0065 g/mL, DCM) = -51.7. Characterisation data is in agreement with the literature data.

6.1.34. (*R,R*)-1,1'-Bis-(α-acetoxyethyl)-ferrocene **32**[4]
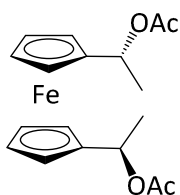
The 1,1'-Bis-(α-hydroxyethyl) ferrocene **31** (4.728 g, 17.4 mmol) was dissolved in dry DCM (60 mL) and stirred for 5 min. 4 mL (4.435 g, 43.4 mmol) of acetic anhydride, 6 mL (4.395 g, 43.4 mmol) of TEA and catalytic amount of DMAP were added successively to the mixture. The reaction was stirred at room temperature overnight. After completion of the reaction, it was quenched with $NaHCO_3$ (80 mL) and extracted with DCM. The aqueous layer was washed with DCM (3 x 100 mL) and then dried on Mg_2SO_4 and evaporated. The crude was purified via flash column chromatography (25% EtOAc and 1% TEA in hexane). A yellow-orange solid was obtained (4.898 g, 79%). ^{1}H NMR (400 MHz, $CDCl_3$) δ 5.81 (q, *J* = 6.5 Hz, 2H), 4.24 (t, *J* = 1.7 Hz, 2H), 4.19 (t, *J* = 1.8 Hz, 2H), 4.14 (t, *J* = 1.9 Hz, 4H), 2.05 (s, 6H), 1.54 (d, *J* = 6.5 Hz, 6H). ^{13}C NMR (101 MHz, $CDCl_3$) δ 170.44 (C=O), 88.69 (ipso Cp), 69.23 (Fc), 68.96 (Fc), 68.85 (Fc), 68.59 (Fc), 66.63 (CH*), 21.39 (CH_3), 20.27 (CH_3). IR (cm^{-1}): 3087 (=C-H), 2997 (CH_2), 2947 (CH_2), 1721 (C=O), 1445 (CH_3), 1367 (OCOCH3), 836 (CH=CH), 703 (CH Ar). Mp 55 °C – 58 °C. Characterisation data is in agreement with the literature data.

6.1.35. (R,R)-1,1'-Bis-(α-N,N-dimethylaminoethyl)-ferrocene **33**[4]
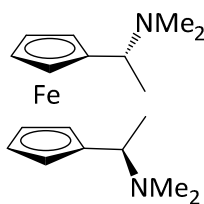
The 1,1'-Bis-ethylacetate ferrocene **32** (2.099 g, 59 mmol) was dissolved in 10 mL of MeOH. 10.8 mL of dimethylamine was added and stirred overnight at room temperature. The reaction was quenched with 20 mL of water and extracted with DCM (3x60 mL), dried on MgSO$_4$, solvent removed *in vacuo* and purified via flash column chromatography (5% MeOH, 2% TEA in DCM) to yield product. A brown-orange oil was obtained (1.474 g, 76%). ^{1}H NMR (300 MHz, CDCl$_3$) δ 3.97 − 3.95 (m, 8H), 3.49 (q, J = 7 Hz, 2H), 1.98 (s, 12H), 1.34 (d, J = 7 Hz, 6H). ^{13}C NMR (101 MHz, CDCl$_3$) δ 87.28 (ipso Cp), 70.31 (Fc), 68.47 (Fc), 68.22 (Fc), 67.09, 58.62 (CH*), 40.70 (CH$_3$), 16.16 (CH$_3$). MS (ES) (m/z) calcd for C$_{18}$H$_{28}$N$_2$^{56}FeNa 351.1500, found 351.1487. [α]$_D$ (c = 0.006 g/mL, DCM) = +16.0. Characterisation data is in agreement with the literature data.

6.1.36. (R,R,S$_p$,S$_p$)-1,1'-Bis-(α-N,N-dimethylaminoethyl)-2-2'-bis-bromo-ferrocene **34a**
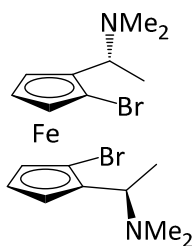
To a stirred solution of dimethylaminoethyl ferrocene **33** (1.474 g, 4.49 mmol) in ether, a solution of n-BuLi in hexane (7.75 mL, 17.9 mmol) was added drop wise over 15 min at room temperature. After few minutes, the colour of the mixture should have turned red. After over night stirring, the reaction was cooled down to -78 °C using a dry ice and acetone mix bath. A solution of dibromotetrachloroethane (6.584 g, 20.2 mmol) in THF was then added drop wise over 15 min. The resulting yellow-dark suspension was allowed to warm up to room temperature over 90 min, stirred for 1 h and then quenched with NaS$_2$O$_3$ (20 mL) at 0 °C. The mixture was washed with water and brine and extracted with ether (30 mL), solvent removed *in vacuo*

and purified via flash column chromatography (5% MeOH, 5% TEA in DCM) to yield product.

A brown-yellow oil was obtained (1.2 g, 55%). ^{1}H NMR (400 MHz, Chloroform-d) δ 4.27 (t, $J =$ 2.0 Hz, 2H), 4.12 (s, 4H), 3.74 (q, $J = 6.8$ Hz, 2H), 2.12 (s, 12H), 1.47 (d, $J = 6.8$ Hz, 6H). ^{13}C NMR (101 MHz, CDCl$_3$) δ 88.22 (ipso Cp), 81.37 (ipso Cp), 75.63 (Fc), 68.90 (Fc), 66.89 (Fc), 55.40 (CH*), 41.05 (CH$_3$), 16.47 (CH$_3$). MS (ES) (m/z) calcd for C$_{18}$H$_{26}$N$_2$^{56}FeBr$_2$ 506.9710, found 506.9720.

6.1.37. (*R,R,S$_p$,S$_p$*)-1,1'-Bis-(α-*N,N*-dimethylaminoethyl)-2,2'-bis-iodo-ferrocene **34**
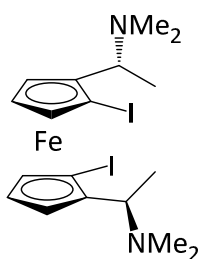
In a 200 mL schlenk tube, **33** (2.01 g, 5.62 mmol) was dissolved in Et$_2$O (30 mL) at room temperature, *n*-BuLi (8.99 mL, 22.46 mmol) was added to the mixture at that temperature and stirred overnight under an inert atmosphere. The reaction mixture was cooled to -78 °C and iodine (6.41 g, 25.27 mmol) dissolved in THF (60 mL) was added over the course of 10 min. The reaction was stirred at -78 °C for 90 min before allowing to warm to room temperature, at which point it was allowed to stirred for an additional 90 min before quenching at 0 °C with sodium thiosulfate$_{(aq)}$ (50 mL, 25% w/v). Dilute with Et$_2$O (30 mL), the layers were separated and the aqueous layer was further extracted with Et$_2$O (50 mL). The combined organic fractions were dried over MgSO$_4$ solvent remove *in vacuo* and purified via flash column chromatography (55% EtOAc, 5% TEA in hexane) to yield product (2.607 g, 80%). ^{1}H NMR (300 MHz, CDCl$_3$) δ 4.18 − 4.15 (m, 6H), 3.58 (q, $J = 7$ Hz, 2H), 2.14 (s, 12H), 1.43 (d, $J = 7$ Hz, 6H). ^{13}C NMR (101 MHz, CDCl$_3$) δ 90.8 (ipso Cp), 82.2 (Fc), 72.2 (Fc), 67.8 (Fc), 56.9 (CH*), 47.58 (ipso Cp), 41.08 (CH$_3$), 15.6 (CH$_3$). MS (ES) (m/z) calcd for C$_{18}$H$_{27}$N$_2$^{56}FeI$_2$ 580.9613, found 580.9619 (M$^+$ + H). Mp 66 °C - 68 °C. [α]$_D$ (c = 0.0053 g/mL, DCM) = +178.8. Opposite enantiomer synthesised by Dr. Nguyen [α]$_D$ (c = 0.0054 g/mL, DCM) = -192.5.

6.1.38. (*R,R,S$_p$,S$_p$*)-1,1'-Bis-(α-*N,N*-acetoxyethyl)-2,2'-bis-iodo-ferrocene **35**
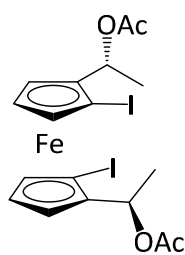
In a 100 mL schlenk tube, **34** (1.52 g, 2.49 mmol) and acetic anhydride (5 mL, 52.99 mmol) was heated at 50 °C under an inert atmosphere for 2.5 h. The excess acetic anhydrides were removed under high vacuum (0.1 mm Hg). Purified via flash column chromatography (5% TEA in hexane) to yield product (1.18 g, 78%). ^{1}H NMR (300 MHz, CDCl$_3$) δ 5.83 (q, *J* = 6.5 Hz, 2H), 4.37(dd, *J* = 2.5, 1.3 Hz, 2H), 4.32 (d, *J* = 2.5, 1.4 Hz, 2H), 4.23(t, *J* = 2.6 Hz, 2H), 2.04 (s, 6H), 1.63 (d, *J* = 6.5 Hz, 6H). ^{13}C NMR (101 MHz, CDCl$_3$) δ 170.1 (C=O), 88.9 (ipso Cp), 82.2 (Fc), 73.2 (Fc), 68.6 (Fc), 67.8 (CH*), 45.51 (ipso Cp) 21.1 (CH$_3$), 18.8 (CH$_3$). MS (ES) (m/z) calcd for C$_{18}$H$_{20}$O$_4$^{56}FeI$_2$Na 632.8698, found 632.8689. Mp 126 °C - 128 °C.

6.1.39. (*R,R,S$_p$,S$_p$*)-1,1'-Bis-(α-hydroxyethyl)-2,2'-bis-iodo-ferrocene **36**
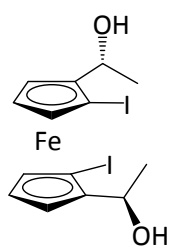
In a 250 mL round bottom flask **35** (1.24 g, 2.36 mmol) was dissolved in EtOH (20 mL). NaOH$_{(aq)}$ (40 mL, 10% w/v) was added and the reaction was heated at 95 °C for 10 min. The reaction was allowed to cool to room temperature and organic layer was extracted with EtOAc (50 mL x 2). The organic layers were dried over Na$_2$SO$_4$, solvent removed *in vacuo* and purified via flash column chromatography (25% EtOAc in hexane) to yield product (1.19 g, 96%) ^{1}H NMR (300 MHz, CDCl$_3$) δ 4.78 (qd, *J* = 6.4, 3.9 Hz, 2H), 4.30 – 4.27 (m, 4H), 4.19 (t, *J* = 2.6 Hz, 2H), 2.08 (d, *J* = 4.1 Hz, 2H), 1.57 (d, *J* = 6.5 Hz, 6H). ^{13}C NMR (101 MHz, CDCl$_3$) δ 92.8 (ipso Cp), 80.6 (Fc), 72.5 (Fc), 67.2 (Fc), 65.6 (CH*), 45.0 (ipso Cp), 21.7 (CH$_3$). MS (ES) (m/z) calcd for C$_{14}$H$_{16}$O$_2$^{56}FeI$_2$Na 548.8487, found 548.8493. Mp 98 - 100 °C. [α]$_D$ (c = 0.0061 g/mL DCM) = +95.1. Opposite enantiomer [α]$_D$ (c = 0.0060/mL g, DCM)= -92.0.

6.1.40. (*R*,*R*,*S*$_p$,*S*$_p$)-1,1'-Bis-(α-methoxyethyl)-2,2'-bis-iodo-ferrocene **37**
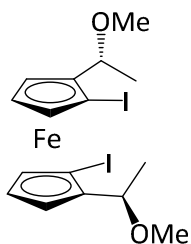
In a 100 mL round bottom flask, **36** (2.12 g, 4.03 mmol) was dissolved in a MeOH/AcOH (20 mL, 9:1) mixture, the reaction was stirred at room temperature for three days. The reaction was quenched with water (10 mL) and extract with DCM (20 mL x 2). The combined organic fractions were dried over MgSO$_4$, solvent removed *in vacuo* and purified via flash column chromatography (25% EtOAc in hexane) to yield product (2.05 g, 81%). ^{1}H NMR (300 MHz, CDCl$_3$) 4.43 (q, *J* = 6.5 Hz, 2H), 4.30 – 4.28 (m, 2H), 4.25 – 4.23 (m, 2H), 4.17 (t, *J* = 2.6 Hz, 2H), 3.27 (s, 6H), 1.63 (d, *J* = 6.5 Hz, 6H). ^{13}C NMR (101 MHz, CDCl$_3$) δ 90.8 (ipso Cp), 81.5 (Fc), 73.5 (Fc), 72.7 (Fc), 67.4 (CH*), 56.2 (CH$_3$), 47.1 (ipso C-I), 19.4 (CH$_3$). MS (ES) (m/z) calcd for C$_{16}$H$_{20}$O$_2$^{56}FeI$_2$Na 576.8800, found 576.8807. Mp 65 °C - 67 °C. [α]$_D$ (c = 0.0054 g/mL, DCM) = +149.6. Opposite enantiomer [α]$_D$ (c = 0.0054 g/mL, DCM) = -155.6.

6.1.41. [(1-Ethoxyvinyl)oxy]trimethylsilane **38**[21]
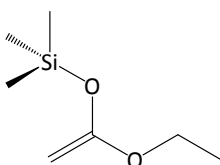
A solution of diisopropylamine (4 g, 39.5 mol) in 30 mL of THF was added to a 2.5 M hexane solution of butyl Lithium (15.857 mL, 39.5 mol) at 0 °C and stirred for 20 min at this temperature. 3.85 mL of EtOAc (35.5 mmol) was then added to the mixture at -78 °C using a dry ice/acetone bath. After 30 min of stirring, 5.51 mL of TMSCl (43 mmol) were added to the mixture at the same temperature. After another 30 min, the mixture was warmed up to RT and stirred for 1 h. The solution was then poured into 80 mL of hexane and 40 mL of water. The organic layer was washed with brine and dried on MgSO$_4$. The pale yellow oil obtained was purified using a glass oven

(Kugelrohr) with the following conditions: 50 °C, high vacuum, 10 to 15 min. A white oil was collected (1.225 g, 20%). ^{1}H NMR (300 MHz, CDCl$_3$) δ 3.53 (q, J = 7 Hz, 2H), 2.97 (d, J = 3 Hz, 1H), 2.83 (d, J = 3 Hz, 1H), 1.07 (t, J = 7 Hz, 3H), 1.01 (t, J = 7 Hz, 3H), 0.00 (s, 9H). The compound was not fully characterised for purity reasons.

6.1.42. (S,S,S_p,S_p)-1,1'-Bis-[α-methyl(2-ethylpropanoate)]-2,2'-bis-iodo-ferrocene 39
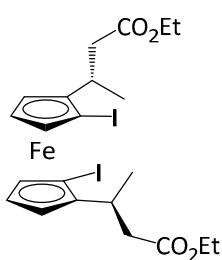
In a 250 mL schlenk tube, **37** (2.05 g, 3.92 mmol) and 1-ethoxyvinyloxytrimethylsilane **38** (2.53 g, 15.68 mmol) were dissolved in DCM (100 mL). The mixture was cooled to -78 °C and BF$_3$.OEt$_2$ (1.11 mL, 8.62 mmol) was added drop wise. The reaction mixture was stirred for 15 min at -78 °C before allowing to be warmed to room temperature. Quenched with saturated NaHCO$_3$ (40 mL), the organic layer was separated and the aqueous layer was further extracted with DCM (40 mL). The combined organic fractions were dried over MgSO$_4$, solvent removed *in vacuo* and purified via flash column chromatography (10% EtOAc in hexane) to yield product (2.40 g, 92%). ^{1}H NMR (300 MHz, CDCl$_3$) δ 4.21 − 4.09 (m, 6H+4H), 3.14 − 2.99 (m, 2H), 2.53 (dd, J = 15.0, 3.7 Hz, 2H), 2.12 (dd, J = 15.0, 10.1 Hz, 2H), 1.40 (d, J = 6.8 Hz, 6H), 1.26 (t, J = 7.1 Hz, 6H). ^{13}C NMR (101 MHz, CDCl$_3$) δ 171.84 (C=O), 94.59 (ipso Cp), 81.12 (Fc), 71.78 (Fc), 66.38 (Fc), 60.30 (CH$_2$), 46.19 (ipso Cp), 42.80 (CH$_2$), 29.91 (CH*), 18.84 (CH$_3$), 14.25 (CH$_3$). MS (ES) (m/z) calcd for C$_{22}$H$_{28}$O$_4$^{56}FeI$_2$Na 688.9324, found 688.9321. IR (cm^{-1}): 3095 (=C-H), 2976 (CH$_2$), 2932 (CH$_2$), 2872 (CH$_2$), 1724 (C=O), 1368 (CH$_3$), 1172 (ester), 1150 (ester), 821 (CH=CH). Mp 62 °C - 64 °C. [α]$_D$ (c = 0.0063 g/mL, DCM) = +128.9. Opposite enantiomer [α]$_D$ (c = 0.0064 g/mL, DCM) = -105.6.

6.1.43. (*S,S,S$_p$,S$_p$*)-1,1'-Bis-[α-methyl-(3-(hydroxyl)propyl)]-2,2'-bis-iodo-ferrocene **40**
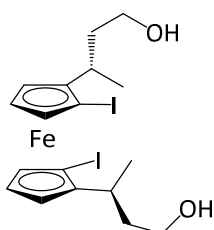
In a 100 mL schlenk tube, **39** (2.01 g, 3.02 mmol) was dissolved in Et$_2$O (50 mL), cooled to 0 °C and stand for 5 min. Diisobutylalumminum hydride (18.1 mL, 18.12 mmol) was added to the reaction slowly at that temperature. The reaction was allowed to stir at 0 °C for 1 h before quenched with aqueous sodium potassium tartrate (30 mL). The layers were separated and the aqueous layer was further extract with Et$_2$O (30 mL). The combined organic fractions were dried over Na$_2$SO$_4$, solvent remove *in vacuo* and purified via flash column chromatography (70% EtOAc in hexane) to yield product (1.56 g, 89%). ^{1}H NMR (300 MHz, CDCl$_3$) 4.16 (t, *J* = 2.0 Hz, 2H), 4.14 – 4.12 (m, 4H), 3.59 (t, *J* = 6.6 Hz, 4H), 2.76 – 2.65 (m, 2H), 1.71 – 1.63 (m, 2H), 1.58 (s, 2H), 1.57 – 1.50 (m, 2H), 1.37 (d, *J* = 6.9 Hz, 6H). ^{13}C NMR (101 MHz, CDCl$_3$) δ 96.29 (ipso Cp), 80.78 (Fc), 71.62 (Fc), 66.04 (Fc), 60.76 (CH$_2$), 46.90 (ipso Cp), 41.82 (CH$_2$), 29.10 (CH*), 19.55 (CH$_3$). MS (ES) (m/z) calcd for C$_{18}$H$_{24}$O$_2$^{56}FeI$_2$Na 604.9113, found 604.9108. IR (cm^{-1}): 3406-3110 (OH), 2963, 1029. Mp 87 °C - 89 °C. [α]$_D$ (c = 0.0019 g/mL, DCM) = +145.3. Opposite enantiomer [α]$_D$ (c = 0.0017 g/mL, DCM) = -112.9.

6.1.44. (*S,S,S$_p$,S$_p$*)-1,1'-Bis-[α-methyl-(3-(benzyloxy)propyl)]-2,2'-bis-iodo-ferrocene **41**
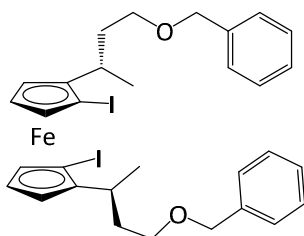
In a 100 mL two necks round bottom flask filled with argon, to the diol **40** (1.01 g, 1.74 mmol) dissolved in DMF (20 mL) was added NaH (0.35 g, 8.70 mmol, 60% w/w in mineral oil) slowly. The reaction was stirred at room temperature for 1 h, after which it was quenched with water (100 mL) and extracted with Et$_2$O (40 mL × 3). The combined ethereal fractions were washed with brine (60 mL), dried over MgSO$_4$, solvent removed *in*

vacuo and purified via flash column chromatography (30% EtOAc in hexane) to yield the yellow oily product (1.06 g, 80%). ^{1}H NMR δ $_H$ (300 MHz, CDCl$_3$) 7.34 – 7.26 (m, 10H), 4.47 (dd, *J* = 30.8, 11.9 Hz, 4H), 4.14 (t, *J* = 2.0 Hz, 2H), 4.11 – 4.08 (m, 4H), 3.49 – 3.39 (m, 4H), 2.75 – 2.65 (m, 2H), 1.86 – 1.47 (m, 4H), 1.34 (d, *J* = 6.9 Hz, 6H). ^{13}C NMR (101 MHz, CDCl$_3$) δ 138.65 (ipso Ph), 128.30 (Ph), 127.61 (Ph), 127.42 (Ph), 96.40 (ipso Cp), 80.81 (Fc), 72.69 (CH$_2$), 71.58 (Fc), 68.33 (CH$_2$), 66.18 (Fc), 46.73 (ipso Cp), 38.35 (CH$_2$), 29.70 (CH*), 19.48 (CH$_3$). IR (cm^{-1}): 2930 (CH$_2$), 2854 (CH$_2$), 1092. MS (ES) (m/z) calcd for C$_{32}$H$_{36}$O$_2$^{56}FeI$_2$Na 785.0052, found 785.0055.

6.1.45. (*S,S,S$_p$,S$_p$*)-1,1'-Bis-[α-methyl-(3-(benzyloxy)propyl)]-2,2'-bis-aldehyde-ferrocene **42**
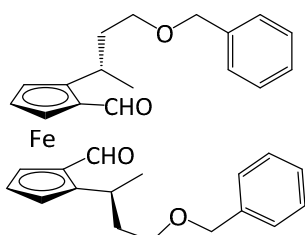
In a 100 mL schlenk tube, **41** (0.80 g, 1.05 mmol) was dissolved in Et$_2$O (30 mL), the mixture was cooled to -78 °C and *n*-BuLi (1.47 mL, 3.66 mmol) was added. After 30 min DMF (0.34 mL, 4.40 mmol) was added and the reaction was stirred at -78 °C for another 30 min before allowing to warm to room temperature, at which point it was quenched with water (10 mL). The phrases were separated and the aqueous layer was extracted with further Et$_2$O (10 mL). The combined ethereal fractions were dried over Na$_2$SO$_4$, solvent removed *in vacuo* and purified via flash column chromatography (2% EtOAc in hexane) to yield the red oily product (0.54 g, 91%). ^{1}H NMR (400 MHz, Chloroform-d) δ 10.04 (s, 2H), 7.37 – 7.26 (m, 10H), 4.82 (t, *J* = 2.1 Hz, 2H), 4.49 – 4.47 (m, 4H), 4.46 – 4.31 (dd, *J* = 30.7, 11.8 Hz, 4H), 3.38 – 3.28 (m, 4H), 3.12 (h, *J* = 6.8 Hz, 2H), 1.74 – 1.58 (m, 4H), 1.36 (d, *J* = 6.9 Hz, 6H). ^{13}C NMR δ 193.1 (C=O), 138.3 (ipso Ph), 128.4 (Ph), 127.8 (Ph), 127.6 (Ph), 99.4 (ipso Cp), 77.7 (ipso Cp), 72.9 (CH$_2$), 72.7 (Fc), 72.0 (Fc), 71.5 (Fc), 67.8 (CH$_2$), 39.9 (CH$_2$), 27.6

(CH*), 19.4 (CH$_3$). MS (ES) (m/z) calcd for C$_{34}$H$_{38}$O$_4$^{56}FeNa 589.2017, found 589.2024. IR (cm$^-$^{1}): 2928 (CH$_2$), 2864 (CH$_2$), 1716 (CHO), 1097 (ether).

6.1.46. (*S*,*S*,*R$_p$*,*R$_p$*)- 1,1'-Bis-[α-methyl-(3-(benzyloxy)propyl)]-2,2'-bis-[(*Z*)-2-((*N*,*N*-6-dibenzoyl)-adenin-9-yl))ethylenyl]-ferrocene **43**

In a 100 mL schlenk tube, **6** (0.768 g, 1.37 mmol) was dissolved in 3 mL of pyridine. The mixture was evaporated on high vacuum. The mixture was then dissolved in 12 mL of dry DMF and NaH (0.035 g, 0.137 mmol) was added in one portion at room temperature. The solution was stirred for 2 h. The aldehyde **42** was dissolved in 7 mL of DMF and added to the mixture, which was stirred overnight at room temperature. The reaction was quenched with 60 mL of a 1:1 EtOAc /water mixture. The phrases were separated and the aqueous layer was extracted with further Et$_2$O. The combined ethereal fractions were dried over Na$_2$SO$_4$, solvent removed *in vacuo* and purified via flash column chromatography (30% EtOAc, 20% Et$_2$O in hexane) to yield product (0.25 g, 43%). ^{1}H NMR (400 MHz, CDCl$_3$) δ 8.70 (s, 2H), 8.02 (s, 2H), 7.87 (d, *J* = 7.0 Hz, 8H), 7.47 (t, *J* = 7.5 Hz, 4H), 7.35 (t, *J* = 7.8 Hz, 8H), 7.31 – 7.19 (m, 10H), 6.90 (d, *J* = 8.8 Hz, 2H), 6.43 (d, *J* = 8.9 Hz, 2H), 4.49 – 4.37 (m, 4H), 4.08 (dd, *J* = 2.6, 1.3 Hz, 2H), 4.01 (t, *J* = 2.6 Hz, 2H), 3.41 – 3.27 (m, 4H), 3.24 – 3.19 (m, 2H), 2.70 – 2.59 (m, 2H), 1.65 – 1.52 (m, 4H), 1.12 (d, *J* = 6.8 Hz, 6H). ^{13}C NMR (101 MHz, CDCl$_3$) δ 172.24 (C=O), 152.98 (ipso adenine), 152.79 (CH adenine), 151.89 (ipso adenine), 144.13 (CH adenine), 138.33 (ipso Ph), 134.20 (ipso Bz), 132.93 (Bz), 129.45 (Bz), 128.68 (Bz), 128.37 (Ph), 127.58 (Ph), 127.01 (ipso adenine), 123.78 (=CH), 116.60 (=CH), 97.49 (ipso Cp), 72.96 (ipso Cp), 69.92 (Fc), 69.29 (Fc), 67.82 (CH$_2$), 67.29 (Fc),

39.76 (CH$_2$), 27.93 (CH*), 19.27 (CH$_3$). MS (ES) (m/z) calcd for C$_{74}$H$_{64}$N$_{10}$O$_6$^{56}FeNa 1267.4257, found 1267.4255. IR (cm^{-1}): 3063 (=CH Fc), 2961 (CH$_2$), 2925 (CH$_2$), 2853 (CH$_2$), 1698 (C=O), 1596 (Amide), 1575 (C=N), 1449 (CH$_2$), 1091 (ether), 1073 (ether), 824 (CH Ar), 699 (C=C). Mp 84 °C - 86 °C.

6.1.47. (*S*,*S*,*S$_p$*,*S$_p$*)-1,1'-Bis-[α-methyl-(3-(*tert*-butyldiphenylsilyl)propyl)]-2,2'-bis-iodo-

ferrocene **44**
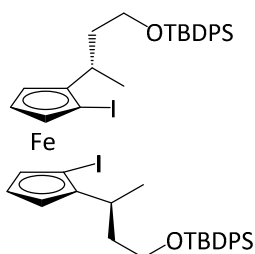
In a 100 mL schlenk tube, the diol **40** (1.2 g, 2.06 mmol) was dissolved in 20 mL DCM at room temperature. TEA (0.861 mL, 6.18 mmol), *tert*-Butyldiphenylsilyl chloride (1.607 mL, 6.18 mmol) and DMAP in catalytic amount were added successively to the mixture. The solution was stirred overnight at room temperature and quenched with water. The phrases were separated and the aqueous layer was extracted with further Et$_2$O. The combined ethereal fractions were dried over Na$_2$SO$_4$, solvent removed *in vacuo* and purified via flash column chromatography (10% EtOAc in hexane) to yield the oily yellow product (2 g, 95%). ^{1}H NMR (400 MHz, CDCl$_3$) δ 7.67 (m, 8H), 7.42 – 7.33 (m, 12H), 4.12 (t, *J* = 1.8 Hz, 2H), 4.06 – 4.01 (m, 4H), 3.66 (dd, *J* = 7.7, 5.6 Hz, 4H), 2.74 – 2.69 (m, 2H), 1.85 – 1.80 (m, 2H), 1.37 – 1.26 (m, 2H), 1.27 (d, *J* = 6.9 Hz, 6H), 1.05 (s, 18H). ^{13}C NMR (101 MHz, CDCl$_3$) δ 135.64 (Ph), 134.06 (ipso Ph), 134.01 (Ph), 129.50 (Ph), 127.60 (Ph), 96.62 (ipso Cp), 80.28 (Fc), 71.16 (Fc), 66.12 (Fc), 61.97 (CH$_2$), 46.67 (ipso Cp), 41.26 (CH$_2$), 29.06 (CH*), 26.95 (tBu), 19.24 (ipso tBu), 18.72 (CH$_3$). MS (ES) (m/z) calcd for C$_{50}$H$_{60}$O$_2$^{56}FeI$_2$Si$_2$Na 1081.1469, found 1081.1481. IR (cm$^-$

[1]): 3071 (=CH Fc), 2958 (CH$_2$), 2930 (CH$_2$), 2856 (CH$_2$), 1589, 1471, 1427 (CH$_2$), 1387 (tBu), 1106 (Si-OR), 1084 (Si-OR), 821 (CH Ar), 699 (C=C). [α]$_D$ (c = 0.0056 g/mL, DCM) = +84.3.

6.1.48. (*S,S,S$_p$,S$_p$*)-1,1'-Bis-[α-methyl-(3-(*tert*-butyldiphenylsilyl)propyl)]-2,2'-bis-aldehyde-ferrocene **45**
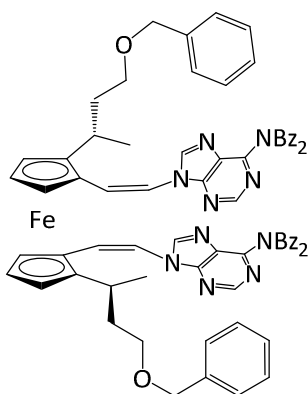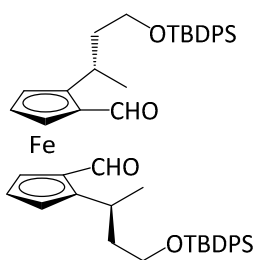
In a 100 mL schlenk tube, **44** (2 g, 1.94 mmol) was dissolved in Et$_2$O (40 mL), the mixture was cooled to -78 °C and *n*-BuLi (2.27 mL, 6.82 mmol) was added. After 30 min DMF (0.63 mL, 8.20 mmol) was added and the reaction was stirred at -78 °C for another 30 min before allowing too warm to room temperature, at which point it was quenched with water (20 mL). The phrases were separated and the aqueous layer was extracted with further Et$_2$O (20 mL). The combined ethereal fractions were dried over Na$_2$SO$_4$, solvent removed *in vacuo* and purified via flash column chromatography (20% EtOAc in hexane) to yield the red oily product (1.31 g, 78%). ^{1}H NMR (400 MHz, CDCl$_3$) δ 10.04 (s, 2H), 7.65 − 7.59 (m, 8H), 7.45 − 7.32 (m, 12H), 4.78 (dd, *J* = 2.7, 1.5 Hz, 2H), 4.44 − 4.40 (m, 4H), 3.64 − 3.52 (m, 4H), 3.16 − 3.02 (m, 2H), 1.68 − 1.62 (m, 2H), 1.55 − 1.48 (m, 2H), 1.28 (d, *J* = 6.9 Hz, 6H), 1.03 (s, 18H). ^{13}C NMR (101 MHz, CDCl$_3$) δ 192.85 (C=O), 135.55 (Ph), 133.81 (ipso Ph), 133.70 (ipso Ph), 129.58 (Ph), 127.63 (Ph), 99.78 (ipso Cp), 76.69 (ipso Cp), 72.41 (Fc), 72.08 (Fc), 71.52 (Fc), 61.56 (CH$_2$), 43.04 (CH$_2$), 27.40 (CH*), 26.86 (tBu), 19.13 (ipso tBu), 18.67 (CH$_3$). MS (ES) (m/z) calcd for C$_{52}$H$_{62}$O$_4$[56]FeSi$_2$Na 885.3434, found 885.3444. IR (cm^{-1}): 3071 (=CH Fc), 2930 (CH$_2$), 2857 (CH$_2$), 1673 (CHO), 1427 (CH$_2$), 1378 (tBu), 1106 (Si-OR), 1085 (Si-OR), 822 (CH Ar), 699 (C=C).

6.1.49. (*S,S,R_p,R_p*)-1,1'-Bis-[α-methyl-(3-(*tert*-butyldiphenylsilyl)propyl)]-2,2'-bis-vinyl-

ferrocene **46**
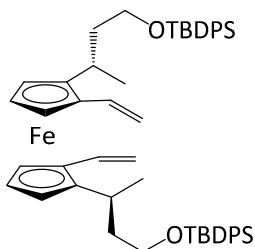
In a 100 mL schlenk tube, trimethylmethylphosphonium bromide (1.293 g, 3.62 mmol), potassium tert-butoxide (0.406, 3.62 mmol) and a catalytic amount of dibenzo-18-crown-6-ether were dissolved in 25 mL of dry THF. The mixture was stirred for 30 min and **45** (1.042 g, 1.21 mmol) previously dissolved in 30 mL of dry THF was added. The reaction was stirred overnight at room temperature, quenched with water and extracted with Et$_2$O (20 mL). The combined ethereal fractions were dried over Na$_2$SO$_4$, solvent removed *in vacuo* and purified via flash column chromatography (10% EtOAc in hexane) to yield the yellow oily product (1.017 g, 98%). ^{1}H NMR (400 MHz, CDCl$_3$) δ 7.72 − 7.59 (m, 8H), 7.44 − 7.32 (m, 12H), 6.48 (dd, *J* = 17.4, 10.8 Hz, 2H), 5.25 (dd, *J* = 17.4, 1.7 Hz, 2H), 5.08 (dd, *J* = 10.8, 1.7 Hz, 2H), 4.20 − 4.18 (m, 2H), 4.04 − 4.01 (m, 4H), 3.63 − 3.59 (m, 4H), 2.87 − 2.82 (m, 2H), 1.72 − 1.61 (m, 2H), 1.36 − 1.30 (m, 2H), 1.25 (d, *J* = 6.9 Hz, 6H), 1.05 (s, 18H). ^{13}C NMR (101 MHz, CDCl$_3$) δ 135.58 (Ph), 134.08 (ipso Ph), 134.00 (ipso Ph), 132.82 (CH vinyl), 129.49 (Ph), 127.57 (Ph), 111.04 (CH$_2$ vinyl), 94.55 (ipso Cp), 82.30 (ipso Cp), 67.86 (Fc), 67.57 (Fc), 66.41 (Fc), 61.79 (CH$_2$), 42.62 (CH$_2$), 26.86 (tBu), 26.67 (CH*), 19.21 (ipso tBu), 18.43 (CH$_3$). MS (ES) (m/z) calcd for C$_{54}$H$_{66}$O$_2$^{56}FeSi$_2$ 858.3951, found 858.3973. IR (cm^{-1}): 3071 (=CH Fc), 2929 (CH$_2$), 2858 (CH$_2$), 1624 (Ar), 1589, 1427 (CH$_2$), 1276 (CH$_3$), 1106 (Si-OR), 1086 (Si-OR), 821 (CH Ar), 699 (vinyl/C=C).

6.1.50. (*S,S,R_p,R_p*)-1,1'-Bis-[α-methyl-(3-(*tert*-butyldiphenylsilyl)propyl)]-2,2'-bis-[2-

(hydroxyl)ethyl]-ferrocene **47**
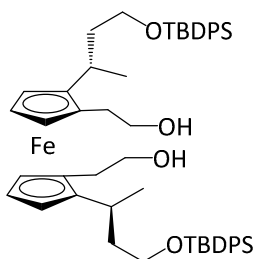
In a 100 mL schlenk tube, **46** (1 g, 1.165 mmol) was dissolved in 30 mL of dry THF. BH_3,THF (6.61 mL, 0.661 mmol) was then added drop wise at room temperature and stirred for 2 h. 1.5 mL of EtOH, 1.5 mL of NaOH (3M) and 1.1 mL of H_2O_2 (30%) were then successively added to the reaction and stirred for 1h at room temperature. The reaction was extracted with DCM, washed with brine and dried over Na_2SO_4, solvent removed *in vacuo* and purified via flash column chromatography (30% EtOAc in hexane) to yield product (0.814 g, 78%). ^{1}H NMR (400 MHz, CDCl$_3$) δ 7.68 – 7.63 (m, 8H), 7.45 – 7.35 (m, 12H), 3.94 (s, 2H), 3.89 (s, 4H), 3.73 – 3.61 (m, 4H+4H), 2.69 – 2.65 (m, 2H), 2.53 (t, *J* = 6.7 Hz, 4H), 1.71 – 1.68 (m, 2H), 1.40 – 1.20 (m, 2H), 1.21 (d, *J* = 6.7 Hz, 6H), 1.06 (s, 18H). ^{13}C NMR (101 MHz, CDCl$_3$) δ 135.61 (Ph), 133.94 (ipso Ph), 129.60 (Ph), 127.64 (Ph), 94.66 (ipso Cp), 82.51 (ipso Cp), 70.58 (Fc), 67.39 (Fc), 65.93 (Fc), 63.11 (CH_2), 61.98 (CH_2), 42.61 (CH_2), 30.73 (CH_2), 27.29 (CH*), 26.92 (tBu), 19.51 (CH_3), 19.23 (ipso tBu). MS (ES) (m/z) calcd for $C_{54}H_{70}O_4{}^{56}FeSi_2Na$ 917.4060, found 917.4020. IR (cm^{-1}): 3309 (OH), 3071 (=CH Fc), 2929 (CH_2), 2858 (CH_2), 1599 (Ar system), 1566, 1427 (CH_2), 1106 (Si-OR), 1077 (Si-OR), 739 (CH-Ar), 699 (C=C). Mp 106 °C - 107 °C. [α]$_D$ (c = 0.0066 g/mL, DCM) = -7.80.

6.1.51. (*S,S,R*_p,*R*_p)-1,1'-Bis-[α-methyl-(3-(*tert*-butyldiphenylsilyl)propyl)]-2-2'-bis-[2-((*N,N*-6-

dibenzoyl)-adenin-9-yl)ethyl]-ferrocene **48**
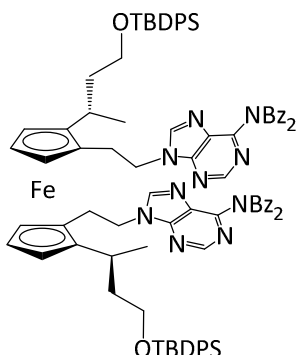
In a 50 mL schlenk tube, triphenylphosphine (0.309 g, 1.176 mmol) and the *N,N*-6-benzoyl-adenine **19** (0.350 g, 1.101 mmol) were dissolved in dry THF and stirred for 10 min at room temperature. **47** (0.351 g, 0.392 mmol) was then added to the mixture pre-dissolved in 7 mL of dry THF. The schlenk tube was then covered with foil and DIAD (0.240 mL, 1.176 mmol) was added at room temperature before the mixture was warmed up to 65 °C for 2 h. The reaction was evaporated, extracted with EtOAc, washed with brine followed by water and dried over Na_2SO_4, solvent removed *in vacuo* and purified via flash column chromatography (40% EtOAc in hexane) to yield product (0.311 g, 52%). ^{1}H NMR (400 MHz, CDCl$_3$) δ 8.54 (s, 2H), 7.86 (d, *J* = 7.1 Hz, 8H), 7.77 (s, 2H), 7.63 − 7.54 (m, 8H), 7.44 (t, *J* = 7.5 Hz, 4H), 7.36 − 7.26 (m, 20H), 4.28 − 4.09 (m, 4H), 3.96 − 3.91 (m, 2H), 3.82 (t, *J* = 2.5 Hz, 2H), 3.66 (dd, *J* = 7.5, 5.3 Hz, 4H), 3.47 (t, *J* = 1.7 Hz, 2H), 2.86 − 2.75 (m, 4H), 2.67 − 2.59 (m, 2H), 1.66 − 1.58 (m, 2H), 1.46 − 1.42 (m, 2H), 1.23 (d, *J* = 6.8 Hz, 6H), 1.00 (s, 18H). ^{13}C NMR (101 MHz, CDCl$_3$) δ 172.27 (C=O), 153.14 (ipso adenine), 152.11 (CH adenine), 151.62 (ipso adenine), 144.96 (CH adenine), 135.53 (Ph), 134.22 (ipso Ph), 133.71 (ipso Bz), 132.87 (Bz), 129.65 (Ph), 129.46 (Bz), 128.65 (Bz), 127.65 (Ph), 127.35 (ipso adenine), 94.83 (ipso Cp), 80.95 (ipso Cp), 69.74 (Fc), 67.97 (Fc), 66.66 (Fc), 61.97 (CH$_2$), 44.68 (CH$_2$), 42.88 (CH$_2$), 28.26 (CH$_2$), 27.28 (CH*), 26.85 (tBu), 19.97 (CH$_3$), 19.16 (ipso tBu). MS (ES) (m/z) calcd for $C_{92}H_{92}N_{10}O_6{}^{56}FeSi_2Na$ 1567.5987, found 1567.5985. IR (cm^{-1}): 3070 (=CH Fc), 2931 (CH$_2$), 2857 (CH$_2$), 1704 (C=O), 1598 (amide), 1575 (C=N), 1448 (CH$_2$), 1235 (CH$_3$), 1106 (Si-OR), 1087 (Si-OR), 699 (C=C). Mp 92 °C - 94 °C. [α]$_D$ (c = 0.0051 g/mL, DCM) = -25.1.

6.1.52. (*S,S,R$_p$,R$_p$*)-1,1'-Bis-[α-methyl-(3-(*tert*-butyldiphenylsilyl)propyl)]-2-2'-bis-[2-((*N*-4-

benzoyl)-uracil-1-yl)ethyl]-ferrocene **49**
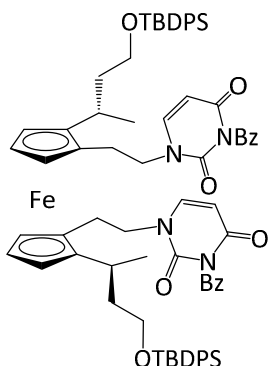
In a 50 mL schlenk tube, triphenylphosphine (0.148 g, 0.563 mmol) and *N*-3-benzoyluracil **20** (0.105 g, 0.4879 mmol) were dissolved in dry THF and stirred for 10 min at room temperature. **47** (0.168 g, 0.187 mmol) was then added to the mixture pre-dissolved in 4 mL of dry THF. The schlenk tube was then covered with foil and DIAD (0.122 mL, 0.563 mmol) was added at room temperature before the mixture was warmed up to 65 °C for 2 h. The reaction was evaporated, extracted with EtOAc, washed with brine followed by water and dried over Na$_2$SO$_4$, solvent removed *in vacuo* and purified via flash column chromatography (50% EtOAc in hexane) to yield product (0.180 g, 75%). ^{1}H NMR (400 MHz, CDCl$_3$) δ 7.82 (d, *J* = 7.1 Hz, 4H), 7.57 – 7.49 (m, 10H), 7.38 (t, *J* = 7.8 Hz, 4H), 7.35 – 7.29 (m, 4H), 7.29 – 7.23 (m, 8H), 6.79 (d, *J* = 8.0 Hz, 2H), 5.45 (d, *J* = 7.9 Hz, 2H), 3.90 – 3.84 (m, 2H), 3.78 (t, *J* = 2.5 Hz, 2H), 3.71 – 3.61 (m, 6H), 3.57 – 3.54 (m, 4H), 2.67 – 2.51 (m, 6H), 1.57 – 1,52 (m, 2H), 1.40 – 1.29 (m, 2H), 1.16 (d, *J* = 1.6 Hz, 6H), 0.94 (s, 18H). ^{13}C NMR (101 MHz, CDCl$_3$) δ 168.90 (C=O Bz), 162.47 (C=O uracil), 149.66 (C=O uracil), 144.29 (CH uracil), 135.52 (Ph), 135.14 (Bz), 133.89 (ipso Ph), 133.76 (ipso Ph), 131.45 (ipso Bz), 130.50 (Ph), 129.74 (Bz), 129.18 (Bz), 127.72 (Ph), 101.78 (CH uracil), 94.46 (ipso Cp), 81.03 (ipso Cp), 70.27 (Fc), 68.14 (Fc), 66.34 (Fc), 61.88 (CH$_2$), 49.55 (CH$_2$), 42.77 (CH$_2$), 27.28 (CH*), 27.11 (CH$_2$), 26.92 (tBu), 19.89 (CH$_3$), 19.26 (ipso tBu). MS (ES) (m/z) calcd for C$_{76}$H$_{82}$N$_4$O$_8$Si$_2$Fe^{56}Na 1313.4918, found 1313.4945. IR (cm^{-1}): 3071 (=CH Fc/CONH), 2930 (CH$_2$), 2857 (CH$_2$), 1747 (C=C-C=O), 1704 (C=O), 1660 (amide), 1428 (CH$_2$), 1382 (CH$_3$), 1107 (Si-OR), 1084 (Si-OR), 700 (C=C). Mp 84 °C - 86 °C. [α]$_D$ (c = 0.0067 g/mL, DCM) = -9.6.

6.1.53. (*S,S,R$_p$,R$_p$*)-1,1'-Bis-[α-methyl-(3-(hydroxy)propyl)]-2-2'-bis-[2-((*N*-6-benzoyl)-adenin-9-yl)ethyl]-ferrocene **50**
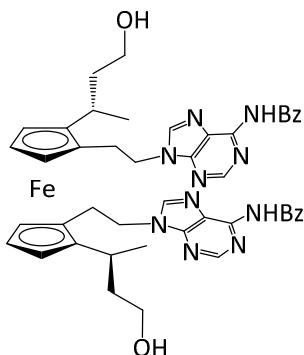
In a 50 mL schlenk tube, **48** (0.5 g, 0.322 mmol) was dissolved in 20 mL of dry THF and Tetra-Butylamino fluoride (0.305 g, 0.967 mmol) was added to the solution. After overnight stirring, the reaction was quenched with water, extracted with DCM, washed with brine, water and dried over Na$_2$SO$_4$. The solvent was removed *in vacuo* and the crude was purified via flash column chromatography (2% MeOH in DCM) to yield product (0.259 g, 92%). ^{1}H NMR (400 MHz, CDCl$_3$) δ 9.35 (s, 2H), 8.72 (s, 2H), 8.03 (d, *J* = 7.3 Hz, 4H), 7.98 (s, 2H), 7.58 (t, *J* = 6.7 Hz, 2H), 7.49 (t, *J* = 6.7 Hz, 4H), 4.38 – 4.23 (m, 4H), 4.04 (dd, *J* = 2.4, 1.2 Hz, 2H), 3.96 (t, *J* = 2.5 Hz, 2H), 3.78 – 3.73 (m, 2H), 3.68 – 3.57 (m, 4H), 3.17 (s, 2H), 3.01 – 2.94 (m, 2H), 2.87 – 2.78 (m, 4H), 1.62 – 1.46 (m, 4H), 1.35 (d, *J* = 6.7 Hz, 6H). ^{13}C NMR (101 MHz, CDCl$_3$) δ 164.83 (C=O), 152.41 (CH adenine), 151.63 (ipso adenine), 149.71 (ipso adenine), 143.13 (CH adenine), 133.54 (ipso Bz), 132.78 (Bz), 128.80 (Bz), 127.97 (Bz), 122.95 (ipso adenine), 94.81 (ipso Cp), 81.10 (ipso Cp), 70.41 (Fc), 68.08 (Fc), 66.20 (Fc), 59.99 (CH$_2$), 45.16 (CH$_2$), 43.47 (CH$_2$), 28.60 (CH$_2$), 26.70 (CH*), 19.96 (CH$_3$). MS (ES) (m/z) calcd for C$_{46}$H$_{48}$N$_{10}$O$_4$^{56}FeNa 883.3107, found 883.3100. IR (cm^{-1}): 3266 (OH), 3070 (=CH Fc), 2931 (CH$_2$), 2857 (CH$_2$), 1694 (C=O), 1608 (amide), 1580 (C=N), 1452 (CH$_2$), 1246 (CH$_3$), 1030 (Si-OR), 796 (CH Ar), 706 (C=C). Mp 122 °C - 125 °C.

6.1.54. (*S,S,R~p~,R~p~*)-1,1'-Bis-[α-methyl-(3-(hydroxy)propyl)]-2-2'-bis-[2-((*N*-4-benzoyl)-uracil-1-yl)ethyl]-ferrocene **51**
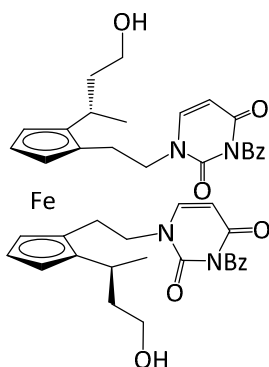
In a 50 mL schlenk tube, **49** (0.198 g, 0.153 mmol) was dissolved in 20 mL of dry THF and Tetra-Butylamino fluoride (0.145 g, 0.459 mmol) was added to the solution. After overnight stirring, the reaction was quenched with water, extracted with DCM, washed with brine, water and dried over Na_2SO_4. The solvent was removed *in vacuo* and the crude was purified via flash column chromatography (7% MeOH in DCM) to yield the oily product (0.025 g, 34%). ^{1}H NMR (400 MHz, CDCl$_3$) δ 7.94 (d, *J* = 7.1 Hz, 4H), 7.66 (t, *J* = 7.5 Hz, 2H), 7.51 (t, *J* = 7.8 Hz, 4H), 7.31 (d, *J* = 7.9 Hz, 2H), 5.72 (d, *J* = 7.9 Hz, 2H), 4.03 (s, 2H), 3.96 (s, 2H), 3.90 – 3.77 (m, 4H+2H), 3.56 (dd, *J* = 7.0, 4.7 Hz, 4H), 2.79 (t, *J* = 7.9 Hz, 4H+2H), 1.60 – 1.41 (m, 4H), 1.33 (d, *J* = 6.7 Hz, 6H). ^{13}C NMR (101 MHz, CDCl$_3$) δ 168.94 (C=O), 162.40 (C=O), 150.03 (C=O), 144.53 (CH uracil), 135.30 (Bz), 131.32 (ipso Bz), 130.52 (Bz), 129.26 (Bz), 102.21 (CH uracil), 94.63 (ipso Cp), 81.10 (ipso Cp), 70.93 (Fc), 68.39 (Fc), 65.98 (Fc), 60.21 (CH$_2$), 50.02 (CH$_2$), 43.13 (CH$_2$), 27.24 (CH$_2$), 26.84 (CH*), 19.67 (CH$_3$). MS (ES) (m/z) calcd for $C_{44}H_{46}N_4O_8Fe^{56}Na$ 837.2563, found 837.2559. IR (cm^{-1}): 3387 (OH), 3088 (=CH Fc), 2930 (CH$_2$), 2871 (CH$_2$), 1734 (C=C-C=O), 1693 (C=O), 1641 (amide), 1597 (C=N), 1439 (CH$_2$), 1348 (CH$_3$), 788 (CH Ar), 687 C=C). Mp 138 °C - 142 °C.

6.1.55. (*S,S,R_p,R_p*)-1,1'-Bis-[α-methyl-(3-(*tert*-butyldiphenylsilyl)propyl)]-2,2'-bis-[2-

(bromo)ethyl]-ferrocene **52**
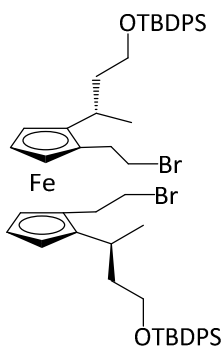
In a 100 mL schlenk tube, NBS (0.483 g, 2.714 mmol) was suspended in dry DCM. A DCM solution of triphenylphosphine (0.682 g, 2.533 mmol) was added drop wise to it. The resulting orange mixture was stirred for 5 min before addition of 0.109 mL (1.805 mmol) of pyridine. The mixture goes brown. **47** (0.405 g, 0.452 mmol) dissolved in 5 mL of dry DCM was added to the mixture. After overnight reaction, the solvent was removed *in vacuo* and the crude was purified via flash column chromatography (3% EtOAc in hexane) to yield the yellow-brown oily product (0.450 g, 97%). ^{1}H NMR (400 MHz, CDCl$_3$) δ 7.68 – 7.63 (m, 8H), 7.45 – 7.36 (m, 12H), 3.94 – 3.89 (m, 4H), 3.87 (t, *J* = 2.5 Hz, 2H), 3.66 – 3.58 (m, 4H), 3.46 – 3.33 (m, 4H), 2.95 – 2.78 (m, 4H), 2.71 – 2.63 (m, 2H), 1.68 – 1.60 (m, 2H), 1.38 – 1.22 (m, 2H), 1.22 (d, *J* = 6.8 Hz, 6H), 1.07 (s, 18H). ^{13}C NMR (101 MHz, CDCl$_3$) δ 135.61 (Ph), 133.91 (ipso Ph), 133.82 (ipso Ph), 129.62 (Ph), 127.67 (Ph), 94.43 (ipso Cp), 83.16 (ipso Cp), 70.18 (Fc), 67.42 (Fc), 66.15 (Fc), 61.72 (CH$_2$), 42.76 (CH$_2$), 31.63 (2xCH$_2$), 27.21 (CH*), 26.97 (tBu), 19.50 (CH$_3$), 19.22 (ipso tBu). MS (ES) (m/z) calcd for C$_{54}$H$_{68}$O$_2$^{56}FeSi$_2$^{79}Br^{81}BrNa 1020.2454, found 1020.2458. IR (cm^{-1}): 3070 (=CH Fc), 2958 (CH$_2$), 2930 (CH$_2$), 2856 (CH$_2$), 1589, 1575, 1472, 1427 (CH$_2$), 1235 (CH$_3$), 1105 (Si-OR), 1085 (Si-OR), 822 (CH Ar), 699 (C=C).

6.1.56. (*S,S,R*$_p$*,R*$_p$)-1,1'-Bis-[α-methyl-(3-(*tert*-butyldiphenylsilyl)propyl)]-2-2'-Bis-[2-((*N-4*-

benzoyl)-cytosin-1-yl)ethyl]-ferrocene **53**
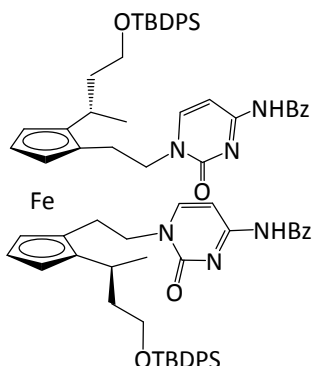
In a 50 mL schlenk tube, **21** (0.126 g, 0.588 mmol) was stirred vigorously in suspension in 2 mL of DMF for 5 min. NaH (0.014 g, 0.588 mmol) was added to the mixture in one portion and stirred for 1 h. At this point the solution was clear. **52** (0.2 g, 0.196 mmol) was dissolved in 1 mL of DMF and added to the mixture. After overnight stirring at 50 °C, the reaction was quenched with water, extracted with chloroform, dried on MgSO$_4$. The solvent was removed *in vacuo* and the crude was purified via flash column chromatography (2% MeOH in DCM) to yield product (0.039 g, 16%). ^{1}H NMR (400 MHz, CDCl$_3$) δ 8.71 (s, 2H), 7.90 (d, *J* = 7.7 Hz, 4H), 7.70 − 7.56 (m, 10H), 7.50 (t, *J* = 8.0 Hz, 4H), 7.44 − 7.29 (m, 14H), 7.20 (d, *J* = 7.0 Hz, 2H), 4.05 − 3.97 (m, 2H), 3.96 (s, 2H), 3.88 (s, 2H), 3.78 (s, 2H), 3.74 (m, 2H), 3.75 (t, *J* = 5.7 Hz, 4H), 2.82 (s, 2H), 2.72 − 2.59 (m, 4H), 1.67 − 1.42 (m, 2H), 1.25 (d, *J* = 6.9 Hz, 6H), 1.02 (s, 18H). ^{13}C NMR (101 MHz, CDCl$_3$) δ 166.19 (ipso C-N), 162.09 (C=O Bz), 155.49 (C=O cytosine), 149.11 (CH cytosine), 135.55 (Ph), 133.88 (ipso Ph), 133.81 (ipso Bz), 133.05 (Bz), 129.70 (Bz), 128.98 (Ph), 127.70 (Bz), 127.61 (Ph), 96.20 (CH cytosine), 94.67 (ipso Cp), 81.65 (ipso Cp), 70.59 (Fc), 68.19 (Fc), 66.55 (Fc), 61.99 (CH$_2$), 51.41 (CH$_2$), 42.68 (CH$_2$), 27.32 (CH*), 26.91 (tBu), 20.07 (CH$_3$), 19.20 (ipso tBu). MS (ES) (m/z) calcd for C$_{76}$H$_{85}$N$_6$O$_6$^{56}Fe 1289.5419, found 1289.5415 (M+H$^+$). IR (cm^{-1}): 3071 (=CH Fc), 2958 CH$_2$), 2930 (CH$_2$), 2856 (CH$_2$), 1661 (C=O), 1625 (C=N), 1552 (Amide), 1482 (C=N), 1427 (CH$_2$), 1361 (tBu), 1236 (Si-tBu), 1106 (Si-OR), 1086 (Si-OR), 822 (CH Ar), 700 (C=C). Mp 86 °C - 88 °C.

6.1.57. 1-Acyl-ferrocene **54**[5]
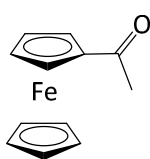
The compound was not synthesised but was recovered from previous work done within the group. It was characterised to check its purity. ^{1}H NMR (300 MHz, Chloroform-d) δ 4.81 – 4.74 (m, 2H), 4.54 – 4.48 (m, 2H), 4.21 (s, 5H), 2.40 (s, 3H). ^{13}C NMR (101 MHz, CDCl$_3$) δ 202.11 (C=O), 79.29 (ipso Cp), 72.35 (Fc), 69.88 (Fc), 69.62 (Fc), 27.45 (CH$_3$). Mp 82 °C - 86 °C. Characterisation data is in agreement with the literature data.

6.1.58. (*R*)-1-(α-Hydroxyethyl)-ferrocene **55**[2]
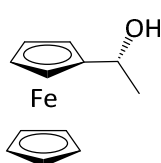
A solution of (S)-CBS (1.82 g, 6.57 mmol) in THF was cooled down to 0 °C under argon. To this solution, BH$_3$.SMe$_2$ (11.066 mL) was added in two steps. First, 2.2 mL were added to the mixture to form the catalyst system. The solution was stirred for 5-10 min. Then 8.85 mL of BH$_3$.SMe$_2$ were added simultaneously with a solution of ketone-ferrocene **54** (5 g, 21.9 mmol) in THF (50 mL) drop wise using a cannula. After 30 min of stirring at 0 °C, the excess of BH$_3$.SMe$_2$ was carefully quenched with MeOH (25 mL, gas evolution). The crude was poured into 100 mL of NH$_4^+$Cl$^-$, washed with ether, water, brine and dried on Na$_2$SO$_4$. The solvent was removed *in vacuo* and the crude was purified via flash column chromatography (75% Et$_2$O in hexane) to yield product (4.29 g, 85%). ^{1}H NMR (400 MHz, CDCl$_3$) δ 4.55 (q, *J* = 6.3 Hz, 1H), 4.22 (d, *J* = 5.3 Hz, 2H), 4.19 (s, 5H), 4.16 (t, *J* = 1.9 Hz, 2H), 1.44 (d, *J* = 6.4 Hz, 3H). ^{13}C NMR (101 MHz, CDCl$_3$) δ 94.82 (ipso Cp), 68.30 (Fc), 67.89 (Fc), 66.09 (Fc), 65.59 (C*H), 23.73 (CH$_3$). MS (ES) (m/z) calcd for C$_{12}$H$_{14}$O^{56}Fe 230.0394, found 230.0389. Mp melt at 82 °C - 84 °C. [α]$_D$ (c = 0.0053 g/mL, DCM)

= +21.9. Opposite enantiomer $[\alpha]_D$ (c = 0.0052 g/mL, DCM) = -22.3. Characterisation data is in agreement with the literature data.

6.1.59. (R)-1-(α-Acetoxyethyl)-ferrocene **56**[2]
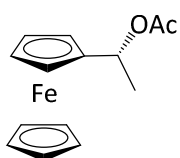
The diol **55** (5.49 g, 23.8 mmol) was dissolved in dry DCM (60 mL) and stirred for 5 min. Then 3.37 mL (3.65 g, 35.8 mmol) of acetic anhydride, 4.99 mL (3.62 g, 35.8 mmol) of TEA and catalytic amount of DMAP were added successively. The reaction was stirred at room temperature overnight. After completion of the reaction, it was quenched with NaHCO$_3$ (50 mL) and extracted with DCM. The aqueous layer was washed with DCM (60 mL x 3) and then dried on Mg$_2$SO$_4$ and evaporated. The solvent was removed *in vacuo* and the crude was purified via flash column chromatography (25% EtOAc in hexane) to yield the yellow-orange product (5.61 g, 86%). ^{1}H NMR (400 MHz, CDCl$_3$) δ 5.83 (q, *J* = 6.5 Hz, 1H), 4.26 (dt, *J* = 2.7, 1.4 Hz, 1H), 4.22 (dt, *J* = 2.7, 1.5 Hz, 1H), 4.18 − 4.13 (m, 5H+2H), 2.03 (s, 3H), 1.56 (d, *J* = 6.6 Hz, 3H). ^{13}C NMR (101 MHz, CDCl$_3$) δ 170.51 (C=O), 87.92 (ipso Cp), 68.91 (Fc), 68.73 (Fc), 68.39 (Fc), 68.34 (Fc), 67.99 (Fc), 66.00 (CH*), 21.43 (CH$_3$), 19.99 (CH$_3$). MS (ES) (m/z) calcd for C$_{14}$H$_{16}$O$_2$^{56}Fe 272.0500, found 272.0497. IR (cm^{-1}): 3087 (=C-H), 2998 (CH$_2$), 2982 (CH$_2$), 2940 (CH$_2$), 1724 (C=O), 1441 (CH$_3$), 1366 (ester), 825 (CH=CH), 722 (CH Ar). Mp 76 °C - 78 °C. $[\alpha]_D$ (c = 0.0064 g/mL, DCM) = +41.3. Opposite enantiomer $[\alpha]_D$ (c = 0.0066 g/mL, DCM) = -38.2. Characterisation data is in agreement with the literature data.

6.1.60. (*R*)-1-(α-*N,N*-Dimethylaminoethyl)-ferrocene **57**[2]
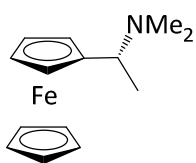
The (ethylacetate)-ferrocene **56** (5.61 g, 20.6 mmol) was dissolved in 40 mL of MeOH. 37.86 mL of dimethylamine were added and the mixture was stirred overnight at room temperature. The reaction was quenched with 20 mL of water and extracted with DCM (40 mL x 3), dried on $MgSO_4$ and evaporated. The solvent was removed *in vacuo* and the crude was purified via flash column chromatography (5% MeOH, 5% TEA in DCM) to yield a brown-orange oil (4.027 g; 76%). ^{1}H NMR (400 MHz, $CDCl_3$) δ 4.15 − 4.09 (m, 9H), 3.59 (q, *J* = 6.9 Hz, 1H), 2.08 (s, 6H), 1.45 (d, *J* = 6.8 Hz, 3H). ^{13}C NMR (101 MHz, $CDCl_3$) δ 87.28 (ipso Cp), 69.36 (Fc), 68.57 (Fc), 67.33 (Fc), 67.19 (Fc), 66.87 (Fc), 58.64 (CH*), 40.72 (NCH_3), 16.11 (CH_3). IR (cm^{-1}): 3426 (amine), 3082 (=C-H), 2990 (CH_2), 2930 (CH_2), 1461 (CH_3), 1381 (CH_3), 819 (CH=CH). MS (ES) (m/z) calcd for $C_{14}H_{19}N^{56}Fe$ 257.0867, found 257.0857. Mp 120 °C - 122 °C. Characterisation data is in agreement with the literature data.

6.1.61. Side product: (*R*)-1-(α-Methoxyethyl)-ferrocene **57a**[20]
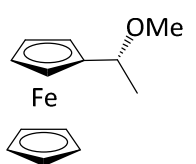
^{1}H NMR (400 MHz, Chloroform-d) δ 4.23 − 4.16 (m, 4H), 4.12 (s, 6H), 3.24 (s, 3H), 1.53 (d, *J* = 6.6 Hz, 3H). ^{13}C NMR (101 MHz, $CDCl_3$) δ 89.12 (ipso Cp), 74.97 (Fc), 68.66 (Fc), 68.01 (Fc), 67.72 (Fc), 65.81 (CH*), 55.71 (CH_3), 20.16 (CH_3). Characterisation data is in agreement with the literature data.

6.1.62. (R,S$_p$)-1-(α-N,N-Dimethylaminoethyl)-2-iodo-ferrocene 58
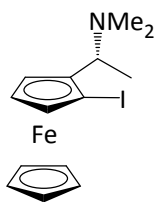
In a 200 mL schlenk tube, **57** (4 g, 15 mmol) was dissolved in Et$_2$O (50 mL) at room temperature, n-BuLi (12 mL, 30 mmol) was added to the mixture at that temperature and stirred overnight under an inert atmosphere. The reaction mixture was cooled to -78 °C and Iodine (9.52 g, 37.5 mmol) dissolved in THF (60 mL) was added over the course of 10 min. The reaction was stirred at -78 °C for 90 min before allowing to warm to room temperature, at which point it was allowed to stirred for an additional 90 min before quenching at 0 °C with sodium thiosulfate$_{(aq)}$ (50 mL, 25% w/v). Dilute with Et$_2$O (30 mL), the layers were separated and the aqueous layer was further extracted with ether (50 mL x 3). The combined organic fractions were dried over MgSO$_4$ solvent remove *in vacuo* and purified via flash column chromatography (5% MeOH, 5% TEA in DCM) to yield product (3.18 g, 55%). ^{1}H NMR (400 MHz, CDCl$_3$) δ 4.46 (dd, J = 2.4, 1.4 Hz, 1H), 4.24 (t, J = 2.6 Hz, 1H), 4.15 (dd, J = 2.7, 1.3 Hz, 1H), 4.12 (s, 5H), 3.62 (q, J = 6.8 Hz, 1H), 2.15 (s, 6H), 1.50 (d, J = 6.8 Hz, 3H). ^{13}C NMR (101 MHz, CDCl$_3$) δ 90.21 (ipso Cp), 74.32 (Fc), 71.67 (Fc), 68.19 (Fc), 65.59 (Fc), 57.59 (CH*), 45.49 (ipso Cp), 41.22 (CH$_3$), 16.01 (CH$_3$). MS (ES) (m/z) calcd for C$_{14}$H$_{18}$N^{56}FeI 382.9833, found 382.9820. IR (cm^{-1}): 3078 (=C-H), 2931 (CH$_2$), 2878 (CH$_2$), 2809 (CH$_2$), 1446 (CH$_3$), 1371 (CH$_3$), 1243, 1087, 821 (CH=CH), 732 (CH Ar). Mp 58 °C - 60 °C. [α]$_D$ (c = 0.0022 g/mL, DCM) = +7.3.

6.1.63. Side product: (S_p)-1-Vinyl-2-idodo-ferrocene **58a**
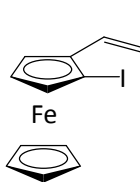
^{1}H NMR (400 MHz, CDCl$_3$) δ 6.54 (dd, J = 17.5, 10.8 Hz, 1H), 5.46 (dd, J = 17.5, 1.5 Hz, 1H), 5.18 (dd, J = 10.8, 1.5 Hz, 1H), 4.52 (dd, J = 2.7, 1.4 Hz, 1H), 4.50 (dd, J = 2.5, 1.4 Hz, 1H), 4.31 (td, J = 2.6, 0.6 Hz, 1H), 4.11 (s, 4H). ^{13}C NMR (101 MHz, CDCl$_3$) δ 134.13 (CH vinyl), 113.13 (CH$_2$ vinyl), 84.16 (ipso Cp), 75.26 (Fc), 72.26 (Fc), 69.43 (Fc), 63.70 (Fc), 44.82 (ipso Cp). MS (ES) (m/z) calcd for C$_{12}$H$_{11}$^{56}FeI 337.9255, found 337.9252. IR (cm^{-1}): 3085 (=C-H), 2954 (CH$_2$), 2922 (CH$_2$), 2851 (CH$_2$), 1628 (C=C), 820 (CH=CH), 715 (CH Ar), 644.

6.1.64. (R,S_p)-1-(α-Acetoxyethyl)-2-iodo-ferrocene **59**
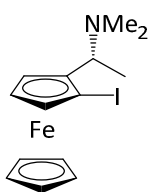
In a 100 mL schlenk tube, **58** (3.26 g, 8.51 mmol) and acetic anhydride (25.68 mL, 272.17 mmol) were heated at 50 °C under inert atmosphere for 2 h. The excess acetic anhydrides were removed under high vacuum (0.1 mmHg). Purified via flash column chromatography (10% EtOAc in hexane) to yield the yellow-brown oily product (2.94 g, 87%). ^{1}H NMR (400 MHz, CDCl$_3$) δ 5.89 (q, J = 6.4 Hz, 1H), 4.51 (dd, J = 2.6, 1.4 Hz, 1H), 4.33 (dd, J = 2.8, 1.4 Hz, 1H), 4.28 (t, J = 2.6 Hz, 1H), 4.15 (s, 5H), 2.01 (s, 3H), 1.66 (d, J = 6.5 Hz, 3H). ^{13}C NMR (101 MHz, CDCl$_3$) δ 170.30 (C=O), 87.54 (ipso Cp), 75.63 (Fc), 71.76 (Fc), 69.71 (Fc), 68.94 (Fc), 65.80 (CH*), 44.03 (ipso Cp), 21.16 (CH$_3$), 18.66 (CH$_3$). IR (cm^{-1}): 3095 (=C-H), 2972 (CH$_2$), 2928 (CH$_2$), 2866 (CH$_2$), 1729 (C=O), 1445 (CH$_3$), 1371 (CH$_3$), 1085, 820 (CH=CH), 703 (CH Ar). [α]$_D$ (c = 0.0086 g/mL, DCM) = -38.1.

6.1.65. (*R,S$_p$*)-1-(α-Hydroxyethyl)-2-iodo-ferrocene **60**
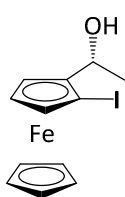
In a 200 mL round bottom flask **59** (2.937 g, 7.37 mmol) was dissolved in EtOH (35 mL). NaOH$_{(aq)}$ (30 mL, 10% w/v) was added and the reaction was heated at 95 °C for 15 min. The reaction was allowed to cool to room temperature and organic layer was extracted with EtOAc (40 mL x 2). The organic layers were dried over Na$_2$SO$_4$, solvent removed *in vacuo* and purified via flash column chromatography (25% EtOAc in hexane) to yield the yellow oily product (2.43 g, 92%) ^{1}H NMR (400 MHz, CDCl$_3$) δ 4.85 (qd, *J* = 6.5, 2.8 Hz, 1H), 4.46 (dd, *J* = 2.5, 1.4 Hz, 1H), 4.29 (dd, *J* = 2.7, 1.3 Hz, 1H), 4.25 (t, *J* = 2.6 Hz, 1H), 4.14 (s, 5H), 1.88 (d, *J* = 3.6 Hz, 1H), 1.62 (d, *J* = 6.5 Hz, 3H). ^{13}C NMR (101 MHz, CDCl$_3$) δ 91.61 (ipso Cp), 75.01 (Fc), 71.59 (Fc), 68.72 (Fc), 66.51 (Fc), 64.98 (CH*), 43.62 (ipso Cp), 21.31 (CH$_3$). MS (ES) (m/z) calcd for C$_{12}$H$_{13}$O^{56}FeI 355.9361, found 355.9352. IR (cm^{-1}): 3255 (OH), 3093 (=C-H), 2967 (CH$_2$), 2920 (CH$_2$), 1445 (CH$_3$), 1369 (CH$_3$), 1099 (C-OH), 816 (CH=CH), 684 (CH=CH). [α]$_D$ (c = 0.002 g/mL, DCM) = +12.0. Opposite enantiomer [α]$_D$ (c = 0.006 g/mL, DCM) = -24.7.

6.1.66. (*R,S$_p$*)-1-(α-Methoxyethyl)-2-iodo-ferrocene **61**
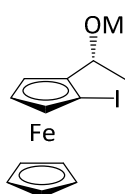
In a 100 mL round bottom flask, **60** (2.43 g, 6.826 mmol) was dissolved in a MeOH/AcOH (20 mL, 9:1) mixture and the reaction was stirred at room temperature for 48 h. The reaction was quenched with water (10 mL) and extract with DCM (2×20 mL). The combined organic fractions were dried over MgSO$_4$, solvent removed *in vacuo* and purified via flash column chromatography (25% EtOAc in hexane) to yield the yellow oily product (2.37 g, 94%). ^{1}H NMR (400 MHz, CDCl$_3$) δ 4.49 (dd, *J*

= 2.4, 1.4 Hz, 1H), 4.34 (q, J = 6.5 Hz, 1H), 4.29 – 4.25 (m, 2H), 4.13 (s, 5H), 3.26 (s, 3H), 1.64

(d, J = 6.5 Hz, 3H). ^{13}C NMR (101 MHz, CDCl$_3$) δ 89.78 (ipso Cp), 74.78 (Fc), 74.22 (Fc), 71.66

(Fc), 68.86 (Fc), 65.35 (CH*), 56.00 (CH$_3$), 39.48 (ipso Cp), 19.63 (CH$_3$). MS (ES) (m/z) calcd for

C$_{13}$H$_{15}$O^{56}FeI 369.9517, found 369.9513. IR (cm^{-1}): 3094 (=C-H), 2974 (CH$_2$), 2926 (CH$_2$), 2871

(CH$_2$), 2815 (CH$_2$), 1448 (CH$_3$), 1371 (CH$_3$), 1085 (C-O-C), 820 (CH=CH). [α]$_D$ (c = 0.0048 g/mL,

DCM) = -16.7. Opposite enantiomer [α]$_D$ (c = 0.003 g/mL, DCM) = +33.3.

6.1.67. (S,S_p)-1-[α-Methyl(2-ethylpropanoate)]-2-iodo-ferrocene 62
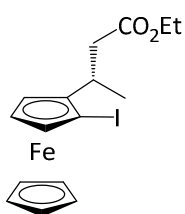
In a 250 mL schlenk tube, **61** (2.37 g, 6.42 mmol) and 1-ethoxyvinyloxytrimethylsilane **38** (8.234 g, 51.37 mmol) were dissolved in DCM (30 mL). The mixture was cooled to -78 °C and BF$_3$.OEt$_2$ (1.774 mL, 14.12 mmol) was added drop wise. The reaction mixture was stirred for 15

min at -78 °C before allowing to be warmed to room temperature. Quenched with saturated

NaHCO$_3$ (40 mL), the organic layer was separated and the aqueous layer was further

extracted with DCM (40 mL). The combined organic fractions were dried over MgSO$_4$,

solvent removed *in vacuo* and purified via flash column chromatography (10% EtOAc in

hexane) to yield the yellow oily product (1.676 g, 61%). ^{1}H NMR (400 MHz, CDCl$_3$) δ 4.42 (dd,

J = 2.4, 1.4 Hz, 1H), 4.18 – 4.08 (m, 8H+2H), 3.14 – 3.05 (m, 1H), 2.53 (dd, J = 15.0, 3.7 Hz,

1H), 2.11 (dd, J = 15.0, 10.3 Hz, 1H), 1.43 (d, J = 6.9 Hz, 3H), 1.25 (t, J = 7.2 Hz, 3H). ^{13}C NMR

(101 MHz, CDCl$_3$) δ 172.00 (C=O), 94.07 (ipso Cp), 74.12 (Fc), 71.52 (Fc), 67.84 (Fc), 64.58

(Fc), 60.26 (CH$_2$), 44.08 (ipso Cp), 43.19 (CH$_2$), 30.72 (CH*), 18.90 (CH$_3$), 14.27 (CH$_3$). MS (ES)

(m/z) calcd for C$_{16}$H$_{19}$O$_2$^{56}FeI 425.9779, found 425.9782.

6.1.68. (*S*,*S*ₚ)-1-[α-Methyl-(3-(hydroxyl)propyl)]-2-iodo-ferrocene **63**
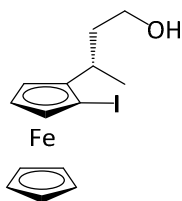
In a 100 mL schlenk tube **62** (1.592 g, 3.73 mmol) was dissolved in Et₂O (50 mL), cooled to 0 °C and stand for 5 min. Diisobutylalumminum hydride (11.2 mL, 11.2 mmol) was added to the reaction slowly at that temperature. The reaction was allowed to stir at 0 °C for 1 h before quenched with aqueous sodium potassium tartrate (30 mL). The layers were separated and the aqueous layer was further extract with Et₂O (30 mL). The combined organic fractions were dried over Na₂SO₄, solvent remove *in vacuo* and purified via flash column chromatography (50% EtOAc in hexane) to yield product (1.413 g, 99%). ¹H NMR (400 MHz, CDCl₃) δ 4.42 (dd, *J* = 2.4, 1.4 Hz, 1H), 4.17 (td, *J* = 2.6, 0.6 Hz, 1H), 4.13 (s, 5H), 4.06 (dd, *J* = 2.7, 1.3 Hz, 1H), 3.59 (t, *J* = 6.6 Hz, 2H), 2.78 – 2.69 (m, 1H), 1.72 – 1.52 (m, 2H), 1.41 (d, *J* = 7.0 Hz, 3H). ¹³C NMR (101 MHz, CDCl₃) δ 95.87 (ipso Cp), 73.76 (Fc), 71.47 (Fc), 67.87 (Fc), 64.18 (Fc), 60.84 (CH₂), 44.73 (ipso Cp), 42.09 (CH₂), 29.81 (CH*), 19.69 (CH₃). MS (ES) (m/z) calcd for C₁₄H₁₇O⁵⁶FeI 383.9674, found 383.9678. IR (cm⁻¹): 3282 br (OH), 3088 (=CH Fc), 2971 (CH₂), 2932 (CH₂), 2854 (CH₂), 1556, 1452 (CH₂), 1376 (CH₃), 680 (C=C). Mp 96 °C - 98 °C. [α]D (c = 0.0083 g/mL, DCM) = +16.9.

6.1.69. (*S*,*S*ₚ)-1-[α-Methyl-(3-(*tert*-butyldiphenylsilyloxy)propyl)]-2-iodo-ferrocene **64**
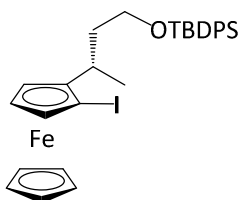
In a 100 mL schlenk tube **63** (1.413 g, 3.67 mmol) was dissolved in 20 mL DCM at room temperature. TEA (0.769 mL, 5.52 mmol), *tert*-Butyldiphenylsilyl chloride (1.435 mL, 5.51 mmol) and DMAP in catalytic amount were added successively to the mixture. The solution was stirred overnight at room temperature and quenched with water. The phrases were separated and the aqueous layer was extracted with further Et₂O. The combined ethereal fractions were dried over Na₂SO₄,

solvent removed *in vacuo* and purified via flash column chromatography (10% EtOAc in hexane) to yield a yellow oily product (2 g, 95%). ^{1}H NMR (400 MHz, CDCl$_3$) δ 7.70 – 7.65 (m, 4H), 7.43 – 7.32 (m, 6H), 4.38 (dd, *J* = 2.4, 1.3 Hz, 1H), 4.10 (s, 5H+1H), 4.00 (dd, *J* = 2.7, 1.3 Hz, 1H), 3.70 – 3.65 (m, 2H), 2.77 – 2.68 (m, 1H), 1.88 – 1.80 (m, 1H), 1.43 – 1.34 (m, 1H), 1.31 (d, *J* = 6.9 Hz, 3H), 1.05 (s, 9H). ^{13}C NMR (101 MHz, CDCl$_3$) δ 135.63 (Ph), 134.10 (ipso Ph), 134.05 (ipso Ph), 129.47 (Ph), 127.58 (Ph), 96.25 (ipso Cp), 73.81 (Fc), 71.38 (Fc), 67.61 (Fc), 64.27(Fc), 62.10 (CH$_2$), 44.45 (ipso Cp), 41.60 (CH$_2$), 30.03 (CH*), 26.94 (tBu), 19.24 (ipso tBu), 18.91 (CH$_3$). MS (ES) (m/z) calcd for C$_{30}$H$_{35}$O^{56}FeISiNa 622.0851, found 622.0846. IR (cm^{-1}): 3071 (=CH Fc), 2958 (CH$_2$), 2929 (CH$_2$), 2856 (CH$_2$), 1472 (CH$_2$), 1387 (CH$_3$), 1361, 1106, 1085, 821 (CH Ar TBDPS), 700 (C=C). [α]$_D$ (c = 0.008 g/mL, DCM) = -5.5.

6.1.70. (*S,S$_p$*)-1-[α-Methyl-(3-(*tert*-butyldiphenylsilyloxy)propyl)]-2-aldehyde-ferrocene 65
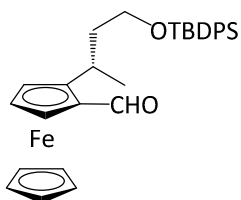
In a 100 mL schlenk tube **64** (2.182 g, 3.505 mmol) was dissolved in Et$_2$O (30 mL), the mixture was cooled to -78 °C and *n*-BuLi (2.32 mL, 7.011 mmol) was added. After 30 min, DMF (0.675 mL, 8.764 mmol) was added and the reaction was stirred at -78 °C for another 30 min before allowing too warm to room temperature, and then quenched with water (20 mL). The phases were separated and the aqueous layer was extracted with Et$_2$O (20 mL). The combined ethereal fractions were dried over Na$_2$SO$_4$, solvent removed *in vacuo* and purified via flash column chromatography (10% EtOAc in hexane) to yield the red oily product (1.686 g, 92%). ^{1}H NMR (400 MHz, CDCl$_3$) δ 10.11 (s, 1H), 7.68 – 7.59 (m, 4H), 7.42 – 7.33 (m, 6H), 4.75 (dd, *J* = 2.7, 1.4 Hz, 1H), 4.48 (t, *J* = 2.6 Hz, 1H), 4.43 (dd, *J* = 2.6, 1.4 Hz, 1H), 4.21 (s, 5H), 3.61 (t, *J* = 7.1, 2H), 3.21 – 3.10 (m,

1H), 1.73 – 1.50 (m, 2H), 1.34 (d, J = 6.9 Hz, 3H), 1.04 (s, 9H). ^{13}C NMR (101 MHz, CDCl$_3$) δ

193.25 (C=O), 135.55 (Ph), 133.94 (ipso Ph), 133.80 (ipso Ph), 129.55 (Ph), 127.61 (Ph), 99.14

(ipso Cp), 76.31 (ipso Cp), 71.04 (Fc), 70.80 (Fc), 70.03 (Fc), 68.89 (Fc), 61.75 (CH$_2$), 43.28

(CH$_2$), 27.90 (CH*)**,** 26.89 (tBu), 22.66 (ipso tBu), 19.17 (CH$_3$). MS (ES) (m/z) calcd for

C$_{31}$H$_{36}$O$_2$^{56}FeSiNa 547.1732, found 547.1727. IR (cm^{-1}): 3071 (=CH Fc), 2958 (CH$_2$), 2929 (CH$_2$),

2856 (CH$_2$), 1673 (C=O), 1589 (C=N), 1427 (CH$_2$), 1376 (tBu), 1106 (Si-OR), 1086 (Si-OR), 821

(CH Ar Ph), 700 (C=C).

6.1.71. (S,R_p)-1-[α-Methyl-(3-(*tert*-butyldiphenylsilyloxy)propyl)]-2-vinyl-ferrocene 66
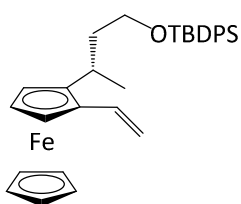
In a 100 mL schlenk tube, trimethylmethylphosphonium bromide (1.722

g, 4.821 mmol), potassium tert-butoxide (0.541 g, 4.821 mmol) and a

catalytic amount of dibenzo-18-crown-6-ether were dissolved in 20 mL

of dry THF. The mixture was stirred for 30 min and **65** (1.686 g, 3.214 mmol) was dissolved in

30 mL of dry THF and added to the mixture. The reaction was stirred overnight at room

temperature, quenched with water and extracted with Et$_2$O (20 mL). The combined ethereal

fractions were dried over Na$_2$SO$_4$, solvent removed *in vacuo* and purified via flash column

chromatography (5% EtOAc in hexane) to yield the yellow oily product (1.497 g, 89%). ^{1}H

NMR (400 MHz, CDCl$_3$) δ 7.69 – 7.63 (m, 4H), 7.44 – 7.33 (m, 6H), 6.62 (dd, J = 17.4, 10.8 Hz,

1H), 5.34 (dd, J = 17.5, 1.8 Hz, 1H), 5.01 (dd, J = 10.8, 1.7 Hz, 1H), 4.43 (dd, J = 2.5, 1.4 Hz,

1H), 4.12 (t, J = 2.6 Hz, 1H), 4.06 (dd, J = 2.5, 1.4 Hz, 1H), 4.03 (s, 5H), 3.62 (dd, J = 7.2, 5.4 Hz,

2H), 2.94 – 2.86 (m, 1H), 1.72 – 1.61 (m, 1H), 1.45 – 1.37 (m, 1H), 1.30 (d, J = 6.8 Hz, 3H), 1.06

(s, 9H). ^{13}C NMR (101 MHz, CDCl$_3$) δ 135.59 (Ph), 134.08 (ipso Ph), 134.02 (ipso Ph), 133.50

(CH vinyl), 129.49 (Ph), 127.56 (Ph), 110.96 (CH_2 vinyl), 94.84 (ipso Cp), 81.37 (ipso Cp), 69.66 (Fc), 66.55 (Fc), 66.27 (Fc), 64.08 (Fc), 61.89 (CH_2), 42.80 (CH_2), 27.65 (CH*), 26.89 (tBu), 19.23 (ipso tBu), 18.92 (CH_3). MS (ES) (m/z) calcd for $C_{32}H_{38}O^{56}FeSi$ 522.2041, found 522.2055. IR (cm^{-1}): 3072 (=CH Fc), 2958 (CH_2) 2930 (CH_2), 2857 (CH_2), 1625 (Ar Ph), 1589, 1427 (CH_2), 1388 (CH_3), 1105 (Si-OR), 1086 (Si-OR), 821 (CH Ar), 699 (vinyl/C=C).

6.1.72. (S,R_p)-1-[α-Methyl-(3-(*tert*-butyldiphenylsilyloxy)propyl)]-2-[2-(hydroxyl)ethyl]-

ferrocene **67**
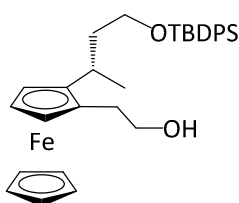
In a 100 mL schlenk tube, **66** (1.497 g, 2.865 mmol) was dissolved in 30 mL of dry THF. BH_3,THF (8.186 mL, 0.818 mmol) was then added drop wise at room temperature and stirred for 2 h. 9.762 mL of EtOH, 9.762 mL of NaOH (3M) and 7.174 mL of H_2O_2 (30%) were then successively added to the reaction and stirred for 1 h at room temperature. The reaction was extracted with DCM, washed with brine and dried over Na_2SO_4, solvent removed *in vacuo* and purified via flash column chromatography (10% EtOAc in hexane) to yield the yellow oily product (1.434 g, 97%). ^{1}H NMR (400 MHz, CDCl$_3$) δ 7.68 − 7.64 (m, 4H), 7.43 − 7.36 (m, 6H), 4.11 − 4.09 (m, 1H), 4.05 (s, 5H), 4.00 (t, *J* = 2.5 Hz, 1H), 3.97 (dd, *J* = 2.5, 1.3 Hz, 1H), 3.75 (tq, *J* = 6.8, 2.6 Hz, 2H), 3.67 − 3.63 (m, 2H), 2.77 − 2.68 (m, 1H), 2.66 − 2.49 (m, 2H), 1.74 − 1.66 (m, 1H), 1.43 − 1.32 (m, 1H), 1.26 (d, *J* = 6.8 Hz, 3H), 1.06 (s, 9H). ^{13}C NMR (101 MHz, CDCl$_3$) δ 135.56 (Ph), 133.96 (ipso Ph), 129.59 (Ph), 127.63 (Ph), 95.01 (ipso Cp), 82.31 (ipso Cp), 69.03 (Fc), 67.36 (Fc), 65.39 (Fc), 65.15 (Fc), 63.00 (CH_2), 61.98 (CH_2), 42.43 (CH_2), 30.93 (CH_2), 27.51 (CH*), 26.91 (tBu), 19.37 (CH_3), 19.22 (ipso tBu). MS (ES) (m/z) calcd for $C_{32}H_{40}O_2^{56}FeSiNa$ 563.2045, found

563.2039. IR (cm^{-1}): 3378 br (OH), 3072 (=CH Fc), 2930 (CH$_2$), 2857 (CH$_2$), 1589, 1472 (CH$_3$), 1427 (CH$_2$), 1388 (tBu), 1361, 1105 (Si-OR), 1086 (Si-OR), 819 (CH Ar Ph), 705 (C=C). [α]$_D$ (c = 0.0056 g/mL, DCM) = -11.4. Opposite enantiomer [α]$_D$ (c = 0.0058 g/mL, DCM) = +23.5.

6.1.73. (*S*,*R$_p$*)-1-[α-Methyl-(3-(*tert*-butyldiphenylsilyl)propyl)]-2-[2-((*N*,*N*-6-dibenzoyl)-adenin-9-yl)ethyl]-ferrocene **68**
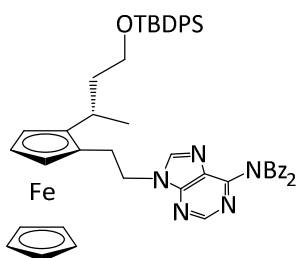
In a 50 mL schlenk tube, triphenylphosphine (0.291 g, 1.109 mmol) and **19** (0.381 g, 1.109 mmol) were dissolved in dry THF and stirred for 10 min at room temperature. **67** (0.300 g, 0.555 mmol) was then added to the mixture pre-dissolved in 5 mL of dry THF. The schlenk tube was then covered with foil and DIAD (0.244 mL, 1.109 mmol) was added at room temperature before the mixture was warmed up to 65 °C for 2 h. The reaction was evaporated, extracted with EtOAc, washed with brine followed by water and dried over Na$_2$SO$_4$, solvent removed *in vacuo* and purified via flash column chromatography (30% EtOAc in hexane) to yield product (0.343 g, 72%). ^{1}H NMR (400 MHz, CDCl$_3$) δ 8.64 (s, 1H), 7.89 − 7.85 (m, 4H), 7.80 (s, 1H), 7.63 − 7.58 (m, 4H), 7.50 − 7.44 (m, 2H), 7.37 − 7.27 (m, 6H+4H), 4.38 − 4.21 (m, 2H), 4.06 (s, 5H), 3.98 (dd, *J* = 2.4, 1.3 Hz, 1H), 3.96 (t, *J* = 2.5 Hz, 1H), 3.69 − 3.63 (m, 2H+1H), 2.96 − 2.80 (m, 2H), 2.76 − 2.68 (m, 1H), 1.68 − 1.61 (m, 1H), 1.49 − 1.41 (m, 1H), 1.28 (d, *J* = 6.7 Hz, 3H), 1.00 (s, 9H). ^{13}C NMR (101 MHz, CDCl$_3$) δ 172.27 (C=O), 153.19 (ipso adenine), 152.15 (CH adenine), 151.63 (ipso adenine), 144.97 (CH adenine), 135.55 (Ph), 134.21 (ipso Bz), 133.75 (ipso adenine), 132.88 (Bz), 129.64 (Ph), 129.46 (Bz), 128.66 (Bz), 127.64 (Ph), 94.99 (ipso Cp), 80.88 (ipso Cp), 69.12 (Fc), 67.09 (Fc), 65.86 (Fc),

65.55 (Fc), 61.96 (CH_2), 44.71 (CH_2), 42.77 (CH_2), 28.52 (CH_2), 27.53 (CH*), 26.84 (tBu), 19.68 (CH_3), 19.16 (ipso tBu). MS (ES) (m/z) calcd for $C_{51}H_{51}N_5O_3{}^{56}FeSiNa$ 888.3008, found 888.3015. IR (cm^{-1}): 3264 (OH), 3074 (=CH Fc), 2930 (CH_2), 2871 (CH_2), 1697 (C=O), 1603 (C=C), 1579, 1450, 1242, 1104, 1091, 821, 705 (C=C). Mp 86 °C - 88 °C. $[\alpha]_D$ (c = 0.0056 g/mL, DCM) = -36.4.

6.1.74. (S,R_p)-1-[α-methyl-(3-(hydroxy)propyl)]-2-[2-((N-6-benzoyl)-adenin-9-yl)ethyl]-ferrocene 69
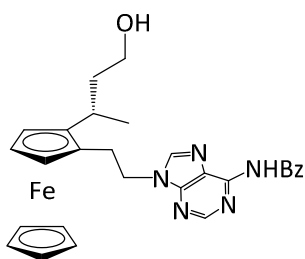
In a 50 mL schlenk tube, **68** (0.3 g, 0.346 mmol) was dissolved in 5 mL of dry THF and tetra-Butylamino fluoride (0.328 g, 1.039 mmol) was added to the solution. After overnight stirring, the reaction was quenched with water, extracted with DCM, washed with brine, water and dried over Na_2SO_4. The solvent was removed *in vacuo* and the crude was purified via flash column chromatography (3% MeOH in DCM) to yield product (0.146 g, 80%). ^{1}H NMR (400 MHz, $CDCl_3$) δ 9.11 (s, 1H), 8.81 (s, 1H), 8.03 (d, J = 7.2 Hz, 2H), 8.00 (s, 1H), 7.60 (t, J = 7.5 Hz, 1H), 7.52 (t, J = 7.9 Hz, 2H), 4.41 − 4.36 (m, 2H), 4.08 (s, 5H), 4.07 − 4.04 (m, 2H), 4.01 (t, J = 1.7 Hz, 1H), 3.65 − 3.61 (m, 2H), 3.10 − 2.89 (m, 2H), 2.88 − 2.83 (m, 1H), 1.64 − 1.48 (m, 2H), 1.39 (d, J = 6.8 Hz, 3H). ^{13}C NMR (101 MHz, $CDCl_3$) δ 164.62 (C=O), 152.54 (CH adenine), 151.78 (ipso adenine), 149.60 (ipso adenine), 143.08 (CH adenine), 133.60 (ipso Ph), 132.80 (Bz), 128.86 (Bz), 127.89 (Bz), 123.03 (ipso adenine), 95.14 (ipso Cp), 80.75 (ipso Cp), 69.29 (Fc), 67.55 (Fc), 66.13 (Fc), 65.42 (Fc), 60.11 (CH_2), 45.10 (CH_2), 43.26 (CH_2), 29.30 (CH_2), 27.04 (CH*), 19.88 (CH_3). MS (ES) (m/z) calcd for $C_{28}H_{29}N_5O_2{}^{56}FeNa$ 546.1568, found 546.1570. IR (cm^{-1}): 3264 br (OH), 3074 (=CH Fc), 2930 (CH_2), 2871 (CH_2), 1697 (C=O), 1603

(Amide), 1579 (C=N), 1452 (CH$_3$), 796 (CH Ar Bz), 705 (C=C). Mp: 104 °C − 106 °C. [α]$_D$ (c = 0.0044 g/mL, DCM) = -40.9.

6.1.75. (*S,R$_p$*)-1-[α-Methyl-(3-(hydroxy)propyl)]-2-[2-(-adenin-9-yl)ethyl]-ferrocene **70**
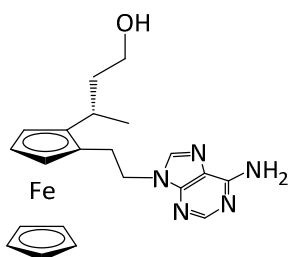
69 (0.043 g, 0.082 mmol) was dissolved in 2 mL of methylamine. The mixture was stirred at room temperature for half an hour under argon. The methylamine was evaporated. The crude was purified via flash column chromatography (5% MeOH in DCM) to yield product.

A yellow solid was obtained (0.025 g, 73%). ^{1}H NMR (400 MHz, DMSO-d6) δ 8.19 (s, 1H), 8.17 (s, 1H), 7.21 (s, 2H), 4.41 − 4.33 (m, 2H+1H (OH)), 4.11 (s, 5H), 4.02 (d, *J* = 2.4 Hz, 2H), 3.99 (t, *J* = 2.4 Hz, 1H), 3.42 − 3.28 (m, 2H), 2.97 − 2.75 (m, 2H), 2.75 − 2.67 (m, 1H), 1.53 − 1.45 (m, 1H), 1.32 (d, *J* = 6.8 Hz, 3H+1H). ^{13}C NMR (101 MHz, DMSO-d6) δ 155.95 (ipso adenine), 152.43 (CH adenine), 149.39 (ipso adenine), 140.71 (CH adenine), 118.75 (ipso adenine), 94.43 (ipso Cp), 81.89 (ipso Cp), 68.80, 66.46, 64.92, 64.74, 58.66, 43.10, 42.43, 27.98, 27.10 (CH*), 19.38 (CH$_3$). MS (ES) (m/z) calcd for C$_{21}$H$_{26}$N$_5$O[56]Fe 420.1487, found 420.1484. IR (cm^{-1}): 3348 br (OH), 3270 (NH$_2$), 3240 (NH$_2$), 3098 (=CH Fc), 2955 (CH$_2$), 2926 (CH$_2$), 2871 (CH$_2$), 1674 (C=N), 1604 (NH$_2$), 1574 (NH$_2$), 1305 (OH), 1076 (C-O), 814 (CH Ar). Mp 90 °C - 92 °C.

^{1}H NMR with addition of D$_2$O: ^{1}H NMR (300 MHz, DMSO-d6) δ 8.18 (s, 1H), 8.16 (s, 1H), 7.22 (s, 0.5H disappearing with D$_2$O), 4.37 (dd, *J* = 8.7, 7.1 Hz, 2H), 4.10 (s, 5H), 4.01 (d, *J* = 2.4 Hz, 2H), 3.99 − 3.96 (m, 1H), 3.40 − 3.28 (m, 2H), 2.95 − 2.73 (m, 2H), 2.72 − 2.66 (m, 1H), 1.53 − 1.42 (m, 1H), 1.30 (d, *J* = 6.7 Hz, 3H+1H).

**6.1.76.** (*S,R_p*)-1-[α-Methyl-(3-(*tert*-butyldiphenylsilyl)propyl)]-2-[2-(bromo)ethyl]-ferrocene

71
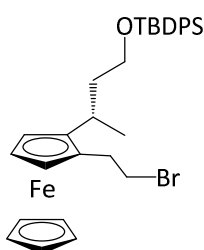
In a 50 mL schlenk tube, NBS (0.198 g, 1.1098 mmol) was suspended in dry DCM. A DCM solution of triphenylphosphine (0.272 g, 1.036 mmol) was added drop wise to it. The resulting orange mixture was stirred for 5 min before addition of 0.045 mL (0.444 mmol) of pyridine. The mixture goes brown. **67** (0.200 g, 0.369 mmol) previously dissolved in 2.5 mL of dry DCM, was added to the mixture. After overnight reaction, the solvent was removed *in vacuo* and the crude was purified via flash column chromatography (10% EtOAc in hexane) to yield the yellow oily product (0.187 g, 84%). ^{1}H NMR (400 MHz, CDCl$_3$) δ 7.68 – 7.64 (m, 4H), 7.44 – 7.37 (m, 6H), 4.10 (dd, *J* = 2.5, 1.3 Hz, 1H), 4.05 (s, 5H), 4.00 (t, *J* = 2.5 Hz, 1H), 3.95 (dd, *J* = 2.6, 1.4 Hz, 1H), 3.66 – 3.60 (m, 2H), 3.46 (dd, *J* = 8.6, 7.5 Hz, 2H), 2.90 (td, *J* = 7.8, 2.8 Hz, 2H), 2.76 – 2.67 (m, 1H), 1.70 – 1.61 (m, 1H), 1.40 – 1.32 (m, 1H), 1.26 (d, *J* = 6.9 Hz, 3H), 1.07 (s, 9H). ^{13}C NMR (101 MHz, CDCl$_3$) δ 135.61 (Ph), 133.95 (ipso Ph), 133.86 (ipso Ph), 129.61 (Ph), 127.68 (Ph), 94.78 (ipso Cp), 83.19 (ipso Cp), 69.06 (Fc), 67.26 (Fc), 65.49 (Fc), 65.22 (Fc), 61.79 (CH$_2$), 42.59 (CH$_2$), 31.94 (CH$_2$), 31.54 (CH$_2$), 27.47 (CH*), 26.99 (tBu), 19.36 (CH$_3$), 19.24 (ipso tBu). MS (ES) (m/z) calcd for C$_{32}$H$_{39}$OFe^{56}Si^{81}Br 604.1282, found 604.1286. IR (cm^{-1}): 3071 (=CH Fc), 2958 (CH$_2$), 2930 (CH$_2$), 1589, 1472, 1427 (CH$_2$), 1389 (tBu), 1105, 1086, 820 CH Ar Ph), 700 (C=C). [α]$_D$ (c = 0.0056 g/mL, DCM) = -28.6.

6.1.77. (*S*,*R*$_p$)-1-[α-Methyl-(3-(*tert*-butyldiphenylsilyl)propyl)]-2-[2-((*N*-4-benzoyl)-cytosin-1-yl)ethyl]-ferrocene **72**
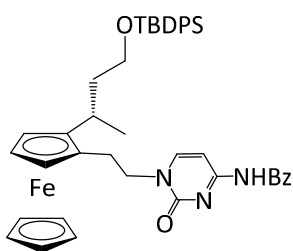
In a 50 mL schlenk tube, the *N*-4-benzoyl-cytosine **21** (0.072 g, 0.331 mmol) was stirred vigorously in suspension in 3 mL of DMF for 5 min. NaH (0.00795 g, 0.331 mmol) was added to the mixture in one portion and stirred for 1 h. At this point the solution was clear. **71** (0.100 g, 0.166 mmol) was dissolved in 2 mL of DMF and added to the mixture. After overnight stirring at room temperature, the reaction was quenched with water, extracted with chloroform, dried on MgSO$_4$. The solvent was removed *in vacuo* and the crude was purified via flash column chromatography (40% EtOAc in hexane) to yield product (0.061 g, 60%). ^{1}H NMR (400 MHz, CDCl$_3$) δ 8.61 (s, 1H), 7.90 (d, *J* = 7.7 Hz, 2H), 7.67 − 7.59 (m, 4H+2H), 7.53 (dd, *J* = 8.4, 7.0 Hz, 2H), 7.45 − 7.34 (m, 4H+2H+1H), 7.14 (d, *J* = 7.1 Hz, 1H), 4.07 (s, 5H), 4.06 − 4.01 (m, 1H (CH$_2$•)), 3.99 (dd, *J* = 5.4, 2.9 Hz, 2H), 3.88 (s, 1H), 3.81 − 3.71 (m, 1H (CH$_2$•)), 3.71 − 3.64 (m, 2H), 2.96 − 2.88 (m, 1H), 2.76 − 2.71 (m, 1H), 2.70 − 2.63 (m, 1H), 1.70 − 1.61 (m, 1H), 1.52 − 1.43 (m, 1H), 1.29 (d, *J* = 6.6 Hz, 3H), 1.04 (s, 9H). ^{13}C NMR (101 MHz, CDCl$_3$) δ 182.20 (C=O), 162.02 (C=O), 149.13 (CH cytosine), 135.55 (Ph), 133.87 (ipso Bz), 133.80 (Bz), 133.16 (ipso Ph), 129.72 (Ph), 129.07 (Bz), 127.71 (Bz), 127.47 (Ph), 95.8 (CH cytosine), 94.8 (ipso Cp), 81.2 (ipso Cp), 69.21 (Fc), 67.80 (Fc), 65.84 (Fc), 65.48 (Fc), 61.96 (CH$_2$), 51.71 (CH$_2$), 42.90 (CH$_2$), 27.44 (CH$_2$), 27.19 (CH*), 26.91 (tBu), 19.76 (CH$_3$), 19.22 (ipso tBu). The CN (ipso) peak could not be characterised. MS (ES) (m/z) calcd for C$_{43}$H$_{47}$N$_3$O$_3$^{56}FeSiNa 760.2634, found 760.2617. IR (cm^{-1}): 3071 (=CH Fc), 2958 (CH$_2$), 2930 (CH$_2$), 2857 (CH$_2$), 1662 (C=O), 1625 (amide), 1553 (C=N), 1484 (CH$_2$), 1363 (tBu), 1237, 1175, 1105 (Si-OR), 785 (CH Ar Ph), 700 (C=C). Mp 72 °C.

6.1.78. (S,R_p)-1-[α-Methyl-(3-(hydroxy)propyl)]-2-[2-((N-4-benzoyl)-cytosin-1-yl)ethyl]-

ferrocene **73**
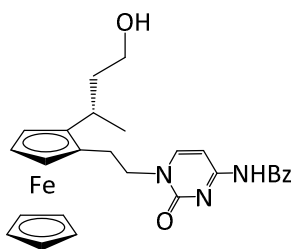
In a 50 mL schlenk tube, **72** (0.053 g, 0.0859 mmol) was dissolved in 2 mL of dry THF and tetra-Butylamino fluoride (0.054 g, 0172 mmol) was added to the solution. After overnight stirring, the reaction was quenched with water, extracted with DCM, washed with brine, water and dried over Na_2SO_4. The solvent was removed *in vacuo* and the crude was purified via flash column chromatography (3% MeOH in DCM) to yield product (0.040 g, 93%). ^{1}H NMR (400 MHz, CDCl$_3$) δ 8.91 (s, 1H), 7.93 − 7.88 (m, 2H), 7.68 (d, J = 7.2 Hz, 1H (CH cytosine)), 7.64 − 7.58 (m, 1H), 7.54 − 7.47 (m, 2H+1H (CH cytosine)), 4.16 − 4.09 (m, 1H (CH$_2$•)), 4.07 (s, 7H), 4.04 (d, J = 2.2 Hz, 1H), 3.85 − 3.78 (m, 1H (CH$_2$•)), 3.72 − 3.60 (m, 1H+1H), 2.98 − 2.76 (m, 2H+1H), 1.71 − 1.62 (m, 1H), 1.51 − 1.43 (m, 1H), 1.36 (d, J = 6.7 Hz, 3H). ^{13}C NMR (101 MHz, CDCl$_3$) δ 165.97 (ipso CN), 162.34 (C=O Bz), 155.7 (C=O cytosine), 149.11 (CH cytosine), 133.20 (Bz), 133.00 (ipso Bz), 129.03 (Bz), 127.58 (Bz), 96.75 (CH cytosine), 95.49 (ipso Cp), 80.93 (ipso Cp), 69.33 (Fc), 67.76 (Fc), 66.01 (Fc), 65.33 (Fc), 60.27 (CH$_2$), 52.36 (CH$_2$), 43.44 (CH$_2$), 27.84 (CH$_2$), 26.92 (CH*), 19.19 (CH$_3$). MS (ES) (m/z) calcd for C$_{27}$H$_{29}$N$_3$O$_3$^{56}FeNa 522.1458, found 522.1456. IR (cm^{-1}): 3315 br (OH), 3075 (=CH Fc), 2958 (CH$_2$), 2929 (CH$_2$), 2874 (CH$_2$), 1692 (C=O), 1646 (Amide), 1623 (C=N), 1555 (NH), 1483, 1363, 1237, 785, 702 (C=C). Mp 90 °C - 92 °C. [α]$_D$ (c = 0.0065 g/mL, DCM) = -4.3.

6.1.79. (*S*,*R*$_p$)-1-[α-Methyl-(3-(hydroxy)propyl)]-2-[2-(cytosin-1-yl)ethyl]-ferrocene **74**
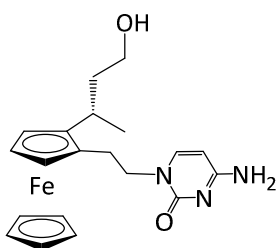
73 (0.018 g, 0.036 mmol) was dissolved in 2 mL of methylamine. The mixture was stirred at room temperature for half an hour under argon. The methylamine was evaporated. The crude was purified via flash column chromatography (10% MeOH in DCM) to yield product.

A yellow solid was obtained (0.014 g, 98%). ^{1}H NMR (400 MHz, CDCl$_3$) δ 7.24 (s, 1H (overlapped by CDCl$_3$ peak), 5.72 (d, *J* = 7.1 Hz, 1H), 4.07 (dd, *J* = 2.4, 1.3 Hz, 1H), 4.04 (s, 5H+1H), 4.01 (t, *J* = 1.3 Hz, 1H), 3.99 – 3.91 (m, 1H (CH$_2$•)), 3.69 (dt, *J* = 10.1, 4.8 Hz, 1H), 3.65 – 3.60 (m, 1H), 3.58 (dd, *J* = 8.4, 3.5 Hz, 1H (CH$_2$•)), 2.94 – 2.83 (m, 2H), 2.74 – 2.64 (m, 1H), 1.73 – 1.62 (m, 1H), 1.46 – 1.40 (m, 1H), 1.35 (d, *J* = 6.8 Hz, 3H). ^{13}C NMR (101 MHz, CDCl$_3$) δ 165.97 (ipso CN), 156.54 (C=O cytosine), 145.71 (CH cytosine), 95.58 (ipso Cp), 94.40 (CH cytosine), 81.28 (ipso Cp), 69.21 (Fc), 67.60 (Fc), 65.77 (Fc), 65.13 (Fc), 60.22 (CH$_2$), 51.77 (CH$_2$), 43.50 (CH$_2$), 28.03 (CH$_2$), 26.82 (CH*), 18.96 (CH$_3$). MS (ES) (m/z) calcd for C$_{20}$H$_{25}$N$_3$O$_2$^{56}FeNa 418.1194, found 418.1198. IR (cm^{-1}): 3333 br (OH), 3210 (NH$_2$), 3097 (=CH Fc), 2917 (CH$_2$), 2851 (CH$_2$), 1650 (amide/urea), 1614 (NH$_2$), 1528, 1483 (C=N), 1383 (CH$_3$), 1237, 1180, 1106 (C-O), 785 (CH Ar), 718 (C=C). Mp 162 °C - 164 °C.

6.2 Electrochemistry

The electrochemical experiments were carried out in DCM solution under an atmosphere of argon containing TBA·PF6 (0.1 M) as supporting electrolyte and decamethylferrocene as an internal reference. DCM was previously dried using Solvent Purification System. A three-electrode cell was used, with Pt as the working electrode, Ag/AgCl as the reference electrode and Pt wire as the auxiliary electrode. All the glassware was cleaned using an ammonia/hydrogen peroxide 1:1 solution for 3-6 hours and then rinsed with MilliQ® water. Before each experiment, the working electrode was polished with an alumina slurry, rinsed with MilliQ water and dried and the auxiliary electrode was cleaned with a Bunsen flame. The solutions were purged with nitrogen before each run. A BAS 100 potentiostat and BAS 100 software were used to record the voltammograms. The confidence limits in the electrode potential values were ±5 mV for CV. For each voltammogram, the reversibility of the redox wave of the analyte broadly matched that of decamethylferrocene under the same experimental conditions (ΔE_p = 70-100 mV). As the solubility of each compound at ca. 1 mM in DCM was low, each sample required filtration through a Whatman 13mm GD/X syringe filter beforehand.

6.2.1 Cells and glassware care

The cell and all the glassware used during the experiments were cleaned using one of the following methods:

- Ammonia : Hydrogen peroxide 1:1 (3/6 h)

- Piranha solution (sulfuric acid : H_2O_2 3:1) (1 h)

- Nitric acid : sulfuric acid 1:1 at 200 ˚C (1 h)

After any of the above methods the glassware should be rinsed several times (*ca.* 10) with MilliQ® water and dried in an oven overnight.

6.2.2 Working Electrodes pre-treatment

Pt and Au electrodes were mechanically polished before any experiment using an alumina water slurry on a microcloth pad, performing a figure of eight pattern for not less than 5 min. Every 2-3 months of usage (or in case major scratches are present) each electrode was polished with a diamond powder solution 3 μm (on a nylon pad). The scans should be carried out until the voltammogram is reproducible. In all cases the electrode was rinsed with MilliQ water and dried under a nitrogen flow.

6.3 Crystal structures

Suitable crystals were selected and datasets from the following structures were measured by the EPSRC UK National Crystallography Service[1] on a Rigaku AFC12 goniometer equipped with an enhanced sensitivity (HG) Saturn 724+ detector mounted at the window of an FR-E+ SuperBright molybdenum rotating anode generator ($\lambda_{Mo-K\alpha}$ = 0.71075 Å) with HF Varimax optics The data collections were driven and processed, and absorption corrections applied by CrystalClear-SM Expert 3.1 b13a[2]. The structures were all solved in SHELXS-97[3] and were refined by a full-matrix least-squares procedure on F^2 in SHELXL-97.[3] All non-hydrogen atoms were refined with anisotropic displacement parameters. The hydrogen atoms were added at calculated positions and refined by use of a riding model with isotropic displacement parameters based on the equivalent

isotropic displacement parameter (U_{eq}) of the parent atom. Figures were produced using

OLEX2[4] and structural analysis was carried out in Mercury 3.0.[5]

Crystal Data for 12:

Table 6-1: Crystal data and structure refinement for 12.

Empirical formula	$C_{24} H_{24} Fe N_{10}$
Formula weight	508.38
Temperature	120 (2) K
Wavelength	0.71073 Å
Crystal system	Monoclinic
Space group	P 2(1)/c
Unit cell dimensions	a = 6.3611 (6) Å $\quad$ α = 90°. b = 8.0936 (11) Å $\quad$ β= 90.135(8)°. c = 20.680 (3) Å $\quad$ γ = 90°.
Volume	1064.7 (2) Å^3
Z	2
Density (calculated)	1.586 Mg/m^3
Absorption coefficient	0.747 mm^{-1}
F(000)	528
Crystal size	0.36 x 0.03 x 0.01 mm^3
Theta range for data collection	2.96 to 25.00°.
Index ranges	-7<=h<=7, -8<=k<=9, -24<=l<=24
Reflections collected	7494
Independent reflections	1860 [R(int) = 0.0739]
Completeness to theta = 25.00°	98.6 %
Absorption correction	Semi-empirical from equivalents
Max. and min. transmission	0.9926 and 0.7747
Refinement method	Full-matrix least-squares on F^2
Data / restraints / parameters	1860 / 0 / 161
Goodness-of-fit on F^2	1.158
Final R indices [I>2sigma(I)]	R1 = 0.0674, wR2 = 0.1285
R indices (all data)	R1 = 0.0932, wR2 = 0.1461
Largest diff. peak and hole	0.546 and -0.437 e.Å^{-3}

The iron atom of the molecule is located on an inversion centre such that only half of the molecule is crystallographically unique. The structure is a merohedral twin with the refined ratio of the two domains being 52:48 and the twin law relating these domains being (1 0 0 0 -1 0 0 0 -1). The hydrogen atoms were fixed as riding models.
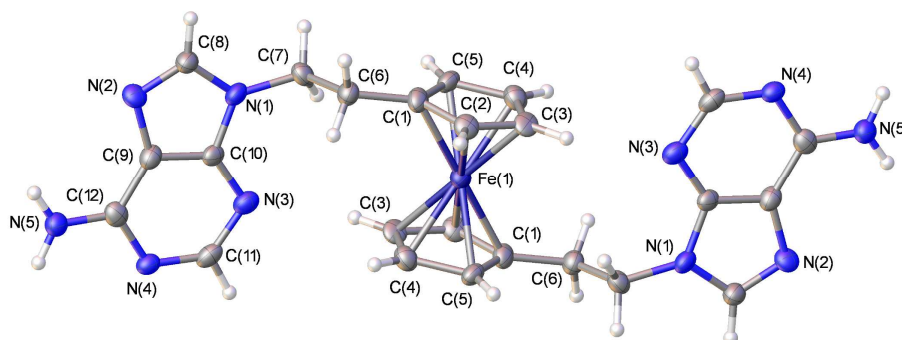

Figure 6-1: *Crystal structure of 12 with ellipsoids drawn at the 50 % probability level. The iron atom is located on an inversion centre such that only half of the molecule is crystallographically independent.*

Crystal Data for 39:

Table 6-2: *Crystal data and structure refinement for 39*

Empirical formula	$C_{22}H_{28}FeI_2O_4$
Formula weight	666.09
Temperature	120(2) K
Wavelength	0.71073 Å
Crystal system	Monoclinic
Space group	$P2_1$
Unit cell dimensions	a = 14.1877 (7) Å α = 90°.
	b = 8.3380 (2) Å β = 101.305 (2)°.
	c = 20.9652 (9) Å γ = 90°.
Volume	2432.00(17) $Å^3$
Z	4
Density (calculated)	1.819 Mg/m^3
Absorption coefficient	3.183 mm^{-1}
F(000)	1296
Crystal size	0.45 x 0.14 x 0.03 mm^3
Theta range for data collection	2.92 to 27.48°.
Index ranges	-17<=h<=18, -10<=k<=9, -27<=l<=27
Reflections collected	29532
Independent reflections	10419 [R(int) = 0.0542]
Completeness to theta = 27.48°	98.5 %
Absorption correction	Semi-empirical from equivalents
Max. and min. transmission	0.9106 and 0.3285
Refinement method	Full-matrix least-squares on F^2
Data / restraints / parameters	10419 / 474 / 624
Goodness-of-fit on F^2	1.039
Final R indices [I>2sigma(I)]	R1 = 0.0464, wR2 = 0.0962
R indices (all data)	R1 = 0.0654, wR2 = 0.1054
Largest diff. peak and hole	1.604 and -0.860 $e.Å^{-3}$

The structure contains two crystallographically independent molecules. The methyl group C(16) / C(16') is disordered over two positions at a percentage occupancy ratio of 73(3):27(3) respectively. The groups C(114)-C(116), O(101), O(102) / C(04')-C(06'), O(01'), O(02') and C(120)-C(122), O(103), O(104) / C(20')-C(22'), O(03'), O(04') are disordered over two positions both at the percentage occupancy ratio of 70(2): 30(2).

Figure 6-2: *Crystal structure of the two crystallographically independent molecules of 39 with ellipsoids drawn at the 50 % probability level. The methyl group C(16) / C(16') and the groups C(114)-C(116), O(101), O(102) / C(04')-C(06'), O(01'), O(02') and C(120)-C(122), O(103), O(104) / C(20')-C(22'), O(03'), O(04') are disordered over two positions. The minor positions and all hydrogen atoms have been omitted for clarity.*

Crystal Data for 47:

Table 6-3: Crystal data and structure refinement for 47

Empirical formula	$C_{54}H_{70}FeO_4Si_2$
Formula weight	895.13
Temperature	100(2) K
Wavelength	0.71075 Å
Crystal system	Triclinic
Space group	P 1
Unit cell dimensions	a = 8.651(7) Å α = 83.74(4)° b = 15.747(15) Å β = 80.13(5)° c = 19.038(17) Å γ = 87.42(5)°
Volume	2539(4) Å^3
Z	2
Density (calculated)	1.171 Mg/m^3
Absorption coefficient	0.386 mm^{-1}
F(000)	960
Crystal size	0.28 x 0.03 x 0.03 mm^3
Theta range for data collection	2.93 to 27.48°.
Index ranges	-9<=h<=11, -20<=k<=20, -24<=l<=24
Reflections collected	45083
Independent reflections	19748 [R(int) = 0.0494]
Completeness to theta = 27.48°	99.8 %
Absorption correction	Semi-empirical from equivalents
Max. and min. transmission	0.9885 and 0.8995
Refinement method	Full-matrix least-squares on F^2
Data / restraints / parameters	19748 / 3 / 1119
Goodness-of-fit on F^2	1.088
Final R indices [I>2sigma(I)]	R1 = 0.0534, wR2 = 0.0809
R indices (all data)	R1 = 0.0617, wR2 = 0.0848
Largest diff. peak and hole	0.364 and -0.437 e.Å^{-3}

The structure of **47** contains two crystallographically independent molecules, with the molecular geometry being the same within experimental error.
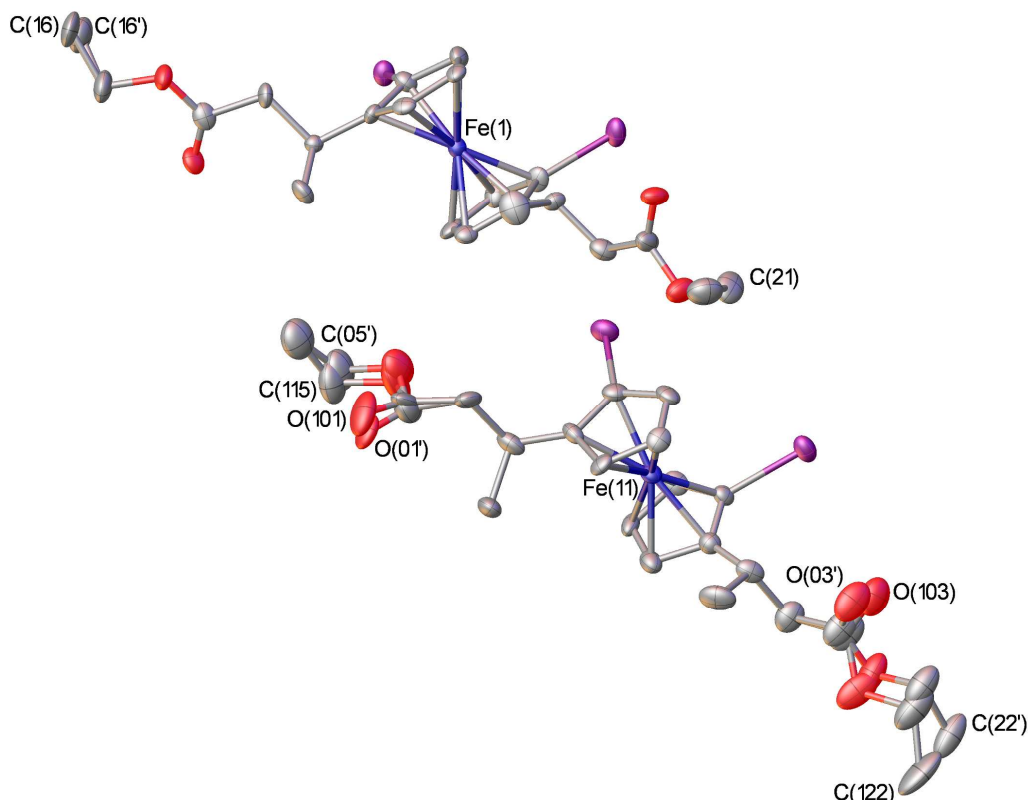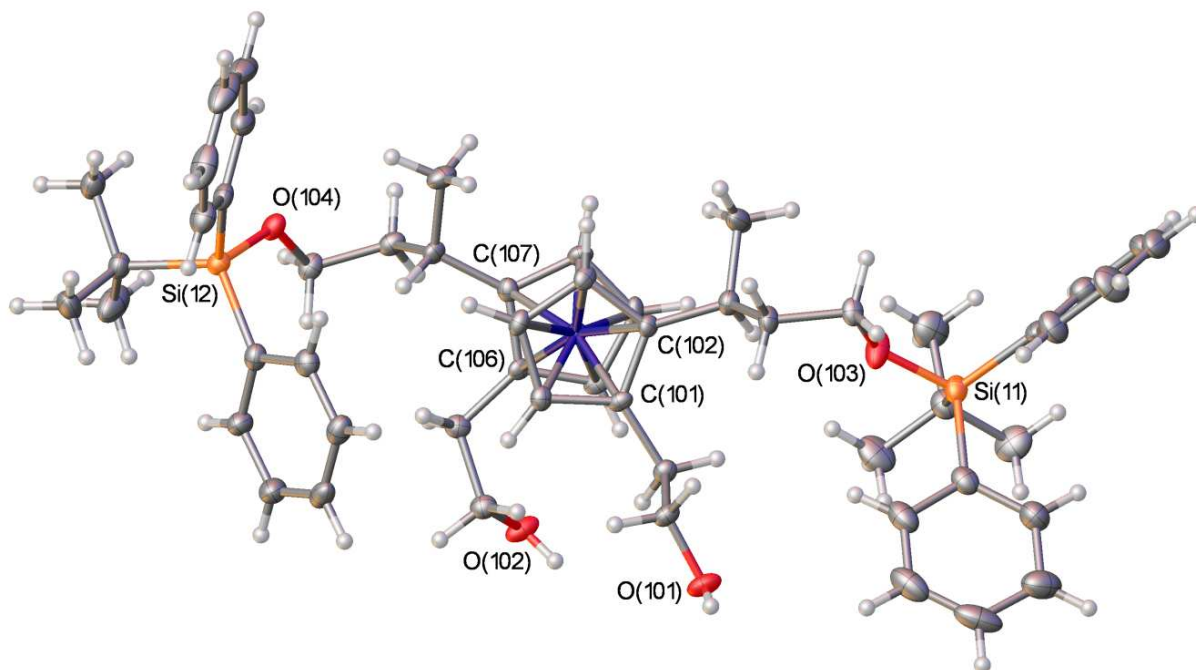

Figure 6-3: *Crystal structure of the second of the crystallographically independent molecules of 47 with ellipsoids drawn at the 50 % probability level.*

Crystal Data for 51:

Table 6-4: Crystal data and structure refinement for 47

|	
Empirical formula	$C_{44}H_{46}FeN_4O_8$, $CDCl_3$
Formula weight	935.10
Temperature	100(2) K
Wavelength	0.71075 Å
Crystal system	Orthorhombic
Space group	$P\,2_1\,2_1\,2_1$
Unit cell dimensions	a = 11.808(5) Å $\quad$ α= 90°
	b = 13.709(6) Å $\quad$ β= 90°
	c = 26.047(11) Å $\quad$ γ = 90°
Volume	4216(3) Å^3
Z	4
Density (calculated)	1.473 Mg/m^3
Absorption coefficient	0.608 mm^{-1}
F(000)	1944
Crystal size	0.11 x 0.11 x 0.02 mm^3
Theta range for data collection	2.91 to 27.48°.
Index ranges	-15<=h<=15, -17<=k<=17, -33<=l<=33
Reflections collected	86280
Independent reflections	9657 [R(int) = 0.0433]
Completeness to theta = 27.48°	99.8 %
Absorption correction	Semi-empirical from equivalents
Max. and min. transmission	0.9879 and 0.9361
Refinement method	Full-matrix least-squares on F^2
Data / restraints / parameters	9657 / 1 / 557
Goodness-of-fit on F^2	1.093
Final R indices [I>2sigma(I)]	R1 = 0.0399, wR2 = 0.0945
R indices (all data)	R1 = 0.0405, wR2 = 0.0948
Absolute structure parameter	0.017(12)
Largest diff. peak and hole	0.558 and -0.500 e.Å^{-3}
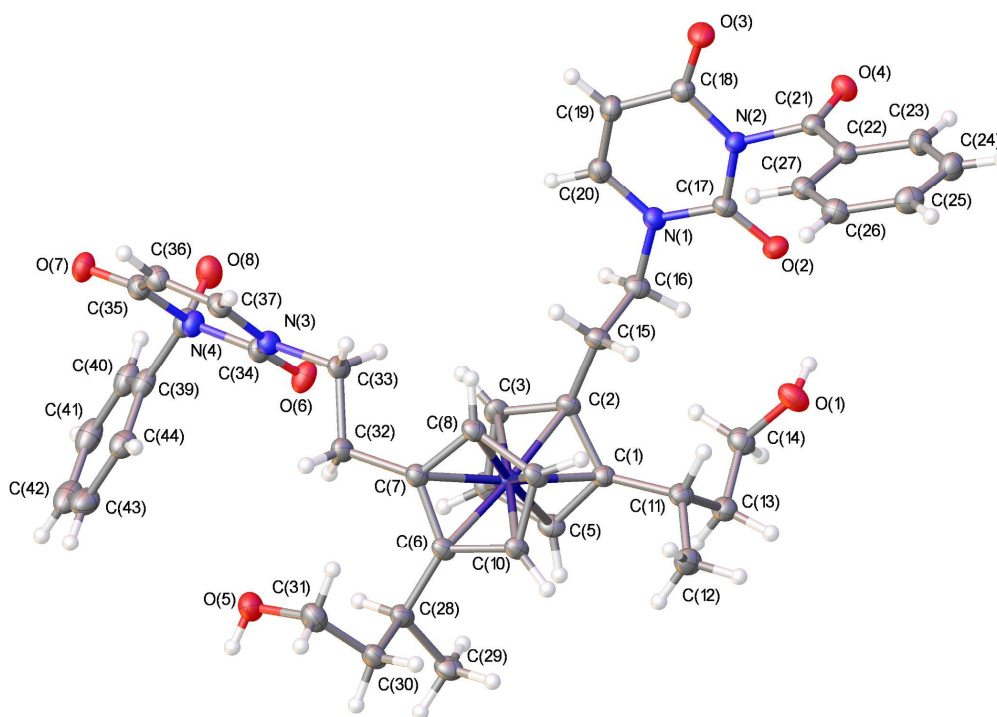
Figure 6-4: *Crystal structure of 51 with ellipsoids drawn at the 50 % probability level. The structure contains a molecule of deuterated chloroform, which has been omitted for clarity.*

6.4   High Performance Liquid Chromatography

Analytical HPLC was recorded using a reverse-phase C18 column with a water acetonitrile method: 0-40 min (0-100% acetonitrile), 40-50 min (100% acetonitrile), 50-60 min (O% acetonitrile) at 1 mL/min and was monitored at 210 nm. Chiral HPLC was conducted on AD or OD chiral columns using IPA/Hexane eluent with a flow rate of 1 mL/min. Three solutions were used to perform the chiral separations: Solvent system **A**: Hexane; Solvent system **B**: 10% IPA in hexane, Solvent system **C:** 20% IPA in hexane. The enantiomeric excess of the compounds was calculated from the area of the peaks obtained. Any opposite enantiomers used in the determination of the *ee* via Chiral HPLC not reporte in the thesis were synthesised by Dr. H. Van Nguyen from Tucker group.

6.5   References

1   S. J. Coles and P. A. Gale, *Chem. Sci.*, **2012**, *3*, 683-689.

2   *CrystalClear-SM Expert 3.1 b13a*, **2012**, Rigaku.

3   G. M. Sheldrick, *Acta Cryst.*, **2008**, *A64*, 112-122.

4   O. V. Dolomanov, L. J. Bourhis, R. J. Gildea, J. A. K. Howard and H. Puschmann, *J. Appl. Crystallogr.*, **2009**, *42*, 339.

5   C. F. Macrae, P. R. Edgington, P. McCabe, E. Pidcock, G. P. Shields, R. Taylor, M. Towler and J. van de Streek, *J. Appl. Cryst.*, **2006**, *39*, 453.

APPENDIX

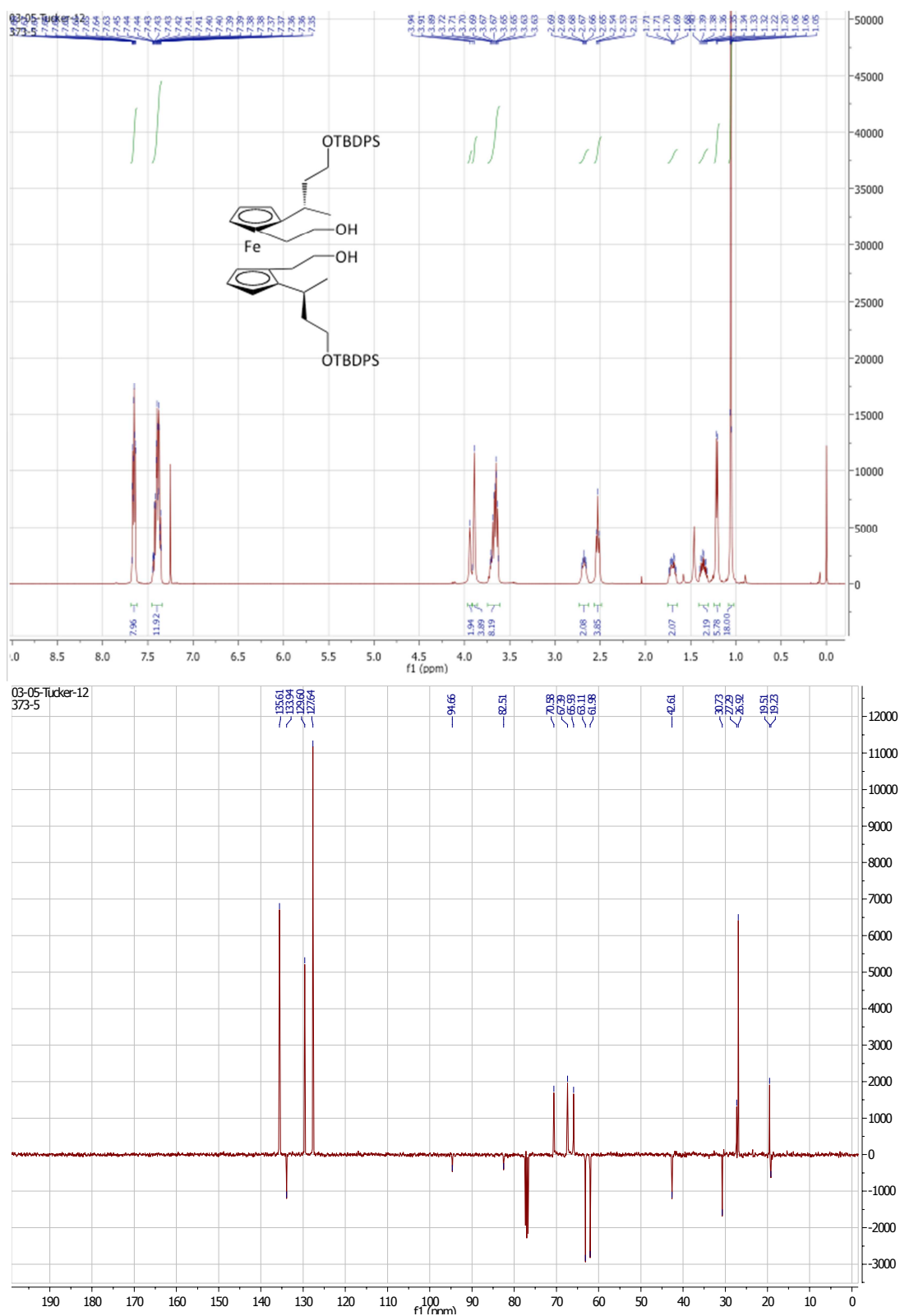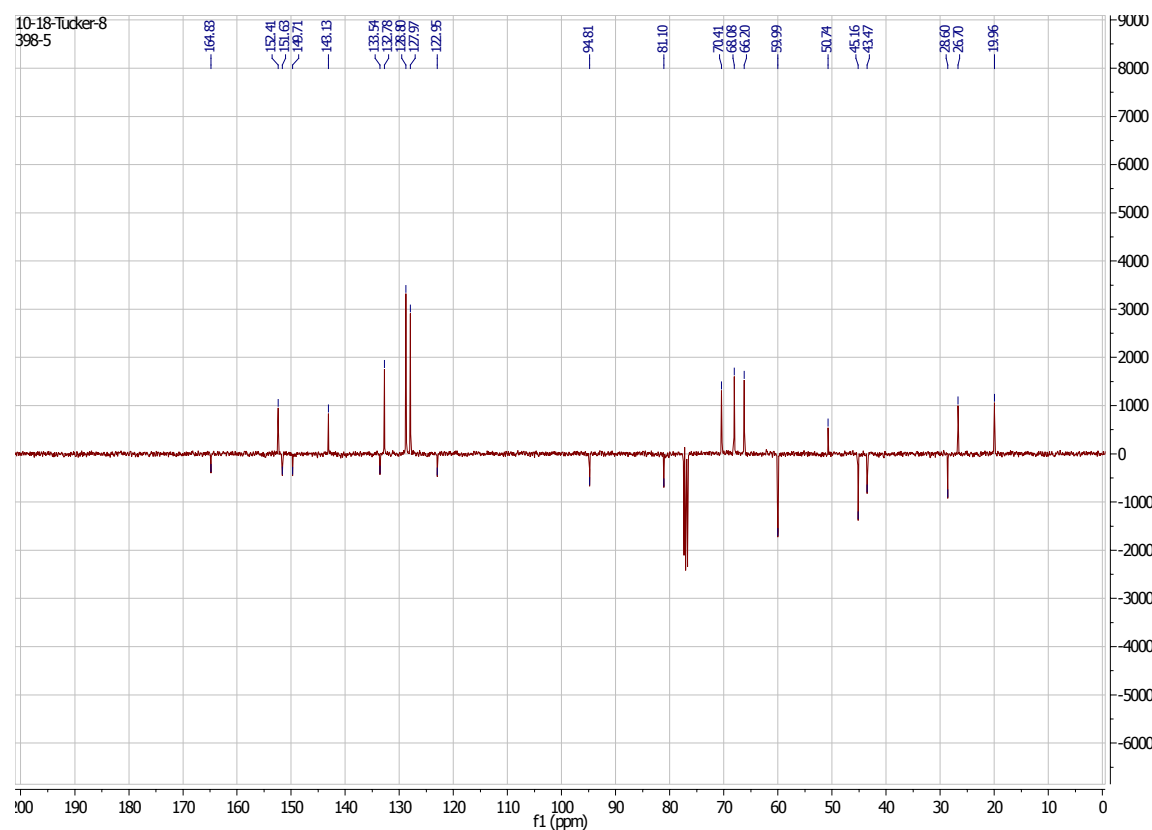***Figure 7-1:*** *^{1}H and ^{13}C NMR of 47 in CDCl$_3$.*
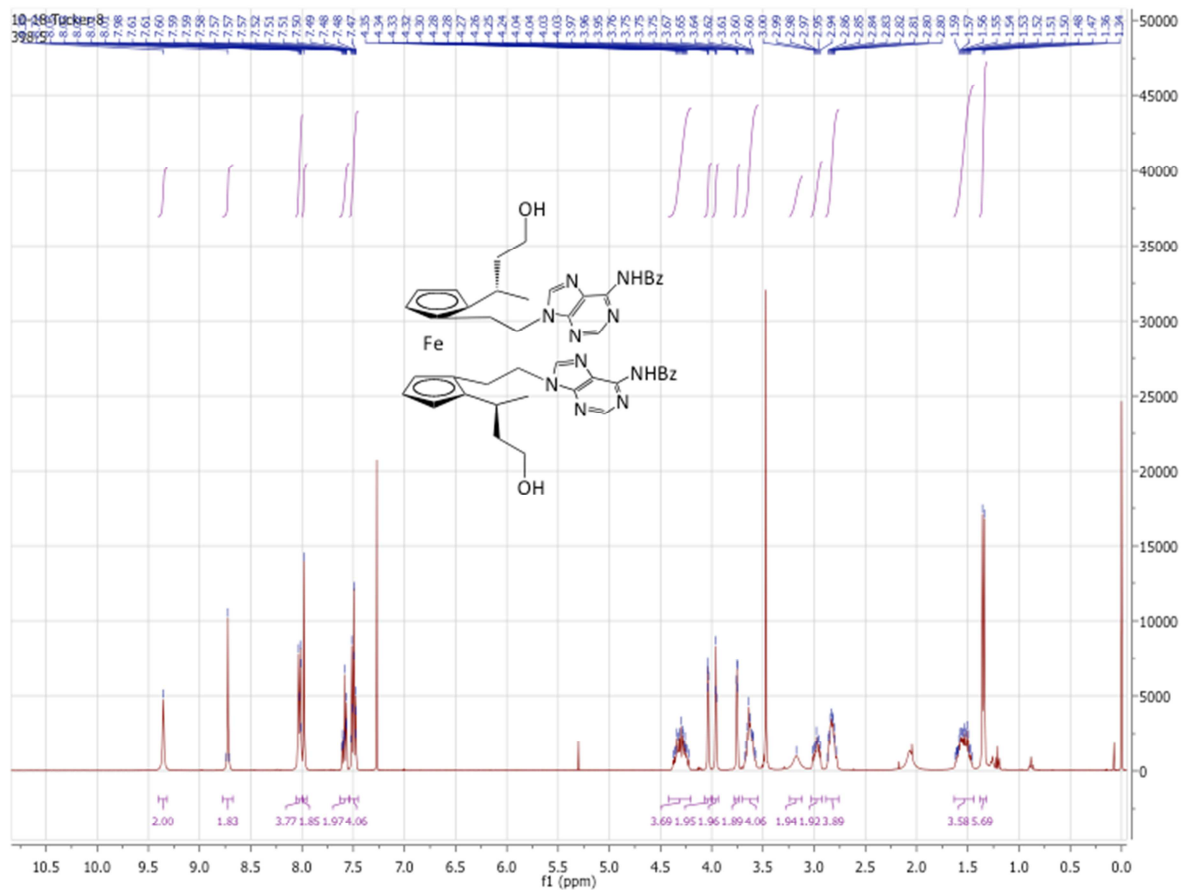
Figure 7-2: *^{1}H and ^{13}C NMR of 50 in CDCl$_3$*
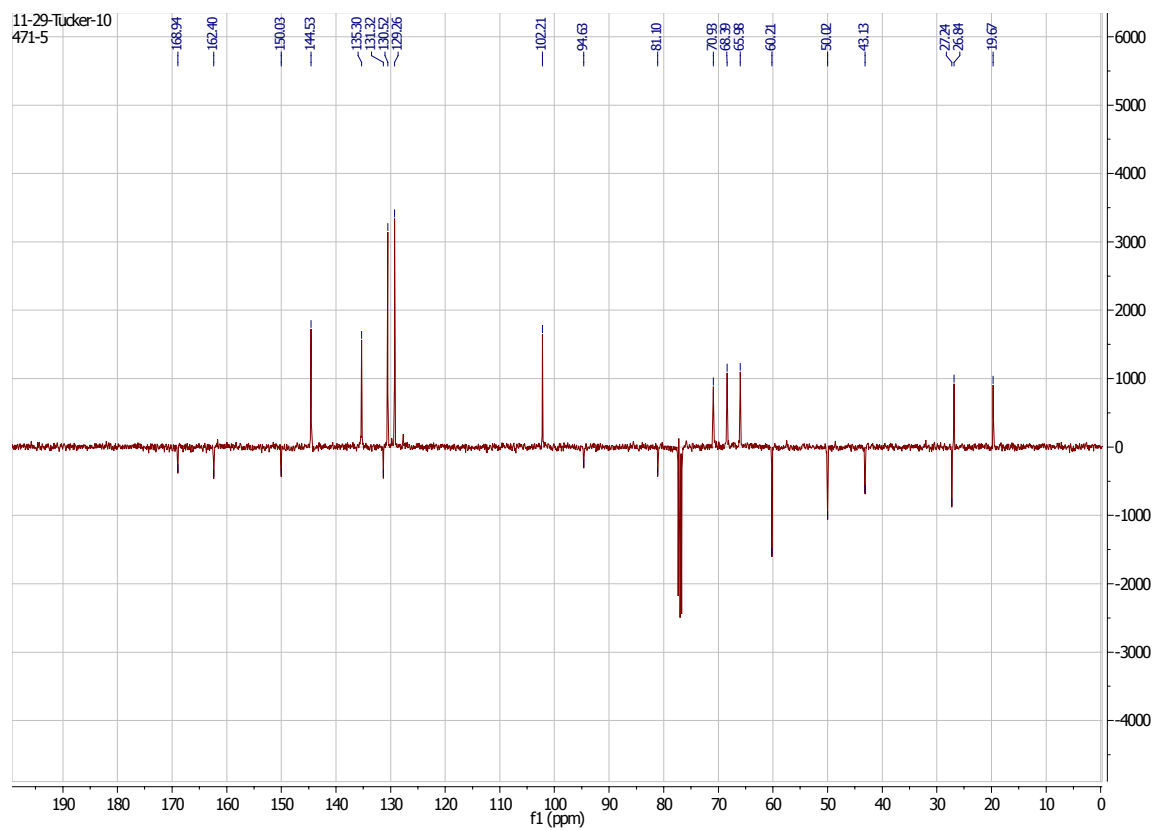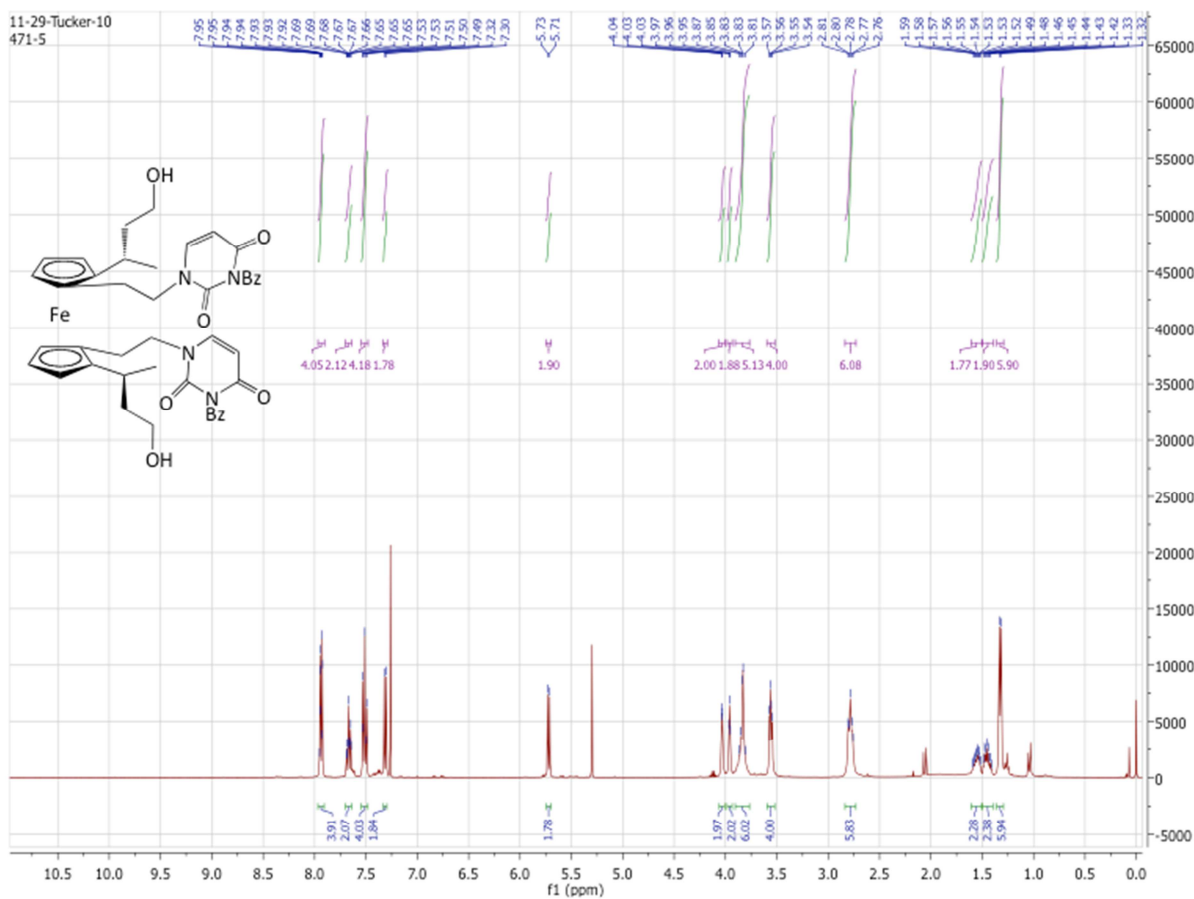
Figure 7-3: *^{1}H and ^{13}C NMR of 51 in CDCl$_3$*
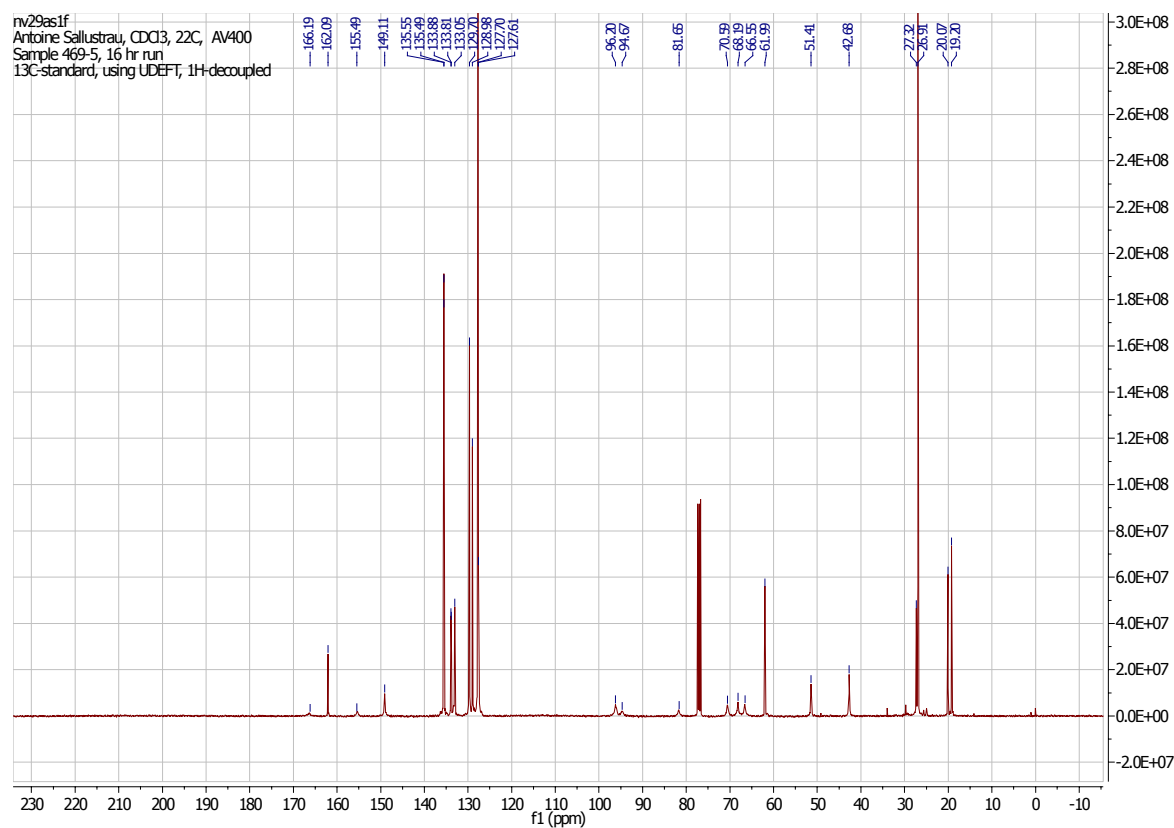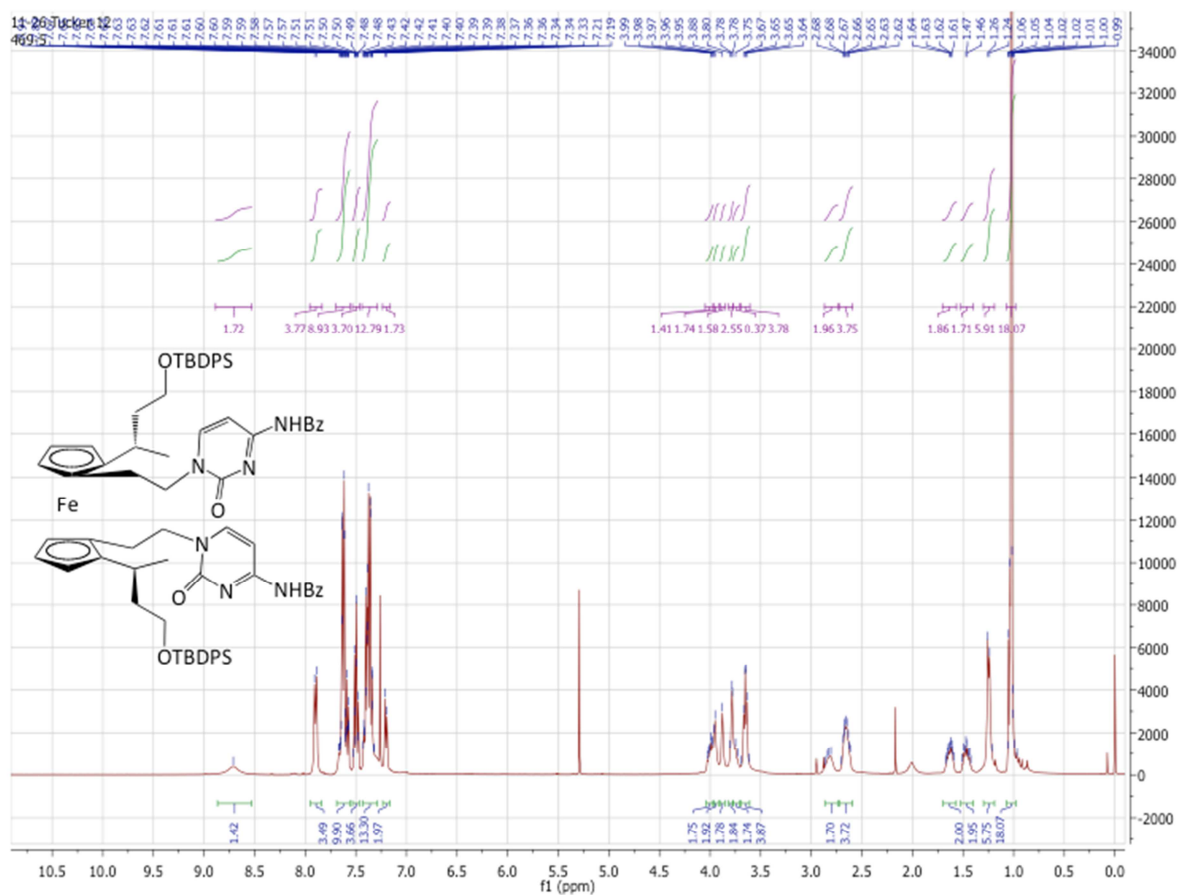
Figure 7-4: ^1H *and* ^{13}C *NMR (UDEFT) of 53 in CDCl$_3$*

Figure 7-5: Chiral HPLC of 34 (10% IPA in Hexane at 1 mL/min, OD column)

No.	Ret.Time min	Peak Name	Height mAU	Area mAU*min	Rel.Area %	Amount	Type
1	4.55	n.a.	859.945	206.296	100.00	n.a.	BMB
Total:			859.945	206.296	100.00	0.000	

No.	Ret.Time min	Peak Name	Height mAU	Area mAU*min	Rel.Area %	Amount	Type
1	4.70	n.a.	9.575	1.849	0.31	n.a.	BMB*
2	18.28	n.a.	720.530	593.685	99.69	n.a.	BMB
Total:			730.105	595.534	100.00	0.000	

Figure 7-6: Chiral HPLC of the opposite enantiomer of 34 (10% IPA in Hexane at 1 mL/min, OD column)

No.	Ret.Time min	Peak Name	Height mAU	Area mAU*min	Rel.Area %	Amount	Type
1	4.59	n.a.	856.722	187.937	28.15	n.a.	BMB
2	18.32	n.a.	608.371	479.647	71.85	n.a.	BMB
Total:			1465.093	667.584	100.00	0.000	

Figure 7-7: *Chiral HPLC of 34 and its enantiomer (10% IPA in Hexane at 1 mL/min, OD column)*

No.	Ret.Time min	Peak Name	Height mAU	Area mAU*min	Rel.Area %	Amount	Type
1	28.80	n.a.	356.756	395.734	100.00	n.a.	BMB
Total:			356.756	395.734	100.00	0.000	

Figure 7-8: *Chiral HPLC of 36 (10% IPA in Hexane at 1 mL/min, AD column)*

No.	Ret.Time min	Peak Name	Height mAU	Area mAU*min	Rel.Area %	Amount	Type
1	28.96	n.a.	0.902	1.617	0.44	n.a.	BMB*
2	36.23	n.a.	248.288	361.857	99.56	n.a.	BMB
Total:			249.190	363.475	100.00	0.000	

Figure 7-9: *Chiral HPLC of the opposite enantiomer of 36 (10% IPA in Hexane at 1 mL/min, AD*

column)

No.	Ret.Time min	Peak Name	Height mAU	Area mAU*min	Rel.Area %	Amount	Type
1	28.80	n.a.	342.160	372.365	44.34	n.a.	BMB
2	36.16	n.a.	314.034	467.339	55.66	n.a.	BMB
Total:			656.193	839.704	100.00	0.000	

Figure 7-10: *Chiral HPLC of 36 and its enantiomer (10% IPA in Hexane at 1 mL/min, AD column)*
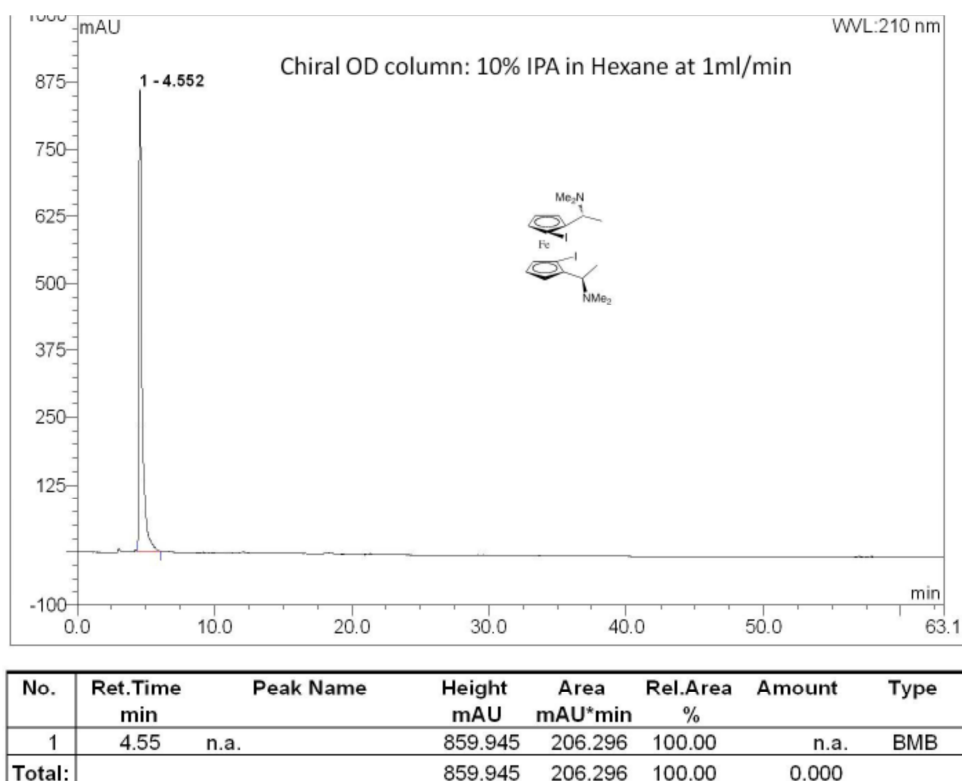
*Figure 7-11: Chiral HPLC of **39** (5% IPA in Hexane at 1 mL/min, AD column)*
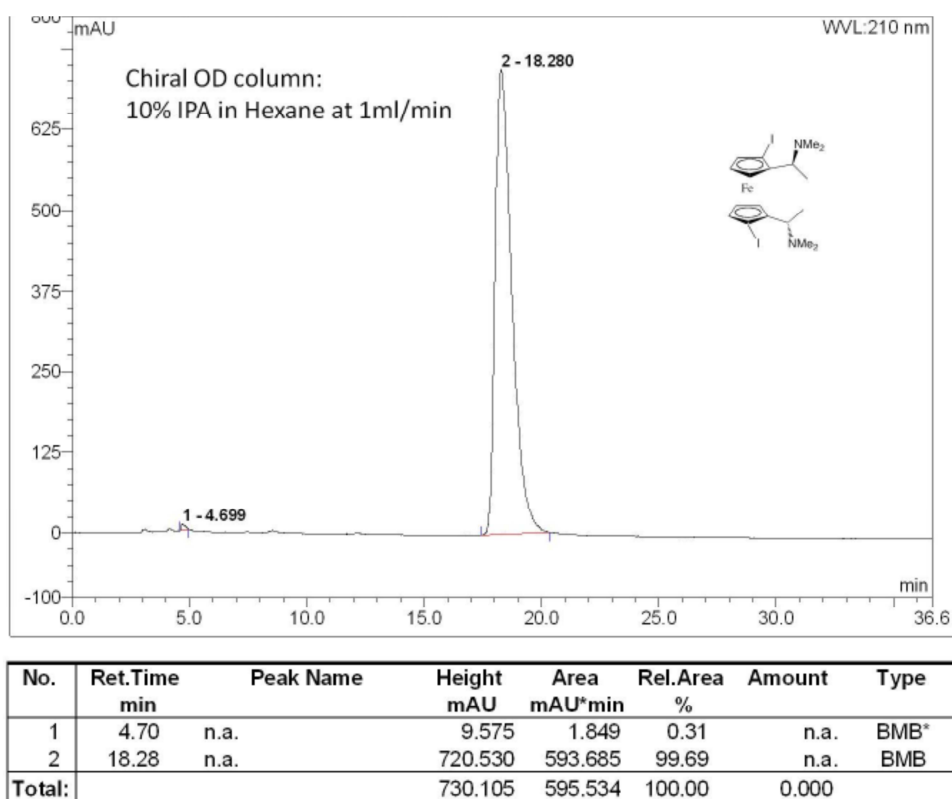

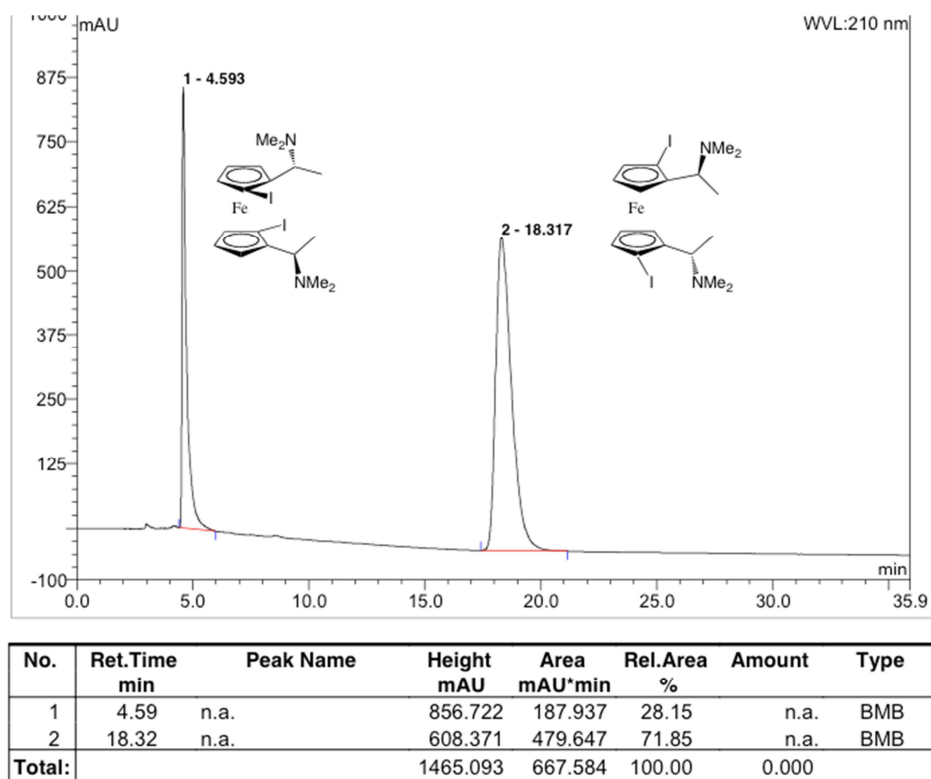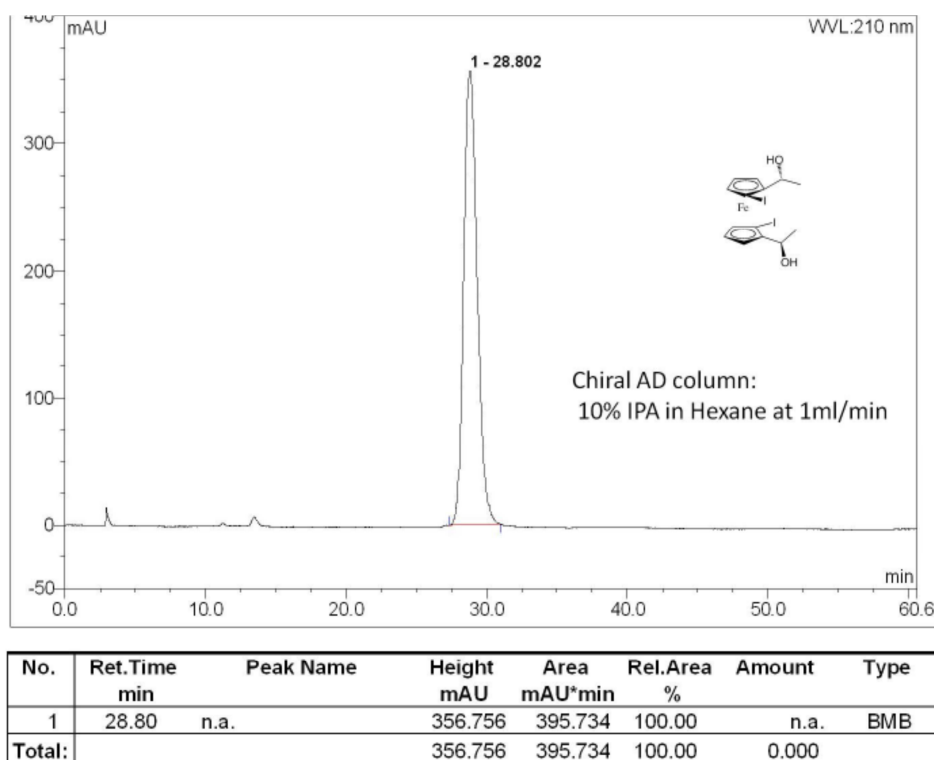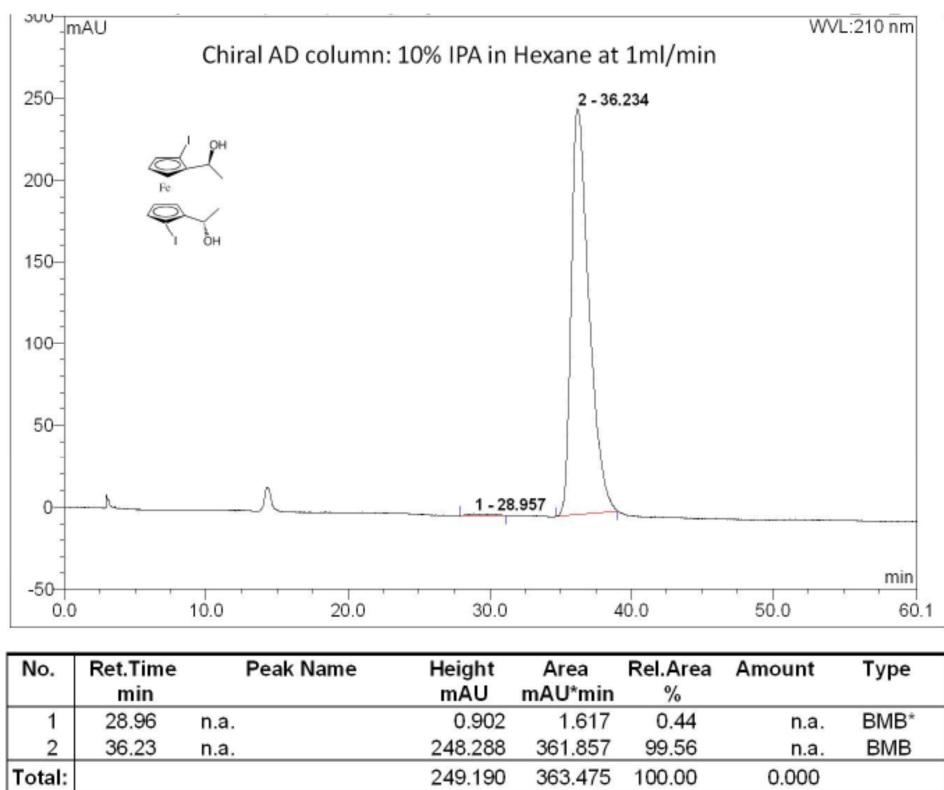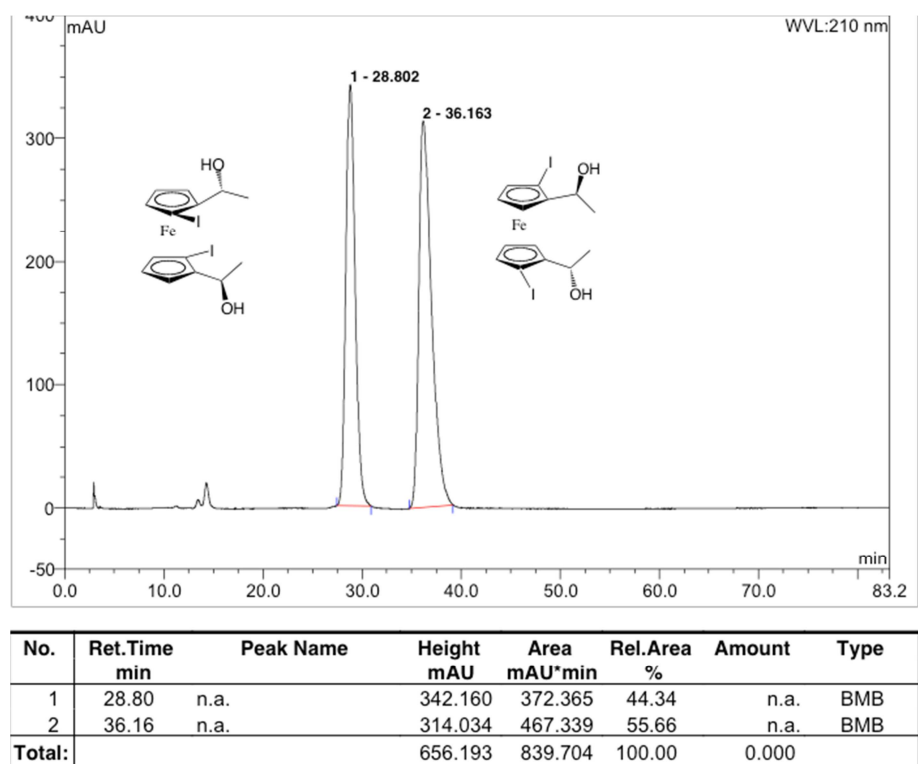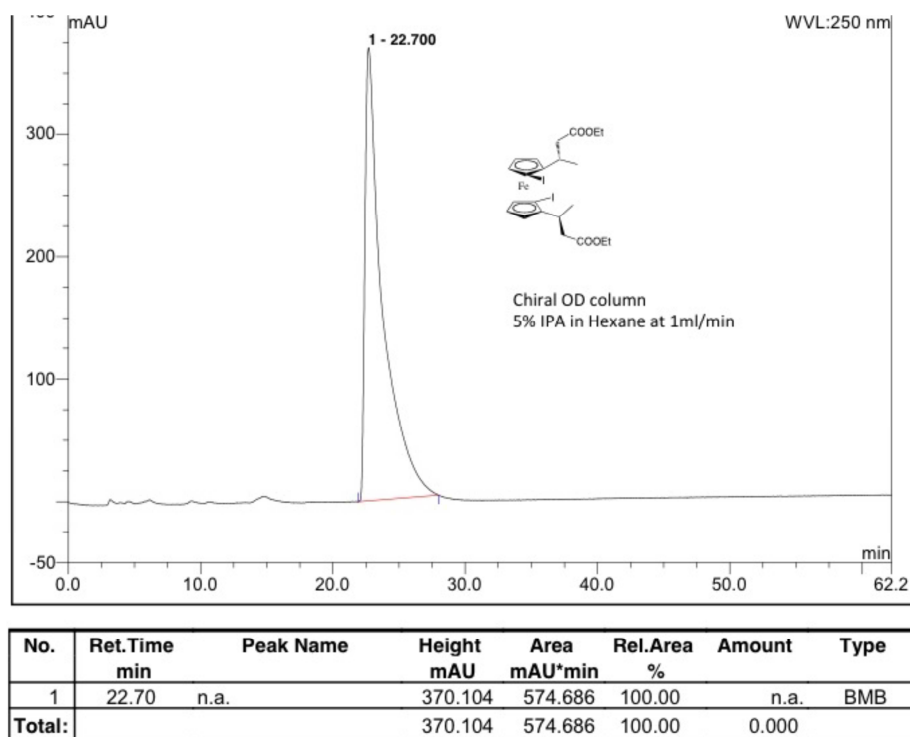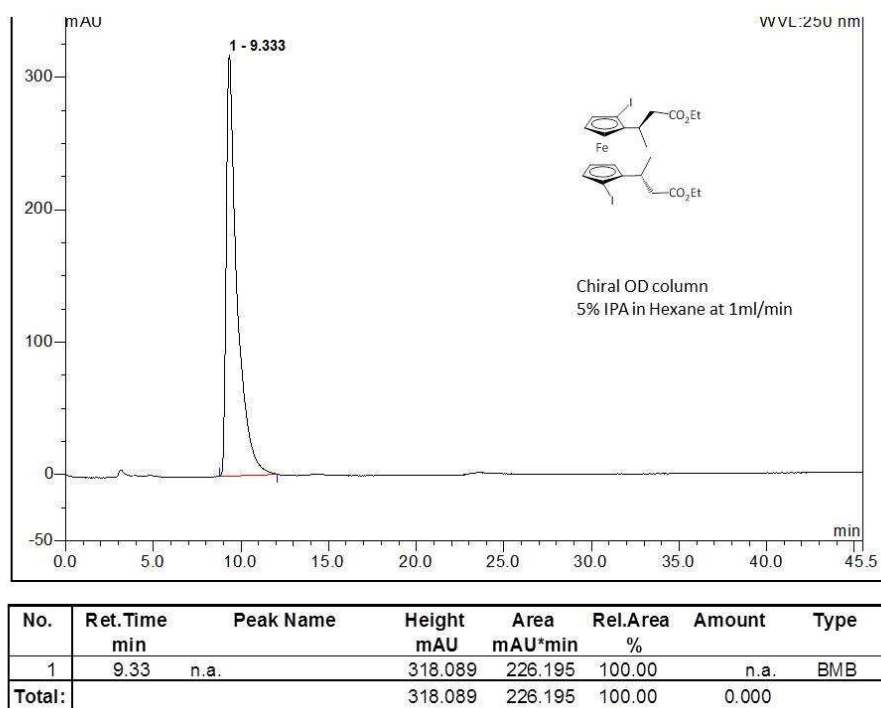*Figure 7-12: Chiral HPLC of the opposite enantiomer of 39 (5% IPA in Hexane at 1 mL/min, AD column)*
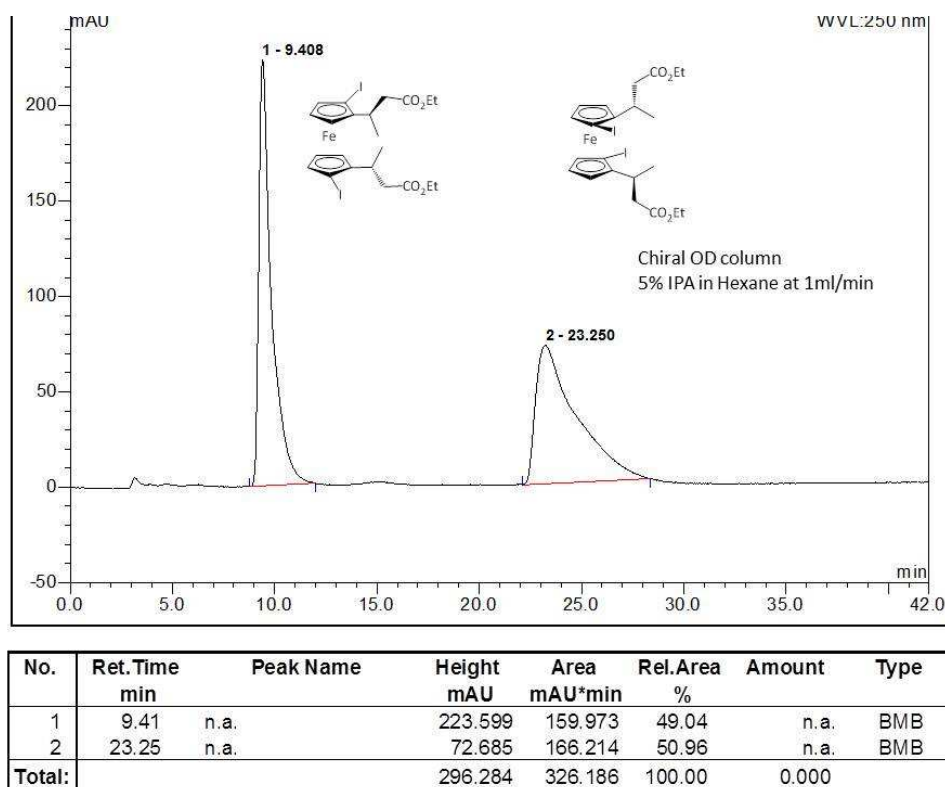
Figure 7-13: *Chiral HPLC of 39 and its enantiomer (5% IPA in Hexane at 1 mL/min, AD column)*

Figure 7-14: *Chiral HPLC of 40 (10% IPA in Hexane at 1 mL/min, AD column)*

No.	Ret.Time min	Peak Name	Height mAU	Area mAU*min	Rel.Area %	Amount	Type
1	43.48	n.a.	459.681	886.055	97.78	n.a.	BMB
2	48.83	n.a.	10.715	20.160	2.22	n.a.	BMB*
Total:			470.396	906.215	100.00	0.000	

Figure 7-15: *Chiral HPLC of the opposite enantiomer of 40 (10% IPA in Hexane at 1 mL/min, AD column)*

| No.	Ret.Time min	Peak Name	Height mAU	Area mAU*min	Rel.Area %	Amount	Type
1	43.48	n.a.	279.315	543.909	53.24	n.a.	BM
2	50.86	n.a.	199.498	477.627	46.76	n.a.	MB
Total:			478.813	1021.536	100.00	0.000	

Figure 7-16: *Chiral HPLC of 40 and its enantiomer (10% IPA in Hexane at 1 mL/min, AD column)*

Figure 7-17: *Chiral HPLC of 47 (2.5% IPA in Hexane at 1 mL/min, AD column)*

No.	Ret.Time min	Peak Name	Height mAU	Area mAU*min	Rel.Area %	Amount	Type
1	53.11	n.a.	1380.048	4607.207	100.00	n.a.	BMB
Total:			1380.048	4607.207	100.00	0.000	

No.	Ret.Time min	Peak Name	Height mAU	Area mAU*min	Rel.Area %	Amount	Type
1	46.53	n.a.	609.508	1258.453	96.72	n.a.	BMB
2	54.13	n.a.	21.598	42.687	3.28	n.a.	BMB*
Total:			631.106	1301.140	100.00	0.000	

Figure 7-18: *Chiral HPLC of the opposite enantiomer of 47 (2.5% IPA in Hexane at 1 mL/min, AD column)*

Figure 7-19: *Chiral HPLC of 47 and its enantiomer (2.5% IPA in Hexane at 1 mL/min, AD column)*
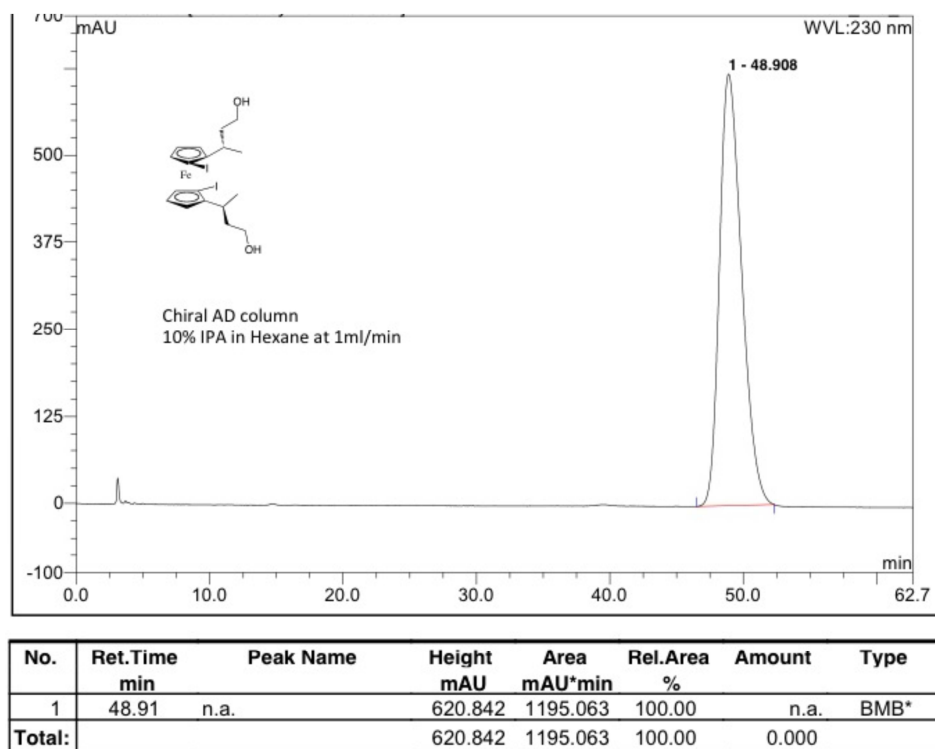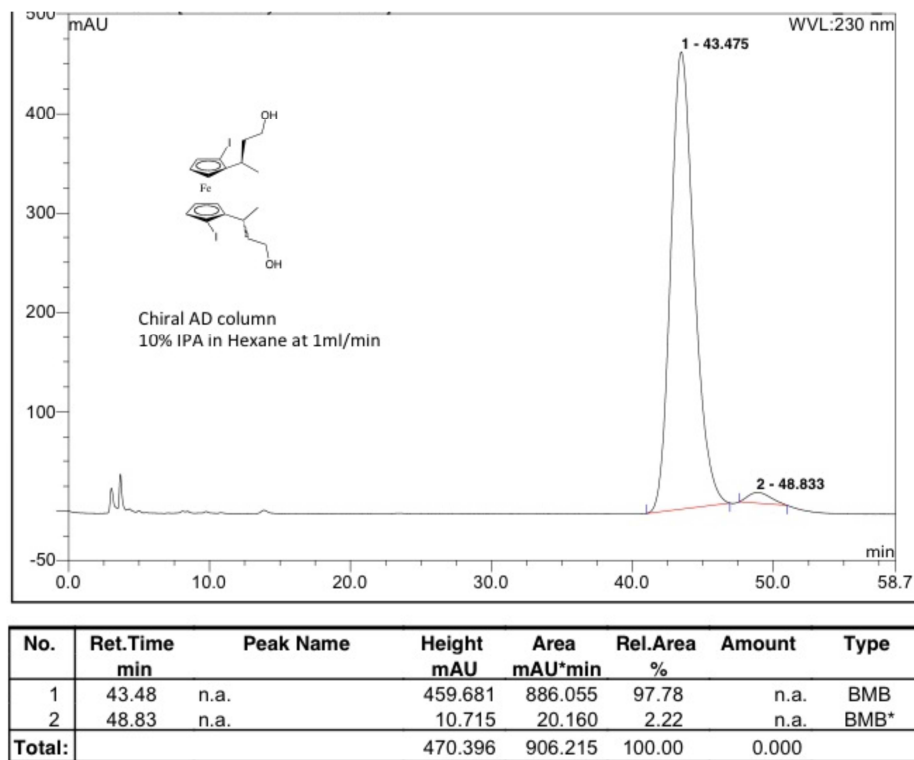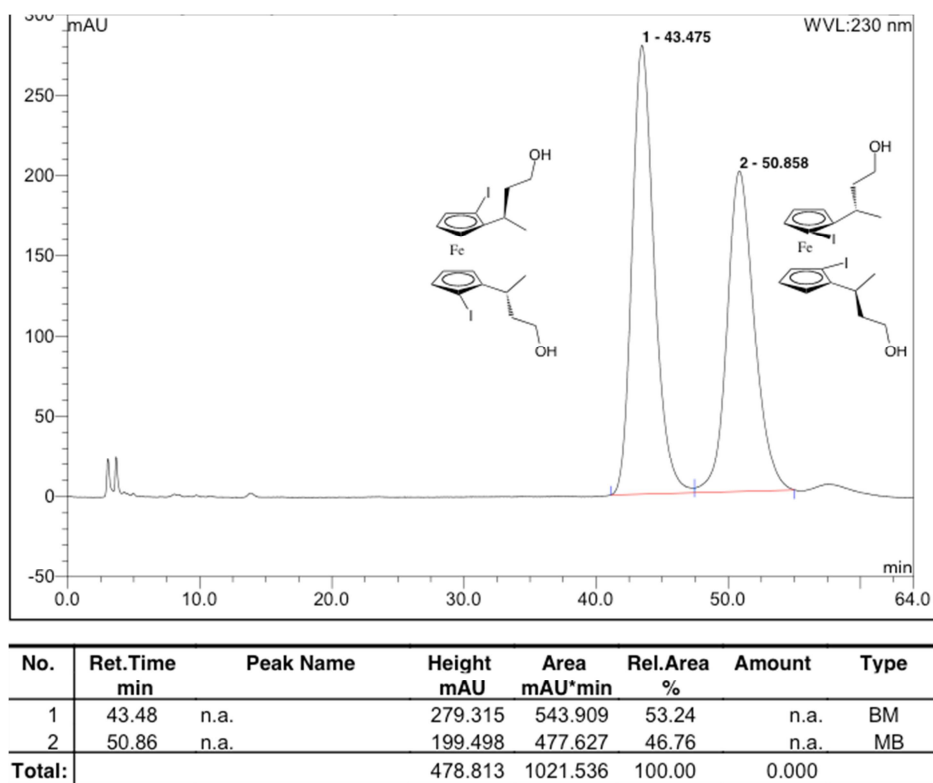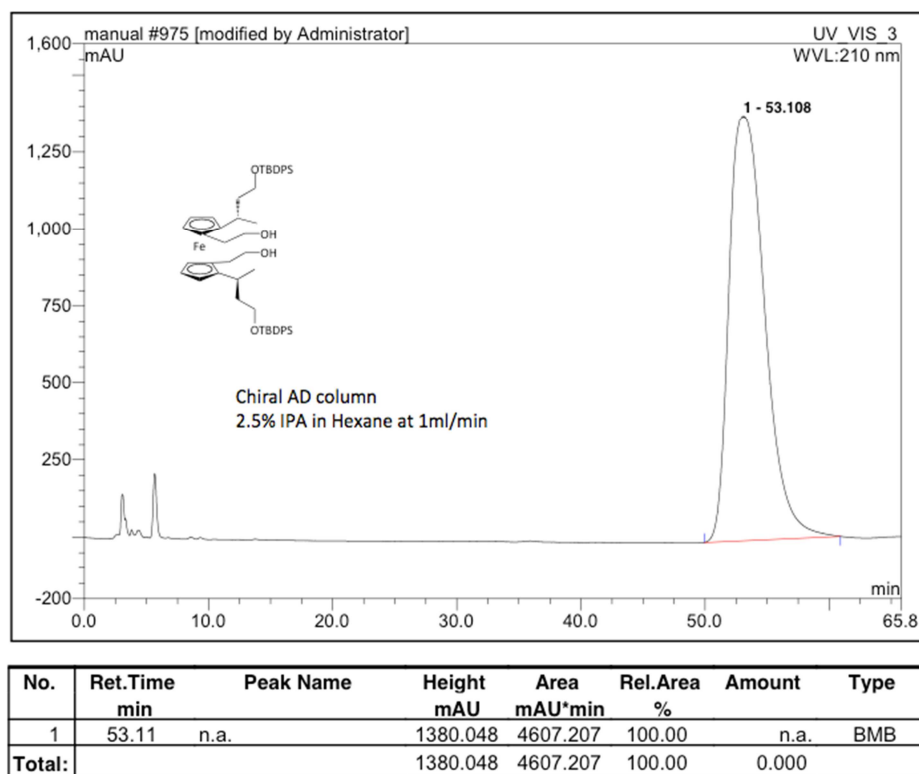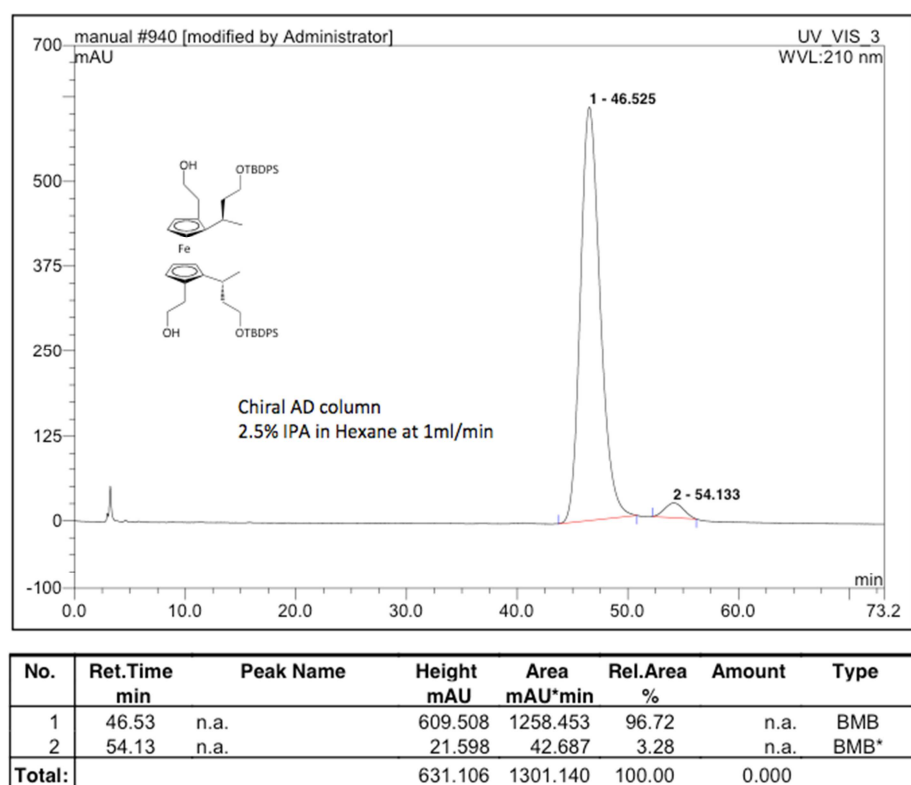
No.	Ret.Time min	Peak Name	Height mAU	Area mAU*min	Rel.Area %	Amount	Type
1	44.84	n.a.	979.453	2180.085	45.65	n.a.	BM
2	53.39	n.a.	967.954	2595.708	54.35	n.a.	MB
Total:			1947.407	4775.793	100.00	0.000	

No.	Ret.Time min	Peak Name	Height mAU	Area mAU*min	Rel.Area %	Amount	Type
1	14.43	n.a.	11.407	6.671	1.69	n.a.	BMB
2	16.85	n.a.	433.553	387.493	98.31	n.a.	BMB*
Total:			444.960	394.164	100.00	0.000	

Figure 7-20: *Chiral HPLC of 67 (1% IPA in Hexane at 1 mL/min, AD column)*

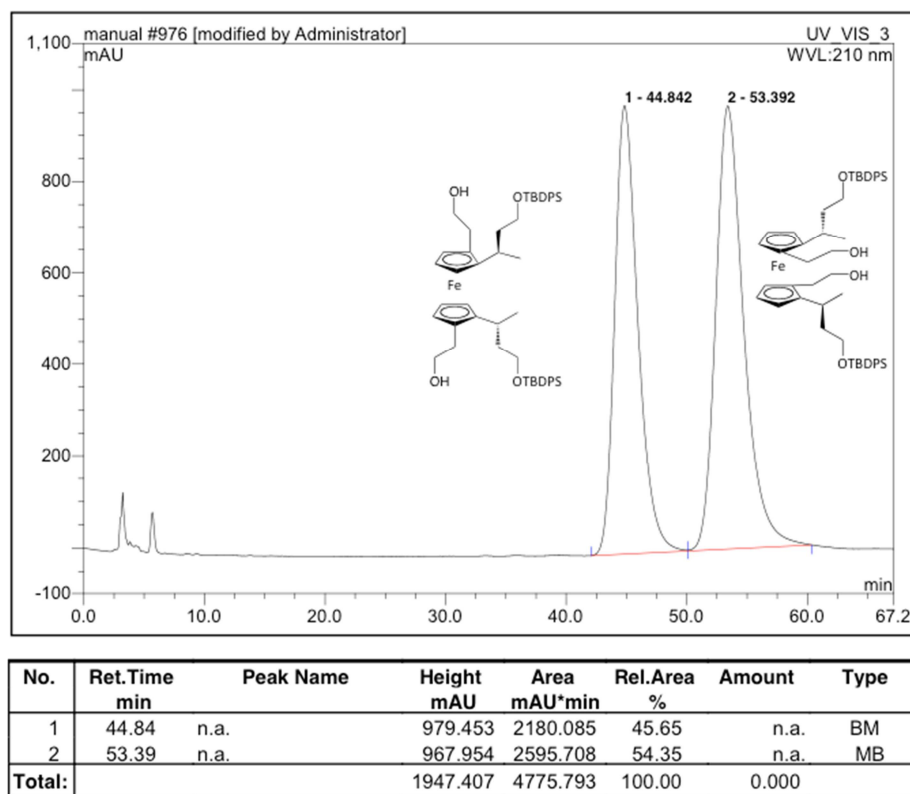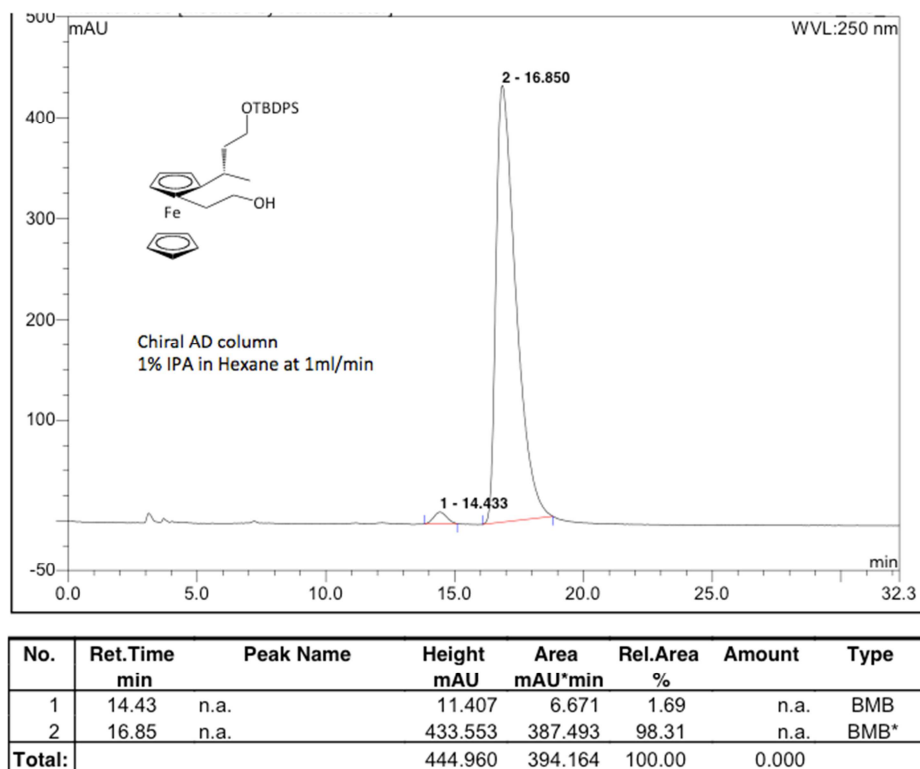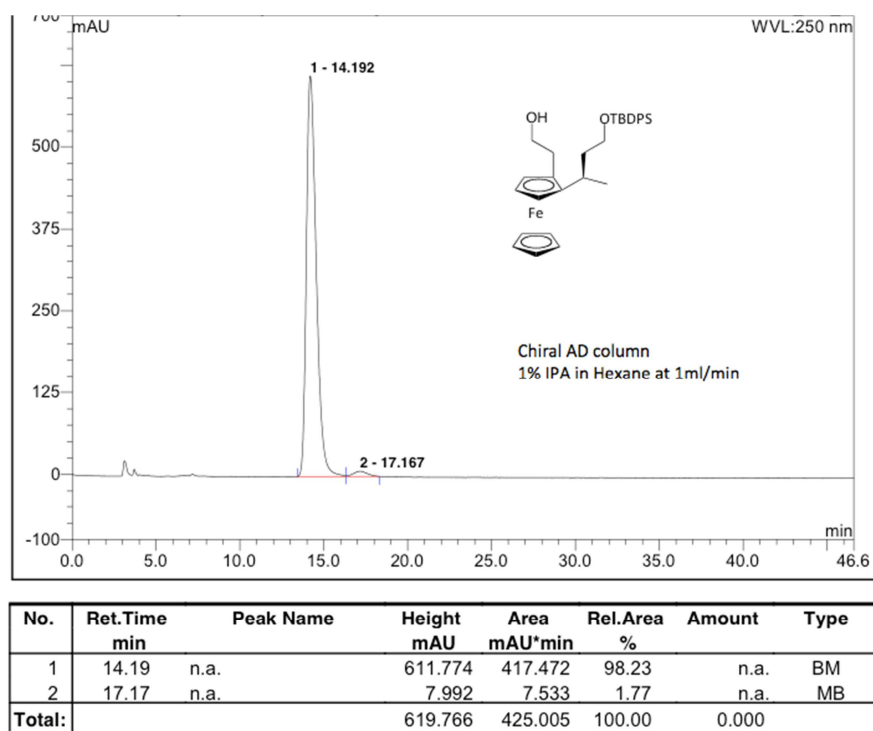**Figure 7-21:** *Chiral HPLC of the opposite enantiomer of 67 (1% IPA in Hexane at 1 mL/min, AD column)*

No.	Ret.Time min	Peak Name	Height mAU	Area mAU*min	Rel.Area %	Amount	Type
1	14.19	n.a.	611.774	417.472	98.23	n.a.	BM
2	17.17	n.a.	7.992	7.533	1.77	n.a.	MB
Total:			619.766	425.005	100.00	0.000	

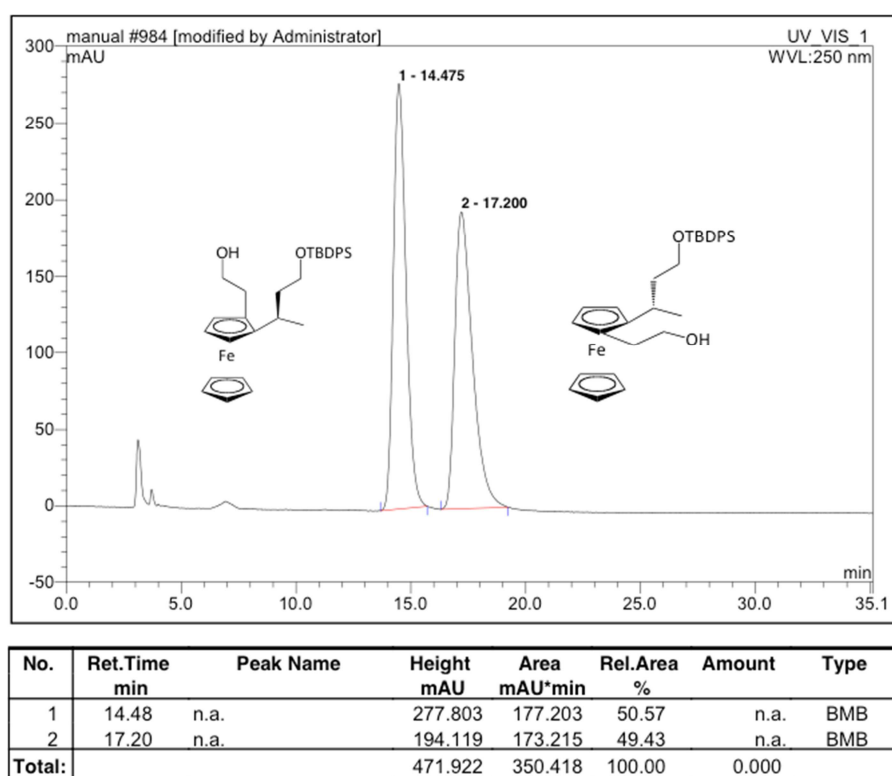| No.	Ret.Time min	Peak Name	Height mAU	Area mAU*min	Rel.Area %	Amount	Type
1	14.48	n.a.	277.803	177.203	50.57	n.a.	BMB
2	17.20	n.a.	194.119	173.215	49.43	n.a.	BMB
Total:			471.922	350.418	100.00	0.000	

Figure 7-22: *Chiral HPLC of 67 and its enantiomer (1% IPA in Hexane at 1 mL/min, AD column)*